N-HETEROCYCLIC CARBENE CATALYSIS: EXPANSION OF SUBSTRATE SCOPE AND SYNTHESIS OF ELECTRONICALLY DIVERSE TETRAARYL *N*-HETEROCYCLIC IMIDAZOLIUM CARBENE LIGANDS

A Dissertation

by

JAMES WILLIAM OGLE

Submitted to the Office of Graduate Studies of
Texas A&M University
in partial fulfillment of the requirements for the degree of

DOCTOR OF PHILOSOPHY

December 2008

Major Subject: Chemistry

N-HETEROCYCLIC CARBENE CATALYSIS: EXPANSION OF SUBSTRATE SCOPE AND SYNTHESIS OF ELECTRONICALLY DIVERSE TETRAARYL *N*-HETEROCYCLIC IMIDAZOLIUM CARBENE LIGANDS

A Dissertation

by

JAMES WILLIAM OGLE

Submitted to the Office of Graduate Studies of
Texas A&M University
in partial fulfillment of the requirements for the degree of

DOCTOR OF PHILOSOPHY

Approved by:

Co-Chairs of Committee,	Stephen Albert Miller
	Kevin Burgess
Committee Members,	Francois P. Gabbai
	Rayford G. Anthony
Head of Department,	David H. Russel

December 2008

Major Subject: Chemistry

ABSTRACT

N-Heterocyclic Carbene Catalysis: Expansion of Substrate Scope and Synthesis of
Electronically Diverse Tetraaryl *N*-Heterocyclic Imidazolium Carbene Ligands.
(December 2008)
James William Ogle, B.S., M.S.; Texas A&M Kingsville

Chairs of Advisory Committee: Dr. Stephen Miller
Dr. Kevin Burgess

Asymmetric hydrogenation as a general route to polypropionates has been
explored for allylic alcohols, acids, and derivatives, which has led to the generation of
2,4-dimethylated hexane derivatives. Quantitative yields in most cases and
enantioselectivities greater than 98% were obtained. A remarkable stereofacial inversion
was observed when an ester or acid was present in the allylic position instead of an
alcohol or alcohol derivative. This led to the construction of all four diastereomers of
the hexanol series from a single enantiomer of hydrogenation catalyst. Also described
are an attempted synthesis of (-)-lardolure, a formal synthesis of the methyl ester portion
of the preen gland extract from the domestic goose *Anser anser*, and a total synthesis of
an extract from the fungi *A. cruciatus*. The synthesis of these compounds demonstrated
shortcomings of the known catalyst system showing enantioselectivities for
polymethylated compounds was high, while diastereoselectivity was low. Methodology
to develop new *N*-heterocyclic carbene catalysts was developed using the cyanide
coupling of aldimines to generate electronically tunable 1,3,4,5-tetraaryl complexes, and
X-ray, IR, and calculations were used to elucidate their electronic characteristics. These
studies indicate that the 4,5-positions have as great an influence on the metal-ligand
bond as the 1,3-positions. In addition, they are among the most electron-donating 2-
metalated *N*-heterocyclic carbenes found thus far. An intrinsic relationship between
catalytic activity and electron donating ability was found in transfer hydrogenations.

TABLE OF CONTENTS

LIST OF FIGURES

LIST OF SCHEMES

LIST OF DIAGRAMS

LIST OF TABLES

CHAPTER I

INTRODUCTION

1.1 Overview

Stereoselective synthesis of natural products has dominated organic chemistry in the last century. Among the most well-defined of these, polypropionate synthesis has had a number of different methodologies developed for the synthesis of these fragments, including enolate chemistry developed by Evans and Myers and alkene functionalizations developed by Negishi and Feringa. These methods are well established as forming 1,3-poly-oxygenated, and in some cases reduced polypropionates, which are ubiquitous in natural products (Diagram 1.1). We turned our attention to fully reduced polypropionates, as they are common fragments of natural products and biologically active molecules, and are interesting oligomer products as well.

This dissertation follows the style of *Organometallics*.

Diagram 1.1. Several natural products with fully reduced polypropionate portions.
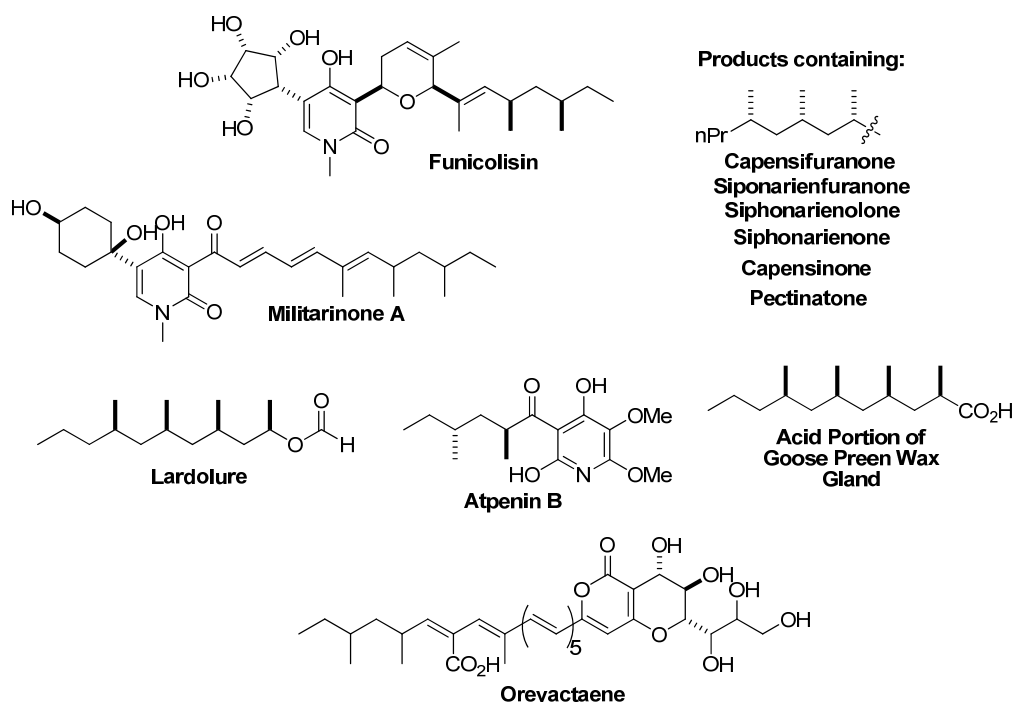
There are many synthetic situations in which hydrogenation of polyenes with concomitant creation of all the chiral centers are conceptually superior to repetitive diastereoselective reactions involving chiral auxiliaries. The missing link which prevented the hydrogenation route being used has been lack of proven enantioselective hydrogenation methods that can be applied to polyenes with little or no other coordinating functionalities. Indeed, there has been almost no work on asymmetric hydrogenations of polyenes of any kind.[1,2] However, data obtained using novel *N*-heterocyclic carbene-oxazoline complexes led us to an opportunity to develop this type of catalytic hydrogenation chemistry. This will be discussed in further detail in Chapter II.

1.2 Background

Most reliable methods to produce these natural product fragments are inefficient from the standpoint of atom-economy, stereospecificity, harsh conditions, and cost of materials. Often, stoichiometric amounts of chiral reagents are used to generate enolates at very low temperatures, and the chiral auxiliaries that induce asymmetric centers are thrown away after hydrolysis of the auxiliary. Other more recent catalytic methods even use 5-10 mol % catalysts; while useful in a laboratory setting, it is not practical for large scale-up procedures should these materials be

needed on an industrial scale, and thus far all require multiple equivalents of either pyrophoric or moisture sensitive reducing agents which are prohibitively dangerous on scale. A great improvement in this field would be the ability to generate the fragments needed in a catalytic method using inexpensive starting materials and milder conditions.

1.3 Current State of the Art in Chiral Auxiliary Methodologies

Myer's work produced some of the cheapest and most general applications in this field. His use of pseudoephedrine as a chiral auxiliary reduced the processing time required of other chiral auxiliaries immensely (Scheme 1.1).[3,4] By forming the *E*-enolate at low temperatures (typically -78 °C), he was able to force kinetic conditions when adding electrophiles, which tended to give the 1,4-*syn* product as the predominant stereoisomer (Diagram 1.2). Also, his development and use of lithium ammonium borate (LAB) as a reducing agent for amides to alcohols gave a protocol to generate either stereocenter with good *ee*'s.[5,6]

Diagram 1.2. Alkylation occurs in a 1,4-*syn* manner.

1,4-syn alkylation

Scheme 1.1. Myer's pseudoephedrine chiral auxiliary can give excellent stereoselectivity.

His process, although highly efficient for generating α chiral centers, lacks efficiency for other systems. Lithium ammonium borane complex (LAB), although efficient for the conversion of amides to alcohols, must be generated from explosive ammonium-borane complex at -78 ^{o}C, and excess material must be quenched carefully as well, generating unwanted salt waste. Pseudoephedrine, although inexpensive, still must be thrown out after reduction, generating a full equivalent of waste material on its own. In addition, for compounds which need multiple stereocenters in sequence, Myer's methodology is not practical unless one stereocenter can be generated independently. For example, if two chiral centers must be generated, one must do an electrophilic attack on the enolate, reduce to alcohol, halogenate, and then react with another enolate, including isolation steps after every step, and generation of the enolate and LAB.

The Myer methodology does give a very viable method to generate a wide variety of mono-chiral compounds, however, and in some cases temperatures up to -40 ^{o}C can be used, and these processes can be scaled up to an industrially useful scale.[7]

1.4 Current State of the Art in Carboalumination Strategies

Negishi has made significant advances in the era of carboalumination strategies to generate poly-propionate systems. In particular, the zirconocene indenyl-menthol based catalyst has

given significant advances in formation of polypropionate natural products, particularly in a catalytic fashion. Thus terminal unfunctionalized alkenes can be reduced with the 1,2-addition of methyl-alanes asymmetrically (Scheme 1.2). The terminal alanes typically are then hydrolyzed to alcohols, with which a two-step sequence of oxidation to aldehyde followed by Wittig reaction generates another terminal alkene which can then be reacted again in sequence. The terminal alcohols do not need to be oxidized exclusively, but can also be functionalized as halogens to react in an enolate fashion as well.[8]

Scheme 1.2. Negishi's carboalumination strategy to reduced polypropionates.
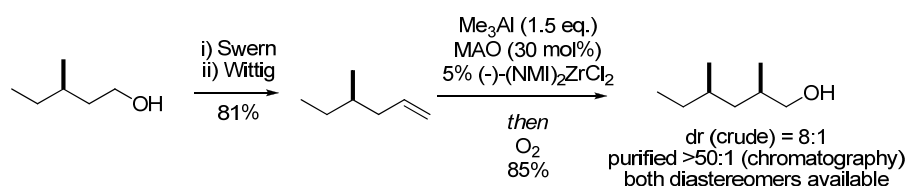
Despite the namesake, catalytic carboalumination with these catalysts is far from efficient. High loading of air sensitive catalyst (5-10 mol %), multiple equivalents of pyrophoric reagents, and anhydrous reaction conditions make the process prohibitively dangerous to use on a large scale. Likewise, selectivity for individual chiral centers (for methyl addition) is only in the range of 75-85% *ee*, and typically has to be carried through so that diastereomeric purification can later improve the apparent selectivity. Likewise, all cases so far require extensive column chromatography for diastereomeric purification, one of the least efficient purification methods available for large-scale reactions. Recently, Negishi has published a specific instance where sequential carboaluminations can be performed *in situ* to generate polypropionates, but these have yet to be made general so far.

Negishi's most significant contribution is the idea of performing asymmetric reductions catalytically to generate the same polypropionates possible from chiral auxiliaries. To this end, he has synthesized a number of natural products and fragments of natural products, including fragments of doliculide, ionomycin, and borrelidin (Figure 1.1).[9-11]
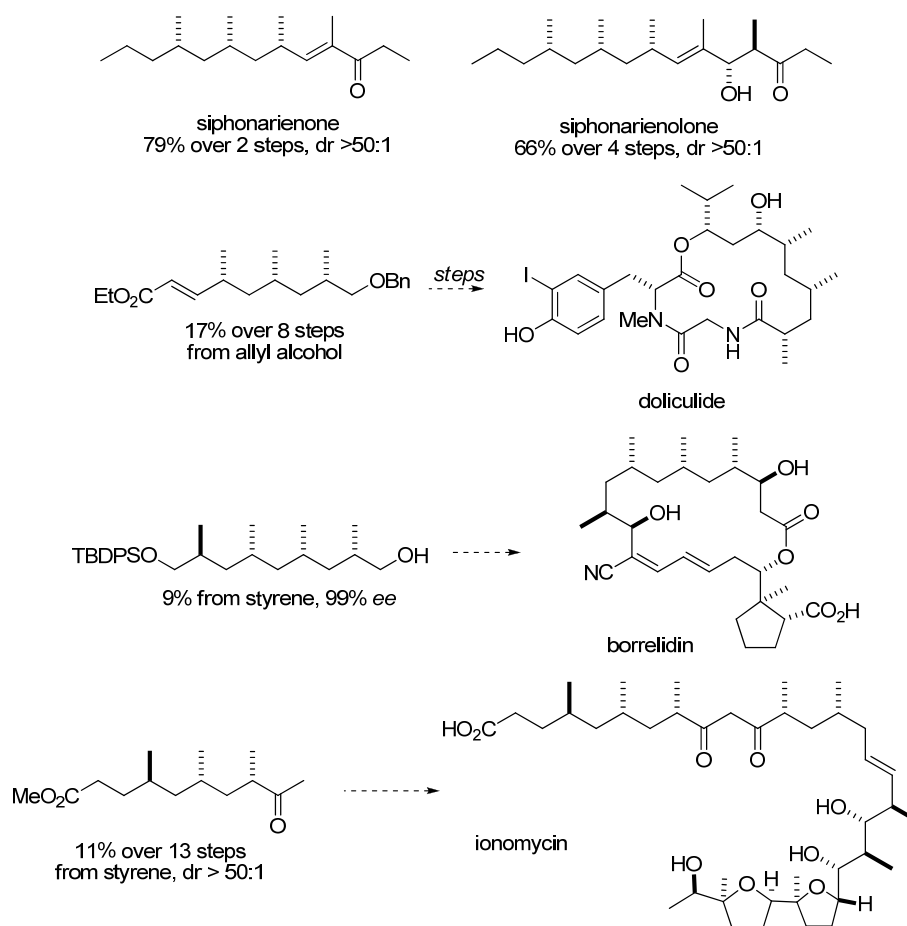
Figure 1.1. Several natural products and natural product fragments developed by the Negishi group.

1.5 Conjugate Addition to Generate Polypropionates

Chiral conjugate addition to Michael acceptors is not a new field, although it has some very significant use. Asymmetric conjugate addition is perhaps more challenging, and Feringa has developed a catalytic asymmetric variant. He found that when adding methyl Grignard to α,β−unsaturated esters, he was able to add conjugatively in a chiral fashion (Figure 1.2).[12-15] In particular, thioesters give better yields and *ee*'s, and have the distinct advantage that they are easily functionalized by transformation into other moieties.[16]
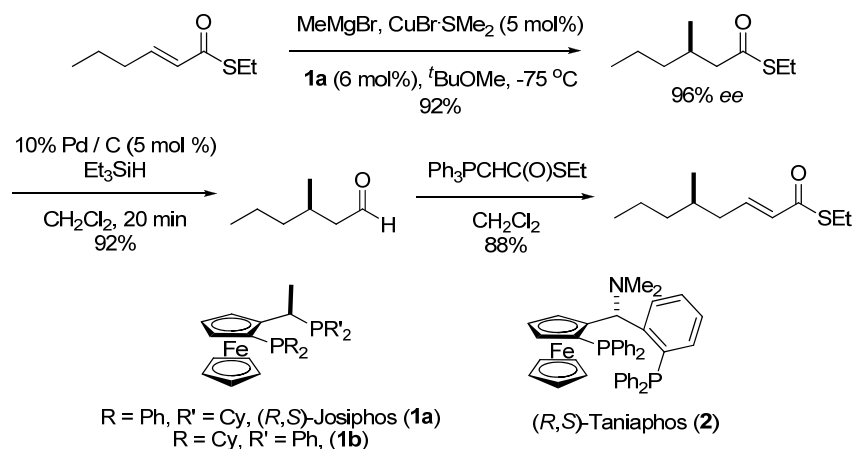
Figure 1.2. Feringa's chief catalysts and reactions.

This conjugate addition methodology enabled him to realize the total synthesis of Lardolure in a concise manner, although the final chiral center was made using a stoichiometric amount of chiral resolving reagent, and has also enabled him with collaboration with Minnard to synthesize *α*-**D**-mannosyl phosphomycoketides from Mycobacterium tuberculosis in a similar manner (Scheme 1.3, Figure 1.3).[16,17]
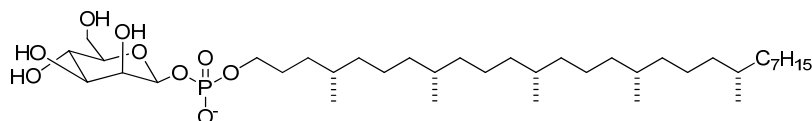
Figure 1.3. Feringa and Minnard's synthesis of a *α*-**D**-Mannosyl Phosphomycoketide from Mycobacterium tuberculosis.

Scheme 1.3. Feringa's total synthesis of Lardolure.

Conditions: (a) MeMgBr (1.2 equiv), **2** (1.2 mol %), CuBr·SMe$_2$ (1 mol %), tBuOMe, -75 °C, 2 h; (b) 10% Pd/C (5 mol %), Et$_3$SiH, CH$_2$Cl$_2$, rt, 20 min; (c) Ph$_3$PCHCOSEt, CH$_2$Cl$_2$, reflux; (d) (S)-MeSOpTol, LDA, THF, -78 °C; (e) DIBAL-H, ZnBr$_2$, THF, -78 °C; (f) Raney-Ni, EtOH, rt; (g) HCOOH, 65 °C.
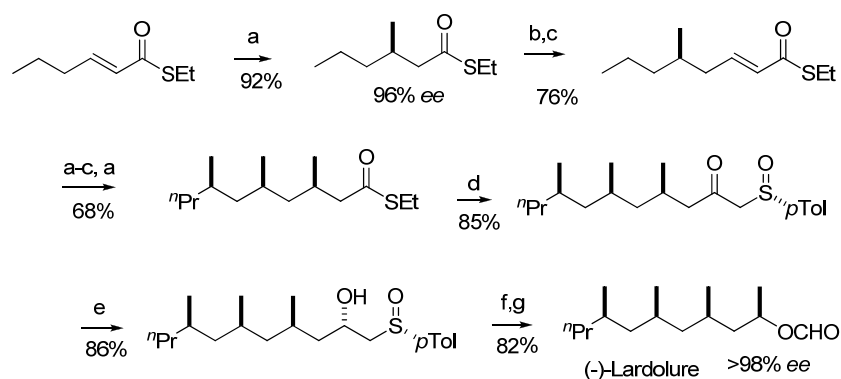
Although Lardolure had been synthesized using his methodology, there are still some serious flaws. Primarily, every step in which a chiral center is made requires a chromatographic step. Likewise, conjugate addition limits the available product structures possible by forcing only certain chiral centers in certain positions, for example as 1,3-dialkylated species (thus, the elaboration of the final chiral center in Lardolure using stoichiometric chiral sulfone auxiliary, Scheme 1.3, steps d-g). Low temperatures (-78 °C) are also required for high stereoselectivity. Thus, the methodology, although extremely effective for certain targets, is neither general nor is it particularly scalable beyond a laboratory setting.

Recently, Feringa has also found that his system can be used in allylic substitution (Scheme 1.4).[12] Typically, a properly substituted allylic compound, *i.e.* one with a suitable leaving group, is subjected to the same reaction conditions as those above, and subsequent allylic substitution gives a chiral center from the alkyl Grignard addition, and leaves the compound with a terminal olefin, in *ee*'s as high as 98%, but more typically around 90-95%. He has demonstrated that these terminal olefins can also be used to generate α,β-unsaturated esters using olefin metathesis, and these in turn can also be used to generate further chiral centers using the methodology above.

Scheme 1.4. Synthesis of some 1,2-dialkyl fragments.
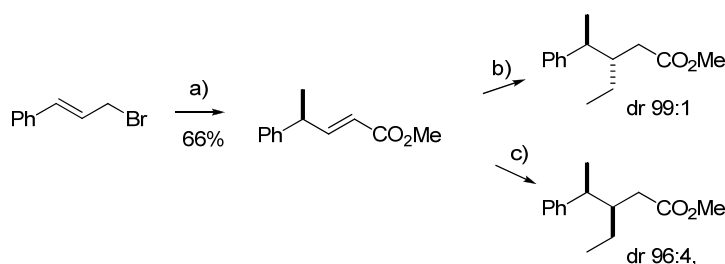
Reagents and conditions: a) i) MeMgBr (1.15 eq.), **2** (1.1 mol%), CuBr·SMe$_2$ (1.0 mol%), CH$_2$Cl$_2$, -78°C; ii) Hoveyda–Grubbs 2nd generation, methyl acrylate (5.0 eq.), CH$_2$Cl$_2$, rt; b) EtMgBr (5.0 eq.), (R,S)-**1b** (6.0 mol%), CuBr·SMe$_2$ (5.0 mol%), CH$_2$Cl$_2$, -78 °C; c) EtMgBr (5.0 eq.), (S,R)-**1b** (6.0 mol%), CuBr·SMe$_2$ (5.0 mol%), CH$_2$Cl$_2$, -78 °C.

Feringa's methodology is much more general than Negishi's in that it applies to many other poly-alkylated natural products: ethyl Grignard, isopropyl Grignard, and others all gave significant *ee*'s and yields. Likewise, the methodology only requires a relatively mild 1.2 equivalents of Grignard reagent per chiral center, making workup and safety concerns much less significant.

1.6 Some Significant Advances in Asymmetric Hydrogenation

Fully reduced polypropionates can also potentially be obtained from asymmetric hydrogenation. Indeed, catalytic hydrogenation is a well known and safe process which has been explored quite thoroughly since Noyori's first publications in the field in the early 1980's. Conversion is usually not as important in these systems, either, since hydrogen is inexpensive and abundant, and large excesses of this reductant can be used with no added workup of the reaction.

Although Noyori's systems typically only reduce the α,β–double bonds on allylic alcohols, stepwise reduction to generate polyenes (by homologation then reduction) could give rise to natural products. Crabtree's catalyst, not requiring a coordinating group to function, and Pfaltz' and Burgess' chiral Crabtree-analogues, both do have greater potential to fully reduce polyene systems without requiring further homologation steps afterwards. Although a wide array of substrates has been used in asymmetric hydrogenation, it is interesting to note that this method has not been used for fully reduced products before.

1.6.1 Crabtree's Catalyst

Crabtree's catalyst was the first of a series of non-coordinating iridium based catalysts which were able to hydrogenate unfunctionalized alkenes (Figure 1.4).[18-22] Not requiring coordination to direct hydrogenation also meant that this catalyst could hydrogenate polyene systems without needing stepwise homologation and elaboration, although work on these particular processes had not been performed before our studies. This chemistry was an important step in realizing a general asymmetric catalyst.

Crabtree's Catalyst
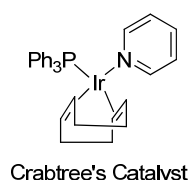
Figure 1.4. Crabtree's catalyst.

1.6.2 Noyori's Catalysts

Noyori's work in asymmetric hydrogenation has had a marked influence on the field of asymmetric catalysis.[23] His catalyst systems, BINAP-based Ruthenium catalysts, bind mildly to oxygen and nitrogen, and can then reduce allylic alkenes and ketones in an asymmetric manner (Figure 1.5).[24-26]

Rh((*R*)-binap)
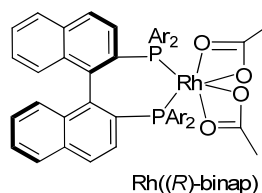
Figure 1.5. One of several of Noyori's catalysts.

Coordination seems to be the key to high stereoselectivity in these kinds of catalysts. For example *E*-1,2-buta-2-enoic acid only gave poor stereoselectivity compared to prochiral allylic alcohols, presumably due to poorer binding to the acid over the alcohol, when prochiral allylic alcohols give much greater *ee*'s.

The stereoselectivity and regioselectivity of these catalysts is remarkable. The catalysts are available as both enantiomers at the same price. Likewise, Noyori found that depending on the olefin geometry, one can pick substrates that will give opposite stereofacial selectivity as well; *E* and *Z* give the opposite enantiomer, thus setting a precedent that careful selection of substrate can have a significant effect on the product regardless of the catalyst.[27,28] Chemoselective hydrogenations can be obtained in certain substrates as well. In the presence of a polyene system, only allylic alkenes are hydrogenated (diagram 1.3). Homoallylic alkenols also can be reduced, although the selectivity for allylic alcohols is much greater.

Diagram 1.3. *E* and *Z* alkenes give opposite facial selectivity, and only allylic alcohols can be hydrogenated.
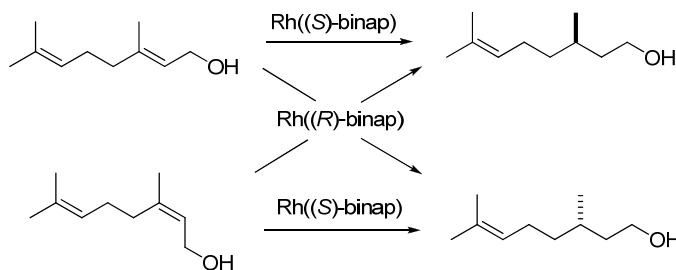
Despite the advantages of the ruthenium and rhodium based Noyori systems, there are some disadvantages. All the common catalysts are air and moisture sensitive, although *in situ* preparative methods are available for some systems. Also, very high pressures are required for a large number of substrates (typically 50 to 100 atm of hydrogen are necessary to effect complete transformation), and, of course, the limited substrates that can react in hydrogenations affect the possible products that can be generated.

1.6.3 Pfaltz and Burgess' Catalyst

Pfaltz and Helmchen developed a useful ligand in asymmetric allylic alkylations.[29] Later, Pfaltz applied this ligand with great success after inserting iridium metal into the ligand and using it in asymmetric hydrogenations.[30,31] The ligand is a logical asymmetric variant of the Crabtree catalyst: replacing the pyridine portion with an oxazoline, and giving a rigid backbone to the phosphine portion forms an enantioselective "pocket" which can force some substrates to be hydrogenated preferentially from a specific side (Figure 1.6).[29]
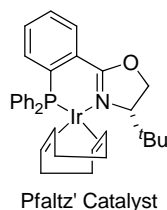
Pfaltz' Catalyst

Figure 1.6. One of several of Pfaltz' catalysts.

This and other similar catalysts give *ee*'s that are very dependent on the specific substrate *i.e.*, although excess hydrogen can give high conversion, the trends in *ee*'s and in absolute facial selectivity are very hard to predict. In addition, there are classes of compounds, mainly sulfur containing compounds and tetra-substituted olefins, which have not been hydrogenated practically yet.[32]

Regardless of these difficulties, the iridium based systems are an improvement in practicality over ruthenium based systems typically due to the lower pressure conditions required to observe complete conversion (only 1-20 atm of hydrogen are needed for most substrates). The Pfaltz group has also recently found that their oxazoline catalyst can also be used to hydrogenate almost completely unfunctionalized polyenes, such as γ-trocotrienyl acetate (reaction 1.1).[33]

Scheme 1.5. Asymmetric hydrogenation of γ-trocotrienyl acetate by Pfaltz.

Pfaltz Catalyst (1 mol%)
50 bar H_2, CH_2Cl_2, 23 °C,
>99% conv.
>98% *d.r.*
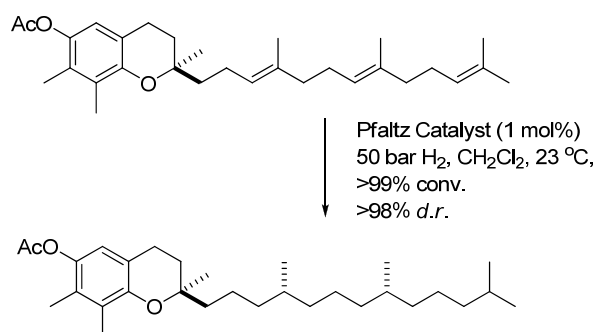
Burgess developed a catalyst almost simultaneously with Pfaltz.[34] In this catalyst, the pyridine is replaced with an oxazoline as in Pfaltz' catalyst, but the phosphine portion is replaced with an imidazole carbene with a rigid backbone instead (Figure 1.7). This catalyst was the first asymmetric iridium based catalyst to give greater than 90% *ee* for prochiral aryl olefins, the first to be used in a systematic study of the hydrogenation of dienes, the first used to determine the

mechanism of the catalytic cycle, and the first used for hydrogenating polyene systems such that each alkene is hydrogenated as the monomer (Figure 1.8).

Ar = 2,6-diisopropylphenyl
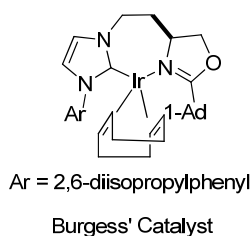
Burgess' Catalyst

Figure 1.7. One of several of Burgess's catalysts.

2,3-disubstituted buta-1,3-dienes
(and related)

yield %   ee %   ent/meso
66-100   31-87   0.35-2.14

(*E,E*)-1,4-diaryl-
2,3-dimethyl buta-1,3-dienes

yield % ee % ent/meso

66-96   96+   1.0-1.3

(*E,E*)-1,4-Diphenyl-
1,3-dimethyl-1,3-butadiene

yield % ee %(major) d.r.

100   95   6:1

(*E,E*)-1,4-Diaryl-
1,4-dimethyl-1,3-dienes

yield % ee % ent/meso

~100   98+   ~14+
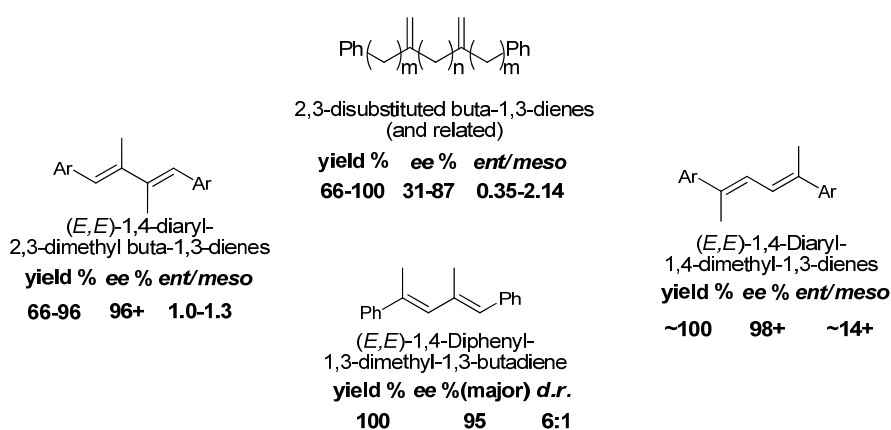
Figure 1.8. Several dienes studied previously in the Burgess group.

1.7 Further Studies

Asymmetric hydrogenation had some precedent for partially reducing polyene systems, particularly in the Noyori systems, but no groups had considered these as important synthetic targets until our initial reports revealed a complex, stepwise hydrogenation with some dependence on initially formed stereocenters affecting future stereocenters.[2,35,36]   Initially, a detailed study of diaryldienes was performed to gain mechanistic insight into further hydrogenations, which revealed step-wise hydrogenation of these substrates. It was with this in mind that efforts were made to explore what further hydrogenations of α,β-unsaturated systems could generate in the sense of natural product synthons.

CHAPTER II

SYNTHESIS OF POLYPROPIONATES USING ASYMMETRIC HYDROGENATION AND APPLICATIONS TO SEVERAL NATURAL PRODUCTS

2.1   Introduction

Although many groups have studied a variety of iridium-based asymmetric hydrogenation catalysts, relatively little variation exists in the substrates used to investigate these catalysts for overall efficacy.[32] Despite the insight gained from our study on diaryl dienes into the mechanism of polyene systems, and the demonstration that unsymmetric diaryl dienes can give good *ee*'s and d.r.'s, the synthetic utility of the products formed from such systems is questionable at best.[1] For this reason, we searched for prochiral tri-substituted alkene units that would give more synthetically useful substrates that could then be used as potential synthons of natural products. Briefly looking through the literature, natural products with low-aryl functionality and that contained few oxygen functionalities seemed particularly attractive.[37,38] As a class, the group of reduced polypropionate natural products could be made from asymmetric hydrogenation of polyenes formed easily from Wittig or similar olefinations, particularly of the stabilized ester-containing phosphor ylides, known to give very high selectivity for the *E* isomer.[39,40] Thus, because of the high *E*/*Z* purity of the products generated from Wittig reactions, the available protocols to generate a wide variety of prochiral substrates, and the ease with which to characterize the absolute configuration of the resulting products, a systematic study on a focused array of alkenes and dienes was begun.

2.2   Model Studies of Monoenes

2.2.1   Monoene Substrates for Catalyst Optimization

The literature revealed that the tiglic systems, *i.e. E*-2-methyl-1-substituted-butenes, could be very attractive substrates for natural product synthons.   Although tiglic substrates had been studied previously with Noyori-style ruthenium catalysts, primarily in studies of transfer hydrogenation with various alcohols, relatively low-chelating iridium-based hydrogenation catalysts, such as catalyst systems based on Crabtree's catalyst, had not been used for these kinds of substrates at the time of these studies.[41a]   A brief study of these hydrogenations on various tiglate systems only revealed moderate *ee*'s, the highest previously reported being around 90% *ee*, but in some cases poor conversions.[41b]   All of the catalysis performed in this manner was exclusively done with *O*-coordinating ruthenium-BINAP based systems, and thus did not have the potential to convert multiple stereocenters at once without exceptionally prepared substrates with multiple allylic systems.

Ethyl tiglate and tiglic acid are both commercially available, and consequently were useful starting materials for optimization and characterization.   Likewise, commercially available *S*-2-methyl butanol gives a common marker that most tiglate derivatives can be chemically modified to; this gives the absolute configuration of the major enantiomer of the products using only chiral GC, making identification of the absolute configuration of the products formed after hydrogenation very simple.

Ethyl tiglate and tiglic alcohol were used early in this search as model substrates for optimizing conditions with, along with several dozen derivatives which gave similar selectivities (Scheme 2.1, reactions 2.1 and 2.2).   Despite similar *ee*'s to what was previously reported,[41] a realization in this study made the two substrates particularly attractive: from the same enantiomer of catalyst, they gave entirely opposite facial selectivity, *R*-products coming generally from the esters and similarly substituted compounds having a carbonyl oxygen, and *S*-compounds coming from the alcohol derivatives.   After hydrogenation, hydride reduction of the ester product, followed by chiral GC analysis revealed the opposite facial selectivity generated from tiglic alcohol (determined by comparison of racemic alcohol and the commercially available *S*-butanol).   This is particularly interesting due to the fact that, in essence, the two substrates are only a few oxidation states away from each other, and can be used quite easily as

synthons for each other as well.[42-44] Thus a general strategy for generation of any combination of *R* or *S* stereocenters along a linear chain was beginning to reveal itself.

Scheme 2.1. Monoene hydrogenations strongly depend on substrate.

reaction 2.1

1 mol% L-Ir* cat.,
20 atm H$_2$, 4 h,
CH$_2$Cl$_2$, 25 °C
100%

2.1f

2.2f
67% *ee*

reaction 2.2

1 mol% L-Ir* cat.,
20 atm H$_2$, 4 h,
CH$_2$Cl$_2$, 25 °C
100%

2.1a

2.2a
83% *ee*
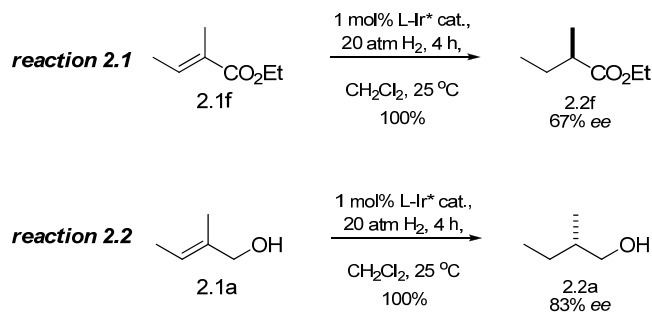
A thorough study to determine the optimum substrates for higher enantioselectivity was performed to find mild modifications that would be easily performed on a large scale (Table 2.1). Despite the lack of discovering any truly remarkable selectivity, some interesting trends emerge. It seems that if the allylic carbon in the tiglic systems is fully oxidized, there is a strong *re*-facial attack of the iridium hydride on the substrate, but if only one oxygen is present on the same allylic carbon, then the *si*-face is preferred for hydride delivery. Whether this is from an electronic effect due to electron density in the alkene, or due to a chelating effect from a lone pair of electrons on the alcohol (or carbonyl on the ester) is yet to be determined. However, some interesting comparisons with the products of prochiral aryl olefins and aliphatic monoenes can be observed (see Diagram 2.1 below).

Table 2.1. Substrates tested to optimize *ee* of asymmetric hydrogenation.

prochiral olefins 2.1 → chiral products 2.2

1 mol% L-Ir* cat., 20 atm H$_2$, 4 h, CH$_2$Cl$_2$, 25 °C, all 98+% conversion

entry	substrate	product	*ee* (%)[a]
a		[b]	83
b		[c]	49
c		[b,e]	54
d		[c]	59
e		[f]	87
f		[c]	67
g		[c]	55
h		[c]	73
i		[c,d]	46
j		[c, h]	42
k		[c]	27
l		[c,g]	57
m		[f]	65
n		[f]	72
o		[f]	42
p		[f]	<20

[a]Unless otherwise listed, *ee* determined by chiral GC analysis of the hydrogenated product with a racemic mixture. [b]Absolute configuration determined by comparison with the available alcohol in chiral GC analysis. [c]Absolute configuration determined by chemical modification to the alcohol followed by comparison with the available alcohol in chiral GC analysis. [d]*Ee* determined after chemical modification to the alcohol and chiral GC analysis. [e]100% reduction of the aldehyde was observed with this substrate. [f]Presumed absolute configuration by comparison with known compounds. [g]Exactly 1:1 d.r. from the racemic substrate, *ee* of the diastereomers was 57% and 52% respectively. [h]Only 22% conversion was obtained with this substrate.

Aryl-substituted prochiral olefins are the most studied and characterized of the substrates in asymmetric hydrogenations, and thus are the most reliable source of data for the substrate's absolute configuration. A comparison of the absolute configuration and facial selectivity of well-known aryl alkenes and tiglic systems reveals which substrates give similar facial selectivity. In general, the L-catalyst gives the same facial selectivity on *E*-aryl substituted alkenes as the alcohol, where the ester and ester-like functionalities give opposite facial selectivity (Scheme 2.2). Considering the bulkiness of the active cavity inside the catalyst, it seems unlikely that all three substrate classes are aligning themselves identically, mainly because this would cause the ester functionality to align itself directly into the middle of the adamantyl group, where the other substrate classes can direct the olefinic hydrogen into the same region (Diagram 2.1).[2] Thus, a more likely scenario is that the electronic deficiency of these substrates causes a complete shift in the substrate-catalyst alignment, perhaps even aligning themselves perpendicular to the alignment of other substrates.

Diagram 2.1. Space-filled model of energy minimized trisubstituted aryl olefin / catalyst complex.
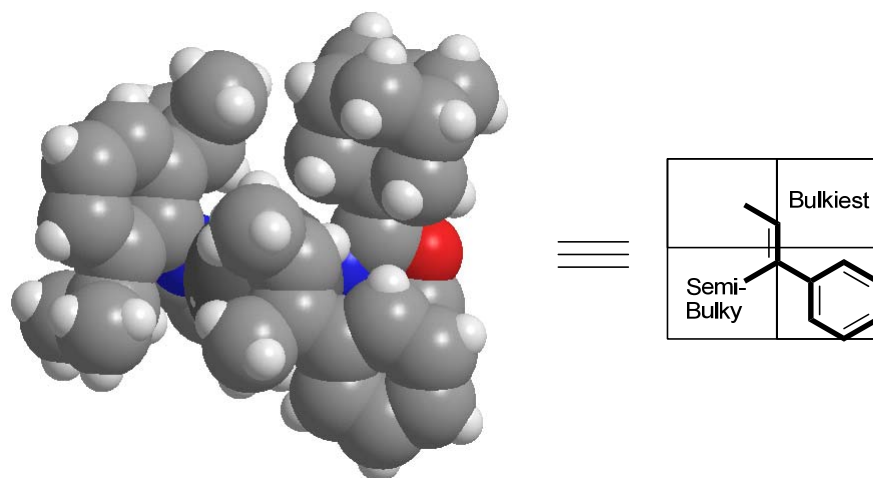
Scheme 2.2. Comparison of substrates. **a** Diaryl olefins are analogous to tiglic alcohol for stereoselectivity. **b** One possible alignment of tiglic ester to avoid steric interactions also explains the reversal in stereochemistry.
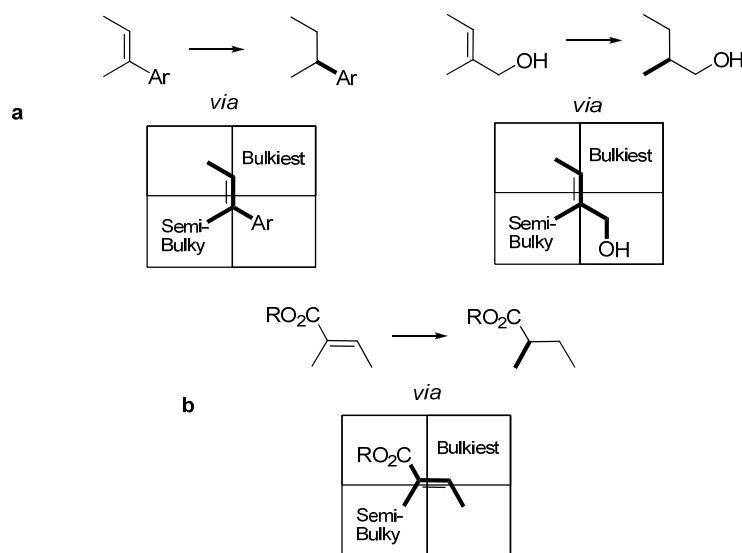
Computational studies were undertaken in order to find the exact nature of the stereofacial inversion.[45a,45b] After undertaking calculations on numerous transition states, the lowest energy of the various transition states had a carbonyl-metal coordination event occurring in tiglic esters that was not present in tiglic alcohol. The carbonyl binding likewise reacted through a different mechanism, where direct bonding in the C3 position to the metal was occurring before releasing the second hydride and giving the fully reduced ester. By contrast, non-coordinating tiglic alcohol reacts giving a C2 metalated species before finally releasing the second hydride and fully reducing the alkene. Schematically, the stereochemistry for simple olefins can be predicted using scheme 2.2.

2.2.2 Early Work on Dienes to Generate Multiple Stereocenters

The first diene studied in this system was methyl *E,E*-2,4-dimethyl-2,4-hexadienoate, made from a Wittig reaction with commercially available tiglic aldehyde and the stabilized phosphorous ylide. The skipped dimethyl systems looked particularly attractive as natural product synthons because their products, after hydrogenation, can produce synthons ubiquitous in nature in skipped polypropionate natural products.

As might be expected, the diastereoselectivity is modest, but the *ee* of the hydrogenation gives an exceptional improvement over the simpler tiglates, favoring the *syn* stereoisomer as the major product, unequivocally assigned from the known method using chiral auxiliaries developed by Meyer (Scheme 2.2).[4] Hydrogenation gives the minor diastereomer relative to that generated by Meyer's methodology, and complementing that method well (Scheme 2.3). The enhanced enantioselectivity and lower diastereoselectivity should be expected, however, due to chiral amplification, or Horeau's principle.[45e] Typically, chiral amplification is performed in a stepwise manner: thus chiral starting materials are allowed to undergo further asymmetric transformations later, and diastereomeric separation at this point is performed. Prochiral polyene substrates undergoing asymmetric hydrogenations are more aligned with Diels-Alder reactions with their potential to form multiple stereocenters simultaneously, and thus chiral amplification occurs simultaneously during the reaction, albeit at the cost of diastereoselectivity. As one may expect, asymmetric hydrogenation of the known alcohol *E,E*-2,4-dimethyl-2,4-hexadienol **2.3b**, a natural defense compound excreted from the daddy longlegs species *Leiobunum leiopenis*, gives even better *ee* than the ester **2.3a**, and the *anti* product as well.

Scheme 2.3. Stereoselectivity of two key dienes, and available stereoselectivity from Meyer's methodology.
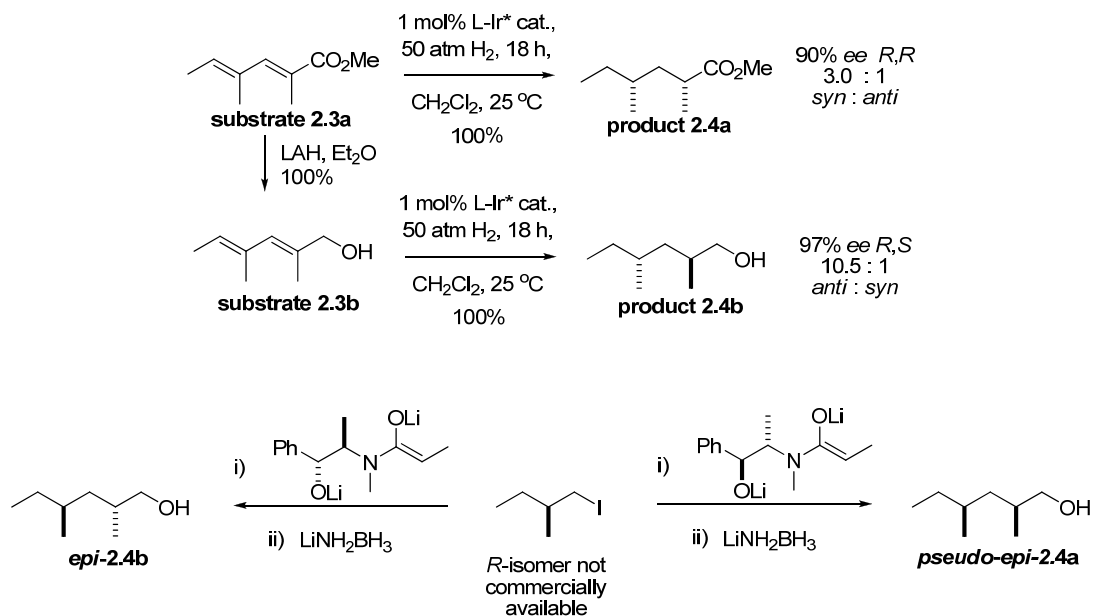
The *anti*-alcohol **2.4b** is a known component in the total synthesis of Atpenin B, an antibiotic compound produced from *Penicillium* sp. FO-125 (Figure 2.1).[46, 47] It consists of a penta-substituted pyridine with the chiral side chain generated from the mixture of 4 isomers of the alcohol. Atpenin B has only been generated as a mixture of diastereomers and enantiomers to our knowledge. The significant steps from addition of the pyridinal unit give 43% yield over 3 remaining steps.
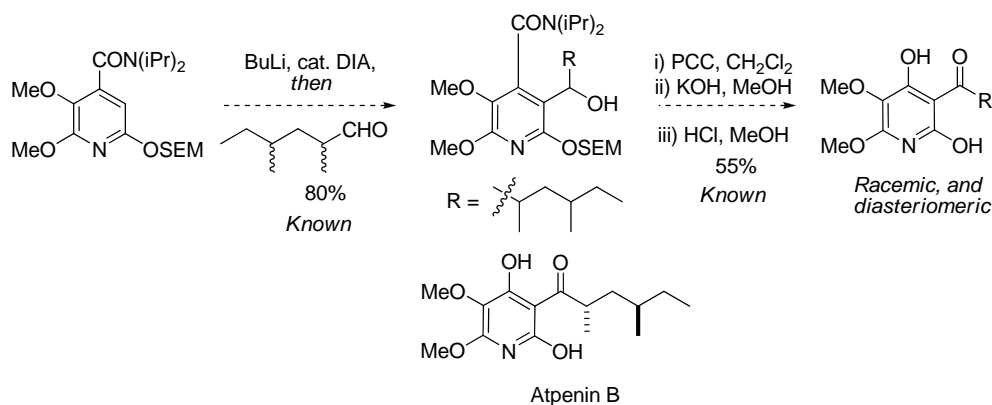
Figure 2.1. Formal synthesis of Atpenin B.

2.2.3 Evidence of a Change in the Substrate / Catalyst Binding of Two Related Dienes

The reversal in stereoselectivity intrigued us. We suspected that there was probably a change in the mechanism from the ester substrates to the alcohol, explaining the reversal of absolute stereoselectivity. There remained the question of whether or not the mechanism changes due to chelation (for example, with the free alcohol) or because of electronic effects (due to the electron withdrawing ester group). If the hydrogenation is completely catalyst driven, independent of the substrate either before or after one hydrogenation, then we would be able to predict the *ee* and diastereomeric ratio of each stereocenter by knowing the stereoselectivity from hydrogenation of each alkene individually, with the other stereocenter having a perfectly racemic center, *i.e. we can predict the statistical distribution of products based off of the individual stereoselectivity at each olefin.*

Although both racemic centers were not made, an approximation of one of the centers as being equivalent to the previously hydrogenated tiglic ester **1f** with respect to stereoselectivity gives a predicted *ee* very similar to that observed experimentally (diagram 2.2). Thus, it seems reasonable that the hydrogenation of functionalized dienyl esters such as **2.3a** occurs in a

stepwise manner, *i.e.* each alkene unit in a diene is hydrogenated as would an alkene in a monoene, with little to no dependence on previous stereocenters. The aliphatic substrates arising from asymmetric hydrogenation of these polyenes can have predictable stereochemistry at each chiral center. Interestingly, applying the same mathematical analysis to the dienyl alcohol **2.3b** does not predict the stereoselectivity at all, implying that this substrate may not be hydrogenated in a purely statistical manner, but rather a chelation effect or dependence on the initial chiral center may be occurring, causing internal manipulation of one stereocenter on the formation of another. Further analysis regarding the absolute configuration of the products formed is discussed in more detail below and reinforces this notion (Diagram 2.3).

Diagram 2.2. Statistical prediction of the **2.3a** hydrogenation products (**2.4a**). **a** Approximation to determine the untested monoene, and **b** hydrogenation of the known monoene.

A question that is important for the application of this methodology to different dienes needed to be addressed: which olefin along a polyene is hydrogenated first? This is important as the dienes become more complicated, it becomes more difficult to predict which stereocenters will be formed at each olefinic unit. If we consider the dienyl alcohol **2.3b**, then there are two possibilities for hydrogenation (Diagram 2.3). In the first case, it is assumed that the γ–δ olefin (farther from alcohol) is hydrogenated first, followed by the allylic olefin. Notice that when this is the case, the stereocenter, as shown in diagram 2.3, should give the *S* stereocenter at this

position, which is not the experimentally observed stereochemical outcome. If, however, the allylic olefin is hydrogenated first, as in the second case, then this creates a stereocenter which, if chelation to the catalyst occurs, could give a diastereomerically produced *re*-facial attack on the γ–δ olefin, which gives the experimentally observed outcome (Diagram 2.3). Thus, there is some evidence that the allylic olefin is hydrogenated first, followed by the γ–δ. This, along with the statistical analysis given above and the failure of products **2.4b** to be predicted by such treatment, strongly suggests that the dienyl alcohol **2.3b** is in fact hydrogenated in a stepwise manner, and that the alcohol moiety manipulates the second olefin hydrogenated after the allylic olefin is hydrogenated. Such arguments are not as persuasive for the corresponding ester **2.3a**, however, as little evidence for chelation to give the experimentally observed stereochemistry can be explained. In fact, if chelation was the deciding factor for the stereochemistry of the γ–δ olefin, then the opposite stereochemistry formed from the allylic olefin would suggest that the *anti* product would be more favorable, which is not experimentally observed. In short, the alcohol and ester olefins and dienes are not easily mechanistically characterized, although some rational for the observed stereochemistry through coordination has been suggested. Whether the non-coordinating statistical hydrogenation of polypropionates is occurring at the molecular level, or if this only models the observed stereochemistry coincidentally has yet to be proven. Regardless, the coordinating model has been able to predict the stereochemistry in multiple systems quite successfully.[45a,45c,45d]

Diagram 2.3. Two possibilities for the hydrogenation of the dienyl alcohol **2.3b**. Enantioselectivity in **2.4b** gives evidence that the allylic olefin is hydrogenated first.
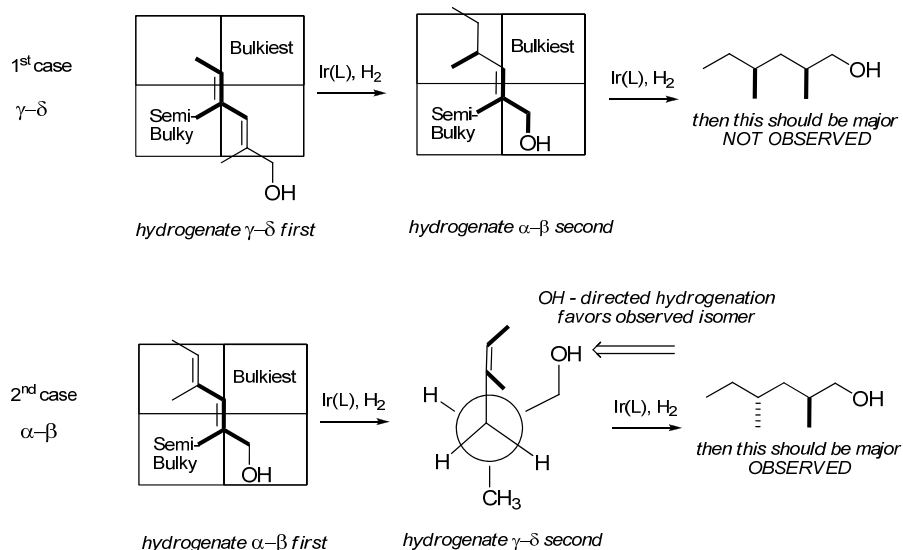
2.2.4 Synthesis of All 4 Isomers of 2,4-Dimethyl Hexane Dyads From a Single Enantiomer of Catalyst

Scheme 2.4. Synthesis of the last two diastereomers of the 2,4-dimethylhexanes.
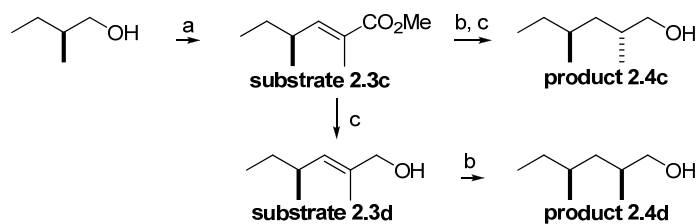
a) 5% TPAP, 2.1 eq. NMO, mol. sieves, *then* Ph$_3$PC(CH$_3$)CO$_2$Me;
b) 1% (1 M) Ir*, 50 atm H$_2$, CH$_2$Cl$_2$, 18 h; c) 3 eq. LAH, Et$_2$O

Given the predictable stereochemistry of diene hydrogenation products **2.3a** and **2.3b**, and the fact that depending on the oxidation state of the allylic carbon one can generate either stereochemical outcome, we sought to generate all possible isomers of the dimethyl aliphatic hexanol or hexanoates from a single isomer of catalyst. Two isomers, the *syn R,R* and *anti R,S* isomers, were already synthesized from the diene ester and diene alcohol, respectively, as described above. Likewise, a stepwise asymmetric hydrogenation of tiglic alcohol to generate *S-*

butanol followed by successive oxidation and a Wittig reaction could easily produce the synthon necessary for the *anti S,R*-product, and the *syn S,S*-product can be formed from the alcohol, reduced from the same synthon (Scheme 2.4). Fortunately, *S*-butanol is commercially available, so simply oxidizing this material followed by a Wittig reaction gives the necessary synthon and saves a step, but the principle of hydrogenating stepwise and following with homologation is still valid.[48]   Of all these synthons, the alcohol-containing synthons are formed in the greatest diastereomeric ratios and *ee*'s of the set (Table 2.2).

Table 2.2. Synthesis of all 4 Isomers of 2,4-Dimethylhexane Series from a Single Enantiomer of Catalyst.

entry	olefins	products	ee^{b} (%)	d.r.[b]
a		CO_2Me c,e	90	2.9:1.0
b		OH d,e	97	11:1.0
c		CO_2Me c	97	5.1:1.0
d		OH d	>98	9.6:1.0

[a]Conversion determined by NMR.   [b]Determined by chiral GC analysis.   [c]Absolute configuration determined by reducing to the alcohols with LAH and comparing by chiral GC analysis with the known alcohols.   [d]Absolute configuration determined by comparison with authentic samples via chiral GC analysis.   [e]Diene substrates required 12 h reaction times and 50 atm H_2 for complete conversion.

2.3 Applications to Total Synthesis

The ultimate test of many methodologies comes from the application of the developed techniques into the synthesis of natural products. Looking through the literature revealed a few substrates that were particularly attractive. Our attention was thus diverted from the general methodology developed above to the total Synthesis of two particularly interesting and challenging compounds with similar core structures: lardolure, an aggregation pheromone excreted by the acarid mite *Lardoglyphus konoi*, and the preen gland wax extract of the domestic goose *Anser anser* (Scheme 2.6).[49-56]   A review of the literature had shown a few totally

syntheses of these products (although one recent synthesis using fully catalytic methodology to synthesis the Preen Wax Gland has recently been submitted).[16,57-62] At this time we are unaware of any synthesis that uses fully catalytic approaches to the synthesis of the four stereocenters of Lardolure; although several total syntheses exist already, none are fully catalytic that generate all four stereocenters. A significant improvement over the existing approaches would be the total synthesis using only catalytic methodologies to generate the requisite stereocenters. The two natural products could easily be produced from each other from a common intermediate: the linear compound containing three stereocenters and containing an ester moiety in the α position, thus the synthesis of this compound was our highest priority.
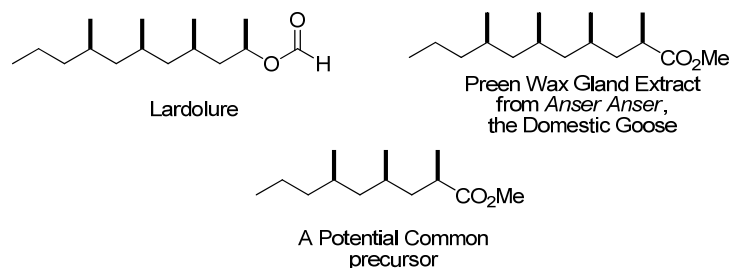

Figure 2.2. Two attractive targets and a common intermediate for total synthesis.

2.3.1 Generation of Multiple Stereocenters with One Hydrogenation: First Generation Aapproach

A quick look at the requisite stereochemistry of Lardolure might give the impression that perhaps all four stereocenters could be formed in a single hydrogenation step. Although the polyene backbone has the potential for such transformations, prochiral enol ether substrates have not been explored yet, and thus this route was not attempted. Our first and perhaps most elegant route to the common polypropionate intermediate (important to both Lardolure and the preen gland extract) involved synthesis of the triene using successive Wittig reactions followed by reduction, reoxidation and further homologation with another Wittig reaction (Scheme 2.5). The methodology, for the most part, had been developed already during the synthesis of the four isomers in the 2,4-dimethyl hexanol series. Thus the *E* triene **2.8** was synthesized in six steps in an overall yield of 20%, and forming *en route* another daddy longlegs defensive excretion, *E,E*-2,4-dimethylhepta-2,4-dien-1-ol, also isolated from *Leiobunum leiopenis*. Successive asymmetric hydrogenation of this species gave complete conversion to alkyl products, but only

poor diastereoselectivity, with all four diastereomers of **2.9** generated in a 2.0 : 1.5 : 1.2 : 1 ratio, as determined from GC analysis of the racemic mixture, although the *ee* of the major diastereomer was greater than 96%. Attempts to separate the diastereomers by column chromatography were in vain, and this route was abandoned for a less aggressive approach that had more precedent in the literature, namely hydrogenation of dienes followed by a single diastereomeric separation, then iterative homologations, hydrogenations, and further diastereomeric separation. Absolute configuration of the major product was not determined in this case, as the mixture of isomers was inseparable regardless.

**Scheme 2.5.** Generation 1 synthesis of an important intermediate in both targets.
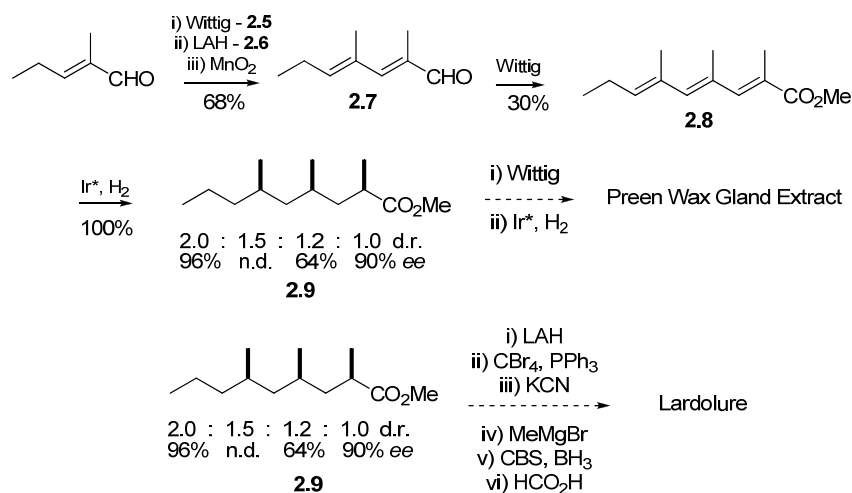
2.3.2 Generation of Multiple Stereocenters with One Hydrogenation: Second Generation Approach

The second approach to Lardolure involved the simpler diene substrate **2.7** generated en route to the triene shown above. A single cycle of Wittig-type homologation gave the requisite *E*-diene in 72% isolated yield (Scheme 2.6a). There was a precedent for the separation of the *syn/anti* diastereomers from Negishi, who reported the isolation of the two diastereomers of the resulting alcohol using simple column chromatography from a ratio of 7:1 *syn:anti* to greater than 40:1 in a single chromatographic operation.[8] This encouraged us to make the heptadienyl ester from the commercially available pentenal in one Wittig step on large scale. Asymmetric hydrogenation of the heptadiene methyl ester revealed selectivity similar to that observed before for the hexadiene substrate, including a similar 2.5:1 diastereomeric ratio when lower catalyst

loading was attempted. Every attempt to separate these two isomers from each other after reduction to the alcohol gave only mild enrichment of the major isomer; indeed, even attempting the separation on a fully automated MPLC instrument, removing all human error from the possibilities, gave only a mild 4:1 *syn:anti* ratio in 67% recovered yield for both diastereomers, identical recovered yield to what has been reported from Negishi.

Scheme 2.6. a) Generation 2 approach to Lardolure and b) Potential formation of the preen wax gland extract.
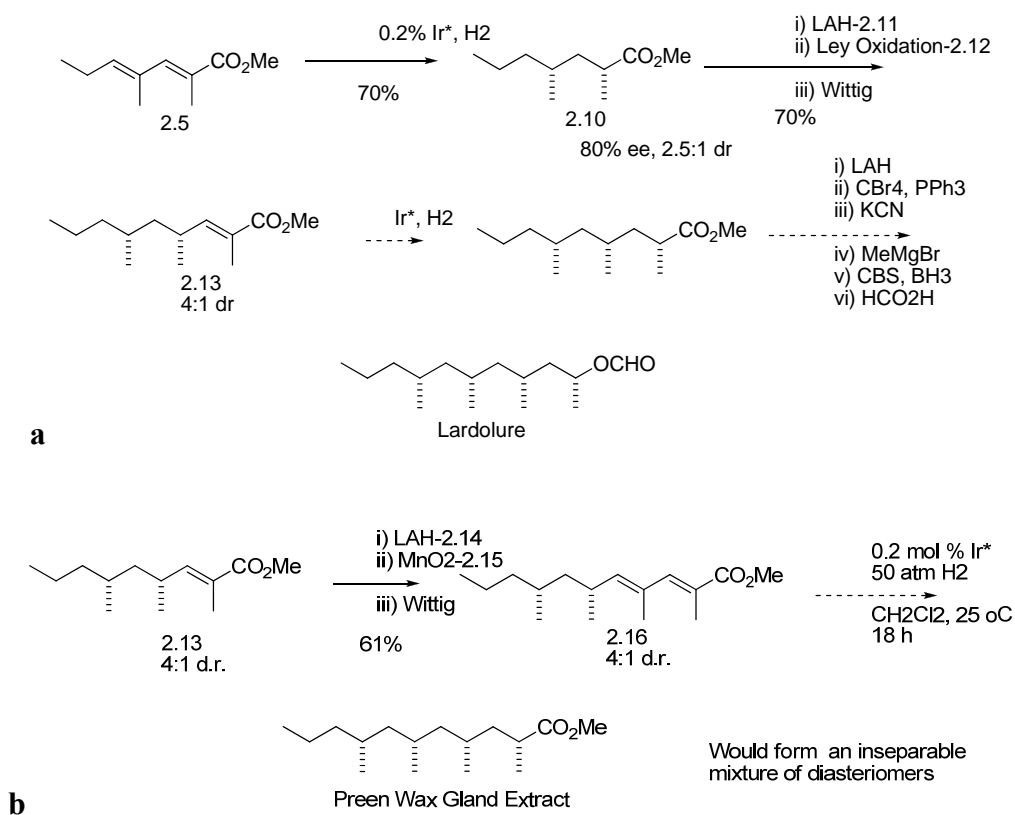
Despite the disappointment in the lower diastereoselectivity, the synthesis was continued further in hopes of the possibility of separation of the diastereomers at a later stage. Thus, the 4 : 1 diastereomeric mixture of alcohols was oxidized using TPAP / N-morpholine-N-oxide and the aldehydes reacted in a successive Wittig reaction, and this ester homologated as described above, giving a 43% isolated yield from the alcohol **2.14**, and 31% overall for 8 steps (Scheme 2.6b). Unfortunately, at no point during the last few steps was any separation by column chromatography possible, marking another failed synthesis at the preen wax gland extract. The

next asymmetric hydrogenation was not performed, as the resulting diastereomers would not be separable by any conventional means.

2.3.3   Matching Substrate and Catalyst for Optimum Selectivity: Generation 3 Approach

Failing to generate the desired all-*syn* isomers from the unconventional, all-catalytic means, we started to favor routes in which the substrates and products would be more conventional, and thus would have more precedent in isolation, separation, and characterization.   Starting the synthesis from the opposite, oxygen-containing end of the molecule could give rise to some allylic strain that would give favorable facial selectivity from both the catalyst and match with the substrate to generate very high stereoselectivity.   Thus, *R*-methyl lactate was homologated after O-protection using the now well-studied Wittig method above (Scheme 2.7).   Asymmetric hydrogenation of the protected allylic silyl ether did not give significantly high *ee*'s, but hydrogenation after removal of the silyl group gave essentially a single enantiomer by GC, and the expected allylic alcohol cyclized to generate the 5-membererd lactone **2.22**, itself a natural product extract from the fungi *Asteromyces cruciatus*.[63]   Reduction of the lactone with DIBAL generated the lactol, which was directly reacted in a Wittig reaction to homologate one more time to form **2.24**.   Alas, the *E/Z* selectivity of this Wittig reaction was less than 100%, thus the linear route to generate Lardolure was again abandoned for another route.

Scheme 2.7. Generation 3 approach to targets – linear, stepwise hydrogenations.
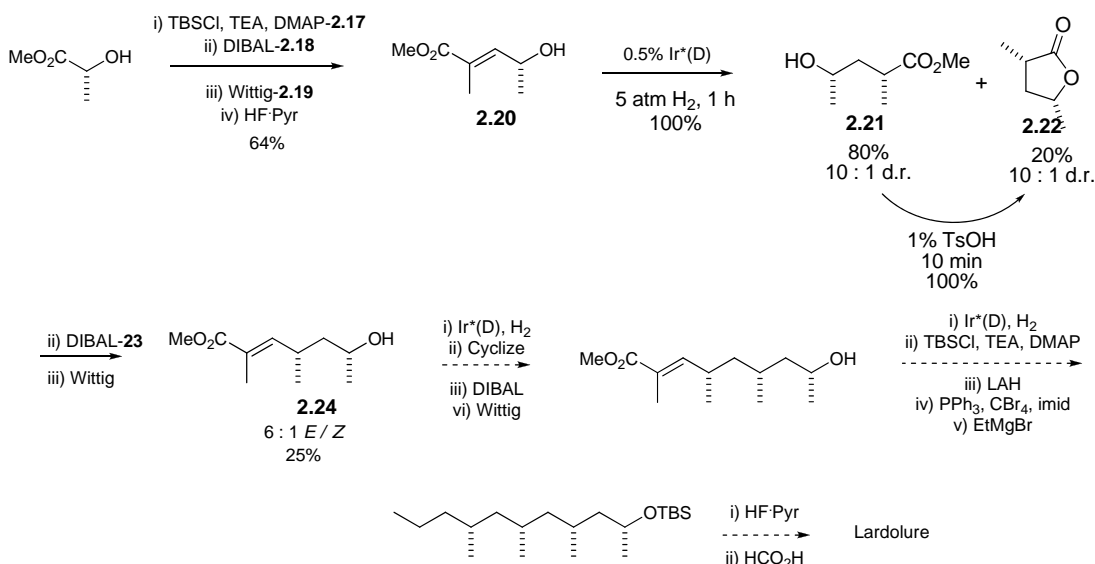
2.3.4   Matching Substrate and Catalyst for Optimum Selectivity: Generation 4 Approach

The high diastereoselectivity of the lactone, generated as above, interested us.   This compound, due to its purity, was a particularly attractive intermediate.   One can envision using this material, after elaboration, in a reaction similar to dimerization, generating all four stereoisomers from a single hydrogenation step.   There is some literature precedent for the ring opening and selective O-protection of 5-membered lactones as well, giving us a linear halide that can either be used as a nucleophile, or further elaborated into the alkyl portion, thus acting as an electrophile, and be dimerized to generate all four stereocenters in a final step (Scheme 2.8).

Scheme 2.8. Generation 4 approach to Lardolure – homo coupling of a key unit.
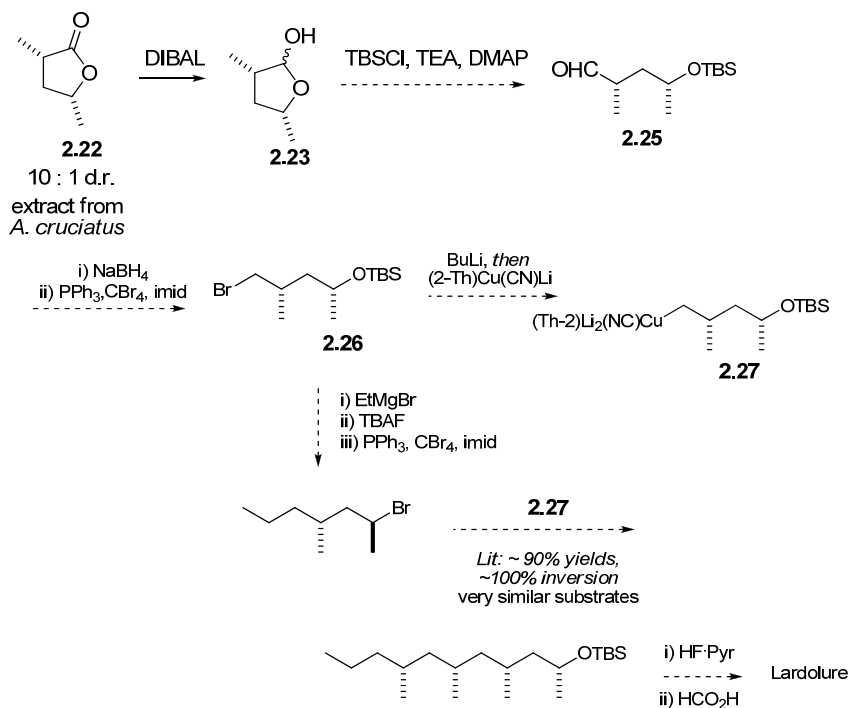
Some of our studies were focused on the optimization of this last route to generate Lardolure. Thus, reducing the number of isolation steps, most of which were column chromatography in initial runs, was a major priority, second of course to yield and stereoselectivity (Scheme 2.9). DIBAL reduction, a key transformation in several steps in the synthesis, has been optimized such that one only need wash a reaction mixture after it is done with an aqueous solution of sodium potassium tartrate, and separate the layers after a few hours, leaving a dichloromethane solution of products.   Likewise, the one step deprotection of the *tert*-butyldimethylsilyl ether without

isolating the earlier α,β-unsaturated ester both decreases the chromatography involved and helps improve the polarity of the reaction mixture, improving the resulting chromatography conditions. Addition of a catalytic amount of acid after hydrogenation gives a quantitative conversion to the lactone product, a natural product extract from the fungi *A. cruciatus*, and subsequent one-pot DIBAL reduction gives the lactol, which in turn can be ring-opened and protected without isolation as well. It is likely that subsequent reduction of the aldehyde could also be performed in a stepwise manner as well, although fewer steps could be telescoped in a one-pot fashion after that.

Scheme 2.9. Optimization studies to reduce isolation steps.
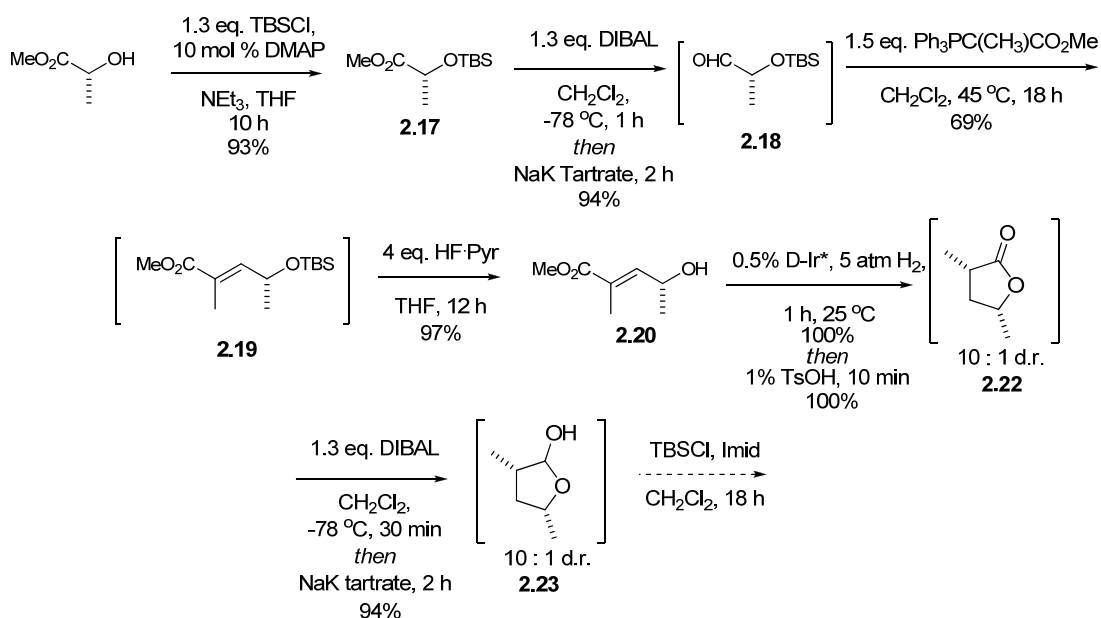
All that remains in the total synthesis of lardolure is the reduction of the aldehyde, halogenation of the resulting alcohol and Grignard reaction with the subsequent halide. The protected silyl ether needs to be deprotected and halogenated in an Appel reaction, *i.e.* halogenation of an alcohol in the presence of triphenylphosphine and carbon tetrabromide, to invert the stereocenter, and the resulting halide needs to be coupled with the higher order cuprate of an earlier derivative. The one-pot deprotection and esterification of the resulting compound could give lardolure in good yield and stereoselectivity.

2.4 Summary

In summation, a new route to 1,3-reduced polypropionates using asymmetric hydrogenation catalysis has been developed. Although the stereofacial selectivity is not as good as in aryl-substituted prochiral olefins, careful consideration of substrate can give higher selectivities through chiral amplification (Horeau's principle). Although the synthesis of the natural product lardolure could be obtained in only a few steps, the novel generation of multiple simultaneous stereocenters failed, as the diastereomeric mixtures could not be separated by conventional means. Catalysts which are more active towards prochiral olefins but with similar stereochemical features could possibly produce 1,3-reduced polypropionates with higher selectivity under milder conditions.

CHAPTER III

SYNTHESIS AND CHARACTERIZATION OF ELECTRONICALLY TUNABLE 1,3,4,5-TETRAARYL *N*-HETEROCYCLIC CARBENE LIGANDS

3.1 Introduction

The recent popularity of *N*-heterocyclic carbenes (NHCs) stems primarily from their utility as ancillary ligands (*e.g.*, phosphine analogues) in organometallic complexes and as metal-free agents for organocatalysis.[86] Hundreds of free and metal-coordinated N-heterocyclic imidazolylidene carbenes have been reported, but 4,5-diaryl substituted heterocyclic imidazolylidene carbenes are relatively rare. One example is that reported by Arduengo, *et al.*, who synthesized the prototypical 1,3,4,5-tetraphenylimidazol-2-ylidene from 1,3,4,5-tetraphenylimidazol-2-thione.[87] Although some insights into the impact of 4,5-substitutents have been reported,[88] improved synthetic methods for such carbenes are necessary for a more comprehensive understanding of the electronic influence these compounds have on the metal. Likewise, although the Burgess catalyst derives its enantioselectivity from the 1,3-substituted positions of the carbene, the 4,5-posistions are relatively open for exploitation. The limits of selectivity found in deoxopolypropionates might be overcome with catalysts more electronically aligned with these substrates.

The Miller group first demonstrated application of the intramolecular cyanide-catalyzed aldimine coupling reaction as a general route for making heterocycles.[89] Here we report the scope and generality of an intermolecular aldimine coupling reaction followed by cyclization with formaldehyde for preparing a wide vareity of 4,5-diaryl substituted NHCs. Somewhat related to our approach, Kison and Opatz have recently reported the synthesis of highly substituted unsymmetrical 1,2-diamines and 1,2-diimines via cross-coupling of α-aminonitriles with N-sulfonylimines—leading to imidazolium salts and imidazolylidenes.[90]

3.2 Synthesis of Tetraaryl NHCs

Although the cyanide-catalyzed aldimine coupling reaction of aromatic Schiff bases was first studied in 1928,[91] few reports since then have applied this reaction toward further synthesis. It is well known that the cognate cyanide-catalyzed benzoin condensation is quite sensitive to the aromatic aldehyde substrates and further oxidation of benzoin to make α-diketone compounds requires relatively harsh conditions.[89a,92] Furthermore, aldimine coupling reactions may be superior for preparing α-diketimine substrates because the corresponding α-diketones generally condense with the second amine equivalent only under rather stringent reaction conditions.[93]

Sixteen aromatic aldimines with varying C-aryl and N-aryl substitutents were prepared and subjected to cyanide-catalyzed C-C coupling conditions (Table 3.1, **3.1a** – **3.1p**). The aldimine substrates were combined with 20 mol% NaCN catalyst in dry DMF and the conversion to intermediate ene-diamines was monitored by ^{1}H NMR spectroscopy. Following subsequent oxidation with 1,4-dibenzoquinone, most substrates afforded the targeted diketimines (**3.2a** – **3.2h**, **3.2k**, **3.2l**, **3.2n**); however, compound **3.1i** and **3.1m** with nitro groups only partially reacted with NaCN to give unidentified products. Although reasonable yields can be obtained from substrates with the electron-donating methoxy group (**1e** and **1h**), the presence of the more electron-donating dimethylamino group (**1j**) renders an extremely slow reaction. This is consistent with diminished stability of the benzyl anion, generally thought to be the nucleophilic intermediate generated following cyanide addition to the aldimine and subsequent tautomerization.[94] Likewise, phenolic substrates such as **3.1o** disable the reaction, even with 1.2 equivalents of NaCN loading, suggesting that a simple loss of HCN is not occuring due to reaction with the acidic phenolic proton. The reaction also gives no conversion when the *N*-sterically hindered **3.1p** is used, which likely is due to the carbanion not being able to react nucleophilicly with a second equivalent of the starting imine.

Table 3.1. Cyanide-Catalyzed Aldimine Coupling Reactions to Prepare Symmetrical α-Diketimines[a].

(a) 20 mol % NaCN, DMF, 25 - 80 °C
(b) 1,4-benzoquinone, CH$_2$Cl$_2$, 25 °C
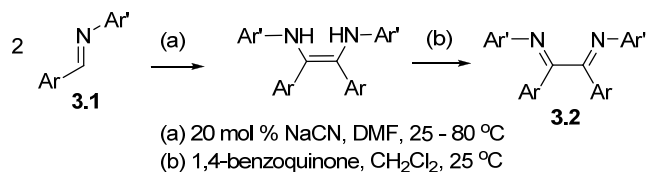
Entry	Ar	Ar'	T (°C)	Time (H)	Yield (%)[b]
3.1a	Ph	Ph	25	24	54
3.1b	4-MeC$_6$H$_4$	Ph	25	40	78
3.1c	4-FC$_6$H$_4$	Ph	25	20	67
3.1d	4-CF$_3$C$_6$H$_4$	Ph	25	20	65
3.1e	4-MeOC$_6$H$_4$	Ph	25	24	57
3.1f	Ph	4-FC$_6$H$_4$	25	22	51
3.1g	4-MeC$_6$H$_4$	4-MeC$_6$H$_4$	80	36	40
3.1h	Ph	4-MeOC$_6$H$_4$	80	24	28
3.1i	4-NO$_2$C$_6$H$_4$	Ph	25	24	-[c]
3.1j	4-NMe$_2$C$_6$H$_4$	Ph	80	120	-[d]
3.1k	4-CF$_3$C$_6$H$_4$	4-MeC$_6$H$_4$	25	18	31
3.1l	4-CF$_3$C$_6$H$_4$	4-MeOC$_6$H$_4$	25	24	55
3.1m	4-MeC$_6$H$_4$	4-NO$_2$C$_6$H$_4$	80	48	-[c]
3.1n	1-naphthyl	Ph	25	24	9[e]
3.1o	2-OH,3-MeOC$_6$H$_3$	4-MeC$_6$H$_4$	25	24	-[d]
3.1p	Ph	2,4,6-Me$_3$C$_6$H$_2$	25	24	0

[a]The reaction was conducted under N$_2$; the crude coupling product was isolated first then oxidized with 1,4-benzoquinone (see experimental). [b]Isolated yield. [c]Imine starting materials were unreactive; some unidentified products were produced. [d]Trace amount of reaction (< 5%) observed by ^{1}H NMR; no isolation was attempted. [e]At 30% conversion, only 80% pure, and repeated crystallizations could not isolate the product from the starting material.

Although Becker discussed the effect of reaction conditions on the aldimine coupling reaction in 1970,[94b] our studies allow some further understanding. NMR analysis provides superior evidence of reactivity and product formation compared to fluorescence data obtained previously. Our results are consistent with Becker's conclusion that DMF is a good solvent for aldimine coupling. Our previous study on the ring-closing of dialdimines to form heterocycles showed

that *intramolecular* aldimine coupling also performs well in MeOH or the biphasic CH_2Cl_2/H_2O system using Bu_4NI as a phase transfer agent. Ethanol is a common solvent for the benzoin reaction; however, no *bimolecular* aldimine coupling could be achieved using NaCN in alcohols or in the biphasic $CH_2Cl_2/H_2O/Bu_4NI$ system. For some substrates, the reaction was sensitive to air, water (including wet DMF not previously dried over $MgSO_4$), or even residual MeOH— lowering the yield or altogether preventing reactivity.

While the initial ene-diamine coupling products were claimed by Becker to be easily oxidized in air,[94b] **3.1a** in DMF with 20% NaCN under dry air—employing a variety of temperature and solvent conditions—for 24 hrs resulted in, at most, a 9:1 mixture of ene-diamine to α-diimine. 1,4-Benzoquinone was found to be a rather competent oxidant for converting the ene-diamines to α-diimines; for example, one equivalent (relative to **3.1a**) provided the diimine **3.2a** within minutes (monitored by NMR), while simply stirring the reaction open to air afforded **3.2a** in only 50% yield after 24 hours. 1,4-Benzoquinone failed as an in-situ oxidant to convert the ene-diamine to diimine—apparently because of unwanted reaction with sodium cyanide. But simple dilution of the reaction mixture with dichloromethane followed by extraction with water is sufficient to remove DMF and NaCN and allows one to skip isolation of the ene-diamine intermediate.

As imidazolium salts are important precursors for NHC synthesis, several different procedures have been reported for converting α-diimines to imidazolium salts. Arduengo originally reported a strategy for cyclizing α-diimines with formaldehyde equivalents which has been fruitful in generating a variety of imidazolium salts.[95] From the diimines **3.2a** – **3.2h**, we modified Noels' procedure[96] (based on Arduengo's strategy) to prepare imidazolium chlorides by reaction with paraformaldehyde and anhydrous HCl; our yields, albeit low, are similar to those previously reported via this method (Table 3.2). The imidazolium salts **3.3a** – **3.3h** have been synthesized, purified and fully characterized by NMR, mass spectrometry and, in the case of **3.3d**, single-crystal X-ray analysis (see Appendix 3).

Table 3.2. Formation of Tetraarylimidazolium Salts and Tetraaryl N-Heterocyclic Silver Carbenes.

Ar'—N   N—Ar'   (a)   Ar'—N$^+$ N—Ar'   (b)   Cl—Ag—C, Ar'—N   N—Ar'

Ar   Ar   Cl$^-$ Ar   Ar   Ar   Ar

3.2   **3.3**   **3.4**

(a) (CH$_2$O)$_n$, HCl·dioxane, THF, 40 °C
(b) Ag$_2$O, CH$_2$Cl$_2$
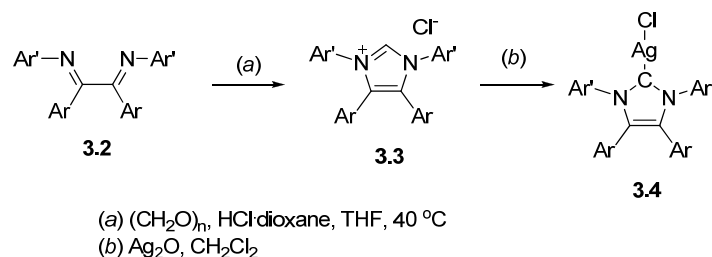
Entry	3.2→3.3 Time (h)	Yield 3.3 (%)[a]	δ 1H 3.3 CH[b]	Yield 3.4 (%)[a]	3.4 Ag-C (Å)[c]
a	12	22	10.81	80	2.079
b	18	33	10.85	-	-
c	18	12	9.85	75	2.087
d	18	16	9.78	-	-
e	12	32	10.58	55	2.051
f	18	33	10.88	88	2.070
g	36	29	10.63	-	-
h	24	31	10.58	80	2.079

[a]Isolated yields. [b]1H NMR shift of the imidazolium ring proton. [c]Determined by X-ray crystallography

NHCs can be directly prepared by deprotonation of the imidazolium chloride salt with KO^{t}Bu using the typical method reported in the literature.[95,96,97] Free carbene compounds from **3.3b** and **3.3e** have thus been prepared and characterized by ^{1}H and ^{13}C NMR spectroscopy. The carbene carbons can be verified with peaks resonating around 220 ppm in the ^{13}C NMR spectra.

Alternatively, the imidazolium chloride salts can be directly transformed into the silver(I) chloride carbene species by refluxing with silver oxide in methylene chloride. Silver carbene complexes **3.4a**, **3.4c**, **3.4e**, **3.4f**, and **3.4h** were targeted for synthesis because of their electronically diverse substitutents. These complexes were prepared and isolated as colorless needles which are neither air nor moisture sensitive. X-ray crystallography confirmed the anticpated structures and these are illustrated in Figure 3.1.
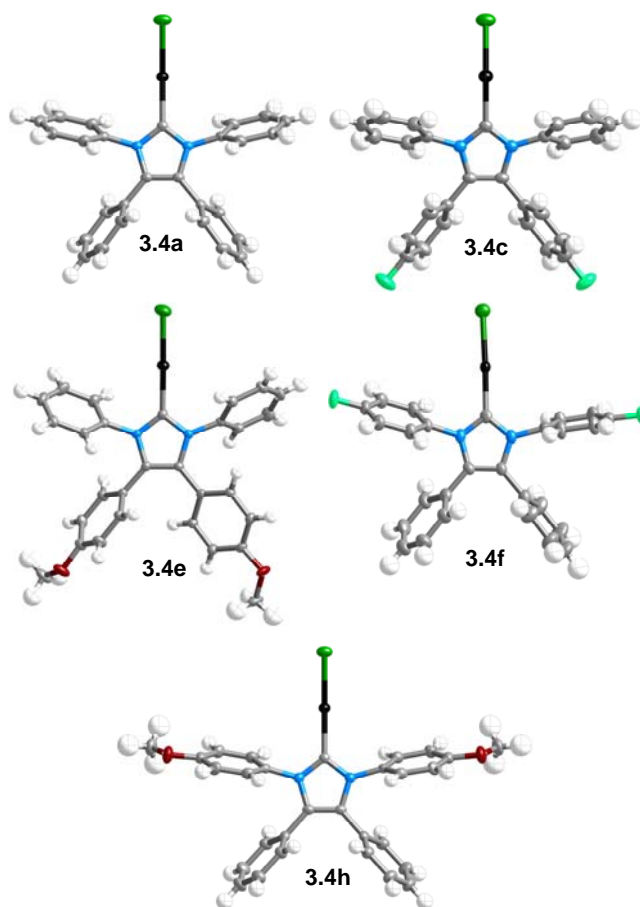
Figure 3.1. Silver carbene complexes **3.4a**, **3.4c**, **3.4e**, **3.4f**, and **3.4h** with 50% probability ellipsoids.

3.3 Electronic Characteristics of Tetraaryl NHCs

Despite the formation and easy characterization of the silver carbene structures, they are not overly useful inherently,[98] so our attention shifted to making complexes that were both more interesting, and for which more comparative data to similar complexes in the literature was already established.

Although numerous studies have been produced analyzing the effect of the NHC 1,3-positions, usually related to steric environment around the metal, relatively little work has been done to study the effect of substitution in the 4,5-positions.[88,99,100] Notable exceptions to this include the works of several groups, given in Figure 3.2. Work by Crabtree, Nolan, and many others all indicate that 4,5-substitution has significant impact on the electronic nature of the metal-ligand

bonding, and little contribution to the steric environment around the metal.[88,100] The possibility of being able to fine-tune the electronic aspects of the NHC with minimal change of the steric environment of the metal is attractive in general to NHC catalyst research.
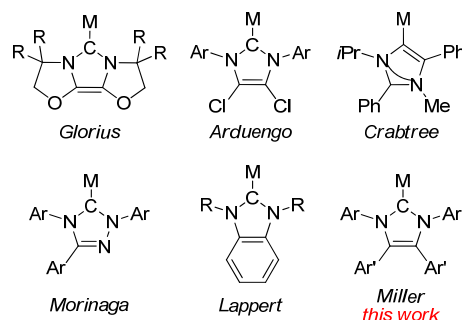
Figure 3.2. Common examples of non-hydrogen 4,5-substitutions.

3.4 Studies of the Electronic Character of 1,3,4,5-Tetraaryl NHC Ligands

Tolman established a system using CO stretching frequencies for $Ni(CO)_3PR_3$ systems to determine the electronic nature the phophine ligands have on the metal-CO bond, as well as a steric parameter associated with the cone angle that the phosphine ligands generated upon bonding.[101] The data also reflected trends in bond-dissociation energies, studied from both NMR and calorimetric data collected on the systems. This was further extended to iridium-based systems by Crabtree and Nolan recently, who found that when plotting CO stretching on the nickel system against the average of the two CO stretching frequencies for the similar iridium system, a straight line resulted, indicating that the iridium CO system was also a suitable method for analyzing electronic character.[100a,b] The main advantage to this system is that the highly toxic $Ni(CO)_4$ precursor to generate the nickel NHC complexes can be avoided, and the iridium precursors are generated much more reliably.[88]

3.4.1 Experimental and Results of Electronic Studies

Having found a reasonable protocol for studying the comparative electronic effects, and methodology to generate several electronically varied NHCs, we then generated the five iridium analogues of the silver complexes already prepared. The strategy used known procedures for the formation of the NHC iridium complexes, and established protocols for the measurement of their electronic variances.[88,102] The already determined X-ray diffraction for the silver chloride NHC

complexes was used for comparative analysis of bond lengths and angles. For the purposes of the following discussions, we have assumed that there are no significant differences between the steric environment around the metal between the five all-aryl analogues studied with respect to a single ligand and metal.

3.4.2 Synthesis of NHC[Ir(COD)X] Complexes

Scheme 3.1. Synthesis of five NHC-Ir(COD)Cl complexes.

Entry	Ar =	Ar' =	yield =
a	Ph	phenyl	68%
c	4-FC$_6$H$_4$	phenyl	88%
e	4-MeOC$_6$H$_4$	phenyl	94%
f	phenyl	4-FC$_6$H$_4$	100%
h	phenyl	4-MeOC6H4	93%
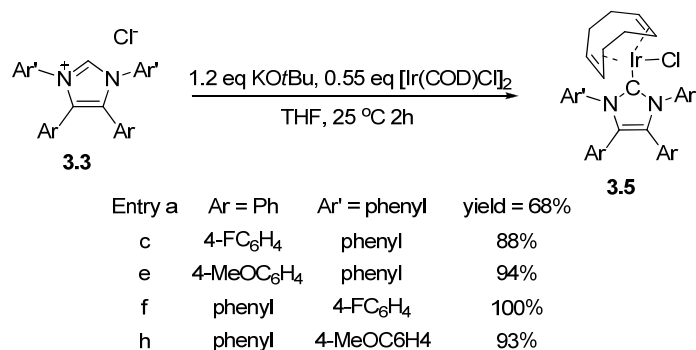
Initial attempts for the transmetalation of the silver NHC in the presence of [Ir(COD)Cl]$_2$ were not successful in forming the desired complexes; however the desired complexes were readily formed from deprotonation of the imidazolium salts **3.3** in the presence of slight excess [Ir(COD)Cl]$_2$ under nitrogen in THF (Scheme 3.1). Workup involved dilution of the reaction mixture in CH$_2$Cl$_2$, washing with water three times, drying over MgSO$_4$, and removal of solvent. The complexes were formed within two hours with no chromatographic separations and in very high yields as dark ocher flakes.

^{1}H, ^{13}C, and ^{19}F (when appropriate) NMR studies confirmed the presence of carbene, single pure isomers, and the inequivalence of the 1,5-cyclooctadiene protons, commonly found in these structures.[88,102] HRMS also confirmed the presence of a single NHC per iridium and the absolute mass of the structures.

3.4.3 Synthesis of NHC[Ir(CO)₂Cl] Complexes

Scheme 3.2. Synthesis of NHC[Ir(CO)₂Cl] complexes.

Entry a	Ar = Ph	Ar' = phenyl
c	4-FC₆H₄	phenyl
e	anisyl	phenyl
f	phenyl	4-FC₆H₄
h	phenyl	anisyl
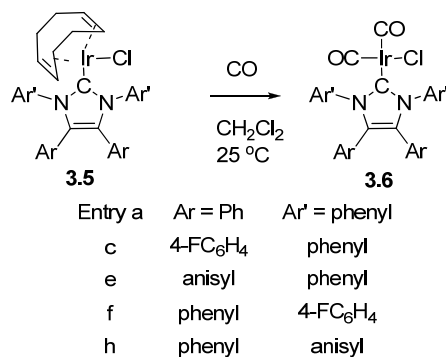
The procedure also used by both Crabtree and Nolan was used to generate the NHC-Ir(CO)₂Cl structures (Scheme 3.2).[88] NHC[Ir(COD)Cl] was dissolved in CH₂Cl₂ and carbon monoxide was bubbled through the solution for 3 seconds. The short reaction time is critical: impurities form in as little time as 10 seconds. The initial dark yellow solution rapidly became a much lighter yellow solution. The CH₂Cl₂ was removed under reduced pressure, and the complexes analyzed by ^{1}H, ^{13}C, and ^{19}F NMR, when appropriate. Multiple methods to remove the cyclooctadiene residues were unsuccessful, but because this would not affect the CO stretching frequencies, the product was taken for IR analysis without further purification.

3.4.4 IR Spectroscopy

The symmetric and asymmetric CO stretching for the iridium based system was used for comparative results against other NHC-Ir(CO)₂Cl systems in the literature. In all five cases the CO stretches were unambiguously assigned. Crabtree suggested that the two CO stretch values for iridium systems be averaged to get a single number for better comparison to the more well-established nickel systems.[88] These values, as well as those of 33 other NHC complexes, are given in Table 3.3, and the full range of these is given in Figure 3.3.
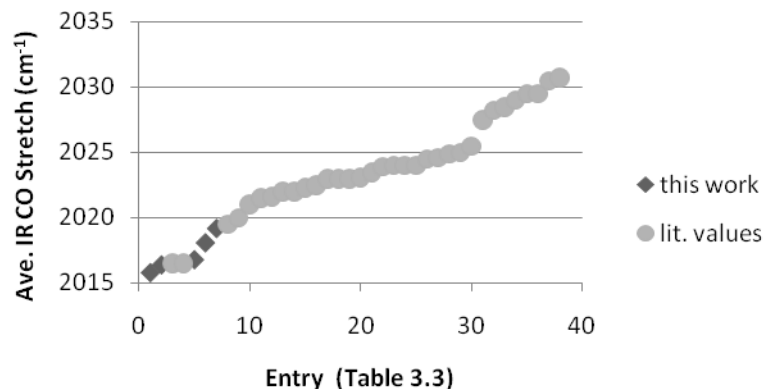
Figure 3.3. Range of IR stretches of common NHC-Ir(CO)$_2$Cl complexes and those reported here (entry 1 omitted for resolution).

Table 3.3. Cumulative List of All the Stretching Frequencies of NHC-Ir(CO)$_2$Cl Complexes Reported in the Literature.
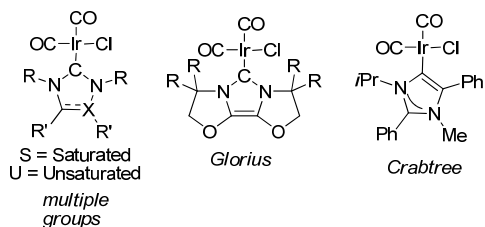
entry	R	R'	X	4,5-saturation	ave. CO stretch[a]	ref.
1	special[b]	special	C	U	2003	103
2	4-MeOC$_6$H$_4$	phenyl	C	U	2015.8	*this work*
3	phenyl	phenyl	C	U	2016.4	*this work*
4	methyl	phenyl	C	U	2016.5	103
5	isopropyl, methyl[c]	phenyl	C	U	2016.5	103
6	phenyl	4-MeOC$_6$H$_4$	C	U	2016.8	*this work*
7	phenyl	4-FC$_6$H$_4$	C	U	2018.1	*this work*
8	4-FC$_6$H$_4$	phenyl	C	U	2019.2	*this work*
9	4-CH$_3$C$_6$H$_4$	H	C	U	2019.5	100a
10	butyl	H	C	U	2020	100a
11	4-NEt$_2$-2,6-dimethylphenyl	H	C	U	2021	104
12	isopropyl, phenyl[c]	H	C	U	2021.5	103
13	1-adamantyl	H	C	U	2021.6	100c
14	C-alkyl[d]	O-Alkyl	C	U	2022	106
15	4-NEt$_2$-2,6-dimethylphenyl	H	C	S	2022	104
16	*tert*-butyl	H	C	U	2022.3	100c
17	C-alkyl[d]	O-Alkyl	C	U	2022.5	105
18	cyclohexyl	H	C	U	2023	106
19	cyclohexyl	H	C	U	2023	100c
20	2,4,6-(CH$_3$)$_3$C$_6$H$_4$	H	C	U	2023	104
21	2,4,6-(CH$_3$)$_3$C$_6$H$_4$	H	C	U	2023.1	100c

Table 3.3
Continued

entry	R	R'	X	4,5-saturation	ave. CO stretch[a]	ref.
22	C-alkyl[d]	O-Alkyl	C	U	2023.5	105
23	2,6-diisopropylphenyl	H	C	U	2023.9	100c
24	isopropyl	H	C	U	2024	106
25	c-alkyl[d]	O-Alkyl	C	U	2024	105
26	2,6-dimethylphenyl	H	C	U	2024	104
27	2,4,6-$(CH_3)_3C_6H_4$	H	C	S	2024.5	104
28	2,4,6-$(CH_3)_3C_6H_4$	H	C	S	2024.6	100c
29	2,6-diisopropylphenyl	H	C	S	2024.9	100c
30	2,6-dimethylphenyl	H	C	S	2025	104
31	4-bromo-2,6-dimethylphenyl	H	C	U	2025.5	104
32	4-bromo-2,6-dimethylphenyl	H	C	S	2027.5	104
33	2,6-diisopropylphenyl	Cl	C	U	2028.25	105
34	S(O)Aryl[e]	H	C	U	2028.5	104
35	S(O)Aryl[e]	H	C	S	2029	104
36	SO_2Aryl[e]	H	C	U	2029.5	104
37	Non-NHC[f]	-	-	-	2029.5	Non-NHC[f]
38	SO_2Aryl[e]	H	N	S	2030.5	104

[a]Average CO stretching frequency from both symmetric and asymmetric CO stretches, in cm^{-1}, listed by increasing value; values labeled *this work* are the average of four measurements taken over several days. [b]This is the non-traditional iridium complex shown above the Table from Crabtree. [c]This compound has two different groups (listed) in the 1,3-positions. [d]These tricyclic carbene iridium complexes from Glorius have cyclic systems interconnecting the R groups of various sizes or are all methyl substituted (shown above the table). [e]The aryl groups for 34-38 are not directly attached to the imidazolylidene ring. [f]For comparison, entry 37 is the electron rich phosphine complex $(PCy)_3Ir(CO)_2Cl$.

We first noticed from the stretching frequency that the all-aryl substituted complexes were among the most electron-donating NHCs reported thus far, only the non-traditional NHC generated by Crabtree has more electron-donating character (Table 3.3, entry 1). Likewise, from the chart, we see that the range of electronic donating character is wider than any other established system thus far (Δ_{max} 3.4 cm^{-1}, Δ_{ave} 0.84 cm^{-1}), with only Glorius's 4,5-dialkoxy system giving comparable ranges (Δ_{max} 2 cm^{-1}, Δ_{ave} 0.67 cm^{-1}).
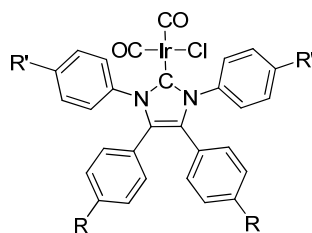
1,3-disubstitution:

more electron donating R' = OCH$_3$ > H > F *less electron donating*

4,5-disubstitution:

more electron donating R' = H > OCH$_3$ > F *less electron donating*

Figure 3.4. Electron donating order of NHC-Ir(CO)$_2$Cl complexes from IR stretching.

   Within the all-aryl series, we see that the 1,3-(4-methoxyphenyl) substituted complex is the most electron donating, followed by the all phenyl complex, then the 4,5-(4-methoxyphenyl) substituted species, then the 4,5-(4-fluorophenyl), and 1,3-(4-fluorophenyl) species (Figure 3.4). In the series, the fluorinated substituents are less electron donating than phenyl substitution and the anisylic substituted complexes can be either more electron donating or withdrawing, depending on their positions. Although the methoxy group is considered to be electron donating for aryl rings in general, it is more electronegative than a hydrogen substituent; the electron donating character arises from pi overlap of the oxygen and the aryl pi orbitals, while the electronegativity arises from sigma interactions. If there is less than perfect pi overlap with the central imidazole ring, as is observed in the silver carbene X-ray structures **3.4**, then the anisyl ring's electron withdrawing character becomes more competitive with the electron donating character. In this case, the electron withdrawing character predominates for the 4,5-substituted complex, though it is not as electron withdrawing as the fluorinated aryl groups.

   Within the tetraaryl system we can compare the effect of 1,3-substitution with 4,5-substitution. Since the IR data suggests that fluorine is acting as an electron withdrawing group, the substitution which has less influence on the CO stretching as compared to the tetraphenyl complex should have less influence on the iridium as well. If we consider the all-phenyl substituted NHC's IR stretch as a baseline to compare the other systems, 4,5-dianisyl NHC gives a shorter wavelength of only 0.4 cm^{-1}, compared to 1,3-dianisyl which gives a 0.6 cm^{-1} lengthening. On the other hand, 4,5-disubstituted 4-fluorophenyl NHC gives a shortening of 1.8

cm^{-1}, while 1,3-disubstituted 4-fluorophenyl gives a shortening of 2.8 cm^{-1}. We can state that for 1,3-substitution patterns, the 4-fluorophenyl group has a larger influence on the CO stretching, and the anisyl has a greater influence in the 4,5-substitution.

3.4.5 X-Ray Studies of NHC[AgCl] Complexes

Table 3.4: Selected Bond Lengths and Angles for Silver NHCs.

entry	Ar	Ar'	M-C (Å)	M-C-N (°)	N-C-N (°)	torsion, Ar (°)	torsion, Ar' (°)
3.4h	Ph	4-MeOC$_6$H$_4$	2.05	128.3	104.7	128.6	60.9
3.4c	4-FC$_6$H$_4$	Ph	2.07	127.2	102.3	116.2	75.9
3.4a	Ph	Ph	2.08	127.9	104.2	112.7	65.2
3.4e	4-MeOC$_6$H$_4$	Ph	2.08	127.9	104.1	114.0	71.4
3.4f	Ph	4-FC$_6$H$_4$	2.09	128.0	103.9	112.8	68.3

Table 3.4 summarizes the bond lengths and relevant angles for the silver carbene complexes 3.4, organized by increasing M-C bond length. Since shorter Ag-C$_{carbene}$ bond lengths indicate stronger electronic donating character,[107] a similar trend to those written for the IR stretches can be written regarding the X-ray determined structures, although the differences in the bond lengths are minor (Figure 3.5).
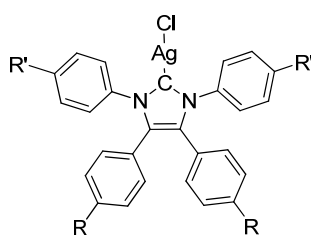
1,3-disubstitution:

more electron donating R' = H > F > OCH$_3$ *less electron donating*

4,5-disubstitution:

R = OCH$_3$ > H > F

Figure 3.5. Electron donating character of NHC-AgCl complexes from X-ray determined Ag-C$_{carbene}$ bond lengths.

The X-ray bond length extension to the electronic character does not agree with the IR trends. We expect the most electron donating all-phenyl substituted complex from the IR studies to likewise give the shortest metal-ligand bond lengths of the five ligands, but both the 4,5-dianisyl and 1,3-di(4-flluorophenyl) complexes showed shorter distances.

The packing arrangements in the crystal lattice likely contributes to this discrepancy. The crystal structures of all the complexes (excluding 4,5-di(4-methoxy)phenyl) have among the shortest intramolecular silver-silver distances we have found thus far. Such tight packing likely skews the bond distances to not be representative of solution-phase bond lengths.[108] The 4,5-dianisyl silver complex did not cocrystallize with solvent, for example, leading to poor intermolecular stacking, large intermolecular metal distances, and shorter metal-$C_{carbene}$ bond lengths. The bond lengths of the other complexes, when compared to other Ag-$C_{carbene}$ structures in the literature, are not much shorter than those already published, indicating that they would not be much more electron donating, and that the CO stretching in the NHC-Ir(CO)$_2$Cl complexes should be of a similar wavelength to those previously reported, which we did not find.[88,100] The distances between metals in the other crystal structures is close enough that there likely is some bonding interaction, increasing the observed Ag-$C_{carbene}$ bond length by reducing the electronic density between those atoms.

3.4.6 Calculations

In order to gain a better understanding of the conflicting data, and see if the packing influences could affect the overall bonding in our Ag-NHCs so dramatically, calculations were run in order to get a better grasp of the 4,5-position's influence among the new NHCs. Molecular orbital modeling calculations were performed using the X-ray coordinates of the free carbene, generated by simply erasing the silver and chlorine from the X-ray structure, with Gaussian at the HF / 6-31G level, and then geometry optimization calculations were used to find the nearest local

minima to remove steric constraints, using the CUBEGEN keyword after both calculations.[109] Figure 3.6 shows the HOMO / LUMO molecular orbitals for the carbenes from compounds **3.3c** and **3.3f** using both the X-ray coordinates as well as computationally geometry optimized coordinates. These two showed the most pronounced difference between the X-ray and optimized molecular orbital overlaps, though there were significantly more pronounced molecular orbitals in all structures (Figures B.1 and B.2).

Although the HOMO does not show much overlap between the central ring and the substitutents, the LUMO shows significantly higher overlap between the 4,5-aryl rings and the central ring in the computationally optimized structures. Other occupied orbitals of lower energy also have significantly greater overlap in the geometry optimized structure rather than the X-ray structure. Likewise, there is a preference for the optimized structures' aryl substituents to be in a symmetrical C_5 configuration, rather than a propellar C_1 conformation when the silver carbene is analyzed directly using DFT / B3LYP 6-31G and the LAN2DZ basis set (necessary for transition metal complexes). The "paddle boat" configuration was only observed for one silver-NHC which did not co-crystalize with solvent (**3.4e**).

The modeled lower occupied orbital overlaps also show more influence of the 1,3-diaryl rings on the electronics of the central ring than the 4,5-aryl rings, which was in agreement with

HOMO

LUMO

X-ray

based on 3.4f

optimized

X-ray

based on 3.4c
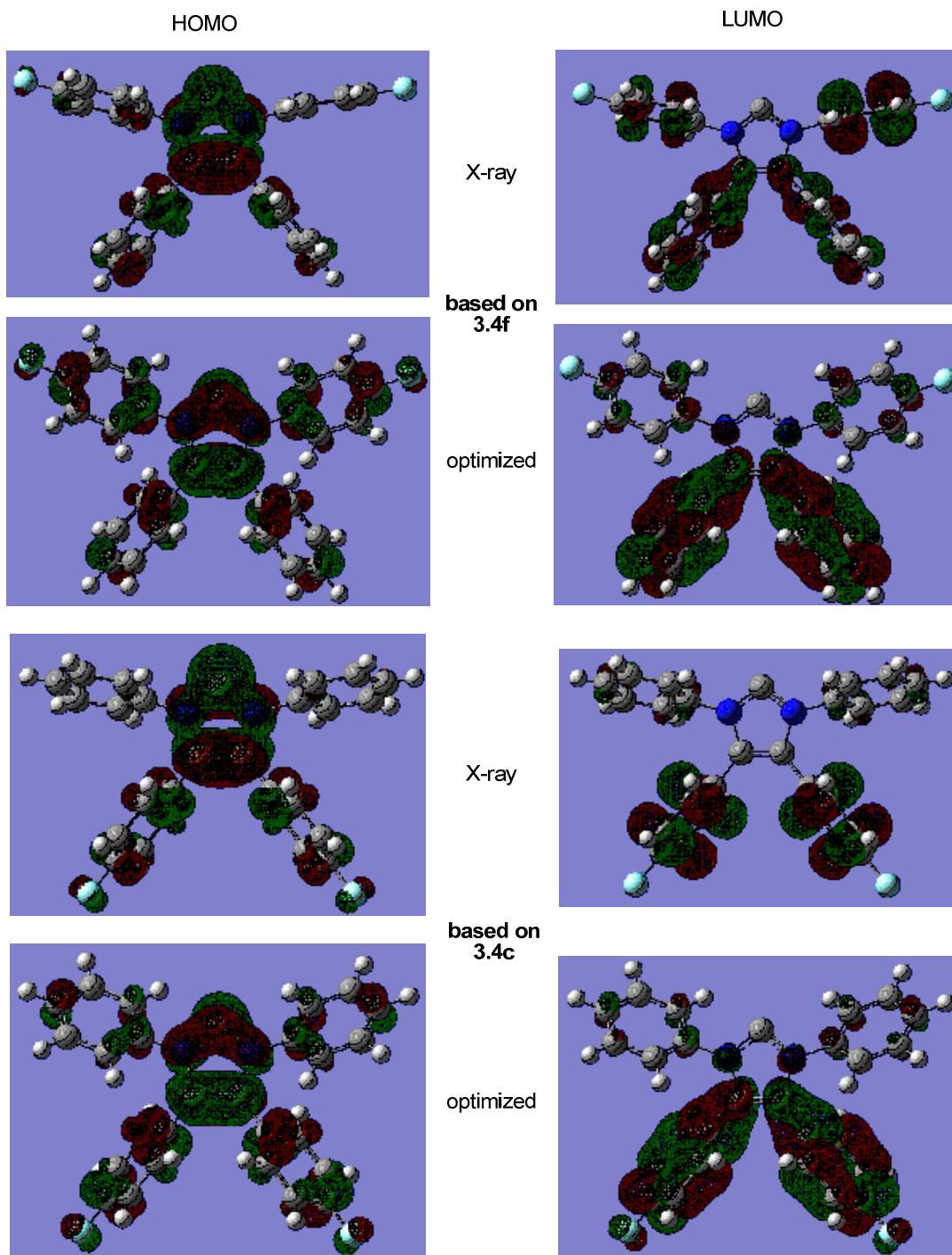
optimized

Figure 3.6. Gaussview depiction of the HOMO / LUMO overlap. Both X-ray coordinates and optimized structure based on the AgCl-NHCs **3.4c** and **3.4f** at eigenvalues of 0.03 are shown.

the studies on the IR stretching of the NHC-Ir(CO)$_2$Cl. We modeled the dicarbonyl iridium complex **3.6a** in order to see if there was some orbital influence between the pi-system of the 1,3-rings and the CO moieties without going through the metal itself (*i.e.* through-space bonding). Calculations on the geometry optimized structure did not indicate that any through-space bonding was occuring (calculations run using DFT / B3LYP, 6-31G, LAND2DZ). There was, however, some influence in some of the occupied orbitals extending through the metal and carbonyl orbitals, indicating some strong through-bond influences from the aryl substituents to the carbonyl.

3.5 Catalytic Studies

  Iridium NHC complexes are well-known for their catalytic properties in homogeneous hydrogenations, transfer hydrogenation, and allylations.[110] In order to get a general sense of the comparitive reactivity of the new Ir-NHC systems, we began a series of transfer hydrogenations with the Ir-NHC chlorides. The acetophenone / isopropanol system is among the simplest of transfer hydrogenations to measure, and we found that even at room temperature, with no additives other than the requisite base, we could get high conversion, and even greater conversion at elevated temperatures.

Table 3.5. Transfer Hydrogenation of Acetophenone Using IrNHC Complexes.[a]
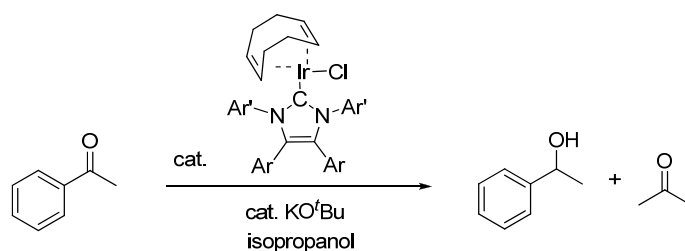
Entry	Cat.	Ar	Ar'	Cat (mol %)	Time (h)	Conv'n (%)[b]	TOF (hr^{-1})[b]
1[c]	5a	Ph	Ph	1.0	12	100	8.3
2[d]	5a	Ph	Ph	0.66	2	70	35
3[e]	5a	Ph	Ph	0.034	1	34	1034
4[e]	5a	Ph	Ph	0.032	1	39	1119
5[e]	5c	Ph	4-FC$_6$H$_4$	0.042	1	13	311
6[e]	5c	Ph	4-FC$_6$H$_4$	0.040	1	14	346
7[e]	5e	Ph	4-CH$_3$OC$_6$H$_4$	0.064	1	86	1260
8[e]	5e	Ph	4-CH$_3$OC$_6$H$_4$	0.059	1	71	1210
9[e]	5f	4-FC$_6$H$_4$	Ph	0.17	1	85	493
10[e]	5f	4-FC$_6$H$_4$	Ph	0.23	1	99	435

Entry	Cat.	Ar	Ar'	Cat (mol %)	Time (h)	Conv'n (%)[b]	TOF (hr⁻¹)[b]

Table 3.5 Continued

Entry	Cat.	Ar	Ar'	Cat (mol %)	Time (h)	Conv'n (%)[b]	TOF (hr⁻¹)[b]
11[e]	5h	4-CH$_3$OC$_6$H$_4$	Ph	0.065	1	50	769
12[e]	5h	4-CH$_3$OC$_6$H$_4$	Ph	0.038	1	27	734

[a]Reactions run at 80 °C under a nitrogen atmosphere with acetophenone (2g, 1.0 eq), KO^{t}Bu (14 - 56 mg, 1.5-2.2 mol %), isopropanol (2.5 - 8.0 mL), and the indicated amount of catalyst for the indicated times unless otherwise stated. [b]Determined by ^{1}H NMR. [c]Reaction performed at 25 °C. [d]Reactions performed using a solution of catalyst in isopropanol. [e]Reactions performed using a solution of KO^{t}Bu in isopropanol.

From Table 3.5, we see that we can achieve among the highest TOF reported for iridium-based NHC catalysts.[111]   Likewise, elevated temperatures give higher rates of conversion, probably driving off acetone. This is in agreement with the proposed equilibrium mechanism for iridium-based transfer hydrogenations, which can reduce or oxidize depending on whether ketone or alcohol is present in excess. TOF has a noticible dependence on time in these systems, and these catalysts are no exception.

We see a clear trend in reactivity, assuming that the IR studies of the CO stretching are indicative of the catalyst electronic character (and that the X-ray studies cannot be trusted for determining the electronic character of these systems). Namely, as CO stretching frequency increases, the TOF of the catalyst systems decreases; *i.e.* the rate of reaction in this system increases with electron density around the metal. Figure 3.7 shows the relationship between the average IR CO stretching frequency from Table 3.3 and the TOF from Table 3.5 (for the reactions that have less than 100% conversion, *i.e.* the entries with accurate TOF not limited by the amount of substrate present under optimum conditions). Many other groups have used the transfer hydrogenation of acetophenone as a standard by which to test their ligands against those already published; however, few have actually made the CO adducts to study the IR stretching. Fortunately, we have found both TOF for acetophenone transfer hydrogenation and IR data for IMes-Ir(COD)Cl (Table 3.3, entry 21).[100c,100d]   We can see that including this point in our comparison of IR and the maximum TOF aligns quite well in a logarithmic plot. Thus, IR-CO stretch seems to be a very strong indicator of how these catalysts will perform in transfer hydrogenation in general.
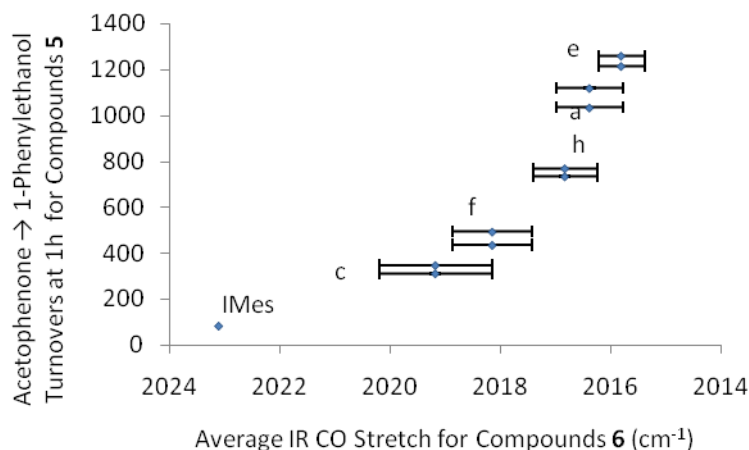
Figure 3.7. Relationship between IR Stretching of Ir(CO)$_2$Cl-NHCs and transfer hydrogenation rate of acetophenone to 1-phenylethanol for Ir(COD)-NHCs.[a]

Some mechanistic studies of transfer hydrogenations have been reported previously. From a calculation study using a simple tridentate phosphoramidate in iridium-based ketone transfer hydrogenation, Bi and coworkers found that the rate limiting step was transferal of hydride to the already coordinated metal-ketone (Figure 3.8).[111d] A more electron rich metal center would facilitate this step, as the metal hydrides are more prone to give the electron donating hydride anion to an electrophile, and thus this proposed mechanism appears to be in-line with our data.
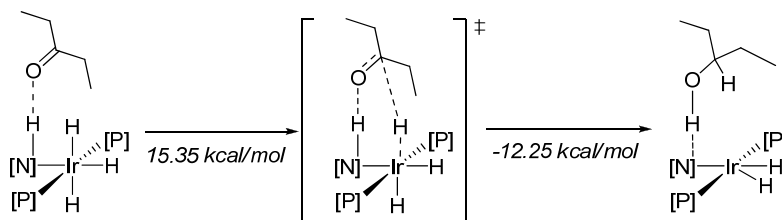
Figure 3.8. The highest energy step in iridium-based transfer hydrogenation as proposed by Bi and coworkers. [111d]

The highest conversion previously obtained in iridium-based transfer hydrogenation is from a complex by Crabtree that gives as high as 14000 TOF per hour (based on 4.5 minutes of reaction, 500 TOF is the highest recorded for 1 full hour). His complex is a bidentate di-NHC complex with an acetate anion. Speculatively, the two NHC groups likely give the complex extra stability, preventing decomposition and/or ligand loss. Our complexes **3.5** do not have this same advantage, and thus may not be the most active for this particular transformation, although they do give higher TOF than most other mono-dentate Ir(COD) complexes. It is important to note that the most active catalyst from Crabtree has alkyl groups in the 1,3-positions of his catalyst, and thus it has a much more electron-rich ligand, agreeing qualitatively with the observed trend. NHC-Ir catalysts are known to lose activity over time, thus basing TOF over such a short amount of time likely is not indicative of its TOF for comparitive analysis at one hour. For example, the IMes ligand listed in chart 3.3, when only measured at 30 minutes, gives an hourly TOF of 228. Likewise, the complexes **3.5** give a much higher TOF when measured for less time as well, though 1 hour conversions are much more commonly reported, and thus easier for comparative analysis.

In order to enhance the activity of our complexes, we attempted to make the non-coordinating NHC-Ir(COD)BF$_4$ or NHC-IR(COD)PF$_6$ complexes for study. Unfortunately, multiple attempts to form either, independently or *in situ*, using AgBF$_4$ and AgPF$_6$ did not yield the desired complexes or even more active catalyst, reducing turnovers in the best cases or stopping the reaction entirely. The expected open-coordinated complex is likely too reactive to be stable under the desired reaction conditions, as is to be expected; the second binding ligand in the Burgess and Crabtree catalysts render those systems less sensitive to environmental deactivation, from water or oxygen.

3.6 Summary

A simple and fairly tolerant methodology for the synthesis of new tetraaryl NHCs has been developed from inexpensive and readily available starting materials. The 4,5-substitution in standard NHC complexes has a definite quantifiable effect on the bonding of the corresponding metal centers. Although the structures studied do not have a wide range of steric difference, a range of about 5 wave numbers of IR stretch on the NHC-Ir(CO)$_2$Cl complexes can be achieved through careful selection of the aryl group substitutions, and the all-

aryl substituted NHC complexes are among the most electron donating traditional mono-dentate NHC complexes synthesized thus far.[112] X-ray crystallographic studies of the silver-carbene complexes did not fully agree with the IR studies, leading us to believe that packing effects can heavily influence bond distances and length. The complexes were all catalytically active towards transfer hydrogenation, though they were not the most active catalyst for the system studied thus far. We also found a linear relationship between the TOF of the five catalysts **3.5** and IMes with the IR stretching frequencies of their CO adducts, strongly suggesting that electron-rich ligands give higher conversions for transfer hydrogenations, and have established a direct comparative protocol for sterically similar catalysts's electronic character (by comparing IR CO stretching with reaction rate). Future studies into the specifics of the short intramolecular silver-silver distances and further substitution of NHCs for other viable catalysts could find material science and other nanostructure applications.

CHAPTER IV

CONCLUSIONS

Our initial review into iridium based hydrogenation gave us indication that this was one of the few catalytic systems capable of generating more than one chiral center at a time without substrate dependence. Our initial research into this concept confirmed this suspicion, and we were able to generate four stereoisomers from a single enantiomer of the catalyst through careful manipulation of the functional groups of the substrate. Calculation and experimental evidence indicated that the polyenes studied were being hydrogenated one at a time in a stepwise manner, and the stereochemistry observed was readily predicted from previous data. Next we undertook an ambitious project to generate several natural products using nothing more than the active catalyst to generate several stereocenters simultaneously. Despite the activity of the catalyst, shortcomings of the targets themselves were encountered, mainly in the inability to separate the diastereomers that resulted by any conventional method. Thus a major limitation was encountered with respect to the asymmetric hydrogenation catalyst and its stereoselectivity towards low-functionalized substrates, which were among the least studied substrates for iridium-based asymmetric hydrogenation.

As none of the iridium based *N*-heterocyclic carbene catalysts with different substituents gave higher selectivities for the substrates studied, electronic variation was investigated to both expand the available NHC ligands available, and to study the impact 4,5-disubstitution of imidazolylidene carbenes has on metal-ligand bonding. Access to this pattern of substitution is generally limited to specific examples in the literature; therefore methodology was developed in order to generate a wide variety of tetraaryl NHCs using Miller's aldimine coupling strategy applied to monoimine substrates. The strategy proved fairly effective; although low yielding, this must be tempered by the ease of the reaction and availability of substrates. Studies into the exact electronic character using IR, X-ray, and computational techniques were able to show the dependence of the metal-carbon bond on all four free positions on the imidazole ring. The compounds studied were also found to be catalytically active without further modification towards transfer hydrogenation in simple, non-chiral substrates. Likewise, a direct correlation

between the electron donation ability of the ligand and reaction rate was found for the transfer hydrogenation of acetophenone into 1-phenylethanol.

N-Heterocyclic imidazolium-based carbene catalysis has been expanded both in the substrates available for reaction, the methodology to form multiple stereocenters simultaneously, and in the expansion of a greater diversity of 1,3,4,5-tetraaryl substituted ligands available. A deeper understanding of the relationship between electron donation of the ligand and the catalytic activity in real systems was also developed. Electronic modification of ligands via 4,5-disubstitution is easily achieved via our developed methodology, and will not, for many complexes, alter the steric environment around the metal in the 1,3-positions significantly.

REFERENCES

(1) Cui, X.; Ogle, J. W.; Burgess, K. *Chem. Commun.* **2005**, 672-674.

(2) Cui, X.; Fan, Y.; Hall, M. B.; Burgess, K. *Chem. Eur. J.* **2005**, *11*, 6859-6868.

(3) (a) Myers, A. G.; Yang, B. H.; Chen, H.; Gleason, J. L. *J. Am. Chem. Soc.* **1994**, *116*, 9361-9362. (b) For a thorough review of several iterative methods of generating deoxypropionates see Hannesian, S.; Giroux, S.; Mascitti *Synthesis* **2006**, *7*, 1057-1076.

(4) Myers, A. G.; Yang, B. H.; Chen, H.; McKinstry, L.; Kopecky, D. J.; Gleason, J. L. *J. Am. Chem. Soc.* **1997**, *119*, 6496-6511.

(5) Myers, A. G.; Movassaghi, M.; Zheng, B. *J. Am. Chem. Soc.* **1997**, *119*, 8572-8573.

(6) Myers, A. G.; Yang, B. H.; Kopecky, D. J. *Tetrahedron Lett.* **1996**, *37*, 3623-3626.

(7) Myers, A. G.; Yang, B. H.; Chen, H.; Kopecky, D. J. *Synlett* **1997**, *5*, 457-459.

(8) Negishi, E.; Tan, Z.; Liang, B.; Novak, T. *Proc. Nat. Acad. Sci. U.S.A.* **2004**, *101*, 5782-5787.

(9) (a) Magnin-Lachaux, M.; Tan, Z.; Liang, B.; Negishi, E. *Org. Lett.* **2004**, *6*, 1425-1427. (b) Zhu, G.; Liang, B.; Negishi, E-i. *Org. Lett.* **2008**, *10*, 1099-1101.

(10) Liang, B.; Novak, T.; Tan, Z.; Negishi, E. *J. Am. Chem. Soc.* **2006**, *128*, 2770-2771.

(11) Novak, T.; Tan, Z.; Liang, B.; Negishi, E. *J. Am. Chem. Soc.* **2005**, *127*, 2838-2839.

(12) (a) Lopez, F.; Van Zijl, A. W.; Minnaard, A. J.; Feringa, B. L. *Chem. Commun.* **2006**, 409-411. (b) For non-catalytic conjugate addition see Hanessian, S.; Chahal, N.; Giroux, S. *J. Org. Chem.* **2006**, *71*, 7403-7411 and references therein.

(13) Martina, S. L. X.; Minnaard, A. J.; Hessen, B.; Feringa, B. L. *Tetrahedron Lett.* **2005**, *46*, 7159-7163.

(14) Lopez, F.; Harutyunyan, S. R.; Meetsma, A.; Minnaard, A. J.; Feringa, B. L. *Angew. Chem., Int. Ed.* **2005**, *44*, 2752-2756.

(15) Suarez, R. M.; Pena, D.; Minnaard, A. J.; Feringa, B. L. *Org. Biomol. Chem.* **2005**, *3*, 729-731.

(16) Des Mazery, R.; Pullez, M.; Lopez, F.; Harutyunyan, S. R.; Minnaard, A. J.; Feringa, B. L. *J. Am. Chem. Soc.* **2005**, *127*, 9966-9967.

(17) Summeren, R. P. v.; Moody, D. B.; Feringa, B. L.; Minnaard, A. J. *J. Am. Chem. Soc.* **2006**, *128*, 4546-4547.

(18) (a) Crabtree, R. H.; Felkin, H.; Morris, G. E. *J. Organomet. Chem.* **1977**, *141*, 205-215. (b) Crabtree, R. H.; Felkin, H.; Fillebeen-Khan, T.; Morris, G. E. *J. Organomet. Chem.* **1979**, *168*, 183-195.

(19) Crabtree, R. H.; Felkin, H.; Khan, T.; Morris, G. E. *J. Organomet. Chem.* **1978**, *144*, C15-C17.

(20) Crabtree, R. H.; Felkin, H.; Morris, G. E. *J. Organomet. Chem.* **1977**, *141*, 205-215.

(21) Crabtree, R. H.; Felkin, H.; Morris, G. E. *Chem. Commun.* **1976**, 716-717.

(22) Pfaltz, A. *CHIMICA* **2004**, *58*, 49-50.

(23) Noyori, R.; Kitamura, M.; Ohkuma, T. *Proc. Nat. Acad. Sci. U.S.A.* **2004**, *101*, 5356-5362.

(24) Noyori, R. *Chem. Soc. Rev.* **1989**, *18*, 187-208.

(25) Noyori, R.; Takaya, H. *Acc. Chem. Res.* **1990**, *23*, 345-350.

(26) Noyori, R.; Ohkuma, T. *Angew. Chem. Int. Ed.* **2001**, *40*, 40-73.

(27) Kitamura, M.; Kasahara, I.; Manabe, K.; Noyori, R.; Takaya, H. *J. Org. Chem.* **1988**, *53*, 708-710.

(28) Takaya, H.; Ohta, T.; Sayo, N.; Kumobayashi, H.; Akutagawa, S.; Inoue, S.; Kasahara, I.; Noyori, R. *J. Am. Chem. Soc.* **1987**, *109*, 1596-1597.

(29) Helmchen, G.; Pfaltz, A. *Acc. Chem. Res.* **2000**, *33*, 336-345.

(30) Schnider, P.; Koch, G.; Pretot, R.; Wang, G.; Bohnen, F. M.; Kruger, C.; Pfaltz, A. *Chem. Eur. J.* **1997**, *3*, 887-892.

(31) Lightfoot, A.; Schnider, P.; Pfaltz, A. *Angew. Chem. Int. Ed.* **1998**, *37*, 2897-2899.

(32) Cui, X.; Burgess, K. *Chem. Rev.* **2005**, *105*, 3272-3296.

(33) Bell, S.; Wuestenberg, B.; Kaiser, S.; Menges, F.; Netscher, T.; Pfaltz, A. *Science* **2006**, *311*, 642-644.

(34) Powell, M. T.; Hou, D.-R.; Perry, M. C.; Cui, X.; Burgess, K. *J. Am. Chem. Soc.* **2001**, *123*, 8878-8879.

(35) Cui, X.; Ogle James, W.; Burgess, K. *Chem. Commun.* **2005**, 672-674.

(36) Cui, X.; Burgess, K. *J. Am. Chem. Soc.* **2003**, *125*, 14212-14213.

(37) Norte, M.; Fernandez, J. J.; Padilla, A. *Tetrahedron Lett.* **1994**, *35*, 3413-3416.

(38) Moses, J. E.; Baldwin, J. E.; Brueckner, S.; Eade, S. J.; Adlington, R. M. *Org. Biomol. Chem.* **2003**, *1*, 3670-3684.

(39) Robiette, R.; Richardson, J.; Aggarwal, V. K.; Harvey, J. N. *J. Am. Chem. Soc.* **2006**, *128*, 2394-2409.

(40) Robiette, R.; Richardson, J.; Aggarwal, V. K.; Harvey, J. N. *J. Am. Chem. Soc.* **2005**, *127*, 13468-13469.

(41) (a) Ohta, T.; Takaya, H.; Kitamura, M.; Nagai, K.; Noyori, R. *J. Org. Chem.* **1987**, *52*, 3174-3176. (b) High enantioselectivities have since been reported using a phosphine-oxazoline iridium hydrogenation catalysts, see Li, S.; Zhu, S-F.; Zhang, C-M.; Song, S.; Zhou, Q-L. *J. Am. Chem. Soc.* **2008**, *130*, 8584-8585.

(42) Majetich, G.; Defauw, J.; Ringold, C. *J. Org. Chem.* **1988**, *53*, 50-68.

(43) Kirrmann, A.; Pourrat, H.; Schmitz, R.; Saito, E. *Bull. Soc. Chim. Fr.* **1952**, 502-504.

(44) Lauchenauer, A.; Schinz, H. *Helv. Chim. Acta* **1951**, *34*, 1514-1523.

(45) (a) Zhou, J.; Ogle, J. W.; Fan, Y.; Banphavichit, V.; Zhu, Y.; Burgess, K. *Eur. J. Org. Chem.*, **2007**, *13*, 7162-7170. (b) Cui, X.; Fan, Y.; Hall, M. B.; Burgess, K. *Eur. J. Chem.*, **2005**, *11*, 6859-6868. (c) Zhou, J.; Burgess, K. *Angew. Chem. Int. Ed. Engl.*, **2007**, *46*, 1129-1131. (d) Zhou, J.; Burgess, K. *Org. Lett.*, **2007**, *9*, 1391-1393. (e) Vigneron, J. P.; Dhaenens, M.; Horeau, A. *Tetrahedron* **1973**, *29*, 1055-1059.

(46) Trecourt, F.; Mallet, M.; Mongin, O.; Queguiner, G. *J. Org. Chem.* **1994**, *59*, 6173-6178.

(47) Kumagai, H.; Nishida, H.; Imamura, N.; Tomoda, H.; Omura, S.; Bordner, J. *J. Antibiotics* **1990**, *43*, 1553-1558.

(48) Ley, S. V.; Armstrong, A.; Diez-Martin, D.; Ford, M. J.; Grice, P.; Knight, J. G.; Kolb, H. C.; Madin, A.; Marby Craig, A.; Mukherjee, S.; Shaw, A. N.; Slawin, A. M. Z.; Vile, S.; White, A. D.; Williams, D. J.; Woods, M. *J. Chem. Soc., Perkin Trans. 1.*, **1991**, 667-692.

(49) Kuwahara, Y.; Yen, L. T. M.; Tominaga, Y.; Matsumoto, K.; Wada, Y. *Ag. Bio. Chem.* **1982**, *46*, 2283-2291.

(50) Honma, L. Y.; Kuwahara, Y.; Sato, M.; Matsuyama, S.; Suzuki, T. *Nippon Noyaku Gakkaishi* **1995**, *20*, 265-271.

(51) Kuwahara, Y.; Asami, N.; Morr, M.; Matsuyama, S.; Suzuki, T. *Applied Entomology and Zoology* **1994**, *29*, 253-257.

(52) Kuwahara, y.; Matsumoto, K.; Wada, Y.; Suzuki, T. *Applied Entomology and Zoology* **1991**, *26*, 85-89.

(53) Kuwahara, Y. *Pestic. Chem.: Hum. Welfare Environ., Proc. Int. Congr. Pestic. Chem., 5th* **1983**, *2*, 111-116.

(54) Schulten, H. R.; Murray, K. E.; Simmleit, N. *Zeitschrift fuer Naturforschung, C: J. Biosciences* **1987**, *42*, 178-190.

(55) Odham, G. *Arkiv foer Kemi* **1963**, *21*, 379-393.

(56) Murray, K. E. *Au. J. Chem.* **1962**, *15*, 510-520.

(57) Hanaki, N.; Ishihara, K.; Kaino, M.; Naruse, Y.; Yamamoto, H. *Tetrahedron* **1996**, *52*, 7297-7320.

(58) Morr, M.; Proppe, C.; Wray, V. *Liebigs Annalen* **1995**, *1995*, 2001-2004.

(59) Kaino, M.; Naruse, Y.; Ishihara, K.; Yamamoto, H. *J. Org. Chem.* **1990**, *55*, 5814-5815.

(60) Mori, K.; Kuwahara, S. *Tetrahedron* **1986**, *42*, 5539-5544.

(61) Mori, K.; Kuwahara, S. *Liebigs Ann. der Chem.* **1987**, *1987*, 555-556.

(62) Liang, B.; Novak, T.; Tan, Z.; Negishi, E.-I. *J. Am. Chem. Soc.*, *128*, 2770-2771.

(63) Holler, U.; Konig, G.; Wright, A. D. *Eur. J. Org. Chem.* **1999**, *1999*, 2949-2955.

(64) Gerecke, M.; Ryser, G.; Zeller, P. (Hoffmann-La Roche, Inc.) US Patent 2912467, **1959**.

(65) Shitangkoon, A.; Vigh, G. *J. Chromatography A* **1996**, *738*, 31-42.

(66) Sreekumar, C.; Darst, K. P.; Still, W. C. *J. Org. Chem.* **1980**, *45*, 4260-4262.

(67) Lynch, C. L.; Hale, J. J.; Budhu, R. J.; Gentry, A. L.; Finke, P. E.; Caldwell, C. G.; Mills, S. G.; MacCoss, M.; Shen, D.-M.; Chapman, K. T.; Malkowitz, L.; Springer, M. S.; Gould, S. L.; DeMartino, J. A.; Siciliano, S. J.; Cascieri, M. A.; Carella, A.; Carver, G.; Holmes,

K.; Schleif, W. A.; Danzeisen, R.; Hazuda, D.; Kessler, J.; Lineberger, J.; Miller, M.; Emini, E. *Org. Lett.* **2003**, *5*, 2473-2475.

(68) Fuganti, C.; Grasselli, P. *Chem. Ind.* **1977**, *24*, 983.

(69) Li, L.; Elliott, W. H. *J. Am. Chem. Soc.* **1952**, *74*, 4089-4090.

(70) Dussault, P. H.; Woller, K. R. *J. Org. Chem.* **1997**, *62*, 1556-1559.

(71) Karminski-Zamola, G.; Jakopcic, K. *Croat. Chem. Acta* **1974**, *46*, 71-78.

(72) Kupchan, S. M.; Balon, D. J.; Fujita, E. *J. Org. Chem.* **1962**, *27*, 3103-3106.

(73) Crump, R. A. N. C.; Fleming, I.; Hill, J. H. M.; Parker, D.; Reddy, N. L.; Waterson, D. *Org. Bio-Org. Chem.* **1992**, 3277-3294.

(74) Hoye, T. R.; Kurth, M. J. *J. Org. Chem.* **1980**, *45*, 3549-3554.

(75) Patel, P.; Pattenden, G. *J. Chem. Soc. Perkin Trans 1* **1991**, 1941-1945.

(76) Patel, P.; Pattenden, G. *Tetrahedron Lett.* **1985**, *26*, 4789-4792.

(77) Venkataraman, H.; Cha, J. K. *Tetrahedron Lett.* **1987**, *28*, 2455-2458.

(78) Katzenellenbogen, J. A.; Utawanit, T. *J. Am. Chem. Soc.* **1974**, *96*, 6153-6158.

(79) Diez-Martin, D.; Grice, P.; Kolb, H. C.; Lev, S. V.; Madin, A. *Synlett* **1990**, *1990*, 326-328.

(80) Collin-Asselineau, C.; Asselineau, J. *Bull. Soc. Chim. Fr.* **1960**, 1776-1784.

(81) Odham, G. *Arkiv foer Kemi* **1967**, *27*, 231-250.

(82) Odham, G. *Fette, Seifen, Anstrichmittel* **1967**, *69*, 164-172.

(83) Marshall, J. A.; Xie, S. *J. Org. Chem.* **1995**, *60*, 7230-7237.

(84) (a) Davies, S. G.; Polywka, R.; Warner, P. *Tetrahedron* **1990**, *46*, 4847-4856. (b) Tamaru, Y.; Mizutani, M.; Fufukawa, Y.; Kawamura, S-i.; Yoshida, Z-i.; Yanagi, K.; Minobe, M. *J. Am. Chem. Soc.* **1984**, *106*, 1079-1085.

(85) Chu, K. S.; Negrete, G. R.; Konopelski, J. P. *J. Org. Chem.* **1991**, *56*, 5196-5201.

(86) (a) Herrman, W. A. *Angew. Chem. Int. Ed.* 2002, *41,* 1290-1309. (b) Herrman, W. A.; Kocheer, C. *Angew. Chem. Int. Ed.* **1997**, *36,* 2162-2187. (c) Garrison, J. C.; Youngs, W. J. *Chem. Rev.* **2005**, *105,* 3978-4008. (d) Huang, J. K.; Stevens, E. D. ; Nolan, S. P.; Petersen, J. P. *J. Am. Chem. Soc.* **1999**, *121,* 2674-2678. (e) Kamber, N. E.; Jeong, W.; Waymouth, R. M.; Pratt, R. C.; Lohmeijer, B. G. G.; Hedrick, J. L. *Chem. Rev.* **2007**, *107*, 5813-5840.

(87) Arduengo III, A. J.; Goerlich, J. R.; Krafczyk, R.; Marshall, W. J. *Angew. Chem. Int. Ed.* **1998**, 37, 1963-1965.

(88) (a) Chianese, A. R.; Li, X.; Janzen, M. C.; Faller, J. W.; Crabtree, R. H. *Organometallics* **2003** *22*, 1663-1667. (b) Kelly III, R. A.; Clavier, H.; Giudice, S.; Scott, N. M.; Stevens, E. D.; Bordner, J.; Samardjiev, I.; Hoff, C. D.; Cavallo, L.; Nolan, S. P. *Organometallics* **2008**, *27,* 202-210. (c) Hillier, A. C.; Sommer, W. J.; Yong, B. S.; Petersen, J. L.; Cavallo, L.; Nolan, S. P. *Organometallics* **2003**, *22*, 4322-4326.

(89) (a) Reich, B. J. E.; Justice, A. K.; Beckstead, B. T.; Reibenspies, J. H.; Miller, S. A. *J. Org. Chem.* **2004**, 69, 1357-1359. (b) Reich, B. J. E.; Greenwald, E. E.; Justice, A. K.; Beckstead, B. T.; Reibenspies, J. H.; North, S. W.; Miller, S. A. *J. Org. Chem.* **2005**, 70, 8409-8416.

(90) Kison, C.; Opatz, T. *Synthesis* **2006**, 21, 3727-3738.

(91) Strain, H. H. *J. Am. Chem. Soc.* **1928**, *50*, 2218-2223.

(92) (a) Ide, W.S.; Buck, J. S. *Org. Reactions* **1948**, *4*, 269-304. (b) Jose, B.; Unni, M. V. V.; Prathapan,S.; Vadakkan, J. J. *Synth. Commun.* **2002**, *32*, 2495-2498. (c) Weiss, M.; Appel, M. *J. Am. Chem. Soc.* **1948**, *70*, 3666-3667.

(93) (a) Siegfried, M. *Chem. Ber.* **1892**, *25*, 2600-2601. (b) Reddelien, G. *Chem. Ber.* **1913**, *46*, 2718-2723. (c) Bock, H.; tom Dieck, H. *Chem. Ber.* **1967**, *100,* 228-246.

(94) (a) Kuebrich, J. P.; Schowen, R. L.; Wang, M.; Lupes, M. E. *J. Am. Chem. Soc.* **1971**, *93*, 1214-1220. (b) Becker, H.-D. *J. Org. Chem.* **1970**, *35*, 2099-2102.

(95) Arduengo III, A. J.; Krafczyk, R.; Schmutzler, R.; Craig, H. A.; Goerlich, J. N.; Marshall, W. J.; Unverzagt, M. *Tetrahedron* **1999**, *55*, 14523-14534.

(96) Delaude, L.; Szypa, M.; Demonceau, A.; Noels, A. F. *Adv. Synth. Catal.* **2002**, *344*, 749-756.

(97) S. Jafarpour, L.; Nolan, S. P. *Organometallics* **2000**, *19*, 2055-2057.

(98) For the utility of silver NHC carbenes in transmetallation and antimicrobial activity see: Garrison, J. C.; Youngs, W. J. *Chem. Rev.* **2005**, *105*, 3978-4008, and references therein.

(99) For some exotic 4,5-disubstituted NHCs see: (a) Altenhoff, A.; Goddard, R.; Lehmann, C. W.; Glorius, F. *J. Am. Chem. Soc.,* **2004**, *126*, 15195-15201. (b) Khramov, D. M.; Lynch, V. M.; Bielawski, C. W. *Organometallics* **2007**, *26,* 6042-6049. (c) Arduengo, A. J. III; Davidson, F.; Dias, H. V. R.; Goerlich, J. R.; Khasnis, D.; Marshall, W. J.; Prakasha, T. K. *J. Am. Chem. Soc.*, **1997**, *119,* 12742-12749. (d) Zetinkayal, E.; Hitchcock, P. B.; Kucukbay, H.;

Lappert, M. F.; Al-Juaid, S. *J. Organomet. Chem.*, **1994**, 89-95. (d) Hiraki, K.; Fuchita, Y.; Morinaga, S. *Chemistry Letters* **1978**, 1-2. (e) McGuinness, D. S.; Cavell, K. J. *Organometallics* **1999**, *18,* 1596-1605. (f) Raubenheimer, H. G.; Cronje, S.; Olivier, P. *J. Chem. Society. Dalton Trans.* **1995**, 313-316. (g) Kucukbay, H.; Bekir Cetinkaya, B.; Guesmi, S.; Dixneuf, P. H. *Organometallics* **1996**, *15,* 2434-2439. (h) Wang, H. M. J.; Lin, I. J. B. *Organometallics* **1998**, *17,* 972-975. (j) Khramov, D. M.; Boydston, A. J.; Bielawski, C. W. *Angew. Chem. Int. Ed.* **2006**, *45*, 6186 –6189.

(100) (a) Fantasia, S.; Petersen, J. L.; Jacobsen, H.; Cavallo, L.; Nolan, S. P. *Organometallics* **2007**, *26,* 5880-5889. (b) Kownacki, I.; Kubicki, M.; Szubert, K.; Marciniec, B. *J. Organomettalic Chem.* **2008**, *693*, 321-328.

(101) Tolman, C. A. *Chem. Rev.* **1977**, *77*, 313-348.

(102) Herrmann, W. A.; Elison, M.; Fischer, J.; Koecher, C.; Oefele, K. German Patent 2339947 **1996**.

(103) Chianese, A. R.; Kovacevic, A.; Zeglis, B. M.; Faller, J. W.; Crabtree, R. H. *Organometallics* **2004**, *23*, 2461-2468.

(104) Leuthäußer, S.; Schwarz, D., Plenio, H. *Eur. J. Chem.* **2007**, *13*, 7195-7203.

(105) Altenhoff, G.; Goddard, R.; Lehmann, C. W.; Glorius, F. *J. Am. Chem. Soc.* **2004**, *126*, 15195-15201.

(106) Frey, G. D.; Retzsch, C. F.; von Presing, D.; Scherg, T.; Mühlhofer, M.; Herdtweck, E.; Herrman, W. A. *J. Organometallic Chem.* **2006**, *691*, 5725-5738.

(107) Shriver, D. F.; Atkins, P. W. *Inorganic Chemistry*, 4th ed., Oxford University Press, Oxford, **2005**.

(108) For some similar studies where the X-ray structures and calculated geometry vary slightly see: (a) Ellis, B. D.; Dyker, A. C.; Deckenc, A.; Macdonald, C. L. B. *Chem. Commun.* **2005**, 1965–1967. For studies into NHC crystal packing see: (b) Liu, Q.; Yin, L.; Feng, J. *J. Organomet. Chem.* **2007**, *692*, 3655–3663. (c) Fürstner, A.; Ackermann, L.; Gabor, B.; Goddard, R.; Lehmann, C. W.; Mynott, R.; Stelzer, F.; Thiel, O. R. *Chem. Eur. J.* **2001**, *7*, 3236 -3253. (d) Lee, C. K.; Vasam, C. S.; Huang, T. W.; Wang, H. M. J.; Yang, R. Y.; Lee, C. S.; Lin, I. J. B. *Organometallics* **2006,** *25,* 3768-3775.

(109) *Gaussian 03, Revision C.02*, M. J. Frisch, G. W. Trucks, H. B. Schlegel, G. E. Scuseria, M. A. Robb, J. R. Cheeseman, J. A. Montgomery, Jr., T. Vreven, K. N. Kudin, J. C.

Burant, J. M. Millam, S. S. Iyengar, J. Tomasi, V. Barone, B. Mennucci, M. Cossi, G. Scalmani, N. Rega, G. A. Petersson, H. Nakatsuji, M. Hada, M. Ehara, K. Toyota, R. Fukuda, J. Hasegawa, M. Ishida, T. Nakajima, Y. Honda, O. Kitao, H. Nakai, M. Klene, X. Li, J. E. Knox, H. P. Hratchian, J. B. Cross, V. Bakken, C. Adamo, J. Jaramillo, R. Gomperts, R. E. Stratmann, O. Yazyev, A. J. Austin, R. Cammi, C. Pomelli, J. W. Ochterski, P. Y. Ayala, K. Morokuma, G. A. Voth, P. Salvador, J. J. Dannenberg, V. G. Zakrzewski, S. Dapprich, A. D. Daniels, M. C. Strain, O. Farkas, D. K. Malick, A. D. Rabuck, K. Raghavachari, J. B. Foresman, J. V. Ortiz, Q. Cui, A. G. Baboul, S. Clifford, J. Cioslowski, B. B. Stefanov, G. Liu, A. Liashenko, P. Piskorz, I. Komaromi, R. L. Martin, D. J. Fox, T. Keith, M. A. Al-Laham, C. Y. Peng, A. Nanayakkara, M. Challacombe, P. M. W. Gill, B. Johnson, W. Chen, M. W. Wong, C. Gonzalez, and J. A. Pople, Gaussian, Inc., Wallingford CT, 2004.

(110) (a) Bower, J. F.; Patman, R. L.; Krische, M. J. *Org. Lett.* **2008**, *10*, 1033-1035. (b) Minnaard, A. J.; Feringa, B. L.; Lefort, L.; de Vries, J. G. *Acc. Chem. Res.* **2007**, *40*, 1267-1277. (c) Takeuchi, R.; Kezuka, S. *Synthesis* **2006**, *20*, 3349-3366.

(111) (a) Hodgson, R.; Douthwaite, R. E. *J. Organomet. Chem.* **2005**, *690*, 5822-5831. (b) Kownacki, I.; Kubicki, M.; Szubert, K.; Marciniec, B. *J. Organomet. Chem.* **2008**, *693*, 321-328. (c) Albrecht, A.; Miecznikowski, J. R.; Samuel, A.; Faller, J. W.; Crabtree, R. H. *Organometallics* **2002**, *21*, 3596-3604. (d) Bi, S.; Xie, Q.; Zhao, X.; Zhao, Y.; Kong, X. *J. Organometallic Chem.* **2008**, *693*, 633-638.

(112) For other tightly packed organometalic silver complexes see: (a) Bosch, E. *Inorg. Chem.* **2002**, 41, 2543-2547 (Ag··Ag 11.746 Å). (b) Cheng, K.; Zhu, H-L.; Li, Y-G., *Z. Anorg. Allg. Chem.* **2006**, 2326-2330 (Ag··Ag 7.438 Å). (c) Wang, J.; Hu, S.; Tong, M-L. *Eur. J. Inorg. Chem.* **2006**, 2069-2077. (d) Sun, D.; Cao, R.; Weng, J.; Hong, M.; Liang, Y. *J. Chem. Soc., Dalton Trans.* **2002**, 291-292.

(113) Reich, B. J. E.; Justice, A. K.; Beckstead, B. T.; Reibenspies, J. H.; Miller, S. A. *J. Org. Chem.* **2004**, *69*, 1357-1359.

(114) Delaude, L.; Szypa, M.; Demonceau, A.; Noels, A. F. *Adv. Synth. Catal.* **2002**, *344*, 749-756.

(115) Arduengo III, A. J.; Krafczyk, R; Schmutzler, R.; Craig, H. A.; Goerlich, J. R.; Marshall, W. J.; Unverzagt, M. *Tetrahedron* **1999**, *55*, 14523-14534.

(116) Tulloch, A. A. D.; Danopoulos, A. A.; Winston, S.; Kleinhenz, S.; Eastham, G. *J. Chem. Soc., Dalton Trans.* **2000**, *24*, 4499-4506.

(117) NMR spectra identical to those of the known compounds were obtained. Jin, W.; Makioka, Y.; Kitamura, T.; Fujiwara, Y. *J. Org. Chem.* **2001**, *66*, 514-520.

(118) NMR spectra identical to those of the known compounds were obtained. Helldorfer, M.; Backhaus, J.; Alt, H. G. *Inorg. Chim. Acta* **2003**, *351*, 34-42.

(119) NMR spectra identical to those of the known compound were obtained. Arduengo III, A. J.; Goerlich, J. R.; Krafczyk, R.; Marshall, W. J. *Angew. Chem., Int. Ed.* **1998**, *37*, 1963-1965.

(120) (a) Chen, M. S.; White, M. C. *Science* **2007**, 318, 783-787.   (b) Cimino, G.; Sodano, G.; Spinella, A. *J. Org. Chem.* **1987**, 52, 5326-5331.

(121) (a) Edson, J. B.; Wang, Z.; Kramer, E. J.; Coates, G. W. *J. Am. Chem. Soc.* **2008**, *130*, 4968-4977. (b) Roberts, J. S. A.; Chen, M-C.; Seyman, A. M.; Li, L.; Zuccacia, C.; Stahl, N. G.; Marks, T. J. *J. Am. Chem. Soc.* **2007**, *129*, 12713-12733. (c) Leclerc, M. K.; Hantzbringer, H. H. *J. Am. Chem. Soc.* **1995**, *117*, 1651-1652. (d) Tsai, J-C.; Kuo, J-C.; Ho, R-M.; Chung, T-M. *Macromolecules* **2006**, *39*, 7520-7526. (e) Cai, Z.; Nakayama, Y.; Shiono, T. *Macromolecules*, **2006**, *39*, 2031-2033. (f) Resconi, L.; Cavallo, L.; Fait, A.; Piemontesi, F. *Chem. Rev.* **2000**, *100*, 1253-1345.

APPENDIX A

EXPERIMENTAL SECTION CHAPTER II

An Asymmetric Hydrogenation Route to Terminal Alkyl-deoxydipropionate Chirons

- synthesis of monoenes and dienes
- asymmetric hydrogenation of monoenes and dienes
- determination of absolute and relative stereochemistry monoenes and dienes
- ^{1}H, ^{13}C spectra of selected monoene, and hydrogenated products

General Procedures.

GC analysis of samples was preceeded by filtering the samples through a small plug of silica, eluting with 2 ml of a 50 / 50 mixture of EtOAc / Hexanes. Freeze-thaw was performed by first cooling the sample to -78 $^\circ$C under nitrogen, applying vacuum for 5 min, then warming to 25 $^\circ$C under nitrogen. Ethyl tiglate, *trans*-2-methyl-2-butenal, antibiotic-2-methyl-2-pentenal, (R)-methyl lactate, methyl-2-bromopropionate and triphenylphosphine were ordered from Sigma-Aldrich or TCI and used without further purification. Silver nitrate was purchased from Strem and used as purchased. Methoxycarbonylethylidene-triphenylphosphorane was generated using the known two-step procedure from methyl-2-bromopropionate and triphenylphosphine[64]. Dichloromethane was distilled from calcium hydride prior to use. Other solvents and reagents were used as received. NMR spectra were recorded on a Varian Unity Plus 300 spectrometer (^{1}H at 300 MHz, and ^{13}C at 75 MHz). Chemical shifts of ^{1}H and ^{13}C spectra were referenced to the NMR solvents. Flash chromatography was performed using silica gel (230–600 mesh). Thin layer chromatography was performed using glass plates coated with silica gel 60 F254 (E. Merck, Darmstadt, Germany). The hydrogenation results were analyzed using GC with a chiral column[65] using two different conditions depending on the products: for hydrogenated products 2a-2d, 2f, 2h-2k, 2m, and 2n: [carrier gas: helium; temperature: 60 °C; flow rate: 2.0 ml/min; retention time varies by product (shown below)]; for hydrogenated products 2e, 2g, 2l, 2o, 2p, and 4: [carrier gas: helium; temperature: 90 °C; flow rate: 2.0 ml/min; retention time varies by product (shown below)]. IR spectra were collected on a Perkin Elmer Spectrum One FT-IR instrument. HRMS data was collected on a PE SCIEX API QSTAR PULSAR instrument.

E-2-Methyl-2-butenol (2.1a).
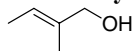
E-2-methyl-2-butenoic acid (3.15 g, 21.6 mmol, 1 eq.) was added slowly in 0.5 g portions to a slurry of 3.3 g (86 mmol, 4 eq.) lithium aluminum hydride in 50 ml dichloromethane cooled to 0-5 °C in an ice bath. This was allowed to warm to ambient temperature over 4 h, after which time it was cooled back to 0-5 °C, and 20 ml of methanol was added slowly, dropwise, to quench the excess hydride. After quenching, a solution of 150 ml of saturated sodium potassium tartrate was added and stirred for 2 h, after which time an additional 50 ml dichloromethane was added, and the layers separated. The aqueous layer was separated an additional 3 times with 50 ml of dichloromethane, and the combined organic extracts dried over anh. sodium sulfate. Concentration of the dichloromethane layers afforded 2.6 g of the title compound, a 96 % isolated yield of the title compound. ^{1}H NMR matched the known compound.[42-44] ^{1}H NMR (CDCl$_3$, 300 MHz): δ (ppm) = 5.52 (qt, J = 6.5, 7.1, 1.3 Hz, 1H), 4.03 (s, 2H), 1.69 (s, 3H), 1.66 (doublet of quintets, J = 6.7, 1.1 Hz, 3H), 1.40 (bs, 1H).
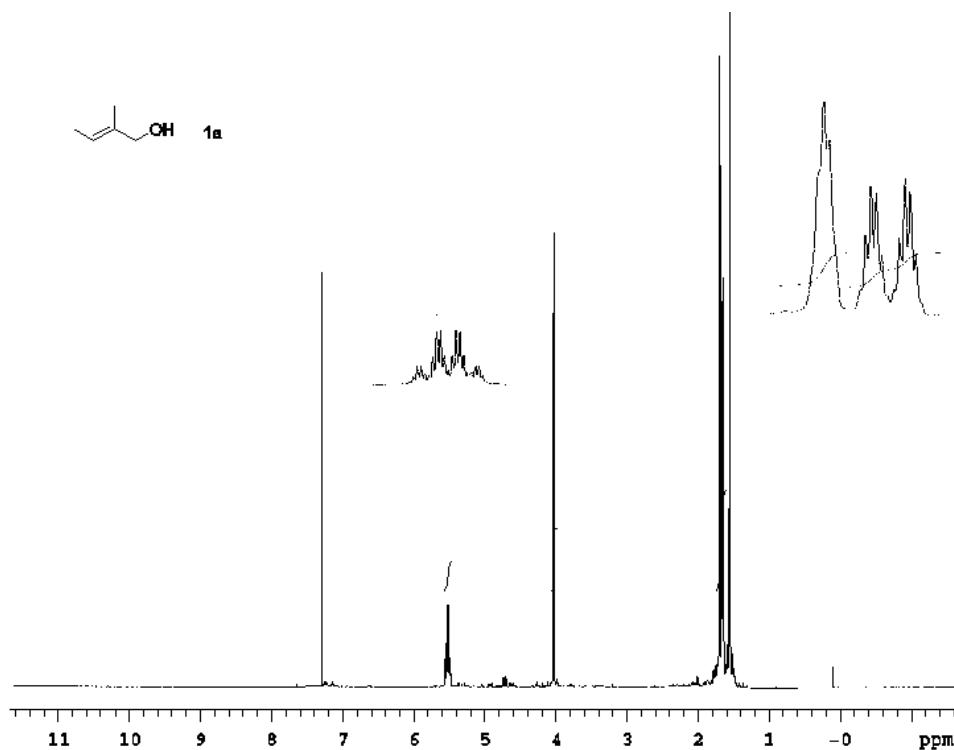
1-(E-2-methyl-2-butenyl)-tertbutyldimethylsilyl Ether (2.1b).
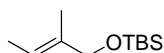
E-2-methyl-2-butenol (1 g, 11.6 mmol, 1 eq.) was added to 335 mg (13.9 mmol, 1.2 eq.) of previously hexane-rinsed sodium hydride (from a 70 % dispersion in mineral oil) in 20 ml of diethyl ether at 0 °C. This was stirred 30 min, at the end of which time 2.1 g (13.9 mmol, 1.2 eq.) tertbutyldimethylsilyl chloride was added all at once, followed by

stirring for 4 h. Concentration under reduced pressure followed by column chromatography with 7.5 % ethyl acetate in hexanes (Rf = 0.8) gave the title compound as a clear oil, 1.15 g, 49 % isolated yield. ^{1}H NMR matched the known compound.[66] ^{1}H NMR (CDCl$_3$, 300 MHz): δ (ppm) = 5.50 (dt, J = 5.3, 1.5 Hz, 1H), 4.40 (s, 2H), 1.65 (q, J = 1.3, 1.1 Hz, 3H), 1.63 (s, 3H), 0.94 (s, 9H), 0.09 (s, 6H).
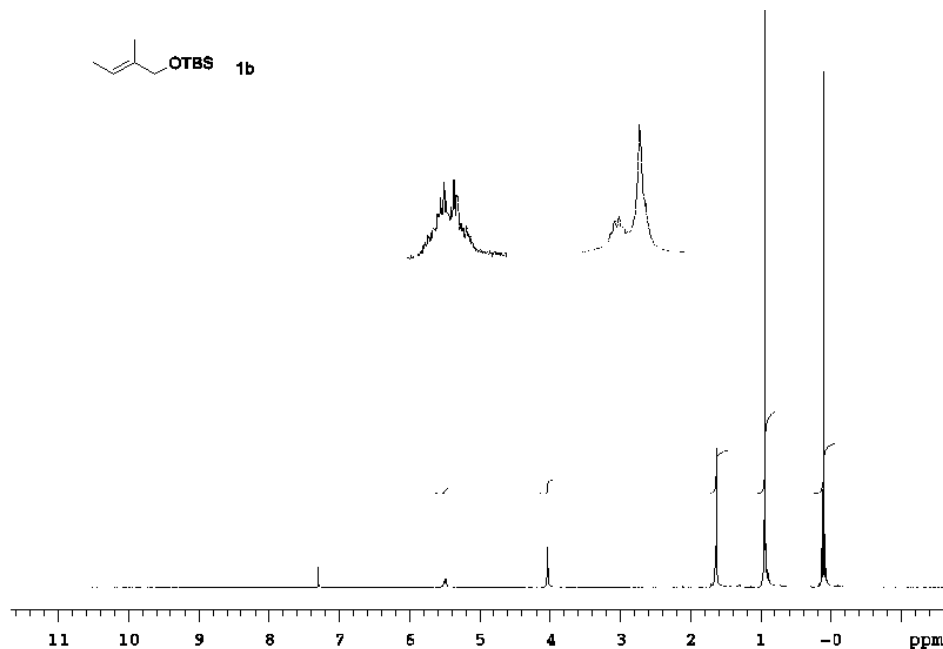
E-3-methyl-4-(oxobenzyl)-2-butene (2.1d).
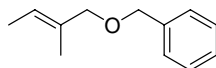
To 28 ml of tetrahydrofuran was added 1.0 g (12 mmol, 1 eq.) tiglic alcohol, then 560 mg (24 mmol, 2 eq.) sodium hydride (70% dispersion in mineral oil) was added after cooling to 0 °C. After stirring for 30 min, benzyl bromide (4 g, 23.2 mmol, 2 eq.) was added, and this was allowed to stir 4 h. Concentration of the reaction mixture under reduced pressure followed by column chromatography with 1.5 % ethyl acetate in hexanes gave 530 mg, a 26 % isolated yield of the title compound as a slightly yellow oil. ^{1}H NMR matched the known spectrum.[67] ^{1}H NMR (CDCl$_3$, 300 MHz): δ (ppm) = 7.35 (m, 5H), 5.54 (qq, J = 6.8, 6.6, 1.2 Hz, 1H), 4.46 (s, 2H), 3.91 (s, 2H), 1.69 (s, 3H), 1.66 (dq, J = 6.7, 1.1, 1.0 Hz, 3H).

E-2-Methylcinnimyl Alcohol (2.1e).
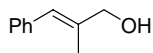
E-2-methyl cinnimic aldehyde (3.15 g, 21.6 mmol, 1 eq.) was added to a slurry of 3.3 g (86 mmol, 4 eq.) lithium aluminum hydride in 50 ml of dichloromethane cooled to 0-5 °C in an ice bath dropwise. This was allowed to warm to ambient temperature over 4 h, after which time it was cooled back to 0-5 °C, and 20 ml of methanol was added slowly, dropwise, to quench the excess hydride. After quenching, a solution of 150 ml of saturated sodium

potassium tartrate was added and stirred for 2 h, after which time additional dichloromethane (50 ml) was added, and the layers separated. The aqueous layer was separated an additional 3 times with dichloromethane, and the combined organic extracts dried over anhydrous sodium sulfate. Concentration of the dichloromethane layers afforded 2.6 g of the title compound, a 92 % isolated yield of the title compound. ^{1}H NMR matched the known compound.[68,69] ^{1}H NMR (CDCl$_3$, 300 MHz): δ (ppm) = 7.33 (m, J = 7.7, 7.0 Hz, 5H), 6.6 (s, 1H), 4.21 (s, 2H), 1.91 (s, 3H), 1.61 (bs, 1H).
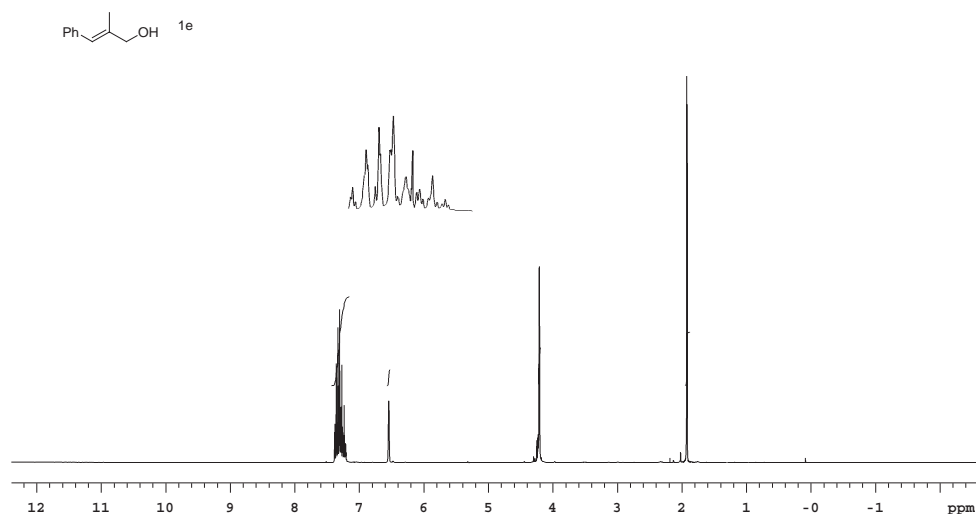
Benzyl *E*-2-Methyl-2-butenoate (2.1g).
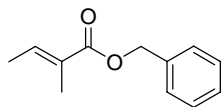
Tiglic acid (2 g, 20 mmol, 1 eq.) was added to 20 ml of tetrahydrofuran, followed by benzyl bromide (3.76 g, 22 mmol, 1.1 eq.) and triethylamine (4.4 ml, 30 mmol, 1.5 eq.). This was stirred at 0 °C for 2 h, then at ambient temperature 18 h. Diethyl ether (30 ml) was then added, followed by 30 ml of sodium bicarbonate, which was then separated. The aqueous extracts were washed with an additional 20 ml of diethyl ether, and the combined organic layers washed with 30 ml of 1 M aqueous HCl solution, then dried over sodium sulfate. Concentration under reduced pressure followed by column chromatography with 2 % ethyl acetate in hexanes (Rf: 0.75) gave 800 mg of the product, 21 % isolated yield, as a viscous colorless oil. ^{1}H NMR matched the known compound.[70] ^{1}H NMR (CDCl$_3$, 300 MHz): δ (ppm) = 7.4 (m, 5H), 6.95 (qq, J = 7.1, 7.2, 1.6, 1.5, 1.3 Hz, 1H), 5.22 (s, 2H), 1.90 (s, 3H), 1.83 (dq J = 7.2, 1.1 Hz, 3H).
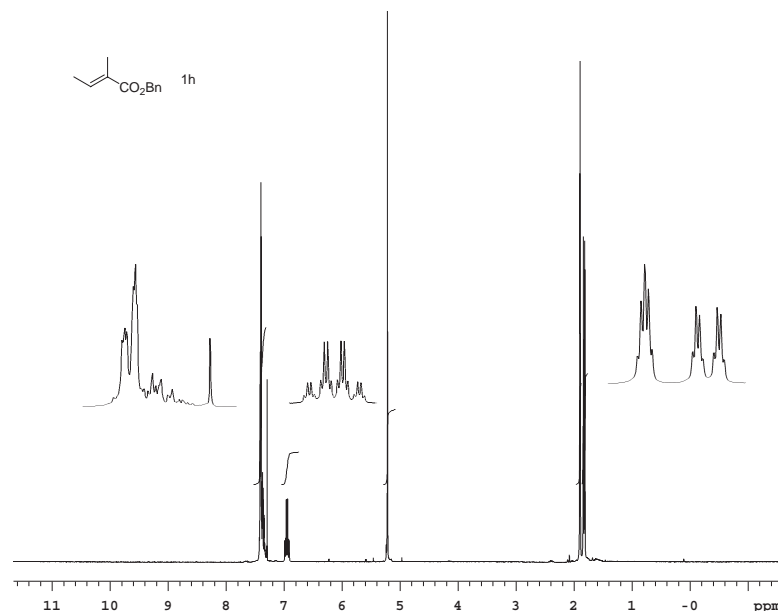
N-methoxy-N,2-dimethyl-(2E)-2-butenamide (2.1h).
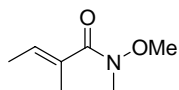
E-2-Methyl-2-butenoic acid (tiglic acid) (1 g, 10 mmol, 1 eq.) was dissolved in 20 ml of dichloromethane and was cooled to 0 °C. Oxalyl chloride (5 ml, 50 mmol, 5 eq.) was added to this solution dropwise, and was stirred for 30 min in ice followed by 30 min at ambient temperature. After concentrating under reduced pressure to remove excess oxalyl chloride, 20 ml of dichloromethane was added followed by cooling to 0 °C, then fresh methoxymethylamine hydrochloride (1.46 g, 15 mmol, 1.5 eq.) and then dimethylaminopyridine (2.44 g, 20 mmol, 2 eq.). This was allowed to stir for 18 h, and allowed to come to ambient temperature over time. After concentrating to a slurry under reduced pressure, the material was subjected to column chromatography with 15 % methanol in dichloromethane (Rf: 0.9) to give 1.1 g of the title compound, 77% isolated yield. ^{1}H NMR matched the known compound[71]. ^{1}H NMR (CDCl$_3$, 300 MHz): δ (ppm) = 5.96 (qq, *J* = 7.0, 7.0, 1.6, 1.5 Hz, 1H), 3.62 (s, 3H), 3.22 (s, 3H), 1.86 (s, 3H), 1.73 (dq, *J* = 6.8, 1.2 Hz, 3H).
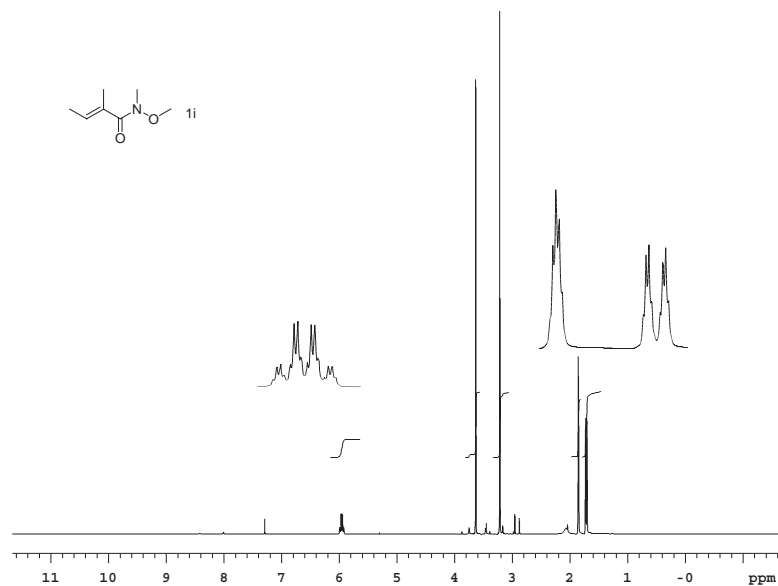
(4-Nitrobenzyl) *E*-2,-Methylbutenoate (2.1j).
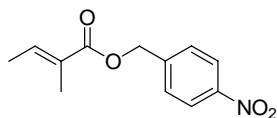
To a solution of tiglic acid (1.0 g, 1.0 eq., 10 mmol) in 10 ml of acetonitrile was added 2.16 g (1.0 eq., 10 mmol) 4-nitrobenzylbromide. This was allowed to stir at reflux for 18 h, after which time the reaction mixture was washed with water then 10 ml of saturated sodium carbonate 3 times. The organic layer was then concentrated *in vacuo* and 1.46 g, 46% isolated yield, was isolated by filtration as it crystallized from solution as an off-white powder identical by ^{1}H NMR to the known compound[72]. ^{1}H NMR (CDCl$_3$, 300 MHz): δ (ppm) = 8.27 (d, *J* = 9.8 Hz, 2H), 7.60 (d, *J* = 9.9 Hz, 2H), 6.95 (q, *J* = 6.8 Hz, 1H), 5.30 (s, 2H), 2.10 (s, 3H), 1.95 (d, *J* = 7.2 Hz, 3H).
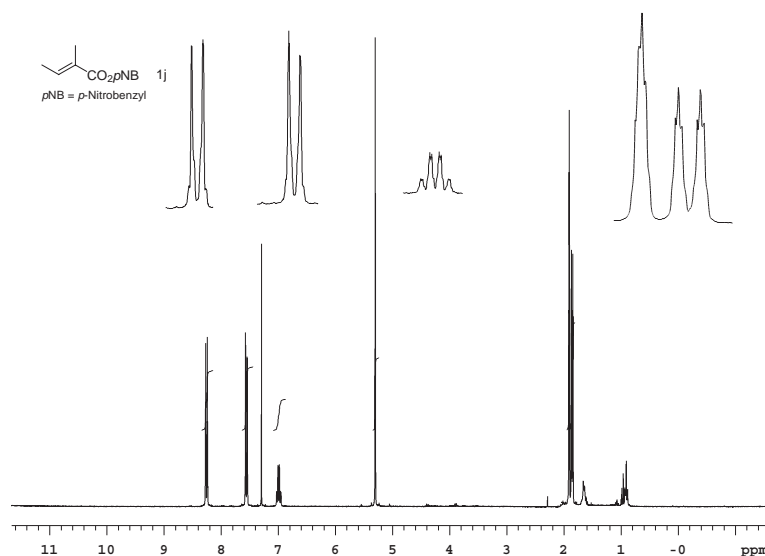
Tetrabutylammonium 2-Methyl-2-butenoate (2.1k).
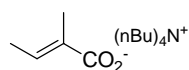
E-2-Butenoic acid (1 g, 10 mmol, 1 eq.) was added to 40 ml of water, and ammonium hydroxide was added until the solution had a slightly ammonical odor and was basic by litmus testing. After heating for 1 h at 70 °C to remove excess ammonia, silver nitrate (1.7 g, 10 mmol, 1 eq.) was added as a solution in 10 ml of water dropwise. Stirring for 20 min at 70 °C produced a solid which was filtered, then washed sequentially with water, ethanol, and ether, and dried 12 h under vacuum to produce 752 mg, 36 % isolated yield, of the silver salt as a white solid. This was then added along with tetrabutyl ammonium iodide (1.3 g, 3.6 mmol, 1 eq.) to 20 ml of methanol, and heated to 40 °C for 18 h. Filtration, and concentration of the filtrate under reduced pressure produced 1.2 g of the title compound, 98 % isolated yield over the second step, or 35 % yield overall. IR: 3389, 2875, 2326, 1649, 1556 cm^{-1} (most had hydrolized from hydration in air). ^{1}H NMR (CDCl$_3$, 300 MHz): δ (ppm) = 6.67 (qt, J = 7.1, 6.7, 1.5 Hz, 1H), 3.33 (t, J = 8.8 Hz, 12H), 1.83 (t, J = 1.1 Hz, 3H), 1.72 (d, J = 1.1 Hz, 3H), 1.70 (d, J = 1.1 Hz, 3H), 1.47 (hexet, J = 7.6, 7.1, 7.1 Hz, 12H), 1.01 (t, J = 7.2 Hz, 14H,). ^{13}C[^{1}H] (CDCl3, 100.4 MHz): δ (ppm) = 131.2, 100.2, 59.1, 24.3, 20.0, 13.9 (the tetrabutylammonium cation slowly precipitated out of solution during the acquisition). MS (M/Z, positive and negative modes): calculated (tiglic anion): 99.04, found (in negative mode): 99.02; calculated (tetrabutyl ammonium cation): 242.28, found (in positive mode): 242.28.
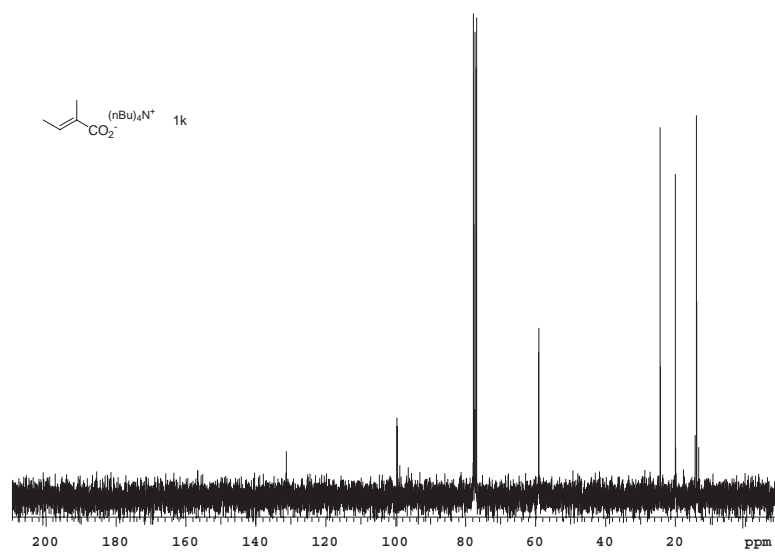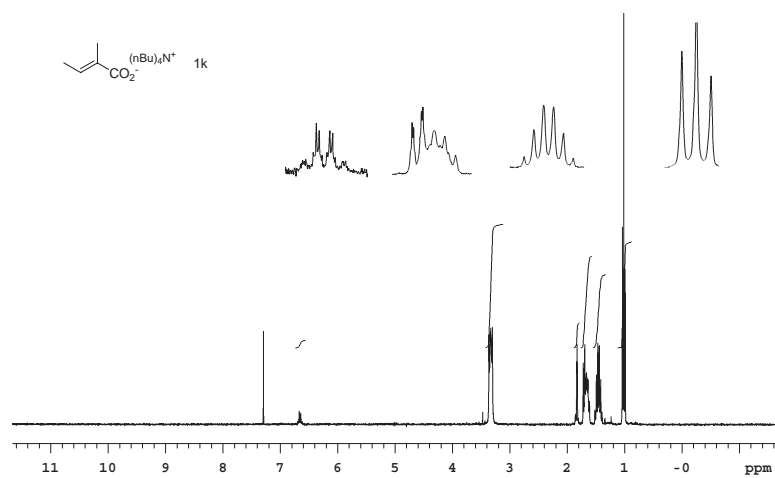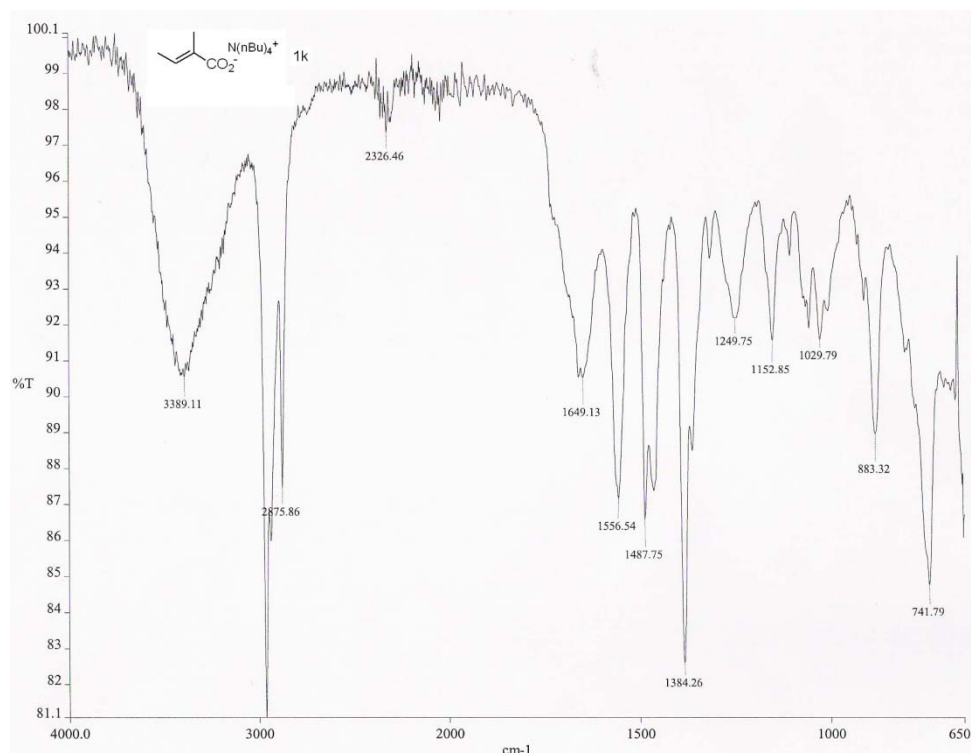
Methyl _E_-2,4-dimethylhexenoate (2.1l).
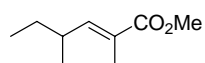
2-methylbutyraldehyde (1 g, 12 mmol, 1 eq.) was added to 4g (12 mmol, 1.05 eq.) methoxycarbonylethylidenetriphenylphosphorane in 30 ml of dichlormethane and was stirred at reflux for 18 h. The reaction mixture was then concentrated onto silica gel, and then column chromatography was performed 15 % ethyl acetate in hexanes to give the desired compound after concentrating under reduced pressure to give 1.24 g of the title compound, 44% yield. [48] ^{1}H NMR was indistinguishable from the pure _S_-compound, and both matched the known compound.[48] ^{1}H NMR (CDCl$_3$, 300 MHz): δ (ppm) = 6.57 (dq, _J_ = 10.0, 1.6, 1.5 Hz, 1H), 3.76 (s, 3H), 2.44 (m, 1H), 1.87 (d, _J_ = 1.3 Hz, 3H), 1.41 (m, 2H), 1.02 (d, _J_ = 6.5 Hz, 3H), 0.88 (t, _J_ = 7.6 Hz, 3H).
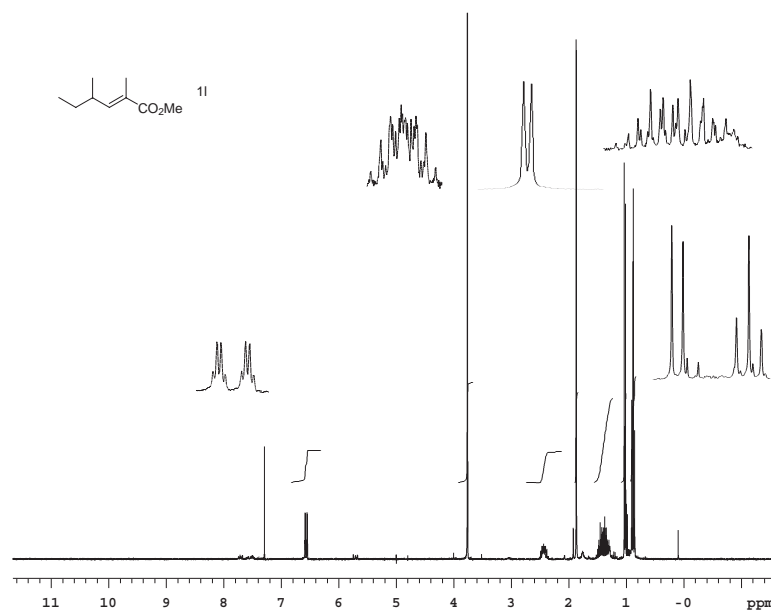
Methyl *E*-2,4-dimethylpentenoate (2.1n).
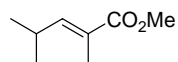
Isobutyraldehyde (1.3 g, 18 mmol, 1 eq.) was added to methoxycarbonylethylidenetriphenylphosphorane (6.1 g, 18.4 mmol, 1.02 eq.) in 30 ml of dichlormethane and was stirred at reflux for 18 h. The reaction mixture was then concentrated onto silica gel, and then column chromatography was performed with 5 % ethyl acetate in hexanes to give the desired compound after concentrating under reduced pressure to give 1.5 g, 59 % yield. ^{1}H NMR matched the known compound.[73] ^{1}H NMR (CDCl$_3$, 300 MHz): δ (ppm) = 6.61 (dq, *J* = 9.6, 1.5 Hz, 1H), 3.77 (s, 3H), 2.7 (m, *J* = 3.0 Hz, 1H), 1.88 (d, *J* = 1.5, 3H), 1.06 (d, *J* = 6.7 Hz, 6H).
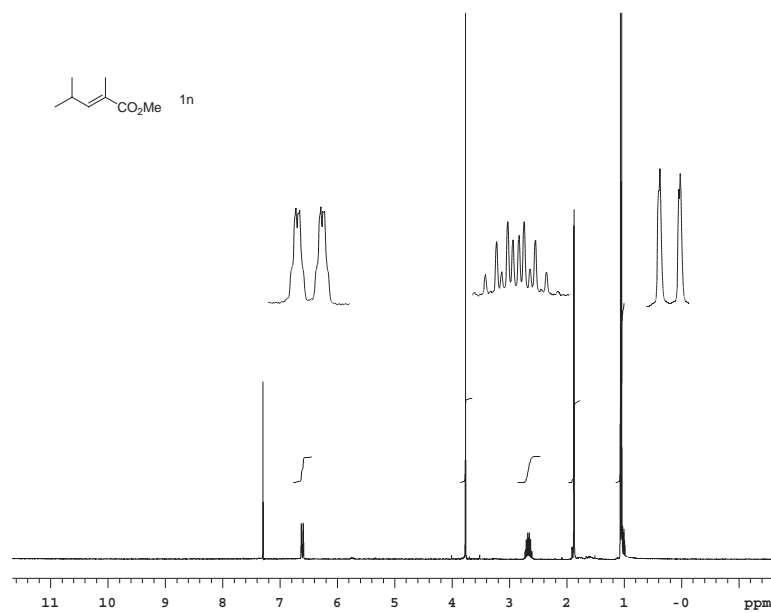
Methyl *E*,3-(4-methylfuryl)-2-methyl-2-butenoate (2.1o).
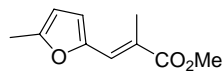
4-Methyl furfural (2.64 g, 24 mmol, 1.2 eq) was added to a solution of methoxycarbonylethylidenetriphenyl-phosphorane (7 g, 20 mmol, 1 eq.) dissolved in 40 ml of dichloromethane. This was then connected with a reflux adaptor and heated for 18 h at reflux. After cooling, concentration under reduced pressure, and forming a slurry with diethyl ether (100 ml), the reaction mixture was purified by column chromatography to produce 2.25 g of the title molecule, 62 % isolated yield. ^{1}H NMR was identical to the known compound.[71] ^{1}H NMR (CDCl$_3$, 300 MHz): δ (ppm) = 7.37 (s, 1H), 6.5 (d, *J* = 3.7 Hz, 1H), 6.09 (d, *J* = 3.7 Hz, 1H), 3.77 (s, 3H), 2.34 (s, 3H), 2.19 (s, 3H).

Methyl _E_-α-Cinnimate (2.1p).

Ph—CH=C(CH₃)—CO₂Me
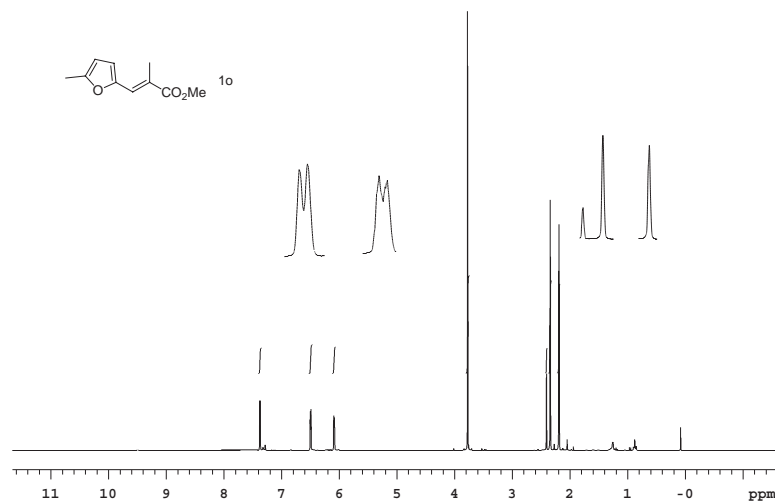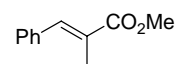
Benzaldehyde (2 g, 18.8 mmol, 1eq.) was added to methoxycarbonylethylidenetriphenylphosphorane (7 g, 20 mmol, 1.05 eq.) in 50 ml of dichlormethane and was stirred at reflux for 18 h. The reaction mixture was then concentrated onto silica gel, and then column chromatography was performed using 15 % ethyl acetate in hexanes to give the desired compound after concentrating under reduced pressure: 2.8 g, 88 % yield. ^{1}H NMR matched the known compound.[74] ^{1}H NMR (CDCl$_3$, 300 MHz): δ (ppm) = 7.70 (s, 1H), 7.36-7.28 (m, 5H), 3.78 (s, 3H), 2.11 (d, _J_ = 2.0 Hz, 3H).
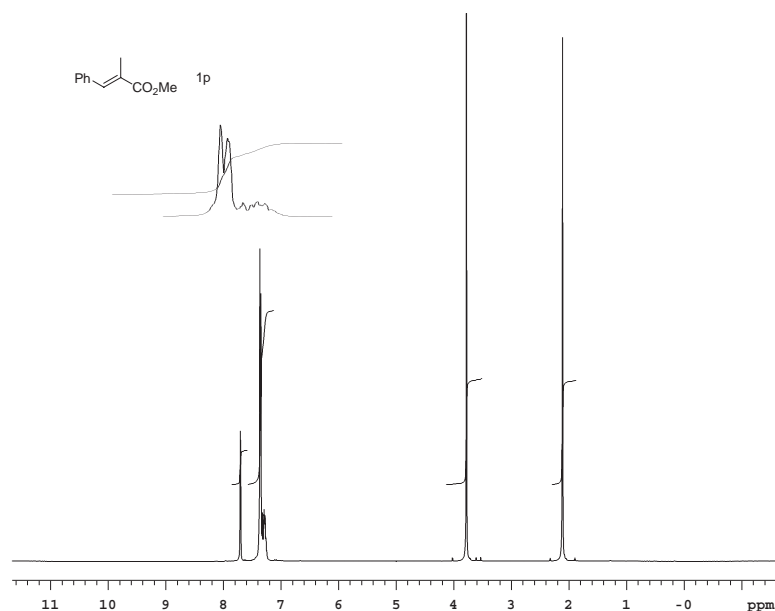
Hydrogenation of substrates 2.1
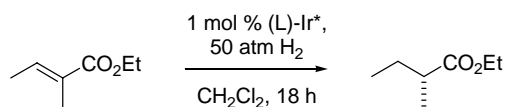
Reaction 2.1

The procedure for hydrogenation of ethyl tiglate is representative for substrates **1**. To ethyl tiglate (129 mg, 1.0 mmol) was added 17.5 mg catalyst (10 μmol, 1 mol %), followed by 100 μl dichloromethane (2M in ethyl tiglate) in a small, 1 cm wide, test tube. This was immediately capped, and was degassed 3 times before placing into a cylindrical Parr bomb (internal dimensions of 2 inches by 6 inches). The Parr bomb was then flooded with a stream of hydrogen, to replace the atmosphere inside of it completely with hydrogen. The external vent was closed, and the pressure increased slowly to 20 atm. Stirring was then started at approximately 800 rpm. After 4 h, the stirring was stopped, the bomb slowly allowed to return to 1 atm, and the sample taken out in order to determine conversion and stereoselectivity (see determination of absolute stereochemistry below). Screening reactions were typically performed on 0.2 mmol of substrate.

Reaction 2.1 scheme and ^{1}H NMR spectrum
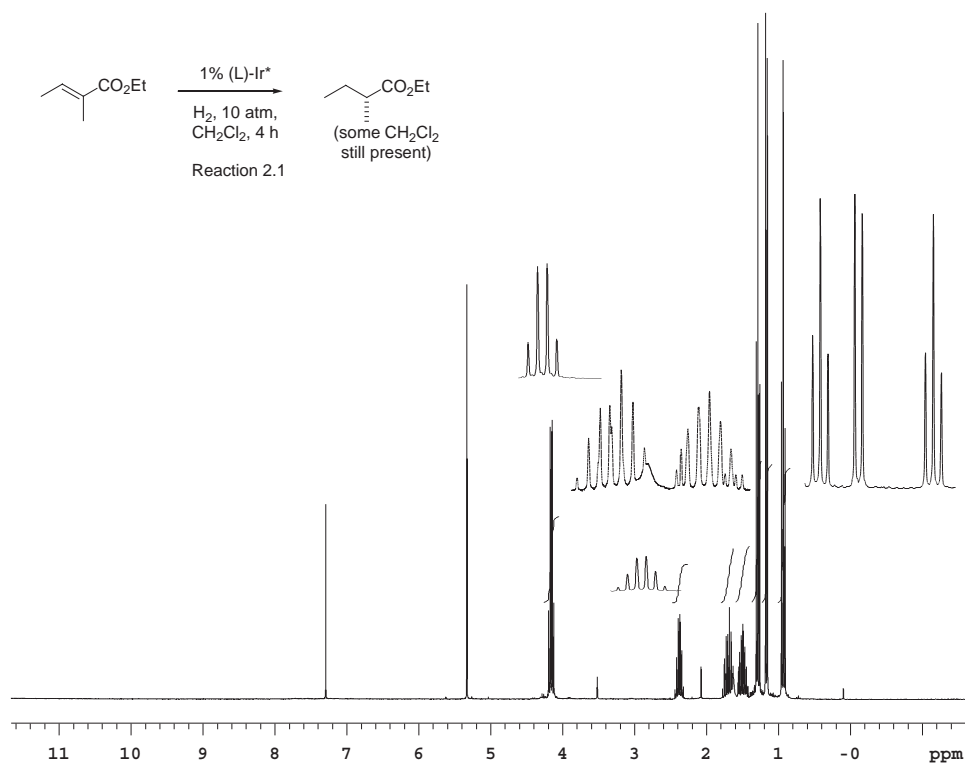
Determination of Absolute Stereochemistry

General. GC analysis of compounds 2 was first performed and compared to racemic samples generated from 10% Pd/C with H_2 to determine *ee* (in most cases, baseline resolution could be obtained, except as noted in Table 2.1 and below). To determine absolute configuration, comparison with commercially available (S)-2-methylbutanol and racemic 2-methylbutanol via chiral GC analysis was performed. Compounds 2f, 2g, 2h, 2i, 2j, and 2k were chemically derived to form their alcohol counterparts by reduction with 3-5 eq. lithium aluminum hydride (noted below) followed by washing with sodium potassium tartrate solution (5-10 ml), extracting the organic phases with additional dichloromethane (10-20 ml), concentrating this sample, diluting with hexanes, filtering through a celite plug, and directly injecting onto chiral GC column. Compound 2d was hydrogenated using 10% Pd/C with H_2 and filtered to give the corresponding alcohol, and 2b was reacted with TBAF followed by extraction with 20 ml of dichloromethane and water to generate the alcohol. After the analysis of hydrogenated tiglic acid (2g), product 2k was acidified and compared to the now known retention time of (R)-2-methyl butanoic acid via GC analysis. The absolute configurations of compounds 2e, 2m, 2n, 2o, and 2p were assigned by analogy.

(S)-2-Methylbutanol (2.1a).
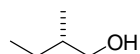
After hydrogenating compound 1a, *E*-2-methyl-2-butenol (tiglic alcohol), the sample was directly injected for analytical comparison with the known compound by chiral GC to give the title compound in 83 % *ee*.
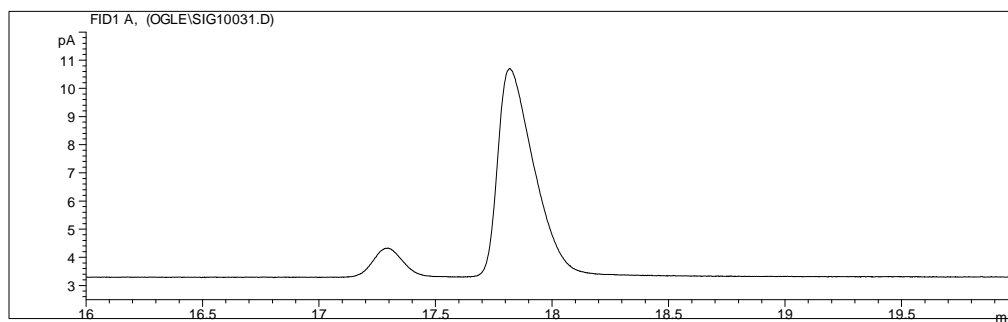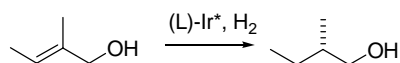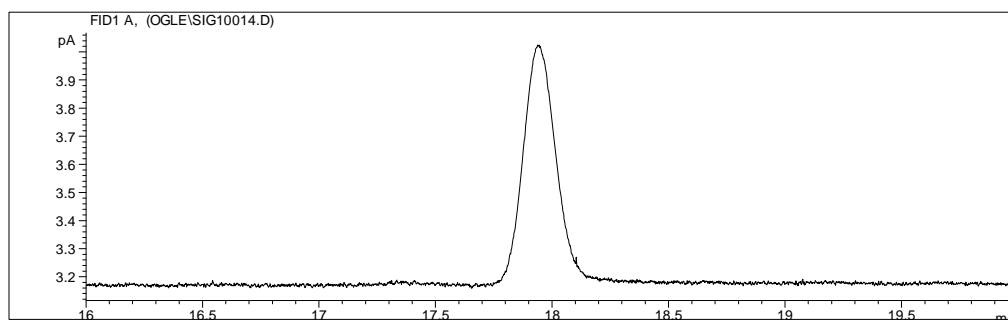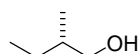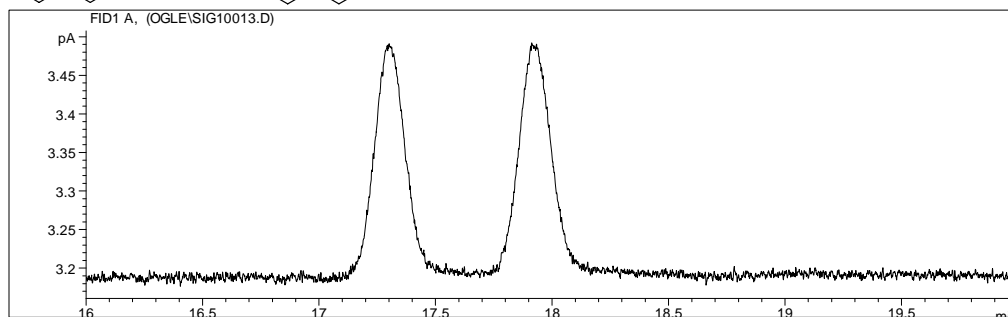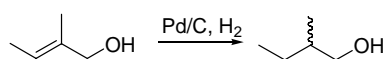
1-((S)-2-methyl-2-butanyl)-*tert*-Butyldimethylsilyl Ether (2.1b).
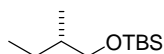
After hydrogenating 1-(E-2-methyl-2-butenyl)-*tert*butyldimethylsilyl ether, the sample was mixed with tetrabutylammonium fluoride for 10 min, then filtered through a silica plug eluted with 30 % ethyl acetate in hexanes, then the sample was directly injected for analysis into chiral GC to give the known butanol compound in 49 % *ee*.
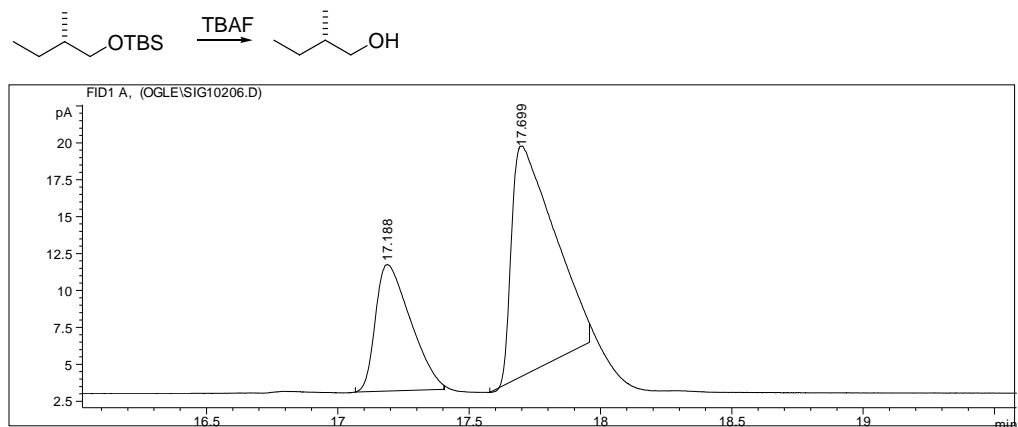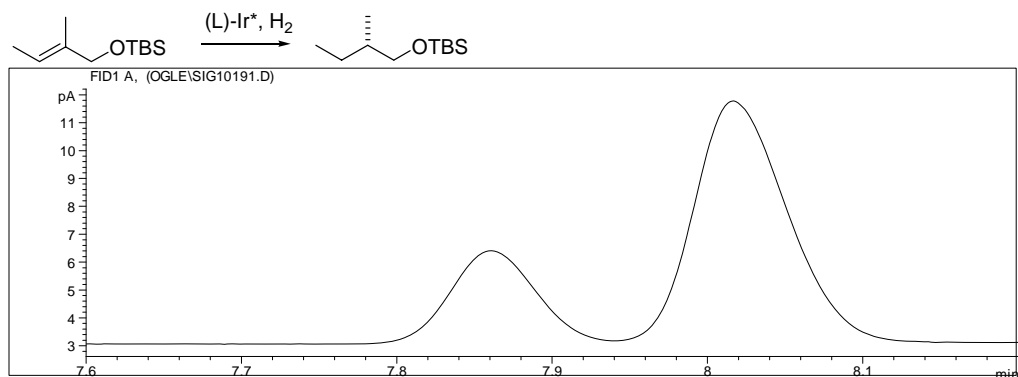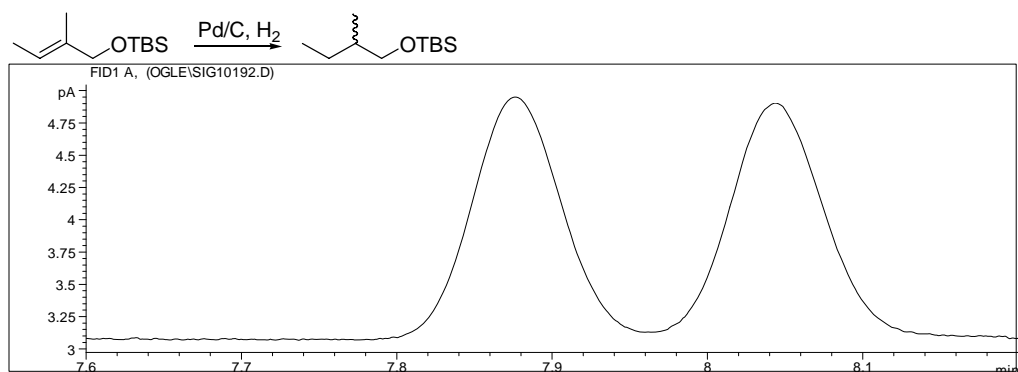
(S)-2-Methylbutanal (2.1c).
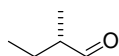
After hydrogenating ethyl *E*-2-methyl-2-butenoate, injecting the reaction mixture directly after hydrogenation revealed fully reduced butanol, indicating reduction of the aldehyde in 54 % *ee*.
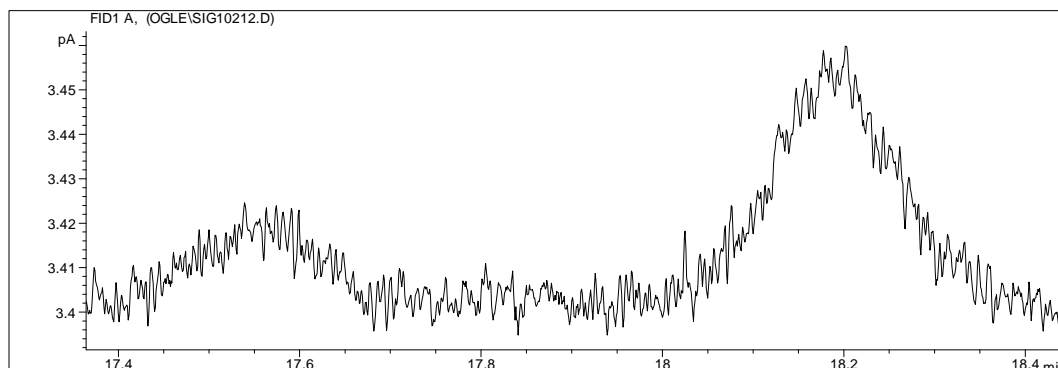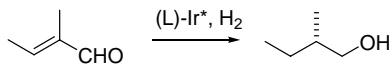
(*S*)-1-(Oxobenzyl)-2-methylbutane (2.1d).
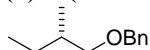
After hydrogenating *E*-1-(oxobenzyl)-2-methyl-2-butene, the sample was reacted with 10 % palladium on carbon with a balloon of hydrogen for 6 h, filtered through a celite then a silica plug with 30 % ethyl acetate in hexanes, and directly injected for analysis into chiral GC to give the known butanol compound in 59 % *ee*.

No resolution at this stage

FID1 A, (OGLE\SIG10198.D)
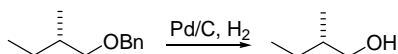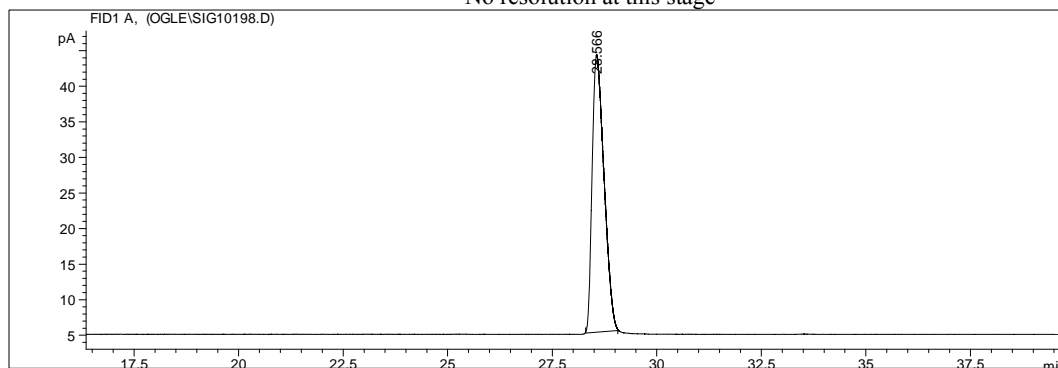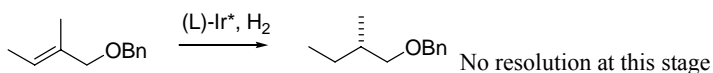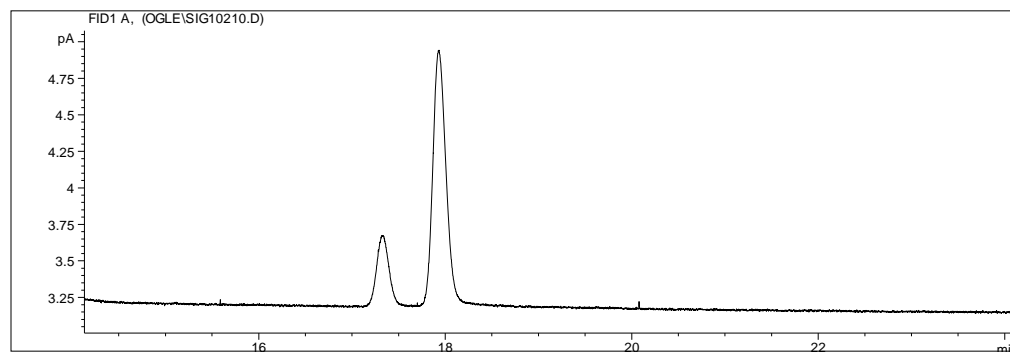
2-Methyl-3-phenylpropanol (2.2e).
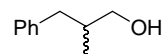
After hydrogenating 2-methylcinnamyl alcohol as above, filtration through a plug of silica followed by GC analysis by comparing with the racemic ester showed 87 % *ee*.

Ethyl (R)-2-Methylbutanoate (2.1f).
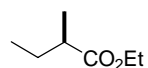
After hydrogenating ethyl E-2-methyl-2-butenoate, the sample was reduced with lithium aluminum hydride as described above to give the title compound in 67 % ee. 10.75 min peak is an impurity form ethyl acetate in this case.

(solvent impurity at 10.75 min)

FID1 A, (OGLE\SIG10032.D)

FID1 A, (OGLE\SIG10164.D)
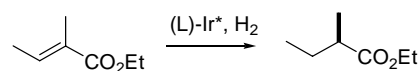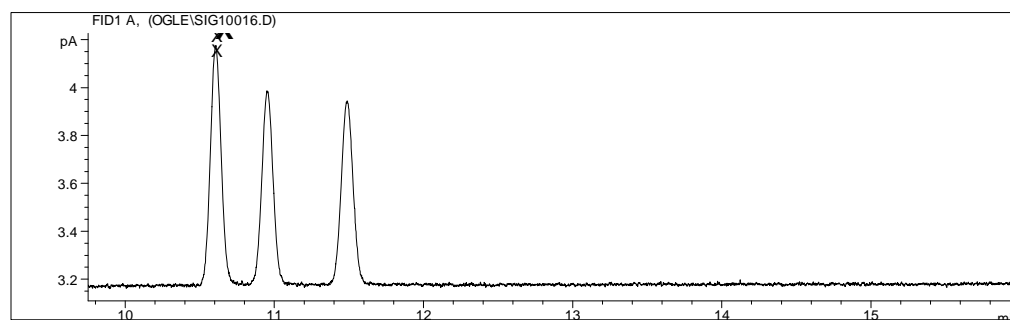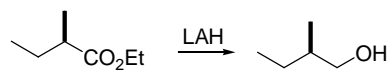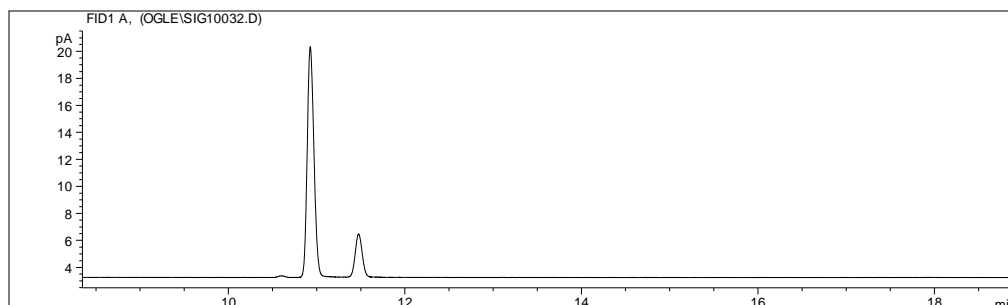
(R)-2-Methylbutanoic acid (2.1g).
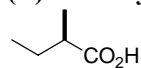
After hydrogenating E-2-methyl-2-butenoic acid (tiglic acid), the sample was reduced with lithium aluminum hydride as described above to give the title compound in 55 % ee.

FID1 A, (OGLE\SIG10169.D)

FID1 A, (OGLE\SIG10261.D)

LAH

FID1 A, (OGLE\SIG10205.D)
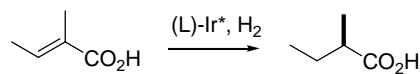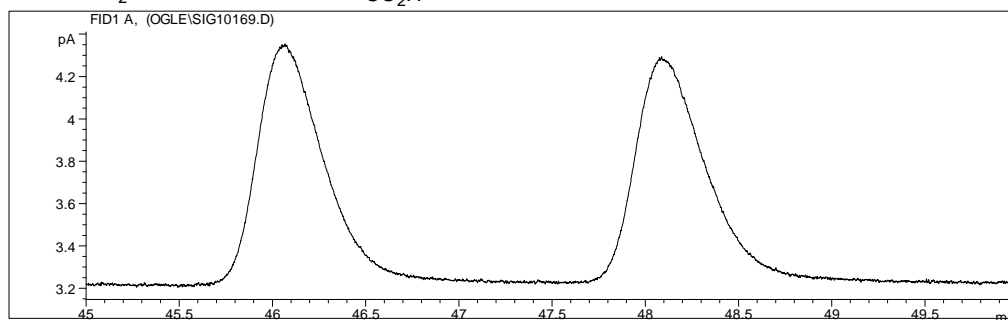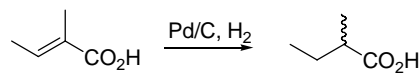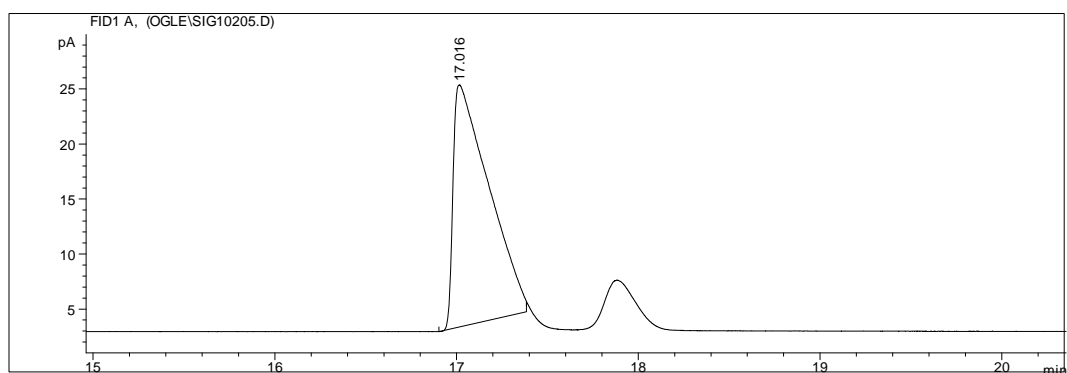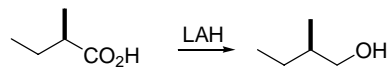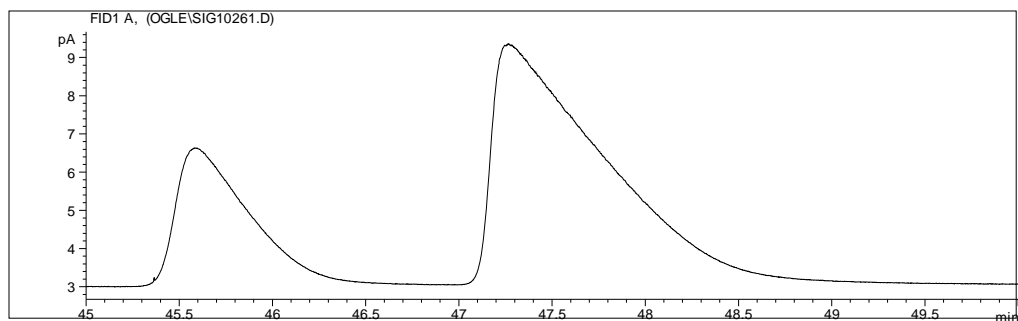
Benzyl (R)-2-Methylbutanoate (2.1h).
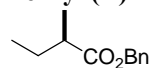
After hydrogenating benzyl *E*-2-methyl-2-butenoate, the sample was reduced with lithium aluminum hydride as described above to give the alcohol compound in 72 % *ee*.

FID1 A, (OGLE\SIG10143.D)

FID1 A, (OGLE\SIG10171.D)

FID1 A, (OGLE\SIG10310.D)
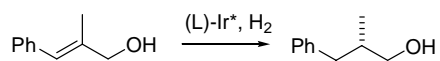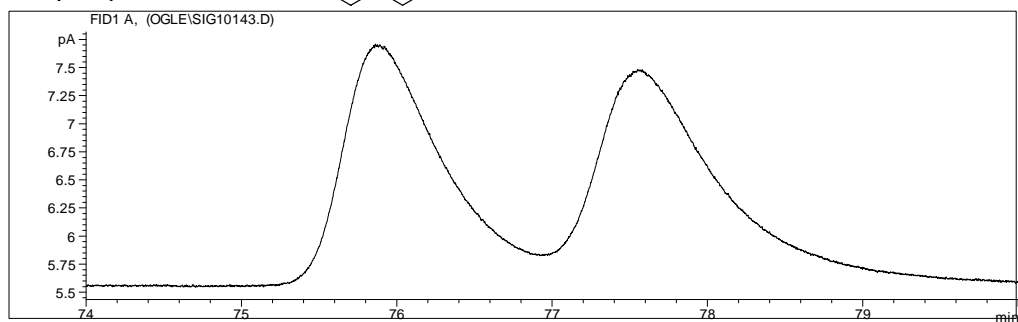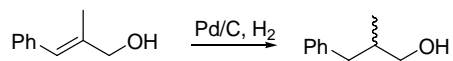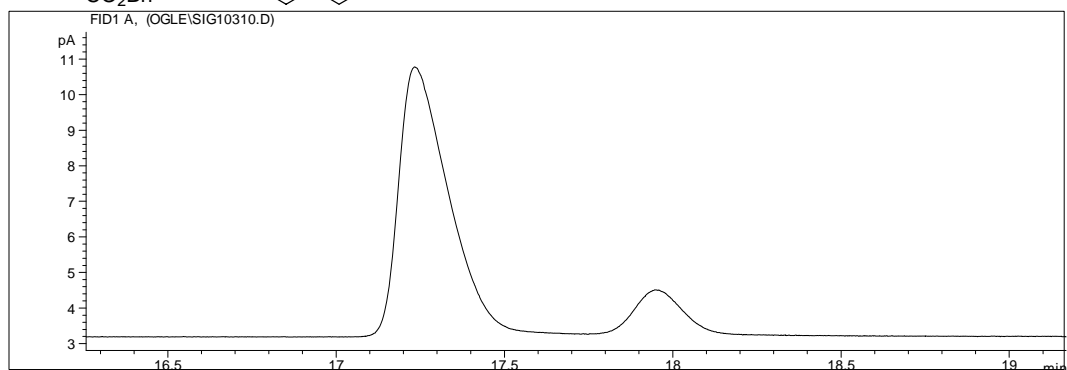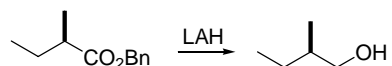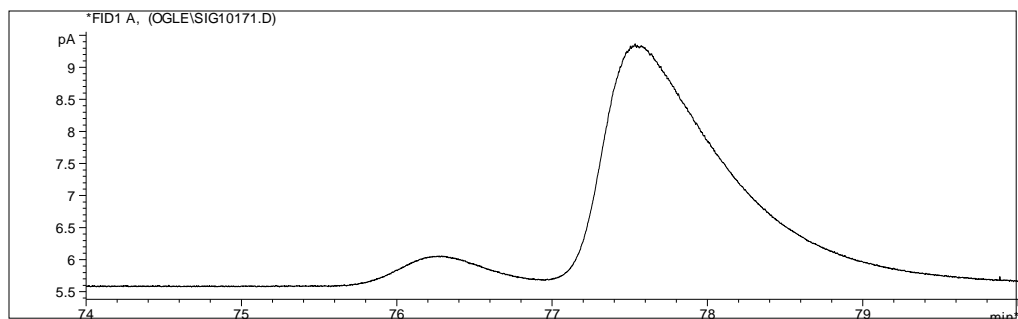
(R)-N,2-Dimethyl-N-methoxybutanamide (2.1i).
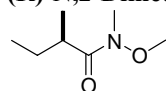
After hydrogenating N-methoxy-N,2-dimethyl-(2E)-2-butenamide, the sample was reduced with lithium aluminum hydride as described above to give the title compound in 46 % ee.

FID1 A, (OGLE\SIG10159.D)

FID1 A, (OGLE\SIG10155.D)

FID1 A, (OGLE\SIG10211.D)
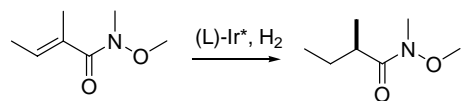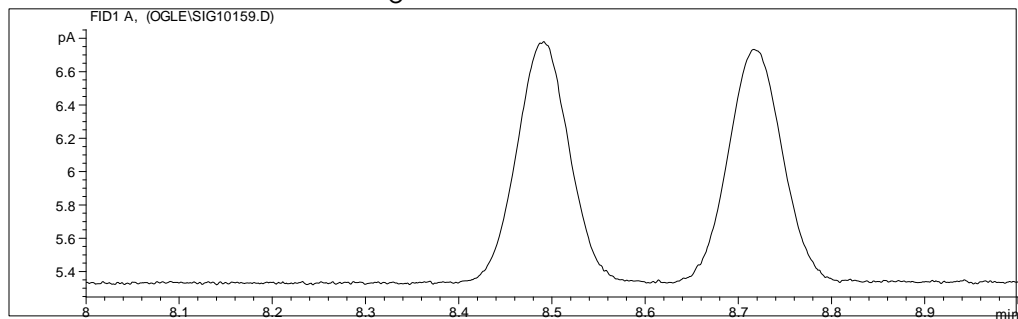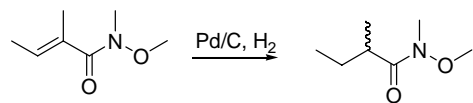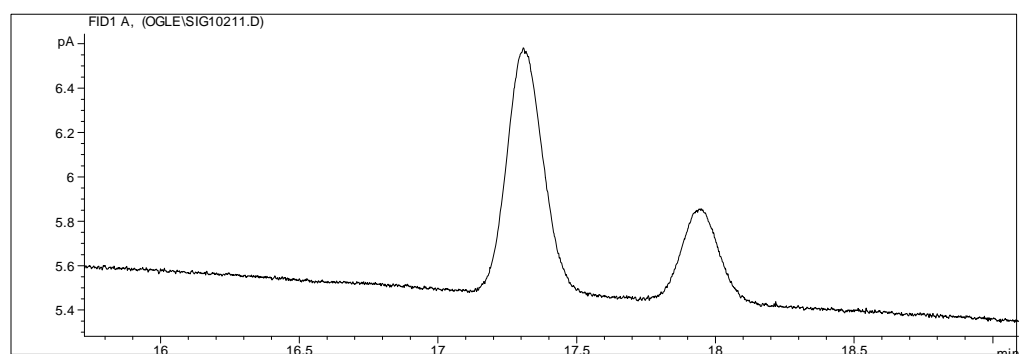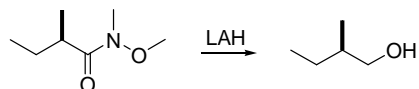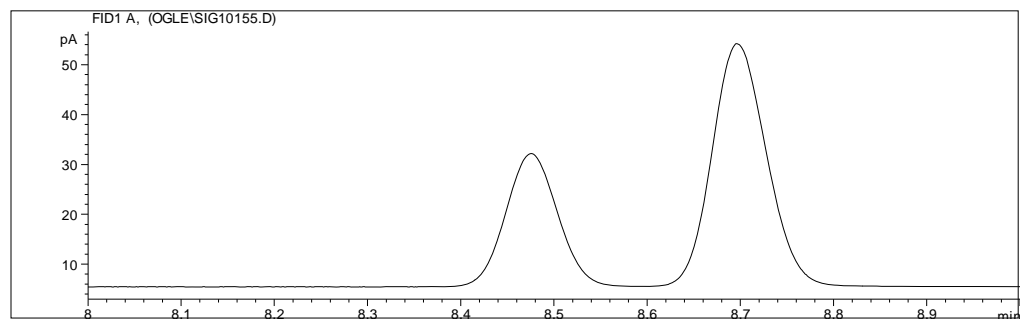
(4-Nitrobenzyl) (R)-2-Methylbutanoate (2.1j).
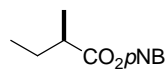
After hydrogenating (4-nitrobenzyl) *E*-2-methyl-2-butenoate, the sample was reduced with lithium aluminum hydride as described above to give the title compound in 42 % *ee*, but only 22 % overall conversion.
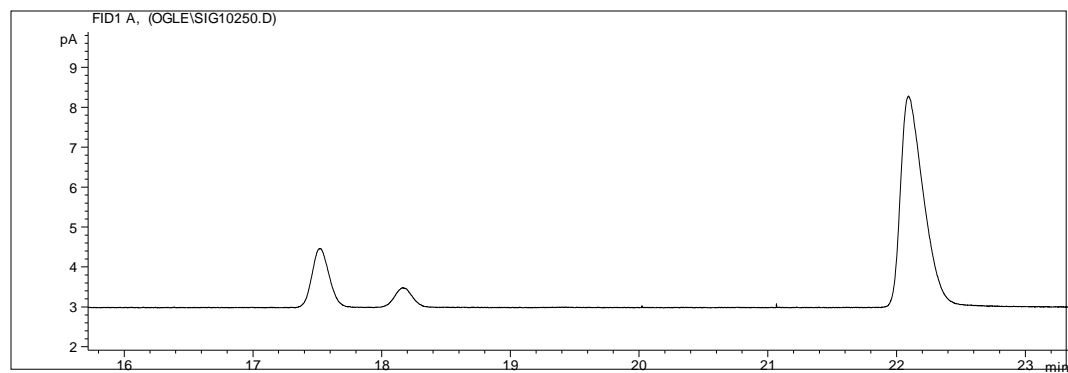
Tetrabutylammonium (R)-2-Methylbutanoate (2.1k).
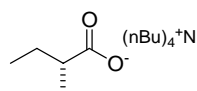
After hydrogenating tetrabutylammonium *E*-2-methyl-2-butenoate, the sample was acidified in 1 M HCl then extracted with dichloromethane for comparison with the known tiglic acid by chiral GC to give the acid in 27 % *ee*.
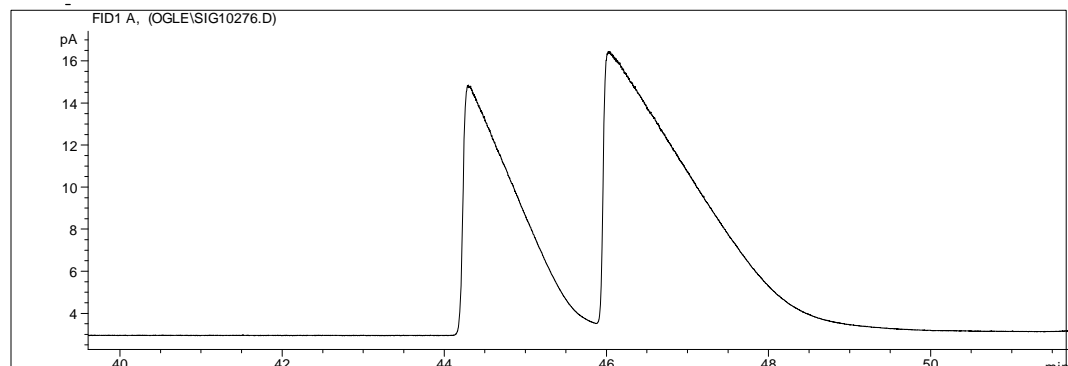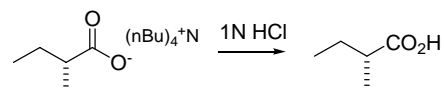
Methyl (2R)-2,4-Dimethylhexanoate (2.1l).
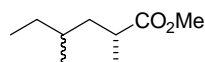
After hydrogenating *E*-2,4-dimethyl-2-hexenoate as above, filtration through a plug of silica followed by GC analysis showed 1.0:1.0 *d.r.* and 57% *ee*. The absolute configuration was determined by later comparison with the known esters (see Products 4a-4d below).
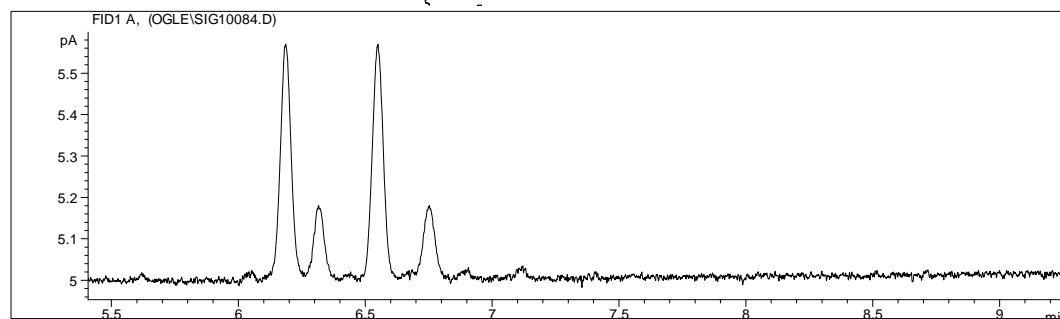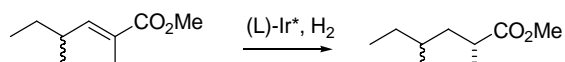
Methyl 2-Methylpentanoate (2.1m).
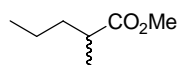
Commercially available methyl *E*-2-methylpenta-2-enoate was hydrogenated as above, filtered through a small plug of silica, and analyzed by chiral GC analysis by comparison with the racemic mixture produced by hydrogenation of the same substrate with 10% Pd / C with 1 atm H$_2$ to give 65 % *ee*, comparable to ethyl tiglate. Absolute determination of stereochemistry was not performed; the proposed R-isomer product is predicted by analogy.
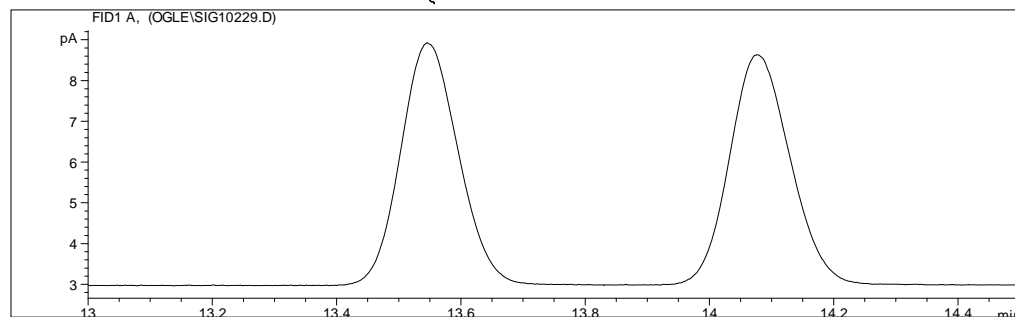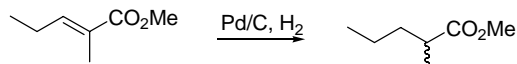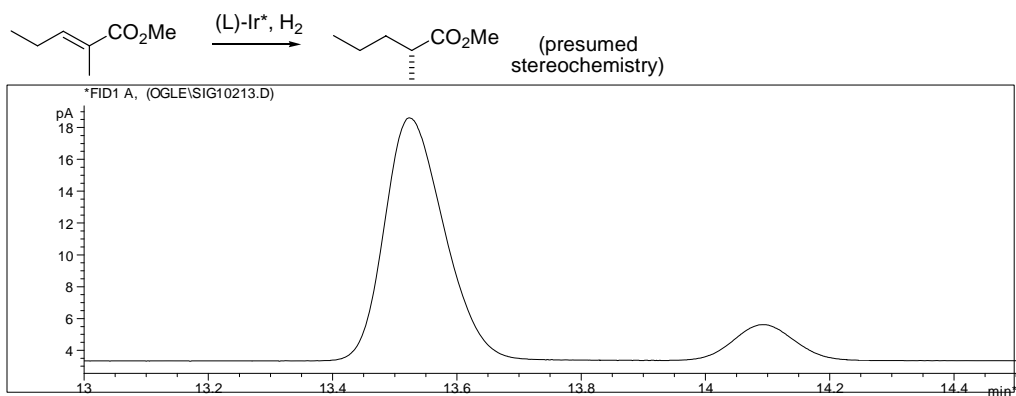
Methyl 2,4-Dimethylpentanoate (2.1n).
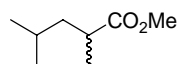
After hydrogenating ethyl *E*-2-methyl-2-butenoate, the sample was filtered to remove excess catalyst in 54 % *ee*. Absolute determination of stereochemistry was not performed; the proposed R-isomer product is predicted by analogy.
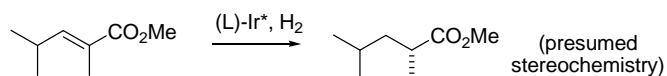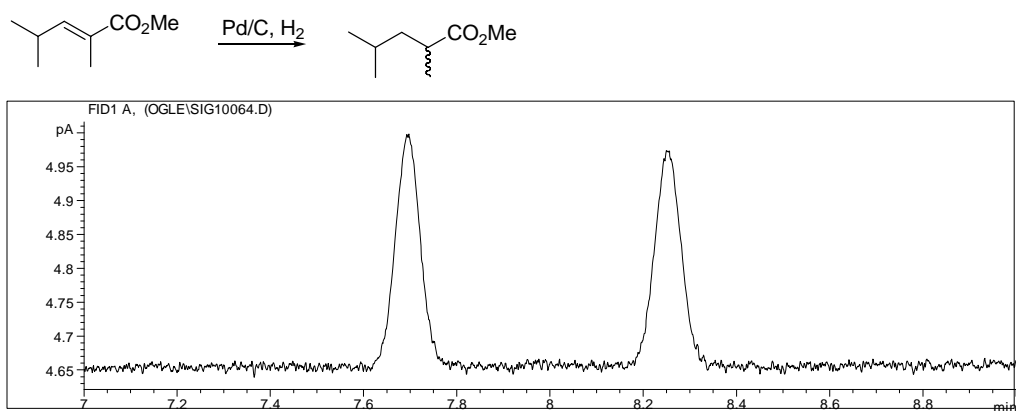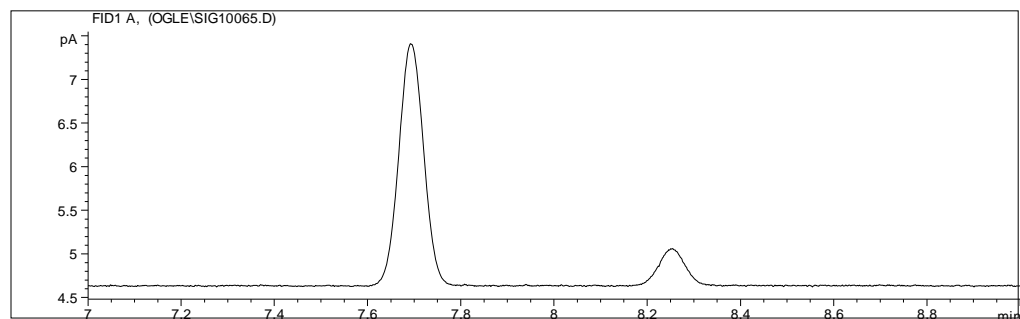
Methyl 2-Methyl-3-(4-methylfuryl)propionate (2.1o).
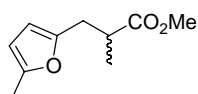
After hydrogenating methyl E,3-(4-methylfuryl)-2-methyl-2-butenoate, the sample was filtered to remove excess catalyst in 42 % *ee*. Injecting the reaction mixture directly after filtration also revealed a qualitatively cleaner reaction than that produced from the Pd/C generated racemic mixture (presumably from partial furyl reduction). Absolute determination of stereochemistry was not performed; the proposed R-isomer product is predicted by analogy.
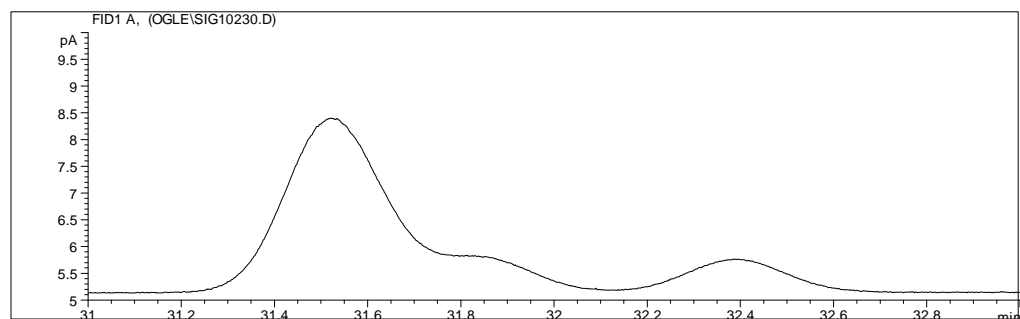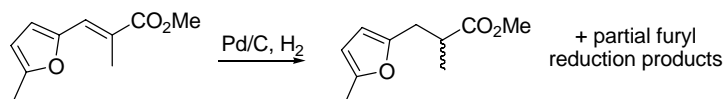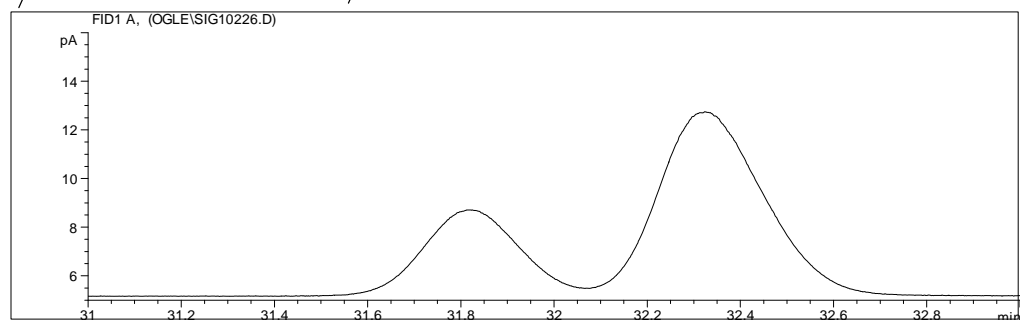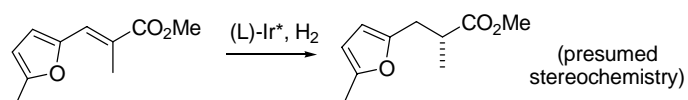
Methyl (2R)-Methyl-3-phenylpropionate (2.1p).
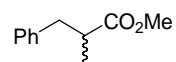
After hydrogenating methyl 2-methylcinnamate as above, filtration through a plug of silica followed by GC analysis by comparing with the racemic ester showed less than 20 % *ee*.
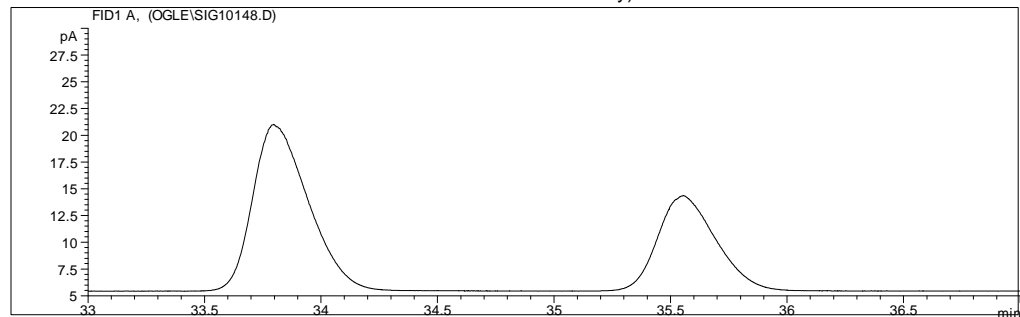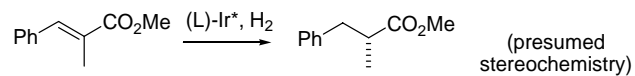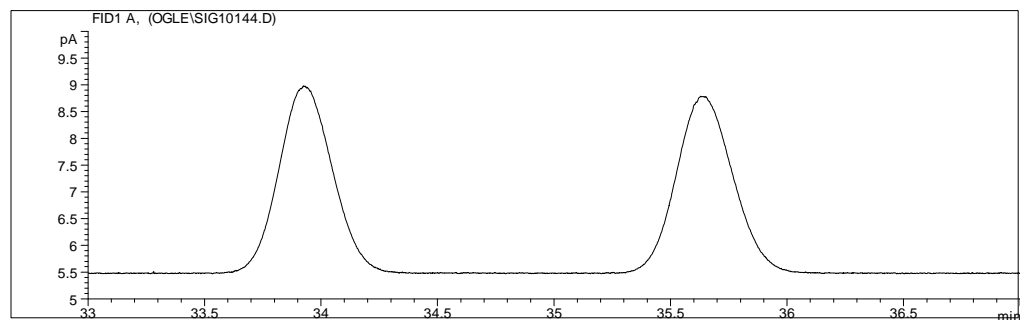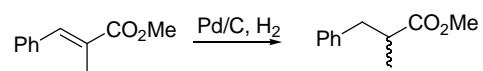
All Four 2,4-Dimethylhexane-1-*O*-dyads from 1 Catalyst

Methyl *E,E*-2,4-Dimethyl-2,4-hexadienoate (2.3a).
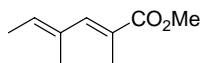
To a solution of methoxycarbonylethylidenetriphenylphosphorane (3.8 g, 11 mmol, 1.05 eq.) in dichloromethane (25 ml) was added *E*-2-methyl-2-butenal (860 mg, 10 mmol, 1 eq.). This solution was then heated at 40 °C for 18 h, at the end of which time it was concentrated *in vacuo* onto silica gel and column chromatography was performed (0-2% EtOAc/Hexanes, Rf = 0.55). Concentration yielded 1.1 g of the title compound as a clear oil, 70% isolated yield. The ^{1}H NMR matches the known compound.[75,76] ^{1}H NMR (CDCl$_3$, 300 MHz): δ (ppm) = 6.52 (s, 1H), 5.12 (q, *J* = 7.5 Hz, 1H), 3.14 (s, 3H), 1.40 (s, 3H), 1.24 (s, 3H), 1.14 (d, *J* = 7.0 Hz, 3H).
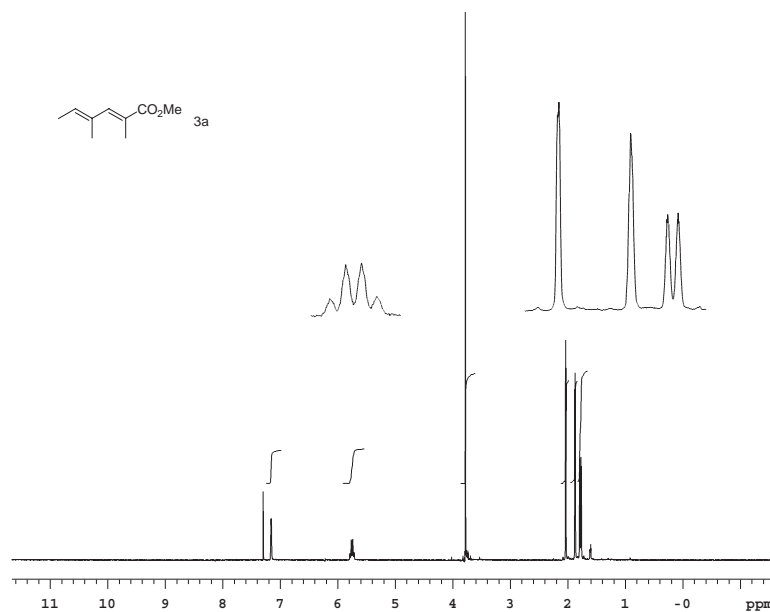
_E,E_-2,4-Dimethyl-2,4-hexadienol (2.3b).
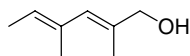
Methyl-*E,E*-2,4-dimethyl-2,4-hexanoate (2.5 g, 16 mmol, 1 eq.) was added to 100 ml of dichloromethane and cooled to 0 °C. To this was added diisobutylaluminum hydride dropwise (43 mmol, 2.7 eq., 1 M in hexanes), and was stirred for 3 h, at which time it was quenched by slow addition of 50 ml of methanol (the addition was slow enough

such that the temperature never raised past 10 °C). After quenching, 100 ml of a solution of saturated sodium potassium tartrate was added and stirred for 2 h, after which time 30 ml of diethyl ether was added, and the layers separated. The aqueous layer was separated an additional 3 times with 30 ml of diethyl ether, and the combined organic extracts dried over anh. sodium sulfate. Concentration of the organic layers followed by column chromatography (20 % ethyl acetate in hexanes, Rf 0.3) afforded 1.54 g, a 75 % yield of the title compound. The ^{1}H NMR matches the known compound.[76,77] ^{1}H NMR (CDCl$_3$, 300 MHz): δ (ppm) = 5.92 (s, 1H), 5.46 (qt, J = 6.8 Hz, 1H), 4.07 (s, 2H), 1.84 (s, 3H), 1.78 (s, 3H), 1.72 (d, J = 7.0 Hz, 3H).
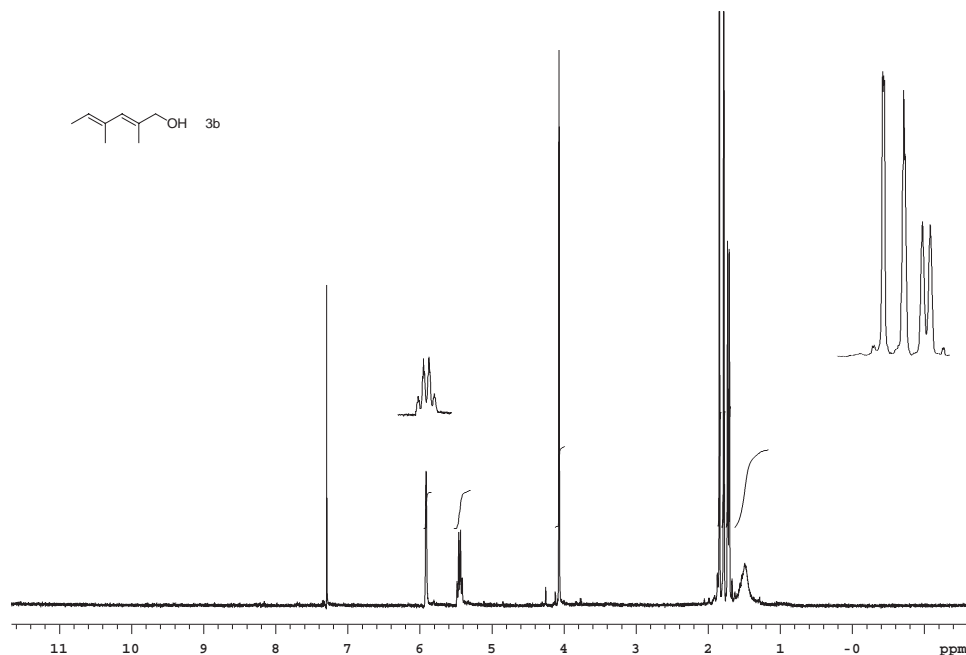
Methyl (S)-*E*-2,4-Dimethyl-2-hexenoate (2.3c).
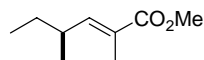
 (S)-2-Methyl butanol (3.4 g, 40 mmol, 1 eq.) was added to a slurry of 200 ml of dichloromethane, 4 A molecular sieves (680 mg), and tetrapropylammonium perruthenate (80 mg, 0.40 mmol, 5 mol%). *N*-Methyl morpholine *N*-oxide (10 g, 84 mmol, 2.1 eq.) was added to this solution all at once, and the resulting heterogeneous mixture was stirred for 6 h at 25 °C. The reaction mixture was filtered through a plug of silica, and the filtercake and silica plug were rinsed with more dichloromethane (200 ml). The combined dichloromethane filtrate was concentrated *in vacuo* to about half volume from a water bath at 5 °C, and the resulting (S)-2-methylbutanal was used in the next step without further purification (^{1}H NMR of the crude mixture matches the known compound: 9.65 (q, J = 2.05 Hz,

1H), 3.54 (m, 1H), 1.8-1.16 (m, 4H), 1.13 (d, J = 6.96 Hz, 3H)). A solution of methoxycarbonylethylidenetriphenyl-phosphorane (5.0 g, 160 mmol, 4.0 eq.) in dichloromethane (100 ml) was made and added to the (S)-2-Methylbutanal from the previous step. This solution was then heated at 40 °C for 18 h, at the end of which time it was concentrated *in vacuo* onto silica gel and column chromatography was performed (0-2% EtOAc / Hexanes). Concentration yielded 4.44 g of the title compound, 71.1% isolated yield over both steps. The ^{1}H NMR is indistinguishable from the enantiomer of the known compound, and was identical in all respects to the racemic ester made above[78]. ^{1}H NMR (CDCl₃, 300 MHz): δ (ppm) = 6.65 (dq, J = 10.3, 1.4 Hz, 1H), 3.74 (s, 3H), 2.40 (m, 1H), 1.85 (s, 3H), 1.75-1.10 (m, 3H), 1.00 (d, J = 6.8 Hz, 3H), 0.85 (t, J = 7.6 Hz, 3H).
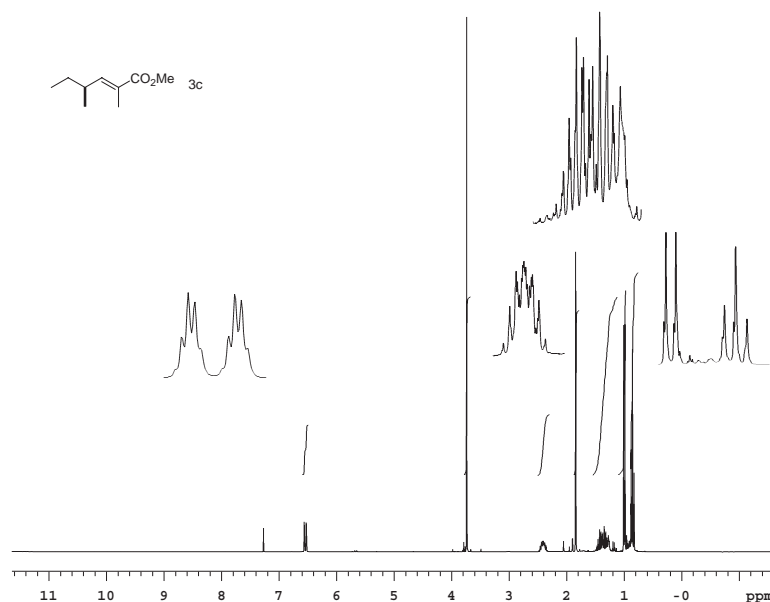
(S)-*E*-2,4-dimethyl-2-hexenol (2.3d).
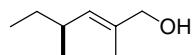
(S)-Methyl-*E*-2,4-dimethyl-2-hexenoate (200 mg, 1.3 mmol, 1 eq.) was added as a solution in 5 ml diethyl ether to 20 ml of diethyl ether with lithium aluminum hydride (150 mg, 3.8 mmol, 3 eq.) at 0 °C, and was stirred for 30 min, at which time it was quenched by slow addition of 5 ml of water (the addition was slow enough such that the temperature never raised past 10 °C). After quenching, the layers were separated, and the aqueous layer washed with 10 ml of diethyl ether 4 times. The combined organic extracts dried over anh. sodium sulfate. Concentration of the ether layers *in vacuo* afforded 142 mg, 85.4% yield of the title compound. The ^{1}H NMR matches the known compound.[48,79] ^{1}H NMR (CDCl₃, 300 MHz): δ (ppm) = 5.16 (quartet of quintets, J = 9.9, 1.2 Hz, 1H), 3.98 (s, 2H),

2.3-2.0 (m, *J* = 8.5, 6.5, 6.7 Hz, 1H), 1.65 (d, 2H), 1.65 (bs, 1H), 1.40-1.15 (m, 2H), 0.93 (d, *J* = 6.6 Hz, 3H), 0.85 (t, *J* = 7.4 Hz, 3H) (some grease in the actual spectra).
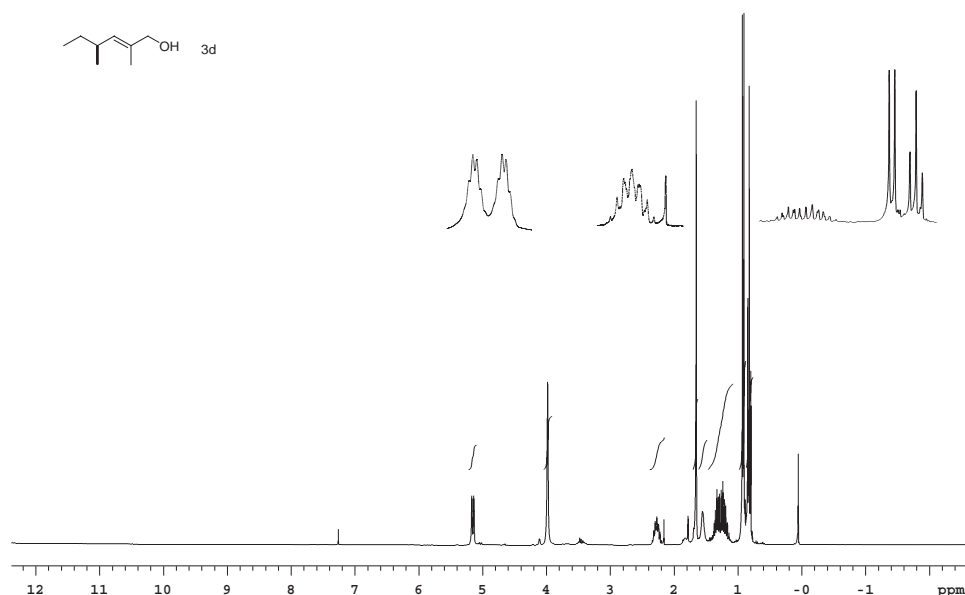
Hydrogenation of Dienes and Mono-enes 3. Hydrogenation of both mono-enes above was performed as described under Hydrogenation of substrates 1 above. Dienes were hydrogenated in the same manner as well, but 18 h and 50 atm was required instead of 4 h for complete conversion. These samples were then filtered through a silica plug as above after diluting with 30 % ethyl acetate in hexanes to remove the catalyst before being analyzed by GC and NMR (see next step, Determination of Absolute Configuration and *ee*).

Determination of Absolute Configuration and *ee*: After hydrogenations, the aliphatic ester product 4a was reacted with 38 mg lithium aluminum hydride (0.6 mmol, 3 eq.) in 1 ml of diethyl ether at 0 °C for 10 min, this reaction mixture slurried with 1 ml methanol at 0 °C followed by stirring with 5 ml water for 1 h. The layers were separated, the aqueous washed twice with 5 ml of diethyl ether, and the combined organic phases dried over sodium sulfate and concentrated under reduced pressure at ambient temperature. Products 4b and 4d were analyzed by GC immediately after filtration, and product 4c was analyzed by comparison with the ester 4a and its known stereochemistry. These samples were all analyzed by chiral GC, comparing the retention times of compounds 4b, 4d, and the alcohol form of 4a to the compounds of known stereochemistry generated by Myer's methodology using pseudoephedrine as a chiral auxillary.[4]
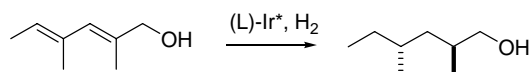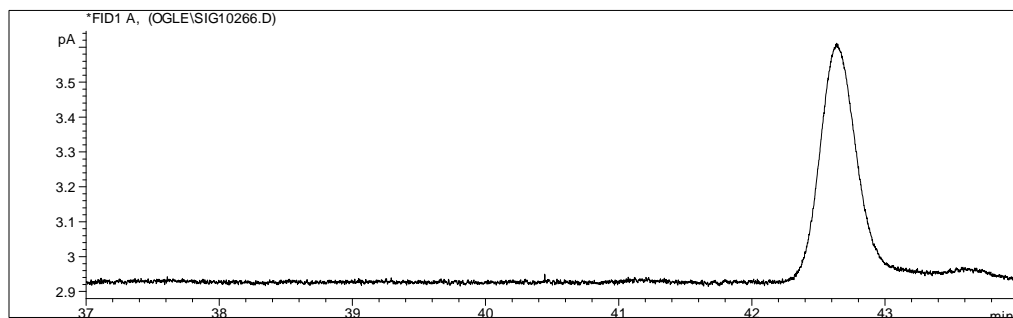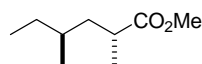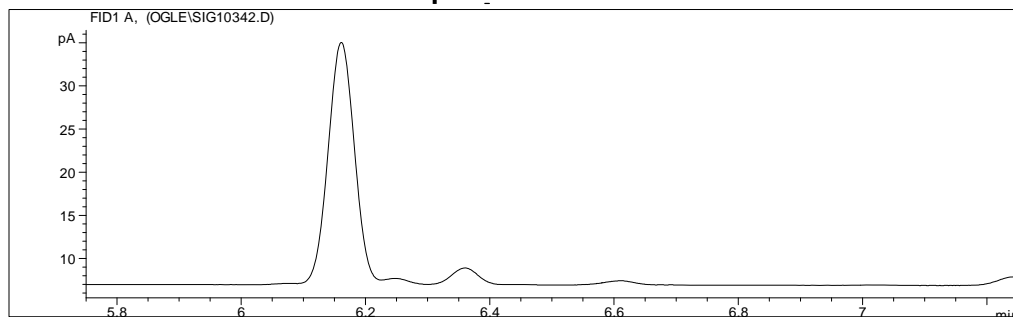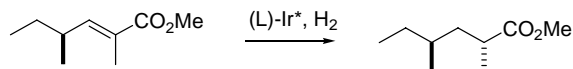
(2R,4R)-2,4-Dimethylhexanol (2.4a).
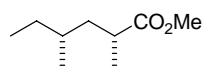
Methyl-*E,E*-2,4-dimethyl-2,4-hexadienoate (32 mg, 0.2 mmol, 1 eq.) was hydrogenated as described above to give the ester 4a as a 2.9:1 mixture of diasteriomers, in 100 % yield, the major isomer having 90 % *ee*. This was then reduced with lithium aluminum hydride (38 mg, 0.60 mmol, 3 eq.) and washed with sodium potassium tartrate to generate the title compound in 85 % isolated yield (same *d.r.* and *ee* of the major diastereomers). The retention time on GC was analogous to the minor isomer generated from Myer's enolate (generated in turn from (2S,4S)-pseudoephedrine).[4]
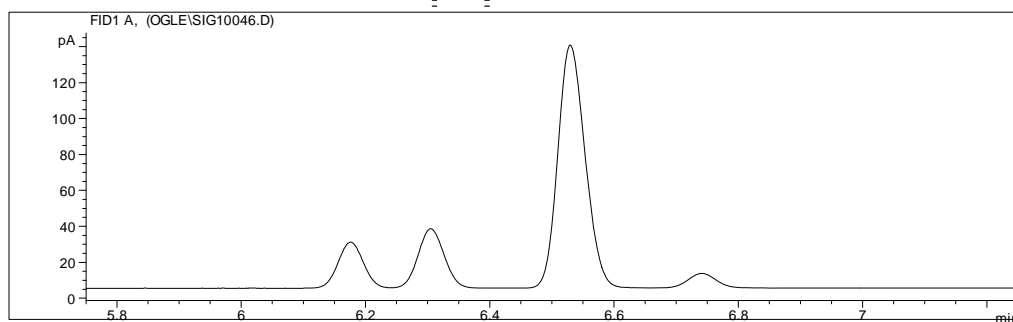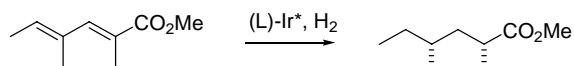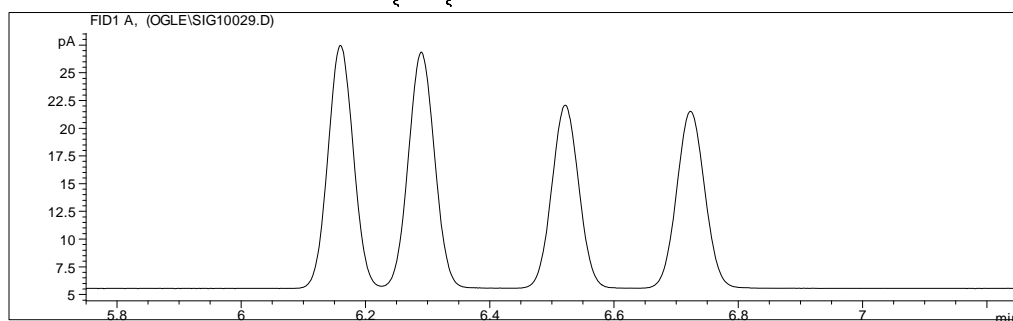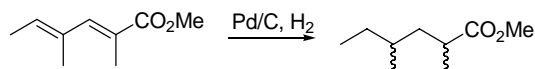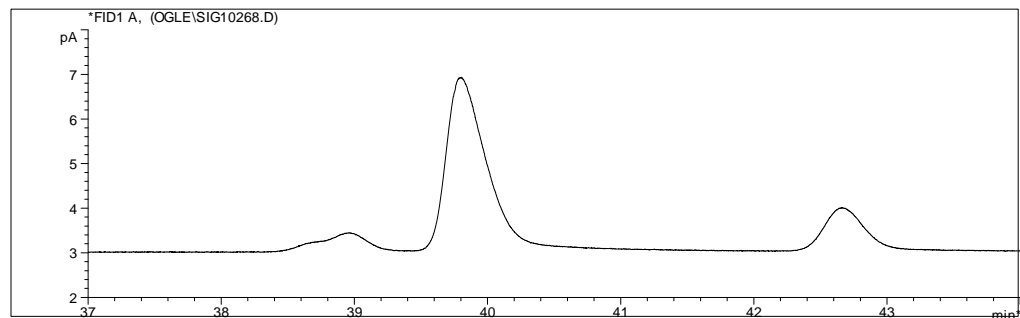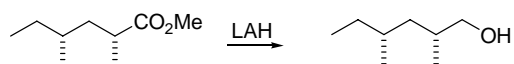
(2S,4R)-2,4-Dimethylhexanol (2.4b).
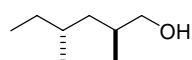
E,E-2,4-Dimethyl-2,4-hexadienol (32 mg, 0.2 mmol, 1 eq.) was hydrogenated as described above to give the title compound as a 10.5:1 mixture of diasteriomers, in 100 % yield, the major isomer having 97 % *ee*. The retention time on GC was analogous to the minor isomer generated from Myer's enolate (generated in turn from (2R,4R)-pseudoephedrine).[4]
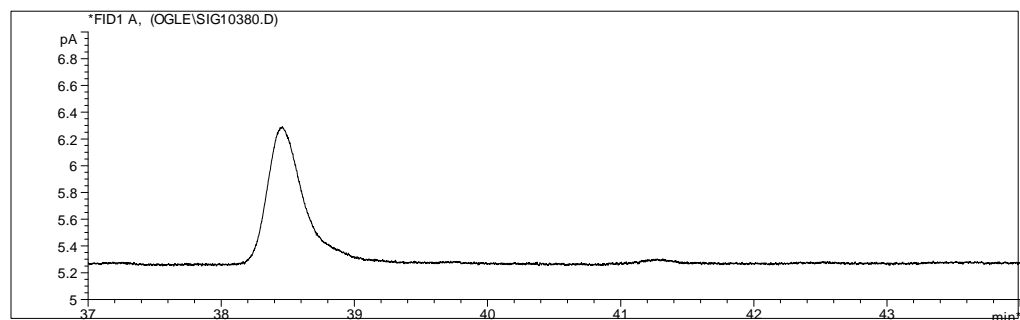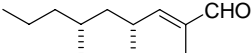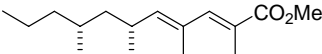
(2R,4S)-2,4-Dimethylhexanol (2.4c).

Methyl-*E,E*-2,4-dimethyl-2,4-hexadienoate (32 mg, 0.2 mmol, 1 eq.) was hydrogenated as described above to give the ester compound as a 5.0:1 mixture of diasteriomers, in 100 % yield, the major isomer having 98+ % *ee*. Comparison of this product with the known diasteriomeric methyl ester (identified above using Myer's methodology) confirmed the predicted anti-relationship of the stereocenters.

(2S,4S)-2,4-Dimethylhexanol (2.4d).
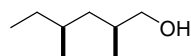
 (S)-*E*-2,4-Dimethyl-2-hexenol (32 mg, 0.2 mmol, 1 eq.) was hydrogenated as described above to give the title compound as a 9.5:1 mixture of diastereomers, in 100 % yield, the major isomer having 98+ % *ee*. The retention time on GC was analogous to the major isomer generated from Myer's enolate (generated in turn from (2R,4R)-pseudoephedrine).[4]
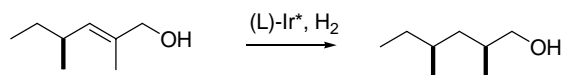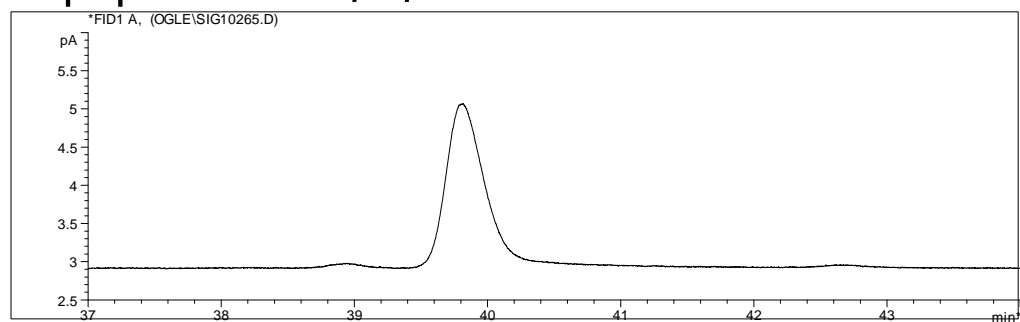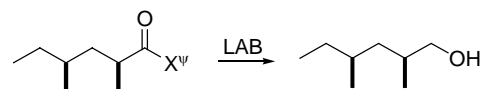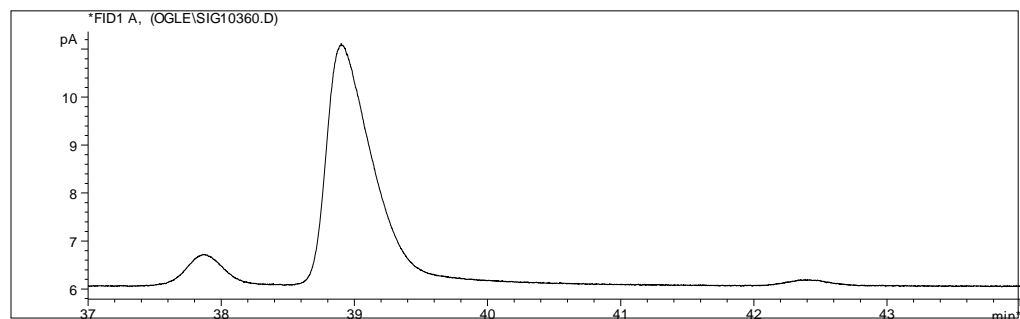
Total Synthesis

Generations 1 and 2

Table A.1 Tabulated Data from the First 2 Generation Approaches to Lardolure and Extract from the Preen Wax Gland of the Domestic Goose.

entry	product	isolated yield (%)	d.r.[a]	ee[a] (%)
5	CO$_2$Me	64	-	-
8	CO$_2$Me	82	-	-
9	CO$_2$Me	100	2.0:1.5: 1.2:1	97
10	CO$_2$Me	100	2.5:1-4:1[b]	80
12	CHO	78	4:1	80
13	CO$_2$Me	70	4:1	80
14	OH	95	4:1	80

15	(structure) CHO	94	4:1	80
16	(structure) CO₂Me	69	4:1	80

a) determined by either ^{13}C NMR or chiral GC analysis by comparison with racemic sample (see experimental), absolute stereochemistry inferred from previous dienes; b) MPLC purification increased the d.r. up to 4:1 from a crude 2.5:1 sample
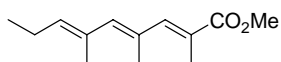
Methyl *E,E*-2,4-Dimethylhepta-2,4-dienoate (2.5).
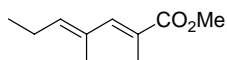
E-2-methyl-2-pentenal (1.9 g, 19 mmol, 1 eq.) was added to a solution of methoxycarbonylethylidenetriphenylphosphorane (10.5 g, 60 mmol, 3 eq.) dissolved in 80 ml of dichloromethane, which was then refluxed for 18 h. Distillation under reduced pressure (bp 84 °C at 15 mm Hg) produced the title compound as a colorless oil, 2 g, 64 % isolated yield, which matched the known compound by ^{1}H NMR [80]. ^{1}H NMR (CDCl₃, 300 MHz): δ (ppm) = 7.12 (1H, s), 5.64 (1H, t, *J* = 7.7 Hz), 3.75 (3H, s), 2.16 (2H, quintet, *J* = 7.5 Hz, *J* = 7.5 Hz), 2.04 (3H, s), 1.87 (3H, s), 1.02 (3H, t, *J* = 7.8 Hz).
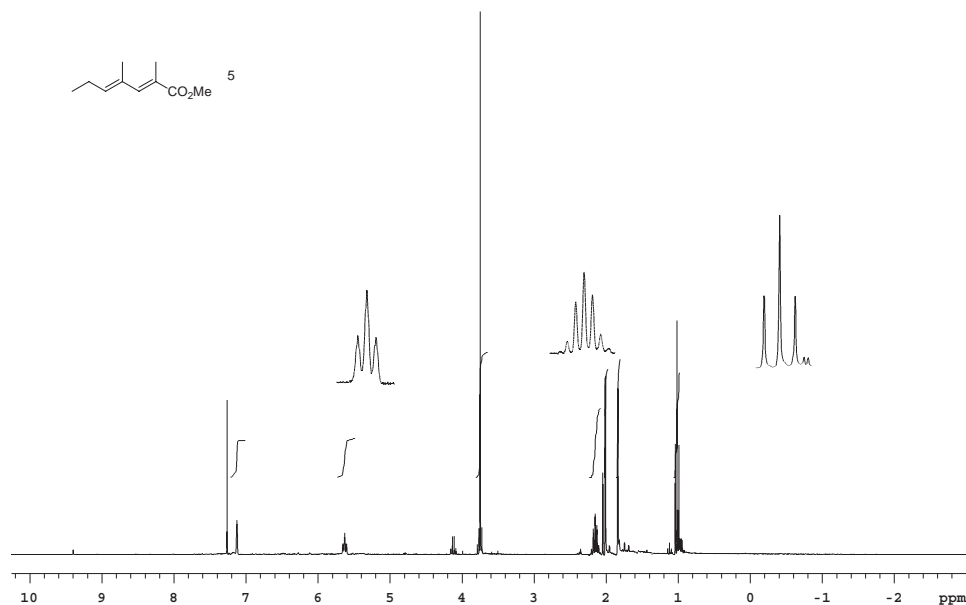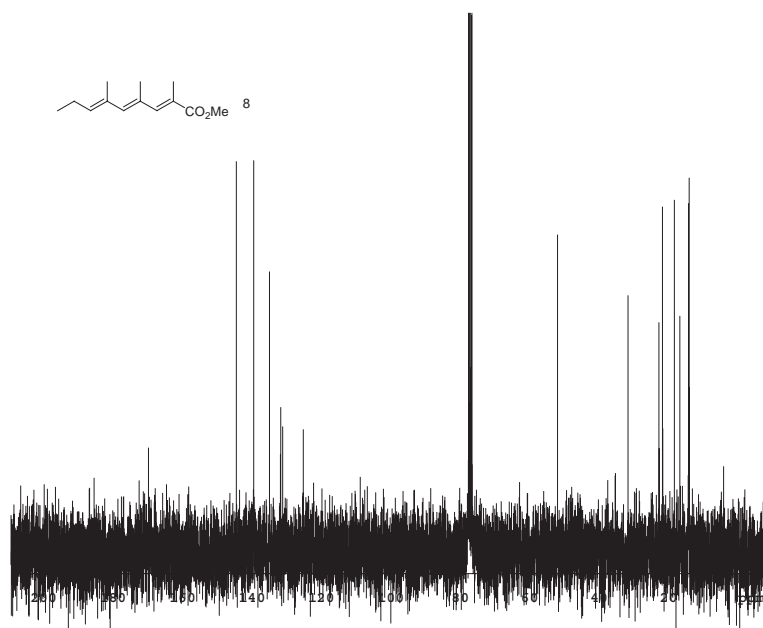

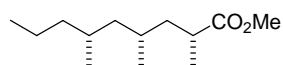**Methyl *E,E,E*-2,4,6-trimethylnona-2,4,6-trienoate (2.8).**

E,E-2,4-Dimethylhepta-2,4-dienal 7 (870 mg, 6.3 mmol, 1 eq.) was added to methoxycarbonylethylidenetriphenylphosphorane (4.6 g, 12.6 mmol, 2 eq) dissolved in 20 ml of dichloromethane. This was heated to reflux for 26 h, followed by concentration under reduced pressure onto silica. Column chromatography was performed using 5 % ethyl acetate in hexanes, followed by concentration of the major fractions to give 1.08 g of the title compound as a colorless oil, 82 % isolated yield. ^{1}H NMR (CDCl$_3$, 300 MHz): δ (ppm) = 7.20 (1H, s), 6.06 (1H, s), 5.49 (1H, t, *J* = 7.5 Hz), 3.70 (3H, s), 2.17 (2H, quintet, *J* = 7.9 Hz, *J* = 7.2 Hz), 2.07 (3H, s), 2.03 (3H, s), 1.81 (3H, s) 1.04 (3H, t, *J* = 7.2 Hz). ^{13}C(^{1}H) (CDCl3, 100.4 MHz): δ (ppm) = 169.96, 144.65, 139.66, 135.11, 131.35, 125.41, 52.14, 21.91, 18.53, 16.92, 14.44, 14.39 (some hexane contaminant in actual spectrum).
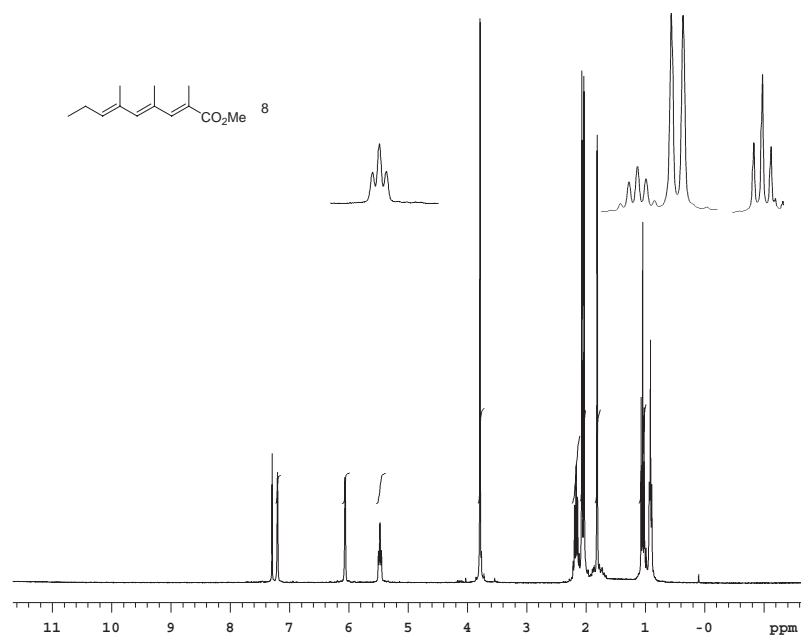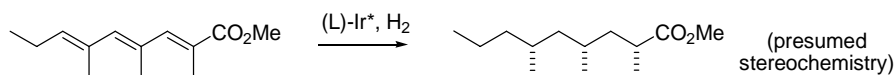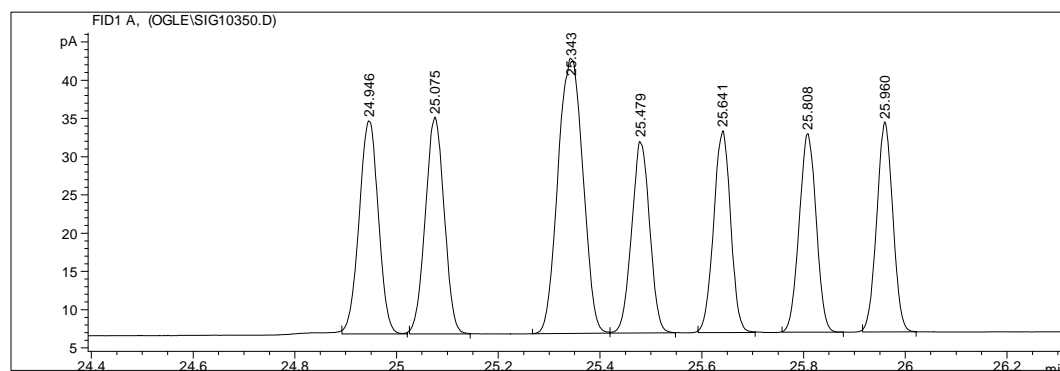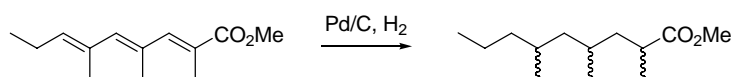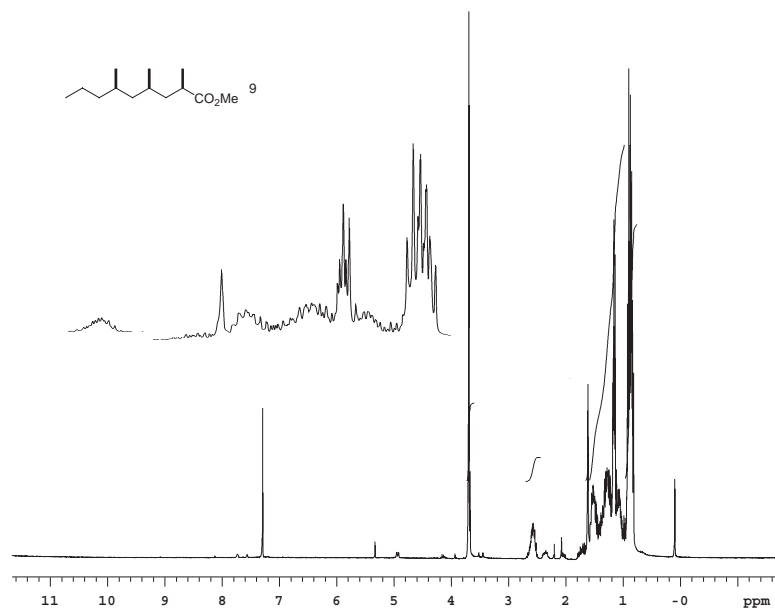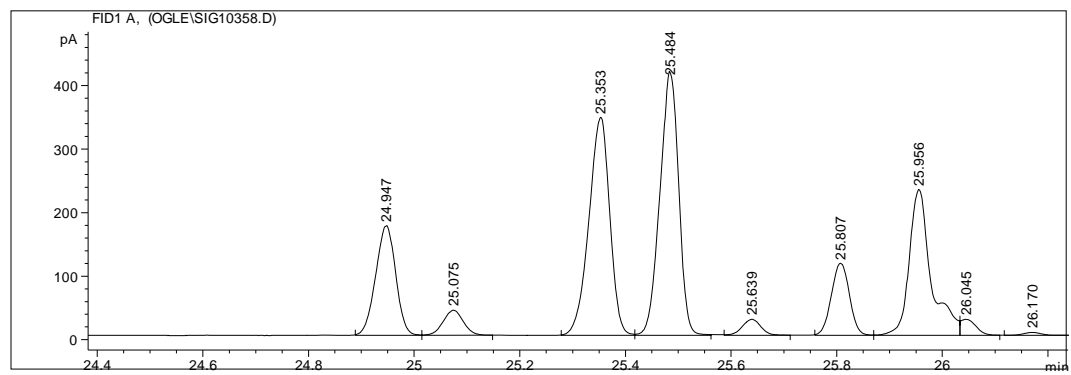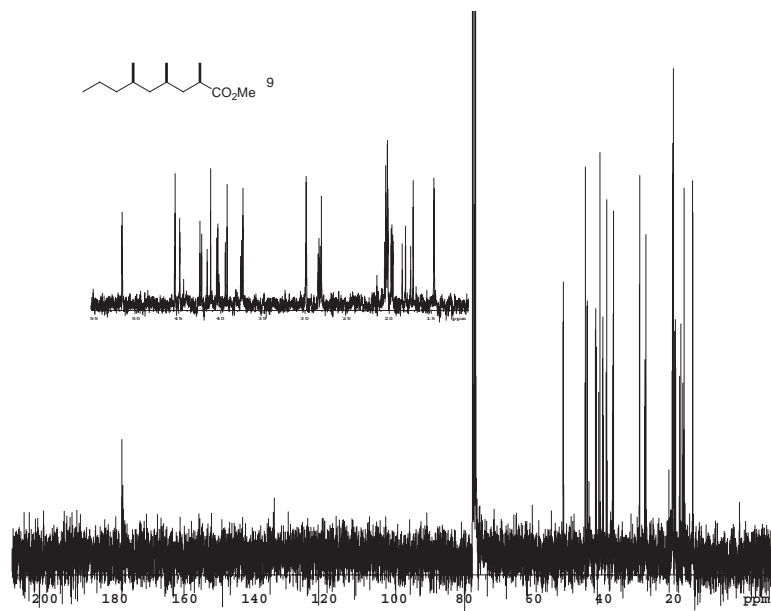
Methyl (2R,4R,6R)-2,4,6-Trimethylnonanoate (2.9).
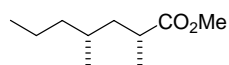

Methyl *E,E,E*-2,4,6-trimethylnona-2,4,6-trienoate (42 mg, 0.20 mmol, 1 eq.) was hydrogenated as diene 5 above. ^{1}H NMR of the mixture was indistinguishable from the known compounds[81,82]. ^{1}H NMR (CDCl$_3$, 300 MHz): δ (ppm) = 3.66 (3H, s), 2.59-2.50 (1H, m), 1.69-1.42 (8H, m), 1.35-0.99 (10H, m), 0.89-0.79 (9H, m).

Methyl *R,R*-2,4-Dmethylheptanoate (2.10).

Methyl *E,E*-2,4-dimethylhepta-2,4-dienoate 5 (9.05 g, 53.9 mmol, 1 eq.), prepared above, was hydrogenated as the dienes above but with reduced catalyst loading (203 mg, 0.12 mmol, 0.2 mol%) to produce 100% of a 2.5:1 mixture of diasteriomers, the greater of which produced in 90 % *ee* (analyzed by chiral GC and compared with the racemic mixture prepared from hydrogenation with palladium on carbon). ^{1}H NMR was indistinguishable from the known compound[81]. ^{1}H NMR (CDCl$_3$, 300 MHz): δ (ppm) = (major diastereomer only) 3.65 (3H, s), 2.52 (1H, q, *J* = 7.7 Hz, *J* = 7.0 Hz), 1.57 (1H, s), 1.51-1.25 (6H, m), 1.14-1.03 (4H, m), 0.88-0.82 (4H, m).
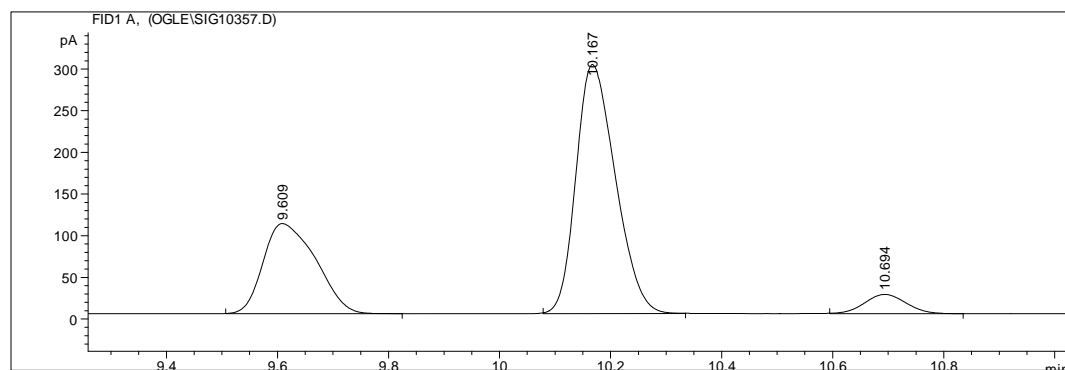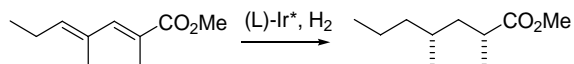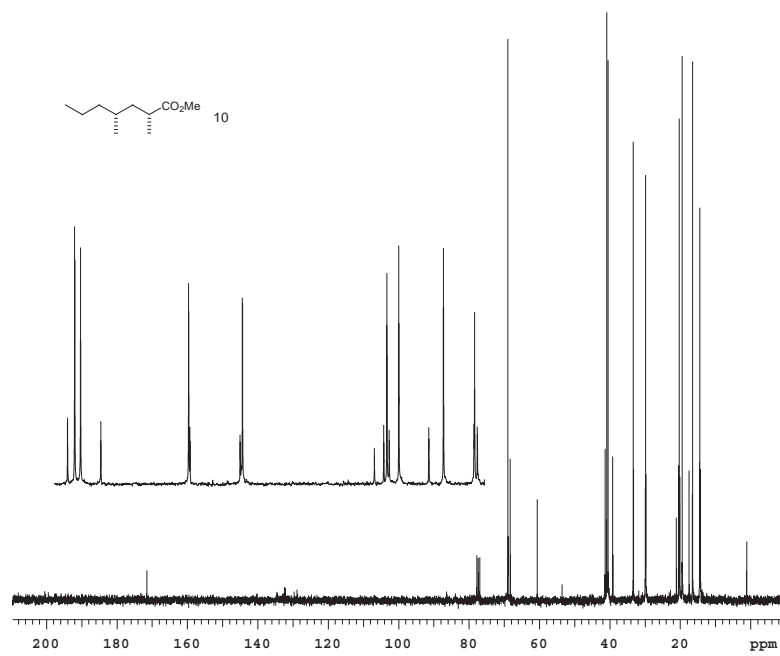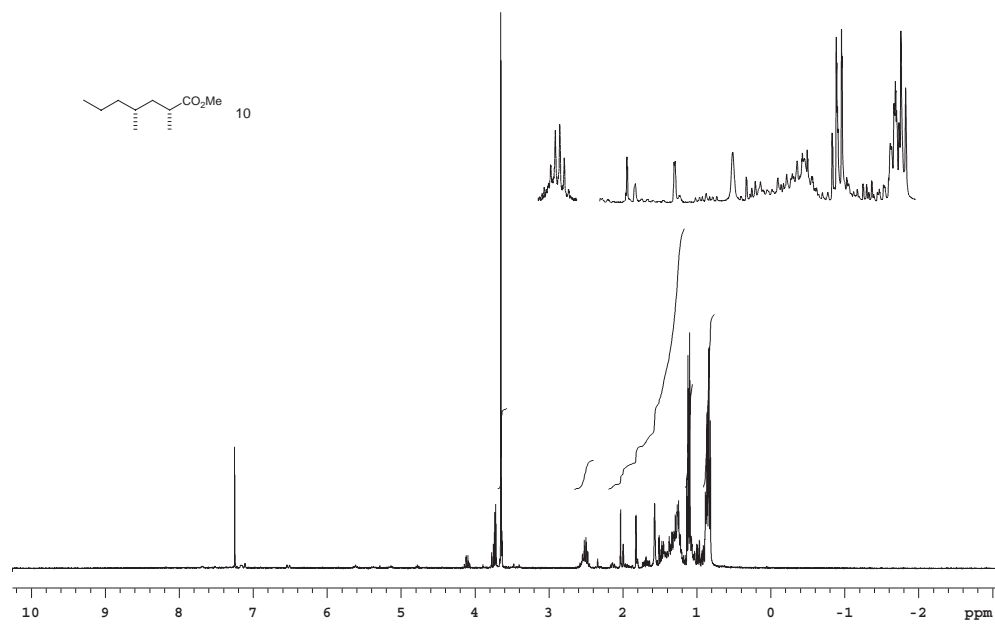
2R,4R-2,4-Dimethylhepanal (2.12).
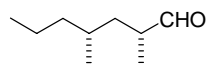
2R,4R-2,4-Dimethylhexanol 11 (1.3 g, 9 mmol, 1 eq.) was added to 90 ml of dichloromethane, followed by 260 mg of 4 Å molecular sieves, N-methylmorpholine-N-oxide (2.25 g, 18.9 mmol, 2.1 eq.), and tetrapropyl ammonium perruthenate (180 mg, 0.9 mmol, 10 mol %). This was stirred 18 h at ambient temperature, at which time analysis by TLC showed complete conversion. Filtration through a silica plug and washing with three portions of 90 ml dichloromethane followed by concentration under reduced pressure at ambient temperature gave the title compound as a clear oil in 1.0 g, 78 % isolated yield which was not stored but immediately reacted in the next step.

Methyl (4R,6R)-*E*-2,4,6-Trimethylnona-2-enoate (2.13).
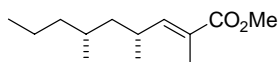
(2R,4R)-2,4-Dimethylheptanal 12 (1 g, 7.0 mmol, 1 eq.) was added to a solution of 50 ml of dichloromethane of methoxycarbonylethylidene-triphenylphosphorane (6 g, 35 mmol, 5 eq.). This was heated to reflux, and allowed to stir for 24 h. This was then filtered through a silica plug and washed with 2 portions of 50 ml of dichloromethane, and concentrated under reduced pressure onto silica gel. Column chromatography was then performed using hexanes, but analyzed with TLC conditions of 30 % ethyl acetate in hexanes (Rf 0.65 on the TLC, but ~ 0.1 using hexanes as eluant). Concentrating the pure fractions gave 1.12 g of the title compound as a clear oil, 70 % isolated yield. ^{1}H NMR (CDCl$_3$, 300 MHz): δ (ppm) = 6.56 (1H, dq, J = 10.1 Hz, J = 1.3 Hz, J = 1.5 Hz), 3.74 (3H, s), 2.61 (1H, m), 1.85 (3H, d, J = 1.5 Hz), 1.43-1.03 (8H, m), 0.97 (3H, d, J = 6.5 Hz), 0.87 (3H, t, J = 7.0 Hz), 0.85 (3H, d, J = 6.5 Hz); [13]C(^{1}H) (CDCl3, 100.4 MHz): δ (ppm) = 169.2, 149.1, 125.7, 51.9, 44.5, 40.1, 39.3, 31.0, 30.4, 20.2, 20.0, 14.6, 12.7; IR: 2971, 2143, 1745, 1456, 1366.
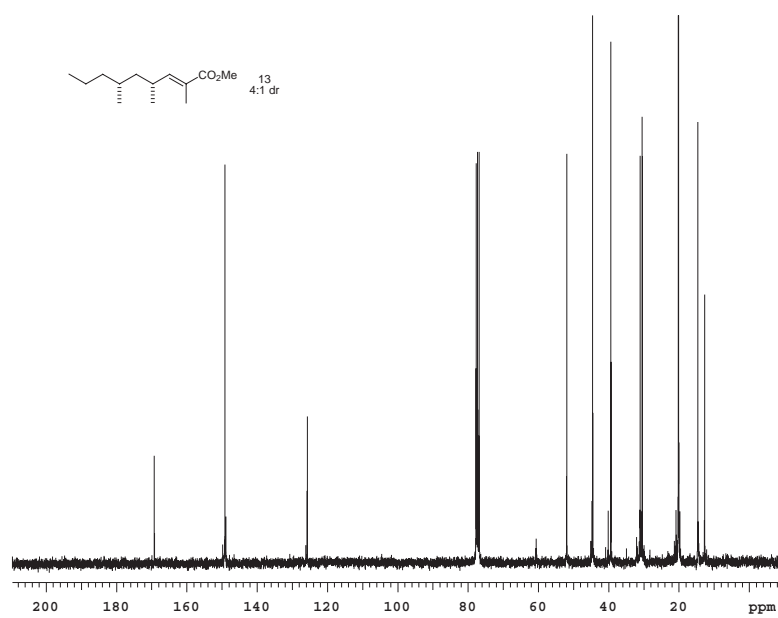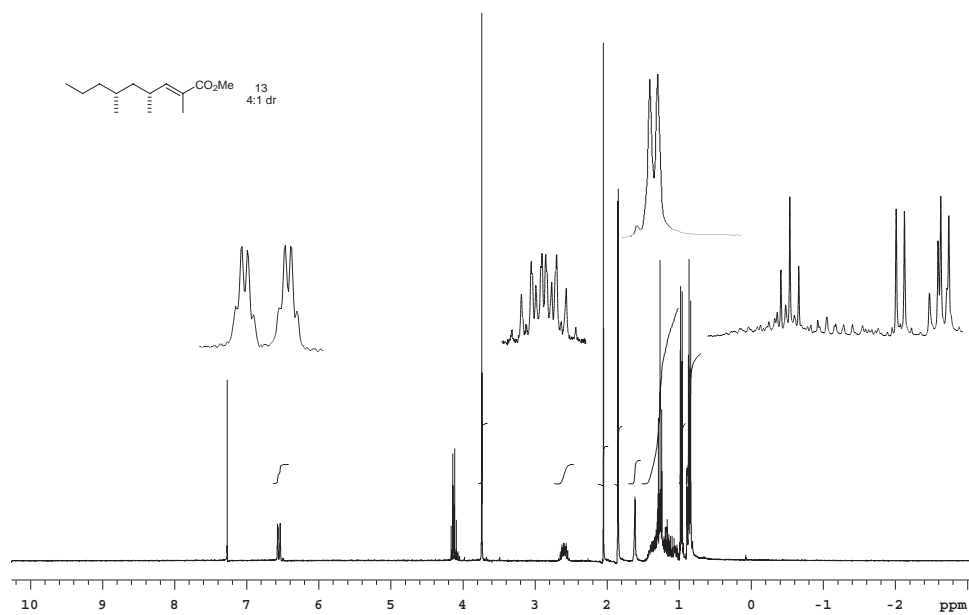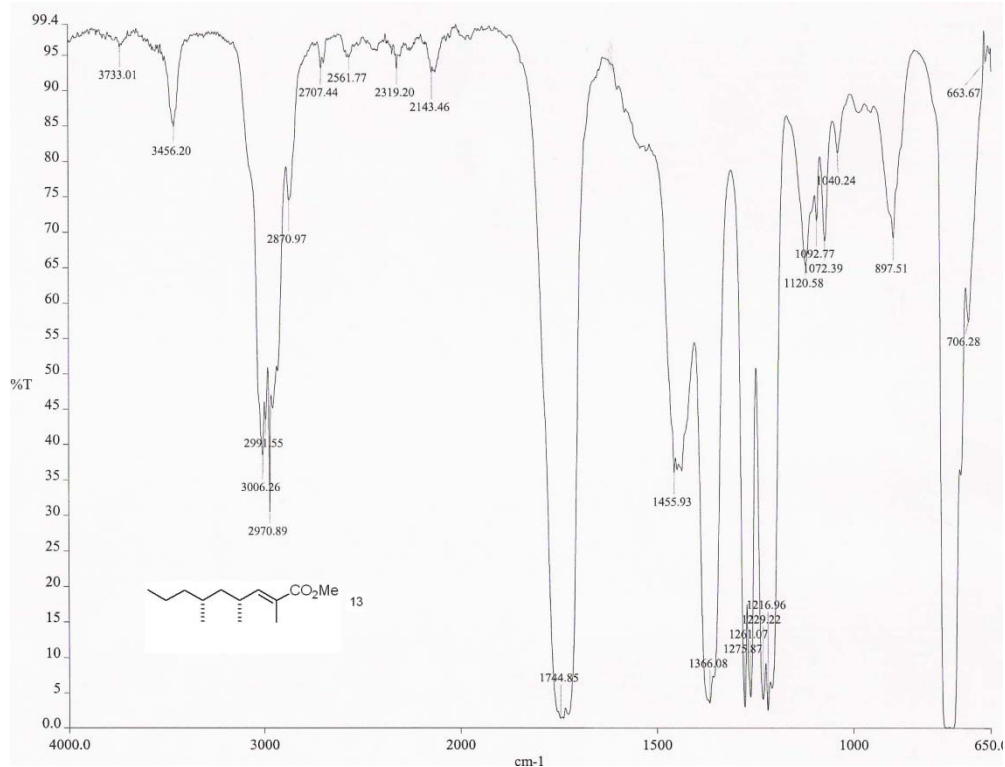
(4R,6R)-*E*-2,4,6-Trimethylnona-2-en-1-ol (2.14).
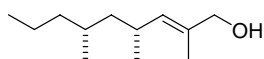
Dry diethyl ether 10 ml was cooled to -5 °C, and lithium aluminum hydride (114 mg, 3 mmol, 3 eq.) was added. After stirring 5 min, methyl (4R,6R)-*E*-2,4,6-trimethylnona-2-enoate 13 (212 mg, 1 mmol, 1 eq.) was added as a solution in 10 ml of diethyl ether dropwise. After stirring 30 min, the reaction mixture was allowed to come to ambient temperature over 1 h, then recooled to -5 °C again, and 5 ml of methanol was added dropwise to quench excess hydride. Then 10 ml of saturated aqueous sodium potassium tartrate was added and stirred for 2 h. The layers were separated, the aqueous washed twice with diethyl ether, and the combined organic phases dried over sodium sulfate and concentrated under reduced pressure at ambient temperature. Column chromatography with 10% ethyl acetate in hexanes was then performed (Rf: 0.22) to give 180 mg, 95 % isolated yield of the title compound as a colorless oil. ^{1}H NMR (CDCl$_3$, 300 MHz): δ (ppm) = 5.10 (1H, d), 3.97 (3H, s), 2.55-2.40 (2H, m), 1.70-1.65 (3H, s), 1.64-1.12 (11H, m), 1.11-0.98 (3H, m), 0.98-0.78 (6H, m), (ethyl acetate also present); IR: 3456, 3006, 2126, 1742; MS (m/e): calculated (M+Li): 191.1987, found: 191.1985.
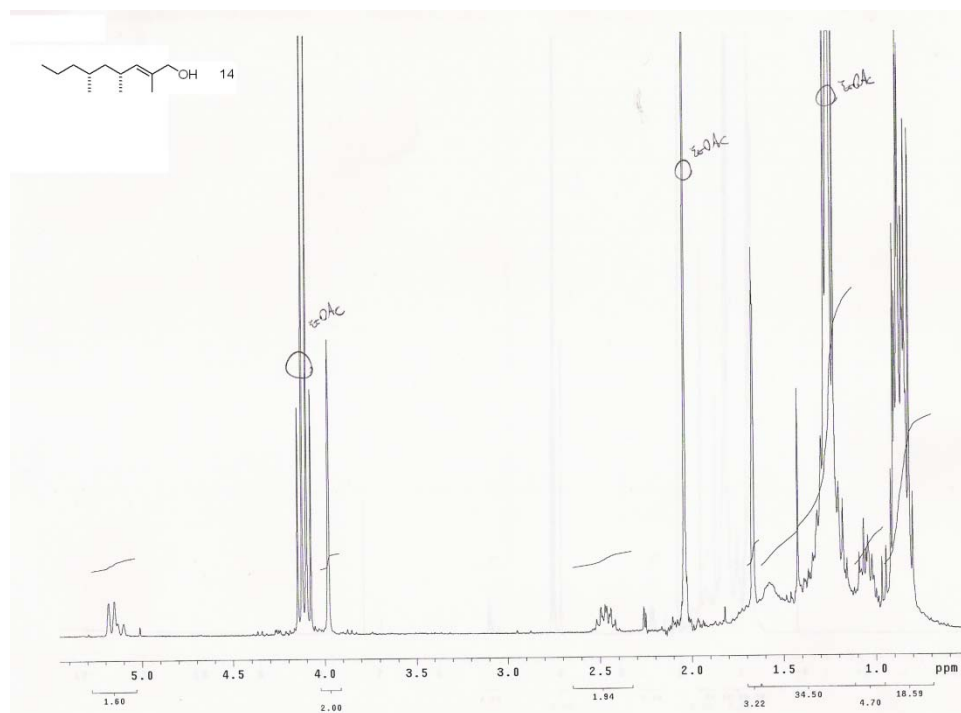
(4R,6R)-*E*-2,4,6-Trimethylnona-2-enal (2.15).

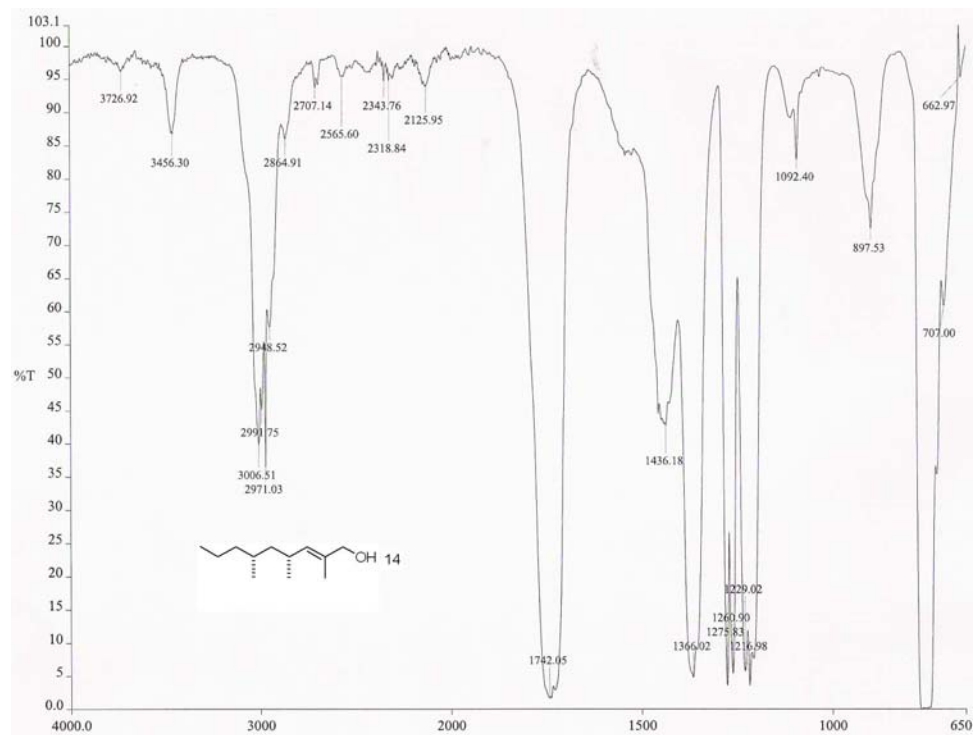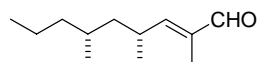Activated manganese dioxide (1.14 g, 13.1 mmol, 20 eq.) was slurried in 5 ml of diethyl ether. A solution of (4R,6R)-*E*-2,4,6-trimethylnona-2-en-1-ol 14 (130 mg, 0.7 mmol, 1 eq.) dissolved in 5 ml of diethyl ether was added. This was stirred 24 h, and filtered first through celite then through a silica plug, eluted with 10 % ethyl acetate in hexanes, and concentrated to produce 121 mg, 94% isolated yield of the title compound, which was not stored but immediately reacted in the next step. ^{1}H NMR (CDCl$_3$, 300 MHz): δ (ppm) = 9.48 (1H, s), 6.25 (1H, d), 2.90-2.68 (1H, m), 1.73 (3H, s), 1.46-0.60 (16H, m); ^{13}C(^{1}H) (CDCl3, 100.4 MHz): δ (ppm) = 195.8, 161.2, 44.5, 44.3, 39.2, 31.3, 30.4, 20.1, 20.1, 19.8, 14.5, 9.4; IR: 2931, 2327, 1733, 1457; MS (m/e): calculated (M+Li): 189.1831, found: 189.1807.
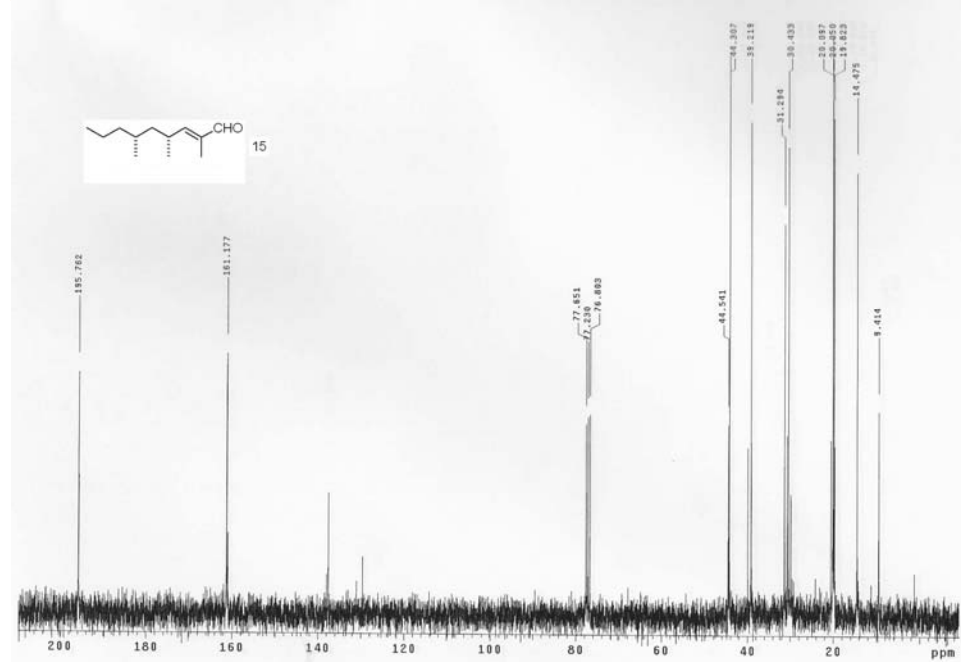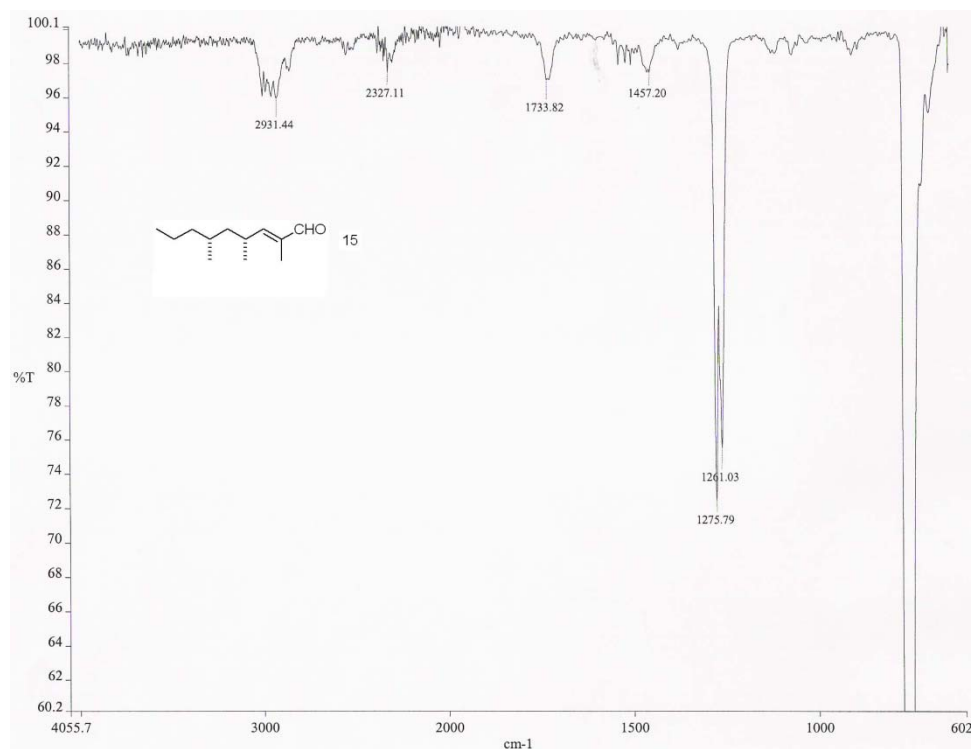
Methyl (6R,8R)-*E,E*-2,4,6,8-Tetramethylundeca-2,4-dienoate (2.16).
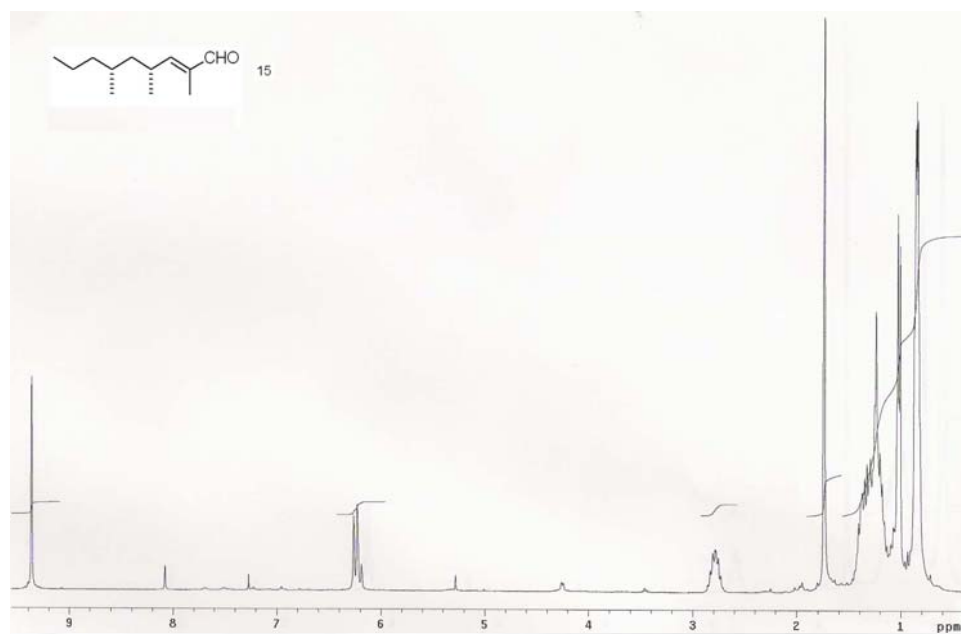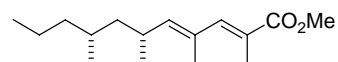

(4R,6R)-*E*-2,4,6-Trimethylnona-2-enal (121 mg, 0.6 mmol, 1 eq.) was added to a solution of 5 ml of dichloromethane of methoxycarbonylethylidenetriphenylphosphorane (1.3 g, 3.7 mmol, 6 eq.). This was heated to reflux, and allowed to stir for 24 h. This was then filtered through a silica plug and washed with 2 portions of 50 ml of dichloromethane, and concentrated under reduced pressure onto silica gel. Column chromatography was then performed using a gradient of 0-2 % ethyl acetate in hexanes, but analyzed with TLC conditions of 10 % ethyl acetate in hexanes (Rf 0.61 on the TLC, but ~ 0.1 using hexanes as eluant). Concentrating the pure fractions gave 108 mg of the title compound, 69 % isolated yield. ^{1}H NMR (CDCl$_3$, 300 MHz): δ (ppm) = 7.11 (1H, s), 5.41 (1H, d), 3.77 (3H, s), 2.70-2.52 (1H, m), 2.02 (3H, s), 1.84 (3H, s), 1.60-1.12 (9H, m), 1.95 (3H, d), 0.92-0.80 (6H, m); ^{13}C(^{1}H) (CDCl3, 100.4 MHz): δ (ppm) = 195.8, 161.2, 44.5, 41.2, 39.2, 31.3, 30.6, 30.4, 30.2, 20.2, 20.1, 20.1, 19.8, 14.5, 9.4 (carboxylic carbon indistinguishable from noise); MS (m/e): calculated (M+Li): 259.2249, found: 259.2267.
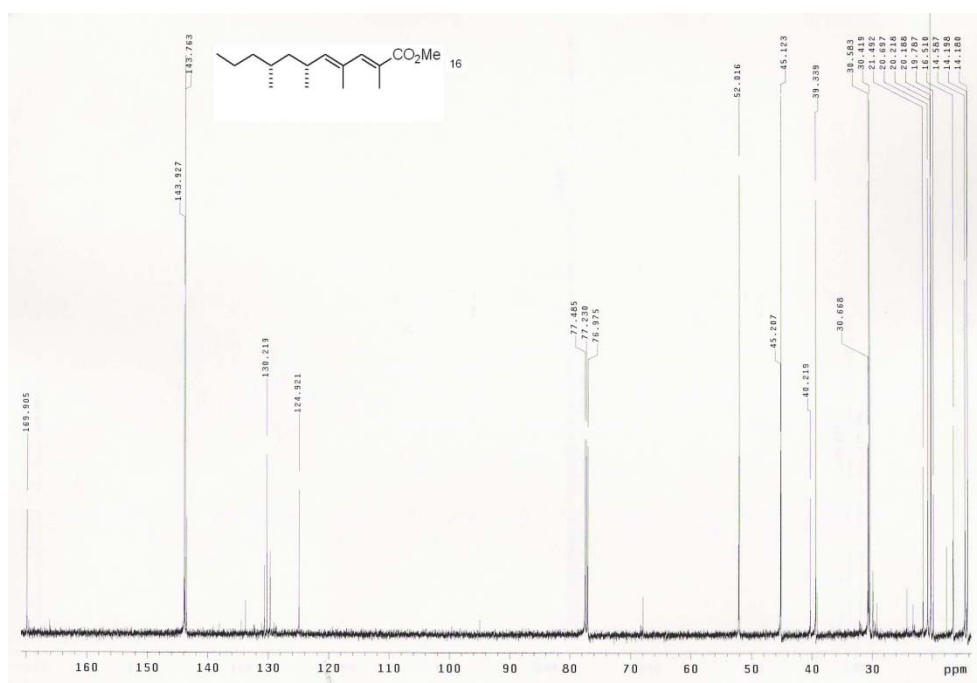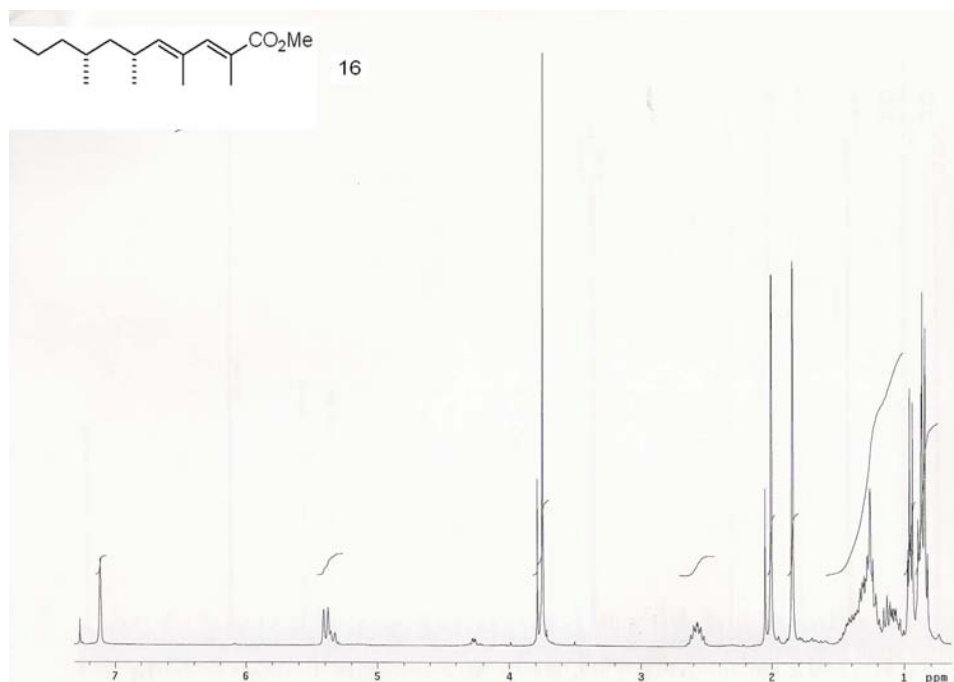
Generations 3 and 4:

Table A.2 Significant Compounds to the Total Synthesis of Lardolure Generation 3 and 4 Approach

Entry	product	isolated yield (%)	d.r.[a]	ee[a] (%)
17	MeO$_2$C OTBS	93	-	>98
18	OHC OTBS	79	-	n.d.
19	MeO$_2$C OTBS	65	-	n.d.
20	MeO$_2$C OH	89	-	>98
22		100	10:1	>98
23	OH	n.d.	40:10: 4:1 [b]	>98
24	MeO$_2$C OH	27[c]	6:1	n.d.

a) determined by either 13C NMR or chiral GC analysis by comparison with racemic sample (see experimental), absolute stereochemistry is inferred; b) the diastereomers of the major and minor acetals were also distinguishable, although this has minor bearing on the subsequent chemistry; c) isolated yield over 2 steps.

Methyl (R)-2-[(tert-Butyldimethylsilyl)oxylpropionate] (2.17).

MeO$_2$C OTBS
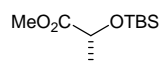
This was made by the known method from (R)-methyl lactate.[83] Isolation by the known method gave 10.2 g, 93% isolated yield. ^{1}H NMR was indistinguishable from the known compound: ^{1}H NMR (CDCl$_3$, 300 MHz): δ (ppm) = 4.31 (1H, J = 6.7 Hz), 3.70 (s, 3 H), 1.38 (3H, d, J = 6.7 Hz), 0.88 (9H, s), 0.074 (3H, s), 0.047 (3H, s).

(R)-2-[(tert-Butyldimethylsilyl)oxylpropanal (2.18).

OHC OTBS
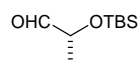
This was made by the known method from Methyl (R)-2-[(tert-Butyldimethylsilyl)oxylpropionate.[83] Isolation of the known compound gave 3.4 g, 79% isolated yield. ^{1}H NMR was indistinguishable from the known compound: ^{1}H NMR (CDCl₃, 300 MHz): δ (ppm) = 9.59 (1H, d, J = 1.3 Hz).0.071 (3H, s), 4.07 (1H, dq, J = 6.9 Hz, J = 1.3 Hz), 1.26 (3H, d, J = 6.9 Hz), 0.90 (9H, s), 0.083 (3H, s).

Methyl (R)-*E*-2-[(tert-Butyldimethylsilyl)oxo]-4-methylpenta-2-enoate (2.19).
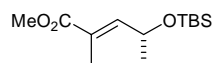
(R)-2-[(tert-Butyldimethylsilyl)oxylpropanal] 18 (856 mg, 4.5 mmol, 1 eq.) was added to a solution of methoxycarbonylethylidenetriphenylphosphorane (4.8 g, 13.5 mmol, 3 eq.) in 20 ml of dichloromethane, which was heated to reflux and stirred for 24 h. Concentration onto silica gel, followed by column chromatography with 30 % ethyl acetate in hexanes followed by concentration under reduced pressure gave a mixture of compounds with very close retention times which were routinely separated after the next step. ^{1}H NMR (CDCl₃, 300 MHz): δ (ppm) = 6.64 (1H, d), 4.75 (1H, pentet), 3.67 (3H, s), 1.77 (3H, d), 1.15 (3H, d), 0.81 (9H, s), -0.03 (6H, d); [13]C(^{1}H) (CDCl3, 100.4 MHz): δ (ppm) = 179.7, 75.0, 39.2, 36.4, 31.7, 22.7, 20.9, 15.1, 14.2; IR: 2930, 2327, 1720, 1463; MS (m/e): calculated (M+H): 259.1729, found: 259.1730.
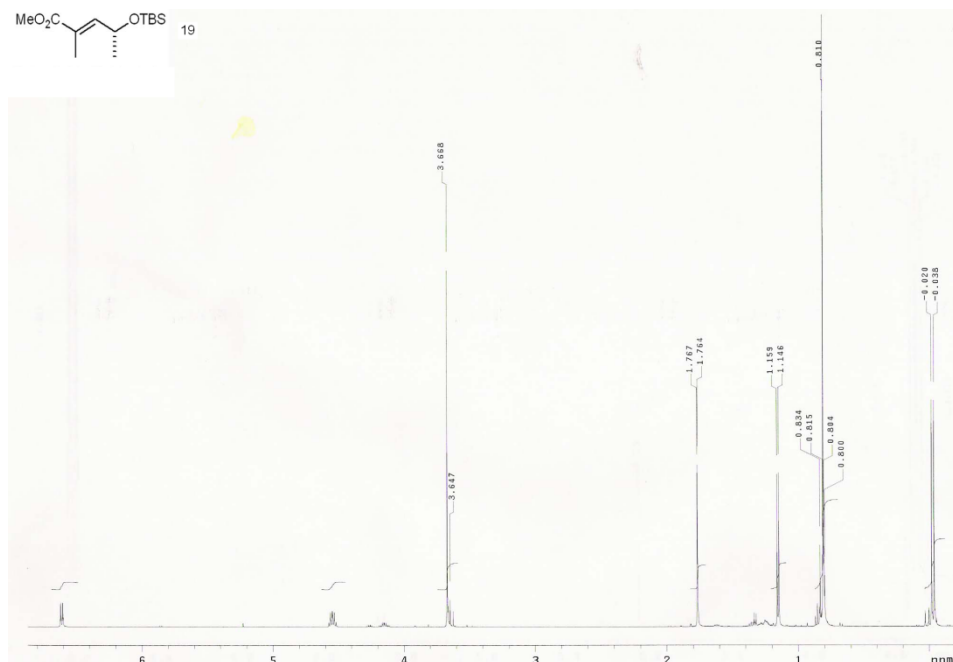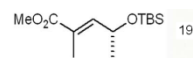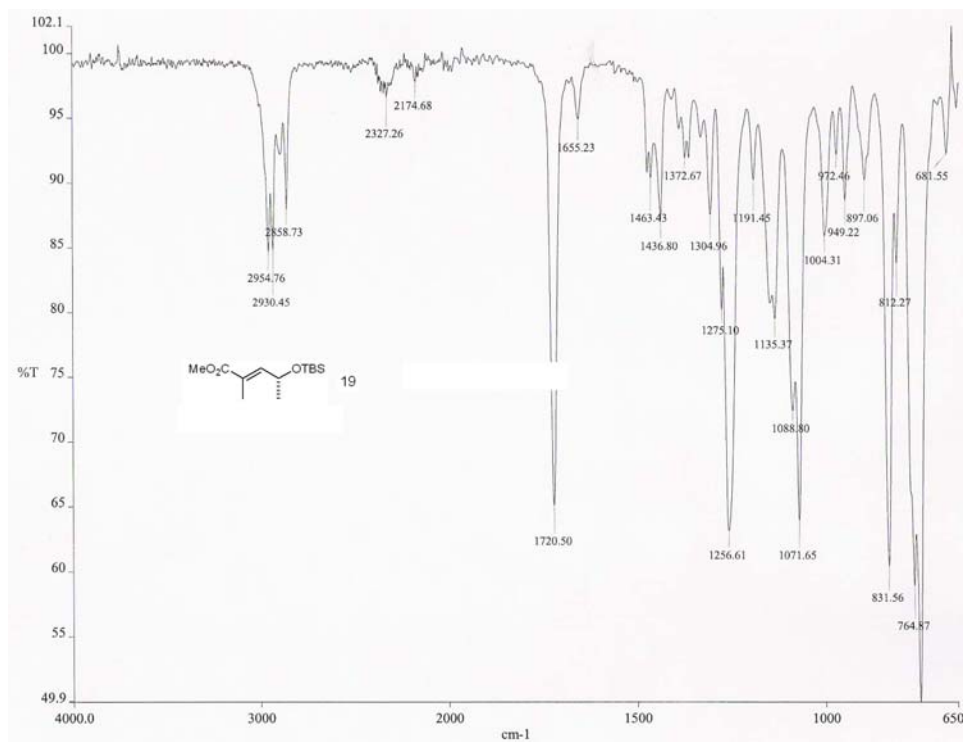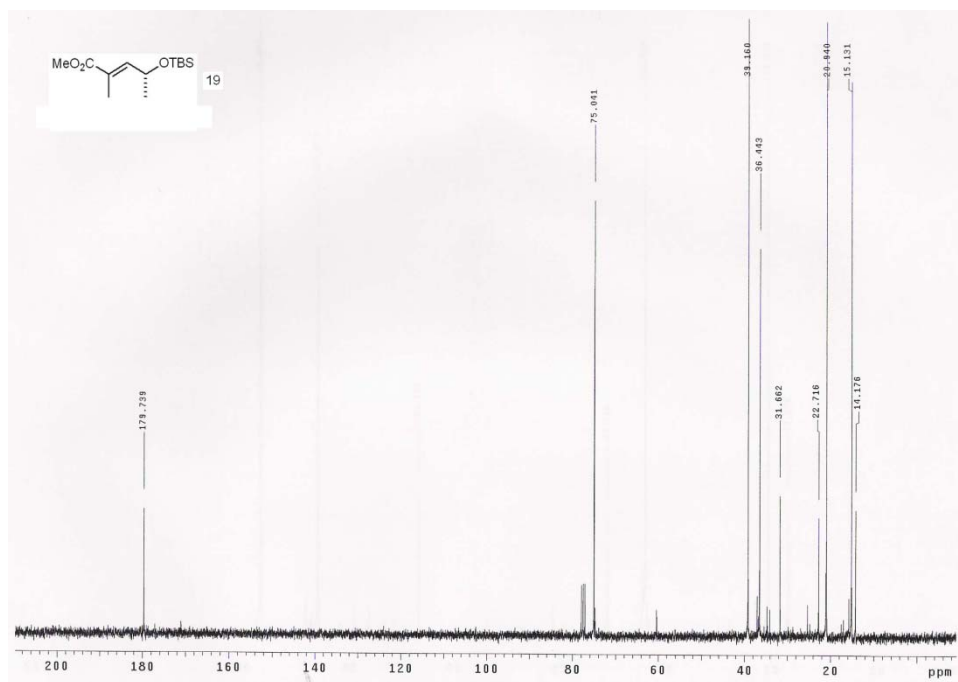
Methyl (R)-*E*-2-Hydroxy-4-methylpenta-2-enoate (2.20).
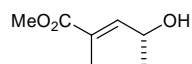
HF·pyridine complex (4.77 ml, 56 mmol, 5 eq.) was added   dropwise to a solution of methyl (R)-*E*-2-[(tert-butyldimethylsilyl)oxo]-4-methylpenta-2-enoate (2.9 g, 11.3 mmol, 1 eq.) in 12 ml of dry tetrahydrofuran. This was stirred for 12 h, at the end of which time 20 ml of saturated solution of sodium bicarbonate was added slowly to quench excess acid, and the solution was extracted with 2 portions of 20 ml diethyl ether. The combined organic phases were then washed sequentially with 50 ml of sodium bicarbonate, brine, 1 M HCl, brine again, and dried over sodium sulfate, concentrated under reduced pressure, and subsjected to column chromatography with 15 % ethyl acetate in hexanes (Rf: 0.25) to produce 1.43 g, 89% isolated yield of the title compound as a light yellow oil. ^{1}H NMR (CDCl$_3$, 300 MHz): δ (ppm) = 6.69 (1H, d), 4.68 (1H, pentet), 3.74 (3H, s), 2.12 (1H, bs), 1.87 (3H, s), 1.31 (3H, d); IR: 3386, 2974, 2326, 1714, 1651, 1437; MS (m/e): calculated (M+H): 145.0865, found: 145.0868.

MeO₂C ⟍⟍⟍OH
20
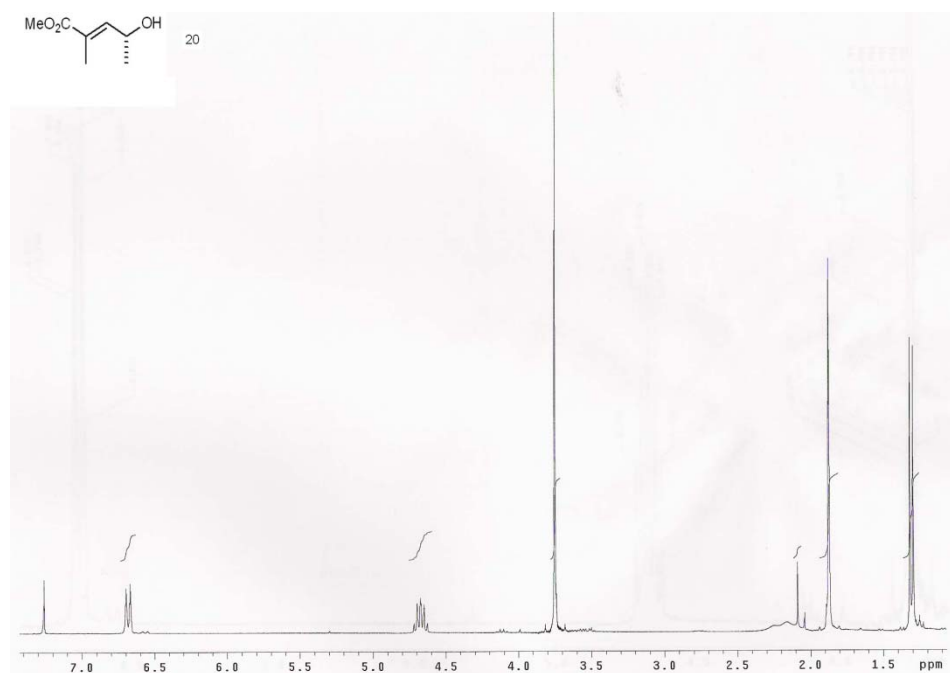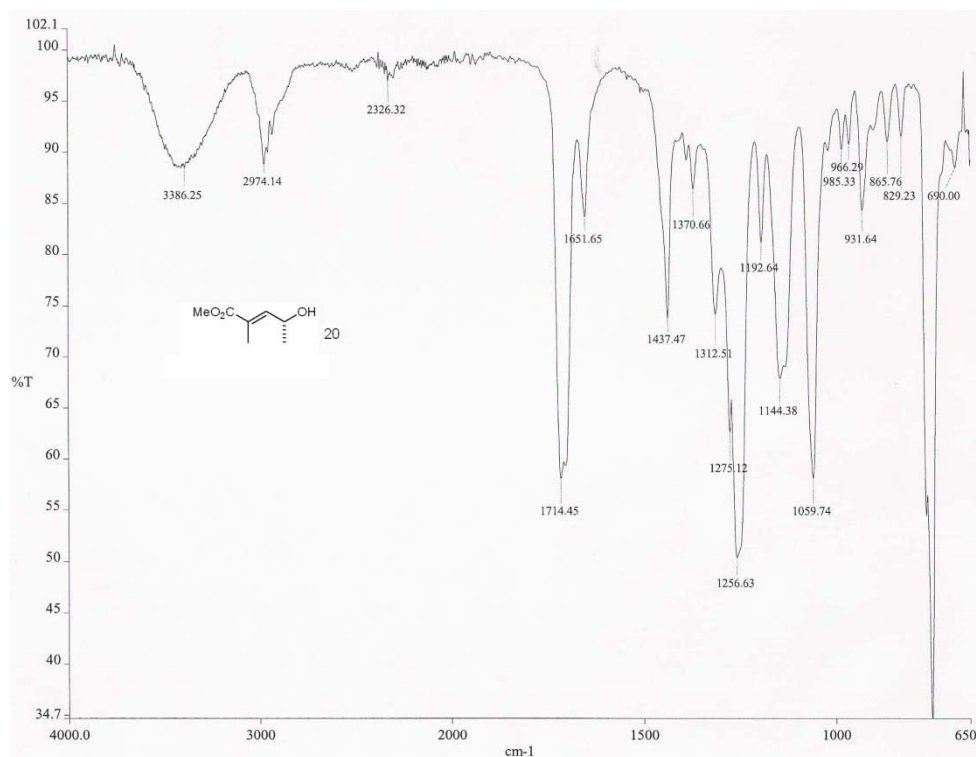
(2S,4R)-2,4-Dimethyl-γ-lactone (2.22).
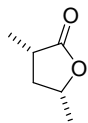
Methyl (R)-*E*-2-hydroxy-4-methylpenta-2-enoate 20 (1.25 g, 8.7 mmol, 1 eq.) was added to 4.3 ml of dichlomethane along with (D)-Ir* catalyst (43 mg, 26 umol, 0.3 mol %). This was freeze-thawed 3 times as in normal hydrogenations, and then placed in a parr bomb, which was subsequently flushed with hydrogen for 5 min open to the air, and then closed off followed by increasing the pressure to 5 atm. Stirring at 800 rpm was allowed for 1 h, at the end of which time the hydrogen was allowed to escape the vessel slowly, and the reaction mixture tested for conversion by ^{1}H NMR of the crude mixture. Although 100% conversion from the alkene had been converted, aproximately 90% had formed a 10:1 mixture of diasteriomers of the linear title compound, with the remaining 10% forming the cyclized lactone below. The linear compound was not isolated, but instead completely cyclized by addition of *p*-toluenesulfonic acid (17 mg, 87 umol, 1 mol %), which after 5 minutes gave 100 % conversion to the lactone in a 10 : 1 ratio of diasteriomers (via ^{1}H NMR, GC analysis revealed a single peak). Isolation routinely was not performed, but an analytic sample can be generated by column chromatography using a 75 % diethyl ether in hexanes mixture. ^{1}H and ^{13}C NMR of the colorless oil matched the known compound[84]: ^{1}H NMR (CDCl₃, 300 MHz): δ (ppm) = (major isomer only): 4.35 (1H, septet), 2.52 (1H, septet), 2.4 (1H, m), 1.25 (3H, d), 1.11 (3H, d);

$^{13}C(^1H)$ (CDCl3, 100.4 MHz): δ (ppm) = 146.2, 66.0, 51.9, 25.9, 23.5, 12.7 (some ethyl acetate in recorded spectra).

More typically, the reaction mixture in dichloromethane was used immediately in the next step.
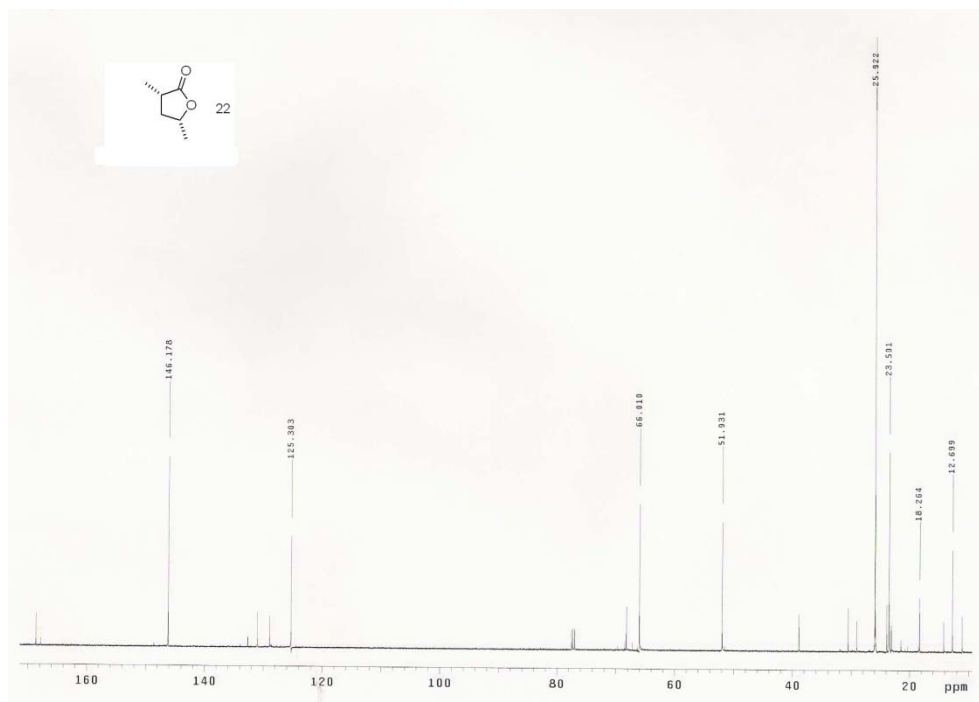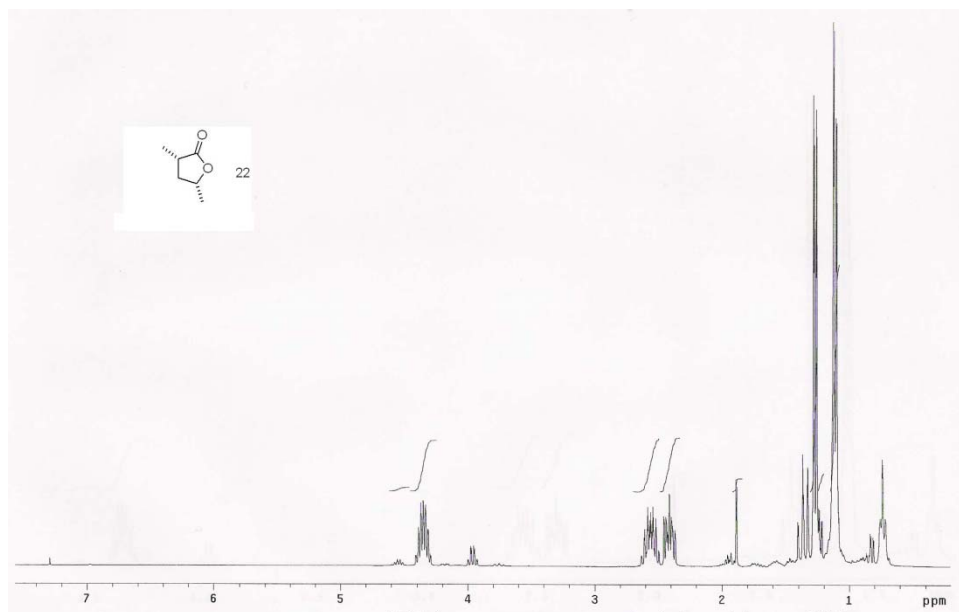
(2S,4R)-2,4-Dimethyl-γ-lactol (2.23).
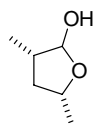
Unisolated lactone 22 (72 mg, 0.65 mmol, 1 eq.) in dichloromethane described above was cooled to -78 °C, and neat diisobutylaluminum hydride (101 mg, 0.72 mmol, 1.1 eq.) was added, dropwise and down the side of the reaction flask. This was stirred for 30 min at –78 °C, at the end of which time 2 ml of saturated aqueous sodium potassium tartrate solution was added and allowed to stir for 2 h. The reaction was diluted with 3 ml of dichlormethane, the layers separated, the aqueous phase extracted with 3 portions of 2 ml dichloromethane, the organic phases combined, dried with sodium sulfate, and filtered. The material can either be used in the next step or isolated by evaporating the dichloromethane by bubbling a thin stream of nitrogen at ambient temperature and pressure. The crude ^{1}H NMR suggested high conversion to the desired γ-lactol in approximately the same diasteriomeric ratio as reported before for the 1 pot formation of the lactol.[85] This compound was not isolated but rather carried through to the next step as a solution in dichloromethane.

Methyl (4S,6R)-*E*-2,4-Dimethyl-6-hydroxyheptenoate (2.24).
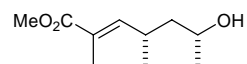
Methoxycarbonyl-ethylidenetriphenylphosphorane (460 mg, 1.3 mmol, 1.5 eq.) was added to a solution of (2S,4R)-2,4-dimethyl-γ-lactol (101 mg, 0.88 mmol, 1 eq.) in 1 ml dichloromethane. This was refluxed for 36 h, at the end of which time the reaction mixture was concentrated onto silica under reduced pressure, and then column chromatography was performed using 15 % ethyl acetate in hexanes (Rf: 0.15) to produce 45 mg, 27 %, of the title compound as a clear oil. ^{1}H NMR showed a mixture of diasteriomers in about a 6 : 1 ratio. ^{1}H NMR (CDCl$_3$, 300 MHz): δ (ppm) = (major isomer only): 6.59 (1H, d), 3.78 (1H, pentet), 3.71 (3H, s), 2.65 (1H, m), 2.84 (3H, s), 1.60-1.38 (4H, m), 1.16 (3H, d), 1.01 (3H, d) 1.11 (3H, d) 1.11 (3H, d); ^{13}C(^{1}H) (CDCl3, 100.4 MHz): δ (ppm) = (major isomer only): 169.0, 147.8, 126.3, 66.4, 51.9, 46.4, 30.5, 24.0, 19.9; MS (m/e): calculated (M+Li): 193.1416, found: 193.1479.
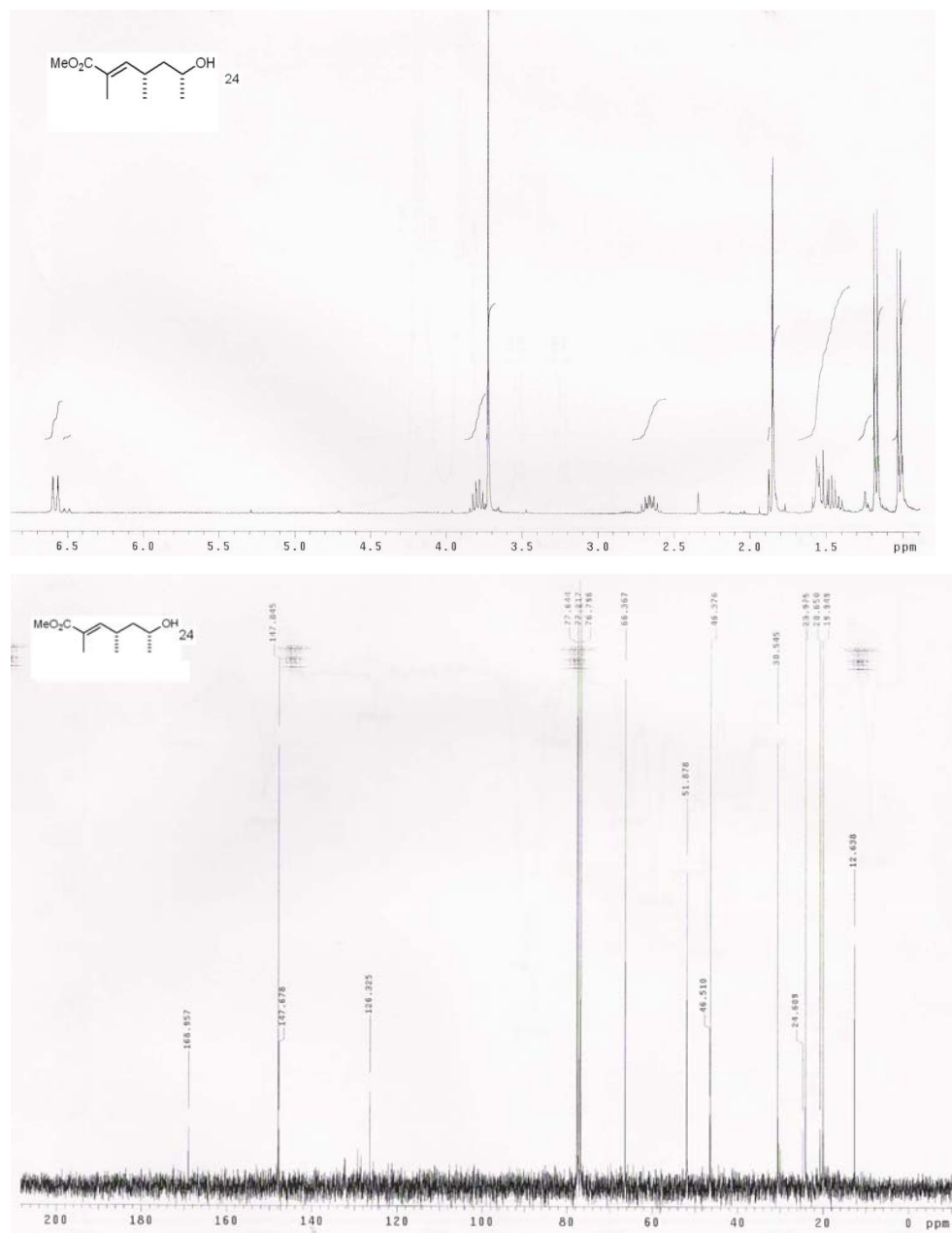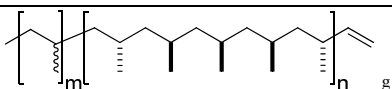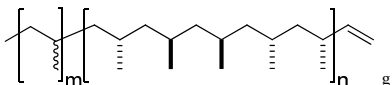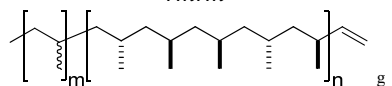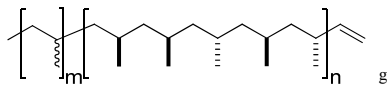
Table A.4. Summary of ^{1}H and [13]C Chemical Shifts for Diastereomeric Methyl Groups.

Entry	Structure	[1]H Shifts[a]	[13]C{[1]H} Shifts[a]	Ref.
2.4d		0.92 (7.0), 0.87 (6.2); *ent* - 0.95-0.8	19.7, 17.2; *ent* - 19.7, 17.2	5,8
reduced 2.4c		0.89 (6.6), 0.84 (6.2); *ent* - 0.95-0.8	18.8, 16.3; *ent* – 18.7, 16.2	5,8

Cont'd

Compound	Structure	¹H shifts (J)	¹³C shifts	Ref.
2.4c	CO₂Me	1.11 (6.9), 0.87 (6.9)	-[d]	120b
anti-2.4a	CO₂Me	1.14 (7.5), 0.87 (6.5); 1.14 (6.9), 0.87 (6.9)[b]	17.7, 16.3	120
A1[c]	CO₂H	1.16 (6.9),	18.8, 16.9	5
A2[c]	CO₂H	1.18 (7.0), 0.87 (6.5)	19.0, 17.9	5
A3[c]	OH	0.88 (6.9), 0.85 (6.3)	19.3, 17.6	9b
A4[c]	OH	1.3-1.0, 0.89 (6.9), 0.84 (6.6)	19.4, 19.2, 17.5, 16.4	9b
A5[c]	OH	0.91 (6.3), 0.86 (6.3)	20.3, 17.3	9b
A6[c]	OH	0.92 (7.2), 0.81 (6.6), 0.79 (6.0), 0.77 (6.3)	20.0, 19.5[f], 19.5[f], 19.3[f], 16.4	9b
2.9	CO₂Me	1.35-0.99, 0.89-0.79[e]	-[e]	*This work*
2.10	CO₂Me	1.14-1.08, 0.88-0.82[e]	-[e]	*This work*
2.13	CO₂Me	0.97 (6.5), 0.85 (6.5)	-[e]	*This work*
A7.1[c]	*mmmm*	-[d]	21.8; 21.8; 21.7[b]	121
A7.2[c]	*rrrr*	-[d]	19.9; 20.5; 20.3; 20.6	121
A7.3[c]	*mmmr*	-[d]	21.6; 21.6; 21.4[b]	121
A7.4[c]	*mmrr*	-[d]	21.1; 21.0; 21.0; 20.9[b]	121
A7.5[c]	*mrrm*	-[d]	20.3; 20.0; 19.8; 19.7[b]	121

Cont'd

A7.6[c]	*rmmr*	_[d]	21.6; 21.3	121
A7.7[c]	*rmrm*	_[d]	21.7; 20.8; 20.6	121
A7.8[c]	*rmrr*	_[d]	21.1; 20.8; 20.9	121
A7.9[c]	*mrrr*	_[d]	20.1	121

[a]Reported as δ shift with coupling constants given in parentheses. [b]Multiple sets of values have been reported, each separated by the semicolon. [c]Values reported for comparative purposes. [d]Values not reported, or are overlapping. [e]Exact values for the shown diastereomer cannot be determined due to mixtures of diastereomers in the sample complicating the spectra. [f]Direct assignment of the methyls cannot be assigned from the data. [g]The pentad descriptions below the structure give the actual repeating units; the fragments **A7** are part of a polymer chain that can include other fragments **A7** - see ref. 121 for full details.

APPENDIX B

EXPERIMENTAL SECTION CHAPTER III

Synthesis and Characterization of Electronically Tunable 1,3,4,5-Tetraaryl *N*-Heterocyclic Carbene Ligands

- synthesis of structures **3.2**, **3.3**, **3.4**, **3.5**, and **3.6**
- ^{1}H, ^{13}C, and ^{19}F NMR spectra and MS of new compounds **3.2**, **3.3**, **3.4**, **3.5**, and **3.6**
- X-ray data for compounds **3.4**
- calculation results for calculations on free carbenes from **3.3** and silver carbenes **3.5**

General Methods and Instrumentation. All air sensitive reactive reactions were carried out in oven-dried glassware and procedures were performed under an atmosphere of dinitrogen in a glovebox or using standard Schlenk techniques. All solvents and reagents were used as received from commercial sources unless otherwise stated. DMF was dried over $MgSO_4$ prior to use. Toluene and dichloromethane used in NHC carbene synthesis were dried using activated alumina columns (MBraun SPS). Hexanes were distilled over CaH_2. $CDCl_3$ and CD_2Cl_2 were stored over 4Å molecular sieves, and after comparison to known spectra using CD_2Cl_2, $CDCl_3$ was used for all compounds under Table 3.1 and 3.2. C_6D_6 was dried over CaH_2 and stored under N_2 in a Straus flask. ^1H, ^{13}C, and ^{19}F NMR measurements were performed on a Varian Mercury 300 or 400 MHz spectrometer and referenced to tetramethylsilane (TMS) using resonances due to residual protons in the deuterated solvents or the ^{13}C resonances of the deuterated solvents. All ^{19}F NMR spectra were recorded on a Varian Mercury instrument operating at a frequency of 376.5 MHz with CF_3CO_2H (-78.5 ppm) as the external standard. All monoimine substrates were obtained by reaction of the aldehyde and the amine in ethanol, followed by removing the solvent, recrystallization from methanol, and drying under vacuum.

Synthesis of the Diketimines 3.2. The general procedure for aldimine coupling is similar to our report in the literature while the oxidation step used 1,4-benzoquinone instead of slow air oxidation.[113] The mono-imine (50 mmol) and NaCN (10 mmol, 20 mol%) were combined in a round bottom flask with a stir bar and DMF was added. The flask was fitted with a 180 degree needle valve and was degassed under vacuum and back-filled with N_2. The reaction was stirred for 24 hours at 25 ^{o}C. Both of the following methods were used for all substrates with no significant difference in the isolated yields:

Method A. The reaction was added to 50 mL of methanol and cooled in the freezer for 1-2 hours. The ene-diamine coupling product with *E*/*Z* isomers was isolated by filtration and dissolved in 50 mL of dichloromethane. One equivalent of 1,4-benzoquinone corresponding to the coupling product was added and the suspension was stirred for 2 hours. This was then washed with 80 mL water. The water layer was extracted with 50 mL of dichloromethane twice, and the combined dichloromethane layers were extracted with water a few times then dried over $MgSO_4$. The solvent was removed and the residue solid was recrystallized from methanol to give solid product, pure by ^1H NMR. Isolated yields are as reported in Table 1 in Chapter III.

Method B. Dichloromethane (100 mL) was added to the reaction mixture. DMF was extracted by washing with distilled water (100 mL) 3 times. One equivalent of 1,4-benzoquinone relative to the coupling product was added and allowed to stir for 2 hours open to air. After this, the reaction mixture was filtered and extracted with water (100 mL) 3 times. The combined aqueous layers were washed with 100 mL dichloromethane, and the combined organic layers were dried over $MgSO_4$. After filtering, the solvent was removed and the residue solid was recrystallized from methanol to give solid product, pure by ^1H NMR. Isolated yields are as reported in Table 1 in Chapter III.

Synthesis of Imidazolium Chloride Compounds 3.3. The modified general procedure was reported in the literature.[114,115] The diketimine (5 mmol) was added to a 20 mL toluene solution of previously dissolved solid paraformaldehyde (7.5 mmol, 1.5 eq.) at 40 °C. After purging with N_2 for 5-10 min, HCl (4.0 M solution in dioxane, 1.5 mL, 1.2 eq.) was syringed in. An immediate color change from orange to red was observed, followed by a change to a yellow colloidal solution after 30 minutes to 1 hour. The reaction was stirred for 12-36 hrs at 40 °C. The mixture was filtered through a fine frit and the solid was washed with some THF and then was washed with 30-50 mL of dichloromethane. The orange dichloromethane solution was transferred to a separation funnel and washed with water until the water layer was colorless. Most dichloromethane was removed *in vacuo*, and the concentrated dichloromethane solution was transferred to a tube and layered with pentane. Slow diffusion of pentane gave light yellow to tan crystalline, mildly hygroscopic solids. High quality single crystals of **3.3d** grown from dichloromethane layered with pentane were used for X-ray diffraction analysis to confirm the imidazolium salt structure. Isolated yields are as reported in Table 2 in Chapter III.

Synthesis of NHC Carbenes. The standard procedure for deprotonation of imidazolium salts was used.[116] A small flask in the glovebox was charged with the imidazolium salt and 1-2 eq of KO^tBu; then, 10-20 mL of dry THF was added to give a brown mixture immediately. The flask was connected to a swivel frit and this was attached to the Schlenk line. After stirring for a few hours at room temperature, the volatiles were removed and to the residue was added 50 mL dry hexanes. After extracting the residue, the filtrate was concentrated and the yellowish precipitate was filtered and dried under vaccum. The two NHC carbene compounds—corresponding to **3.3b** and **3.3e**—were isolated in low yield (around 30 %).

Synthesis of NHC Silver Chloride Carbenes 3.4. The general reaction scheme accompanying Table 2 of Chapter III was used to synthesize these compounds and this procedure is based on several known methods.[117] Imidazolium chloride salts **3.3** (3 mmol, 1 eq.) were added to silver oxide (3 mmol, 1 eq.), and to this was added 10 mL dichloromethane. After flushing with N_2 for 5 minutes, the flask was equipped with a condenser and heated to reflux. After 4 hours, the solution was filtered through a plug of celite, concentrated *in vacuo*, layered with 5 mL pentane, and allowed to crystallize at -4 °C for 18 hours. Filtration followed by washing with 20 mL pentane gave the silver complexes **4** as colorless needles. Single crystals for X-ray diffraction analysis were grown by a mixed solvent method (pentane layered over a dichloromethane or 1,2-dichloroethane solution of the complex at -4 °C) or by a slow diffusion method (pentane diffused into a dichloromethane or 1,2-dichloroethane solution at -4 °C). The ^{13}C NMR peak for the carbene carbons could not be detected for these complexes (a common occurrence[116]), and high resolution mass spectrometry (HRMS) only detected the free carbene ligands; thus, single crystal X-ray diffraction spectroscopy was used to provide positive identification. Isolated yields are as reported in Table 2 in Chapter III.

Summary of ^{1}H, ^{13}C, ^{19}F NMR, and MS Data

Benzil dianil, CAS [7510-33-0] (**3.2a**).[117]
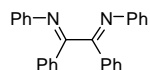
^{1}H NMR (CDCl$_3$): δ 7.90 (m, 4H, phenyl), 7.40 (m, 6H, phenyl), 7.06 (6H, m, phenyl), 6.53 (m, 4H, phenyl). ^{13}C{^{1}H} NMR (CDCl$_3$): δ 164.1 (s, *C*=N), 149.6, 137.9, 131.4, 129.0, 128.6, 128.5, 125.1, 120.3 (phenyl carbons). The NMR showed no appreciable difference in CD$_2$Cl$_2$ or CDCl$_3$.

N,N'-[1,2-bis(4-methylphenyl)-1,2-ethanediylidene]bis-benzenamine, CAS [21854-88-6] (**3.2b**).[117]
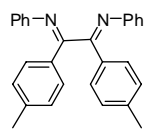
^{1}H NMR (CDCl$_3$): δ 7.79 (d, 4H, J_{HH} = 8.0 Hz, phenyl), 7.21 (d, 4H, J_{HH} = 8.0 Hz, phenyl), 7.03 (m, 6H, aryl), 6.47 (m, 4H, aryl), 2.39 (s, 6H, C*H*$_3$). ^{13}C{^{1}H} NMR (CDCl$_3$): δ 164.2 (s, *C*=N), 149.8, 141.8, 135.5, 129.7, 128.6, 128.5, 124.9, 120.4 (aryl carbons), 21.8 (s, *C*H$_3$). The NMR showed no appreciable difference in CD$_2$Cl$_2$ or CDCl$_3$.

N,N'-(1,2-bis(4-fluorophenyl)ethane-1,2-diylidene)dianiline (**3.2c**).
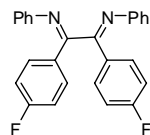
^{1}H NMR (CDCl$_3$): δ 7.90 (m, 4H, aryl), 7.14-7.04 (m, 10H, overlap), 6.55 (m, 4H, aryl). ^{13}C{^{1}H} NMR (CDCl$_3$): δ 166.4 (*C*=N), 163.1, 162.6, 149.2, 125.4, 120.3 (aryl carbons), 133.8 (d, J_{CF} = 3.2 Hz), 130.6 (d, J_{CF} = 9.0 Hz), 116.2 (d, J_{CF} = 22 Hz, F*C*). MS Calc'd [M+Na]$^+$: 397.1511, Found: 397.1537.

¹H
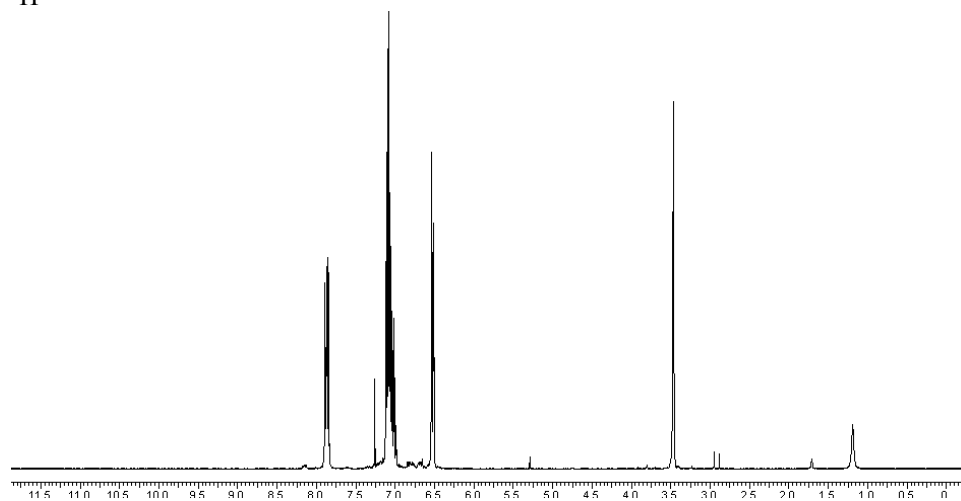
¹³C
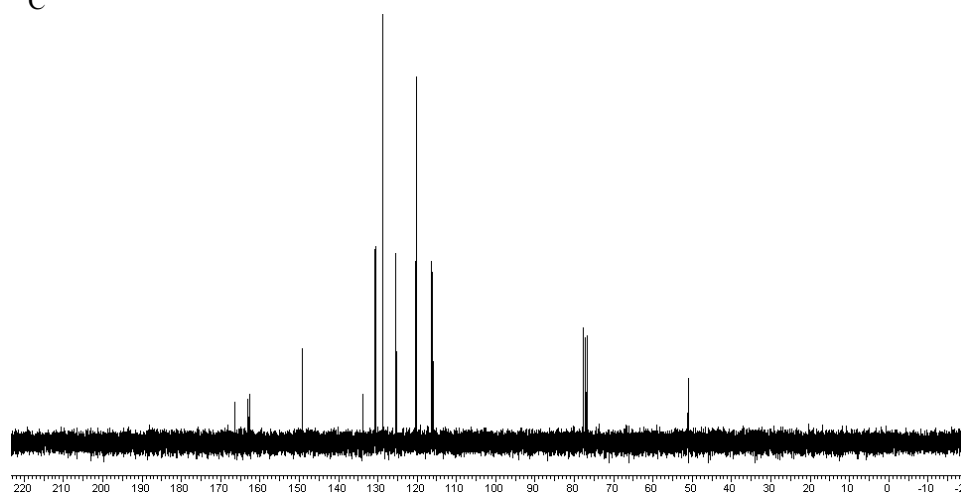
¹⁹F
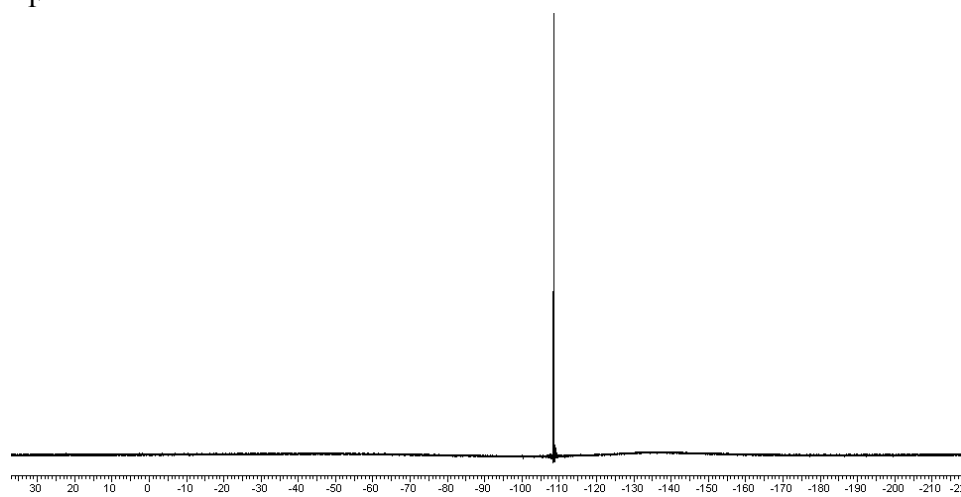
N,N'-(1,2-bis(4-(trifluoromethyl)phenyl)ethane-1,2-diylidene)dianiline (**3.2d**).
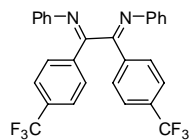
^{1}H NMR (CDCl$_3$): δ 8.02 (d, 4H, J_{HH} = 8.0 Hz, aryl), 7.71 (d, 4H, J_{HH} = 8.0 Hz, aryl), 7.13 (m, 6H, aryl), 6.58 (m, 4H, aryl). ^{13}C{^{1}H} NMR (CDCl$_3$): δ 162.2 (*C*=N), 148.9, 140.3, 133.3, 132.9, 128.9, 128.8, 126.0, 120.3 (aryl carbons), 126.2 (q, J_{CF} = 4 Hz, *C*F$_3$). ^{19}F NMR (CDCl$_3$): δ -64.3 (s). MS Calc'd [M+H]$^+$: 497.1447, found 497.1487.

^{1}H
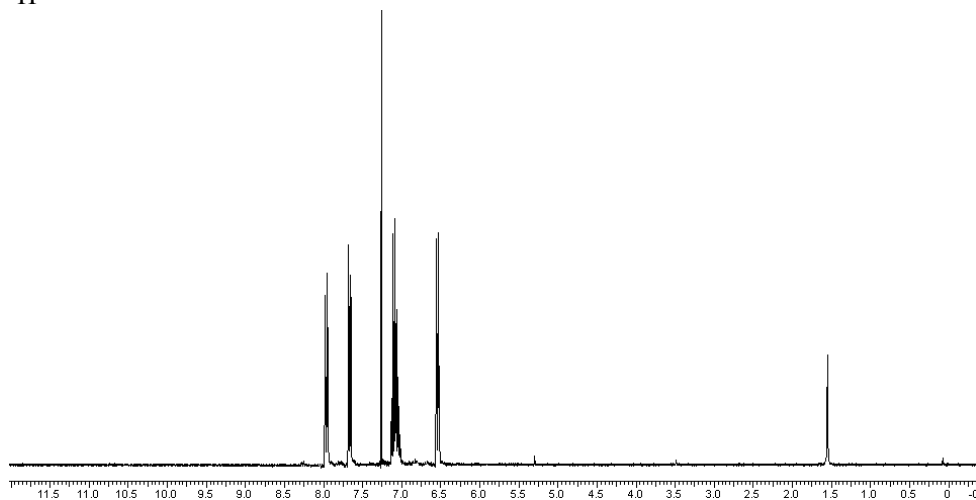
^{13}C
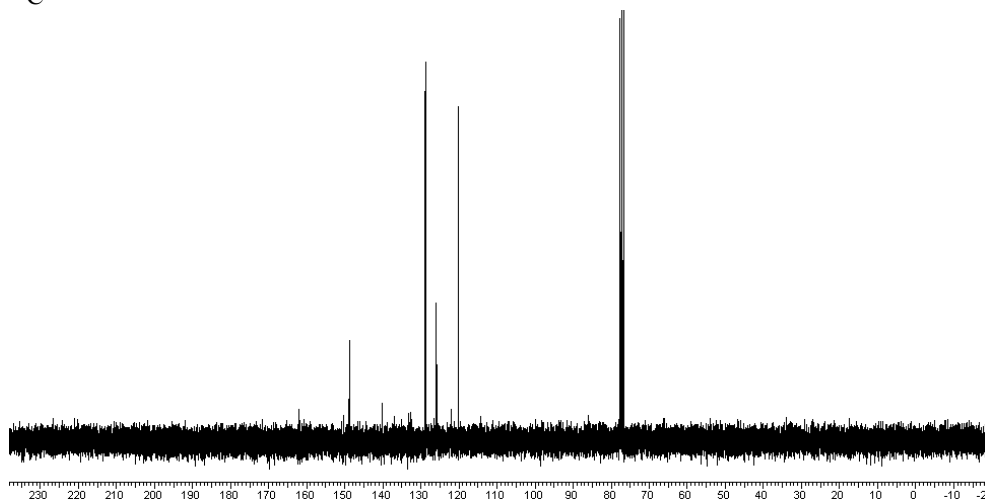
^{19}F
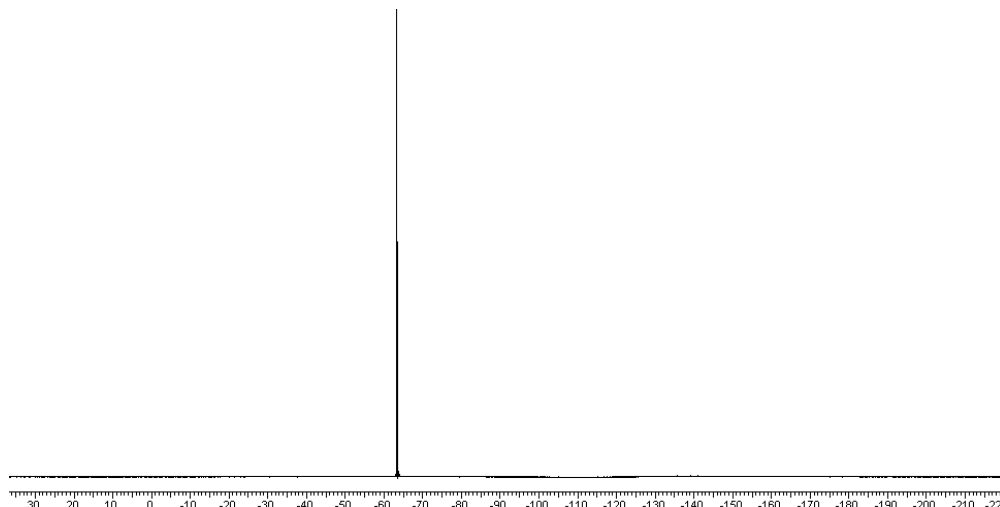
N,N'-[1,2-bis(4-methoxyphenyl)-1,2-ethanediylidene]bis-benzenamine, CAS [21854-89-7] (**3.2e**).[117]
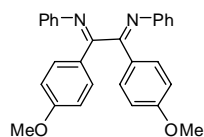
^{1}H NMR (CDCl$_3$): δ 7.89 (d, 4H, J_{HH} = 8.0 Hz, aryl), 7.10 (m, 10H, aryl), 6.50 – 6.48 (m, 4H), 3.84 (s, 6H, CH_3). ^{13}C{^{1}H} NMR (CDCl$_3$): δ 163.6 (*C*=N), 162.2, 149.9, 130.9, 130.4, 128.6, 124.8, 120.5, 114.3 (aryl carbons), 55.6 (*C*H$_3$). The NMR showed no appreciable difference in CD$_2$Cl$_2$ or CDCl$_3$.

N,N'-(1,2-diphenyl-1,2-ethanediylidene)bis-4-fluoro- Benzenamine, CAS [616895-35-3] (**3.2f**).[118]
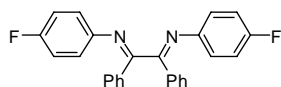
^{1}H NMR (CDCl$_3$): δ 7.90 (m, 4H, aryl), 7.44 (m, 6H, phenyl), 6.80 (m, 4H, phenyl), 6.54 (m, 4H, phenyl). ^{13}C{^{1}H} NMR (CDCl$_3$): δ 164.4 (*C*=N), 162.2, 159.0, 145.6, 137.6, 131.6 (aryl carbons), 128.8 (d, J_{CF} = 50 Hz, F-*C*), 122.0 (d, J_{CF} = 8 Hz, FCCH*C*H), 115.5 (d, J_{CF} = 22 Hz, FC*C*H).

N,N'-[1,2-bis(4-methylphenyl)-1,2-ethanediylidene]bis-4-methylbenzenamine, CAS [77014-38-1] (**3.2g**).[117]
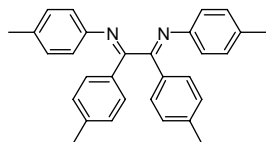
^{1}H NMR (CDCl$_3$): δ 7.70 (d, 4H, J_{HH} = 8.0 Hz, tolyl), 7.18 (d, 4H, J_{HH} = 8.0 Hz, tolyl), 6.87 (d, 4H, J_{HH} = 8.0 Hz, phenyl), 6.47 (d, 4H, J_{HH} = 8.0 Hz, tolyl), 2,37 (s, 6H, CH$_3$), 2.24 (s, 6H, Me). ^{13}C{^{1}H} NMR (CDCl$_3$): δ 164.1 (C=N), 147.1, 141.6, 135.3, 134.5, 129.7, 129.2, 128.5, 120.6 (tolyl carbons), 21.7 (CH$_3$), 21.2 (CH$_3$).

Benzildi-*p*-anisil, CAS [32349-49-8] (**3.2h**).[117]
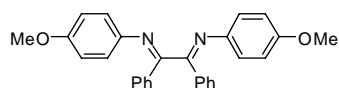
^{1}H NMR (CDCl$_3$): δ 7.87 (m, 4H, aryl), 7.38 (m, 6H, aryl), 6.66 (m, 8H), 3.72 (s, 6H, OCH$_3$). ^{13}C{^{1}H} NMR (CDCl$_3$): δ 163.6 (C=N), 157.7, 142.8, 137.8, 131.2, 129.1, 128.4, 122.5, 114.1 (aryl carbons), 55.7 (CH$_3$).

N,N'-(1,2-bis-(4-methylphenyl)ethane-1,2-diylidene)di(4-trifluoromethyl)phenyl (**3.2k**).
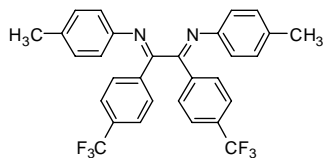
^{1}H NMR (CDCl$_3$): δ 7.94 (d, *J* = 7.9 Hz, 4H), 7.63 (d, *J* = 8.2 Hz, 4H), 6.93 (d, *J* = 8.2 Hz, 4H), 6.59 (d, *J* = 8.5 Hz, 4H), 2.26 (s, 6H). ^{13}C{^{1}H} NMR (CDCl$_3$): δ 161.9, 146.2, 140.2, 136.0, 129.5, 128.5, 126.0 (q, *J* = 4.0 Hz), 122.2, 120.7, 118.6, 21.2. ^{19}F NMR (CDCl$_3$): δ -63.3 (s). MS calc'd: 525.1760 [M+H]$^+$, Found 525.1760 [M+H]$^+$.

^{1}H
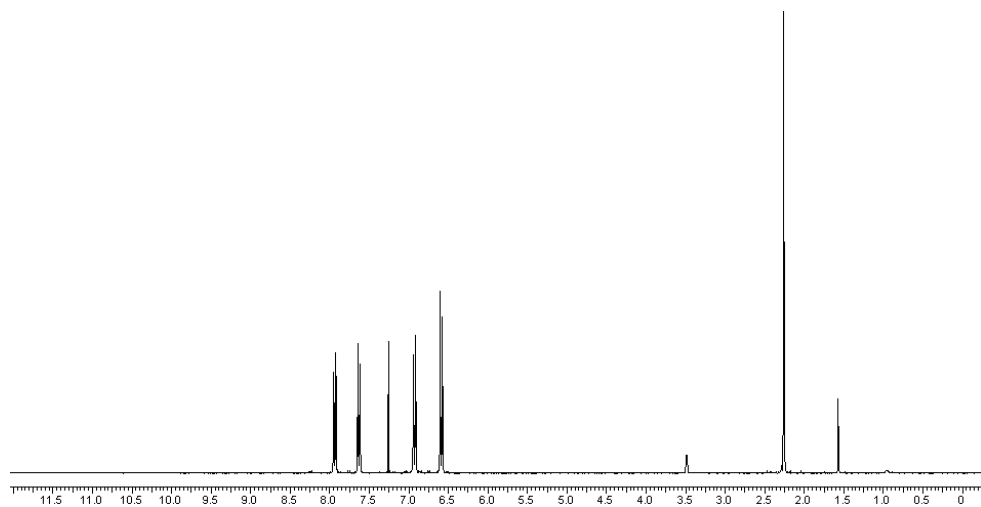
^{13}C
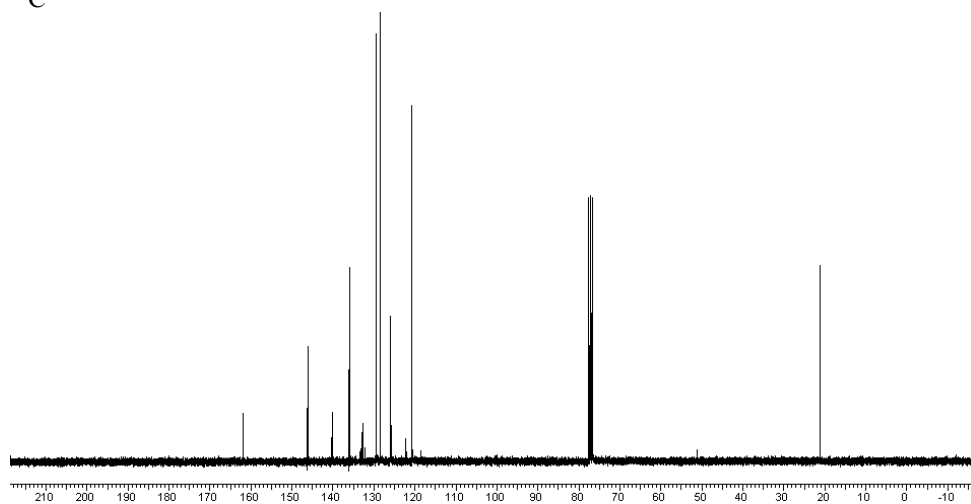
^{19}F
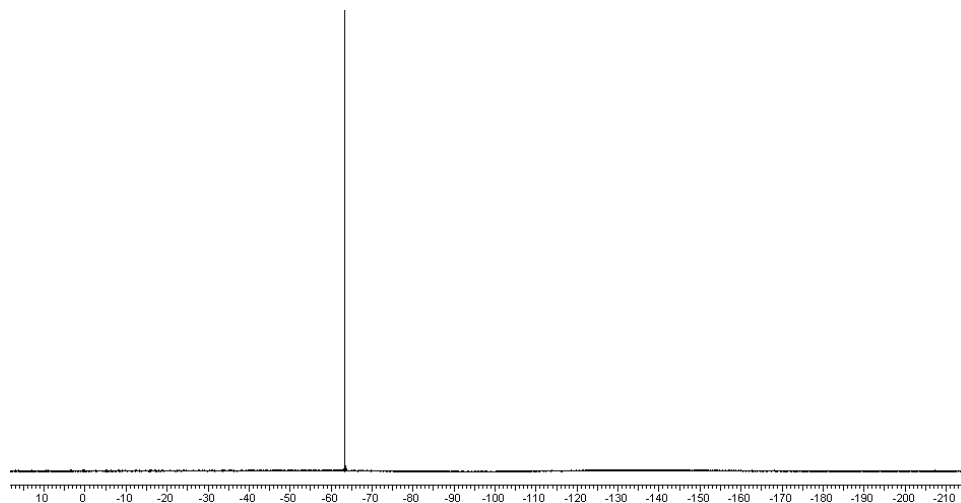
N,N'-(1,2-bis-(anisyl)ethane-1,2-diylidene)di(4-trifluoromethyl)phenyl (**3.2l**).
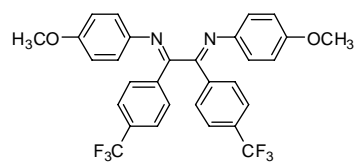
^{1}H NMR (CDCl$_3$): δ 7.93 (d, *J* = 8.3 Hz, 4H), 7.61 (d, *J* = 8.3 Hz, 4H), 6.79 (d, *J* = 9.4 Hz, 4H), 6.68 (d, *J* = 9.1 Hz, 4H), 3.74 (s, 6H). ^{13}C{^{1}H} NMR (CDCl$_3$): δ 161.2, 158.4, 141.7, 140.0, 129.7, 128.9, 128.3, 126.0 (q, *J* = 3.4 Hz), 122.8, 114.1, 55.5. ^{19}F NMR (CDCl$_3$): δ -64.5 (s). MS calc'd: 557.1658 [M+H]$^{+}$, Found 557.1681 [M+H]$^{+}$.

^{1}H
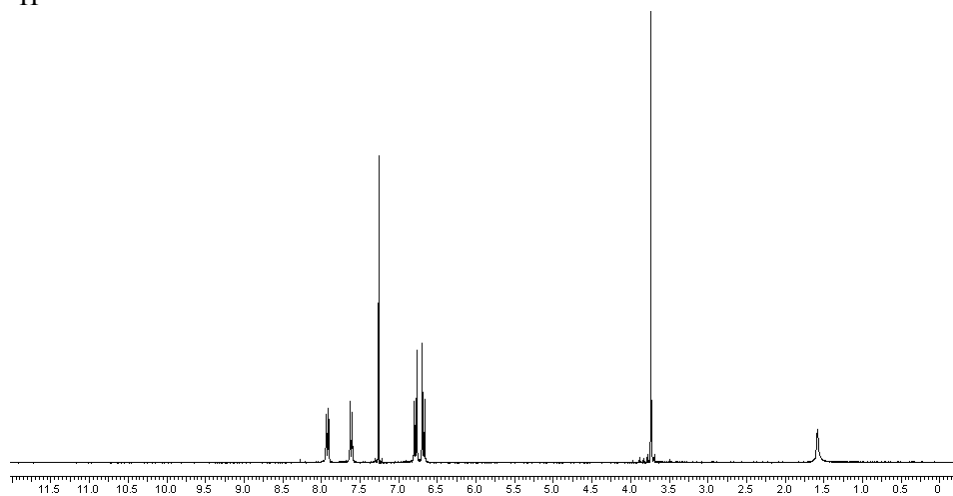
^{13}C
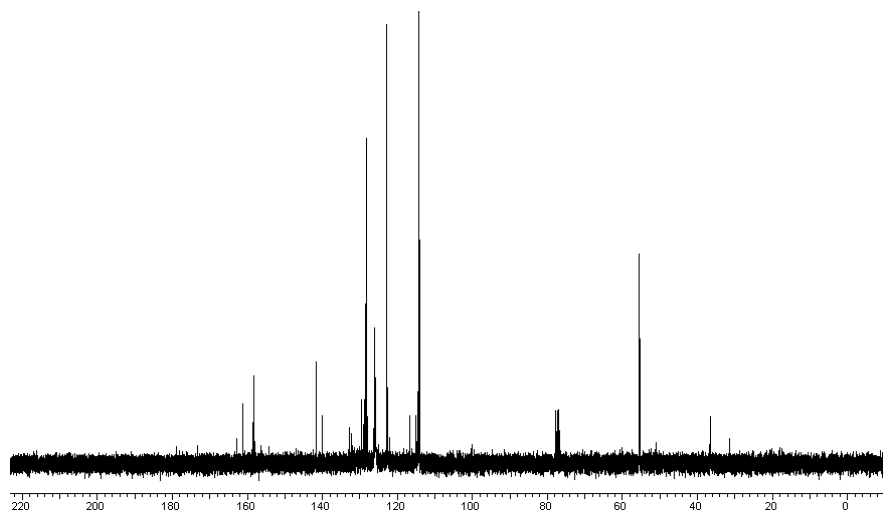
^{19}F
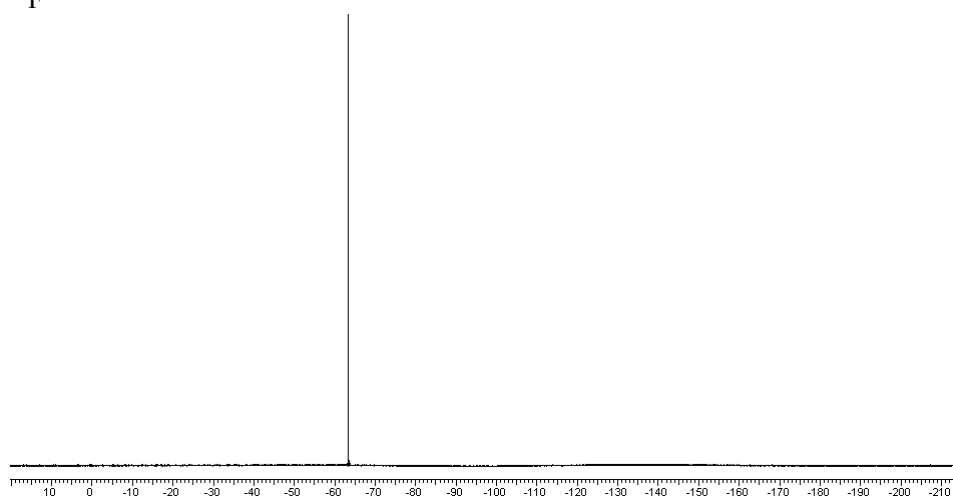
N,N'-(1,2-bis-(phenyl)ethane-1,2-diylidene)di(1-naphthyl) (**3.2n**).
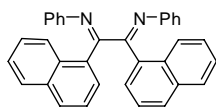
^{1}H NMR (CDCl$_3$): δ 8.86-6.39 (m, 24H), approximately 20% unreacted starting material in spectra. ^{13}C{^{1}H} NMR (CDCl$_3$): δ 133.3, 130.1, 129.5, 128.9, 128.8, 128.7, 128.2, 127.7, 126.5, 126.2, 126.0, 124.5, 124.4, 121.2, 119.8. MS calc'd: 461.2012 [M+H]$^+$, Found 461.2019 [M+H]$^+$.

^{1}H

^{13}C
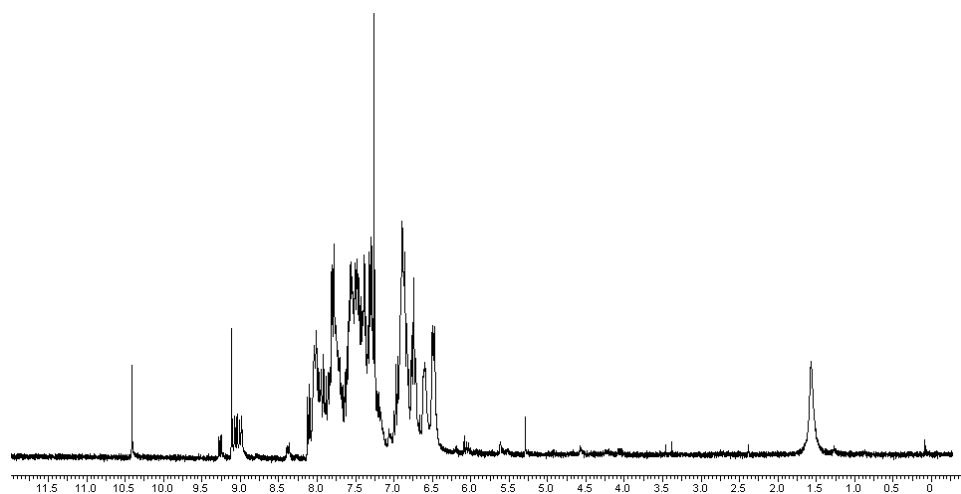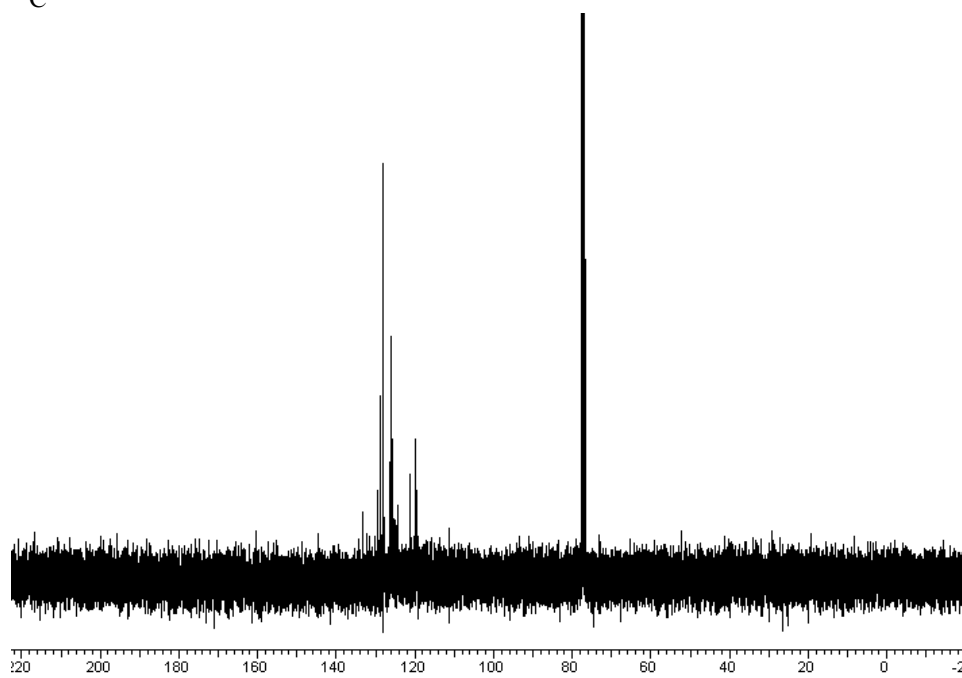
1,3,4,5-Tetraphenyl-1H-imidazolium chloride, CAS [213181-17-0] (**3.3a**).[119]
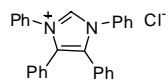
^{1}H NMR (CDCl$_3$): δ 10.81 (s, 1H, NCHN), 7.7 – 7.2 (m, 20H, phenyl). ^{13}C{^{1}H} NMR (CD$_2$Cl$_2$): δ 138.0 (NCH), 134.0, 132.7, 131.5, 130.9, 130.5, 130.2, 129.2, 127.0 (phenyl carbons), 125.0 (NC). The NMR showed no appreciable difference in CD$_2$Cl$_2$ or CDCl$_3$.

4,5-Di(4-methylphenyl)-1,3-diphenyl-1H-imidazolium chloride (**3.3b**).
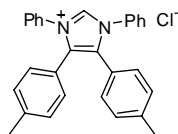
^{1}H NMR (CDCl$_3$): δ 10.85 (s, 1H, NCHN), 7.67 (m, 4H, aryl), 7.45 (m, 6H, aryl), 7.08 (m, 8H, aryl), 2.27 (s, 6H, CH_3). ^{13}C{^{1}H} NMR (CDCl$_3$): δ 140.7 (NCH), 137.6, 134.0, 132.4, 131.2, 130.6, 130.0, 129.8, 126.8 (aryl carbons), 122.3 (NC), 21.4 (CH_3). MS Calc'd: 401.2012, Found 401.2041.

^{1}H

^{13}C
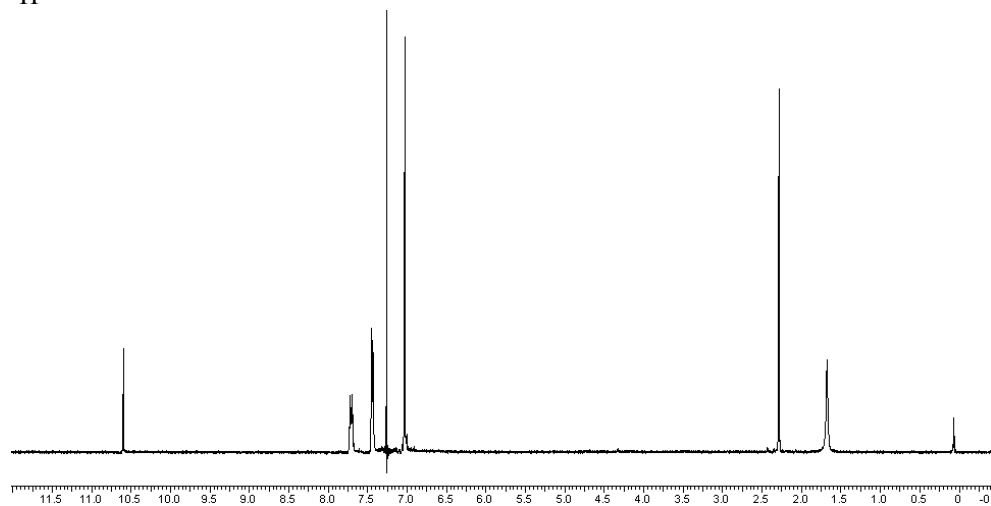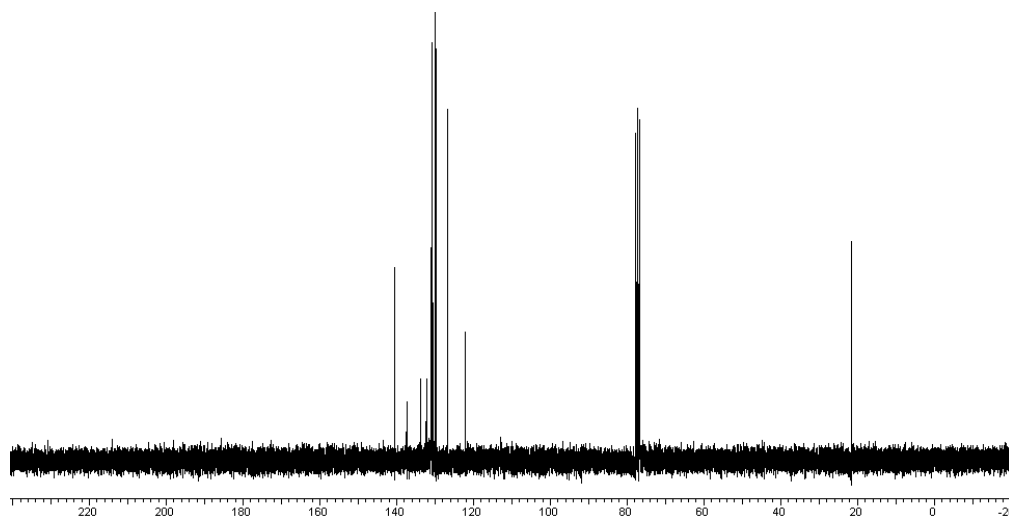
4,5-Di(4-fluorophenyl)-1,3-diphenyl-1H-imidazolium chloride (**3.3c**).
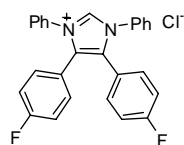
^{1}H NMR (CDCl$_3$): δ 9.86 (s, 1H , NC*H*N), 7.76 (m, 4H), 7.41-7.49 (m, 6H), 7.25 (dd, 4H), 6.97-6.91 (m, 4H).
^{13}C{^{1}H} NMR (75 MHz, CDCl$_3$): δ 133.5, 133.4, 133.3, 132.1, 130.9, 130.1, 127.0, 121.0, 116.6, 116.3. ^{19}F NMR
(CDCl$_3$): δ -109.14 (s, 1 F). MS calc'd: 409.1511, Found: 409.1546.

^{1}H
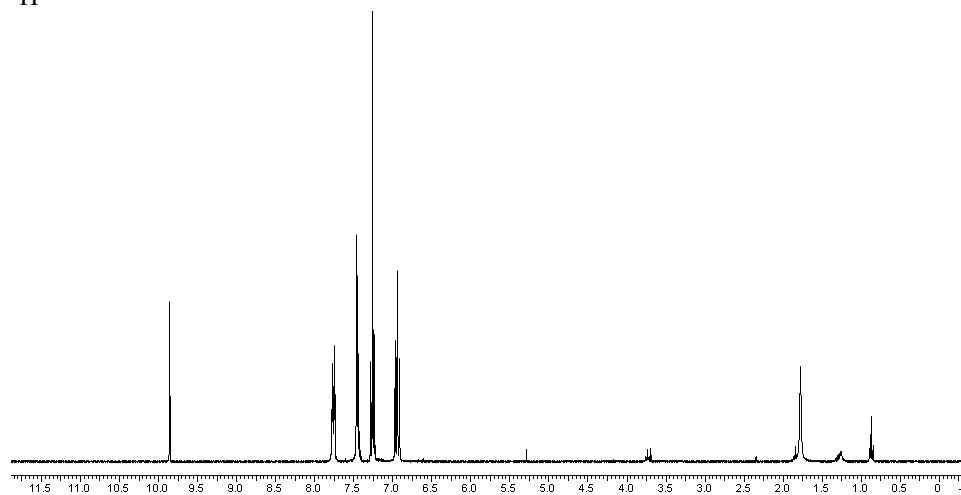
^{13}C
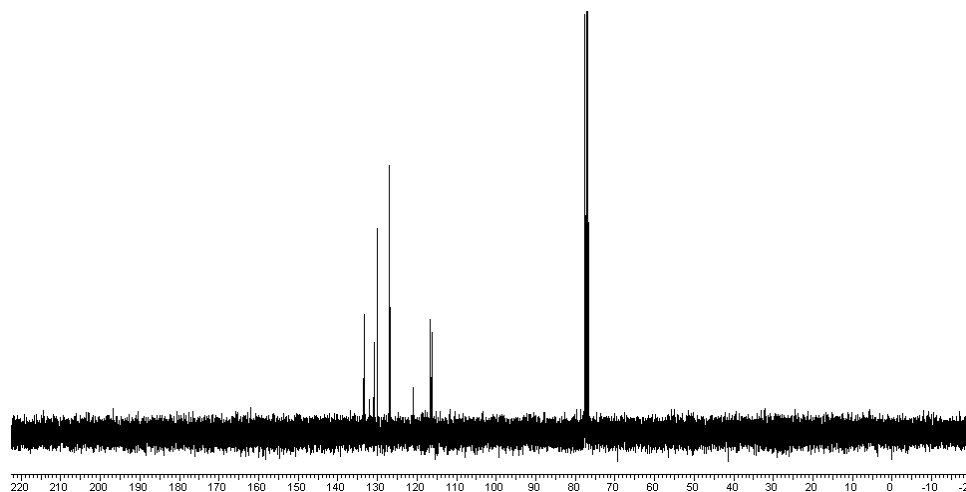
^{19}F
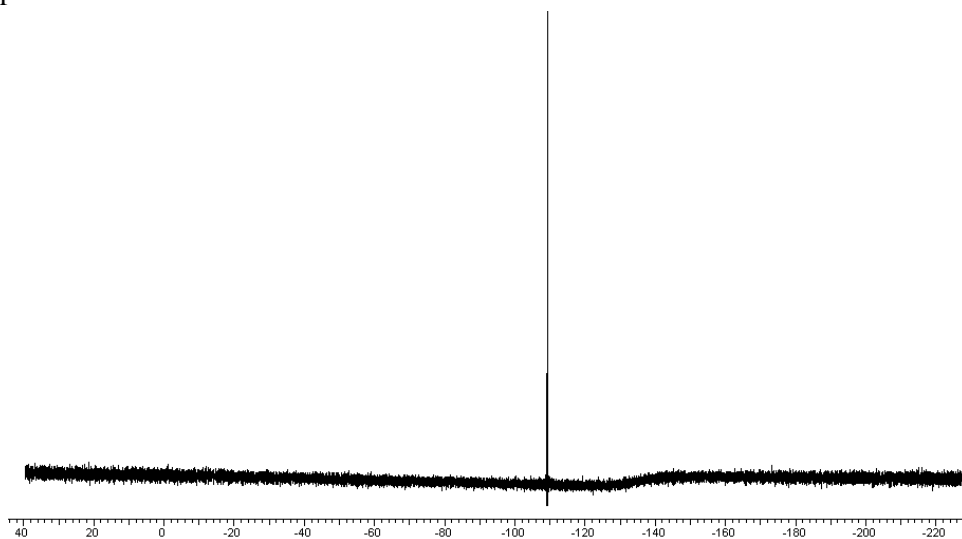
4,5-Di(4-trifluoromethylphenyl)-1,3-diphenyl-1H-imidazolium chloride (**3.3d**).
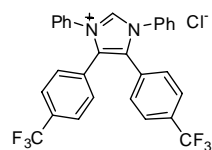
^{1}H NMR (CDCl$_3$): δ 9.70 (s, 1H, NC*H*N), 7.74 (m, 4H, aryl), 7.43 (m, 14H, aryl). ^{13}C{^{1}H} NMR (CD$_2$Cl$_2$, δ): 138.2 (N*C*H), 133.3, 132.6, 132.1, 131.8, 131.1, 130.2, 128.5, 127.0 (aryl carbons), 126.0 (q, J_{CF} = 4 Hz), 121.8 (N*C*). ^{19}F NMR (CDCl$_3$): δ -62.9 (s). MS Calc'd: 509.1447, Found: 509.1458.

^{1}H

^{13}C

^{19}F
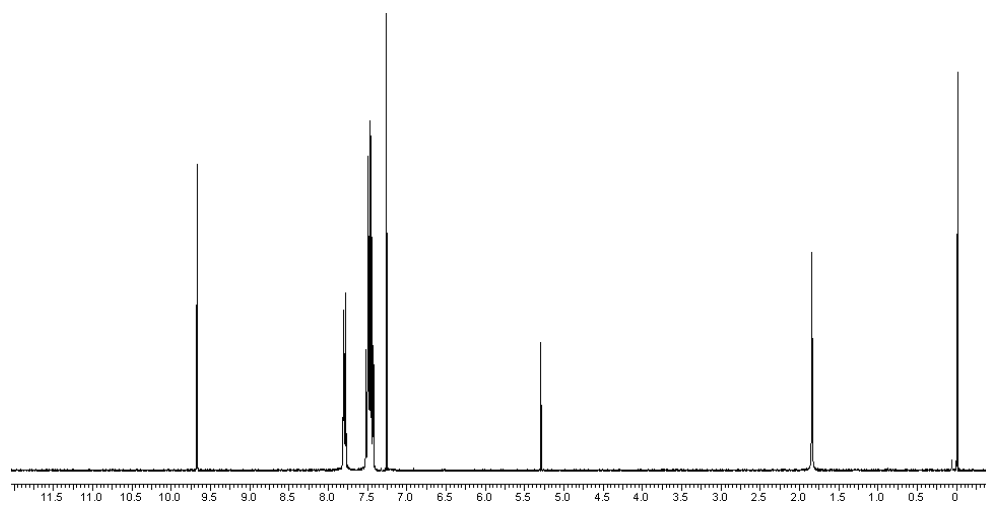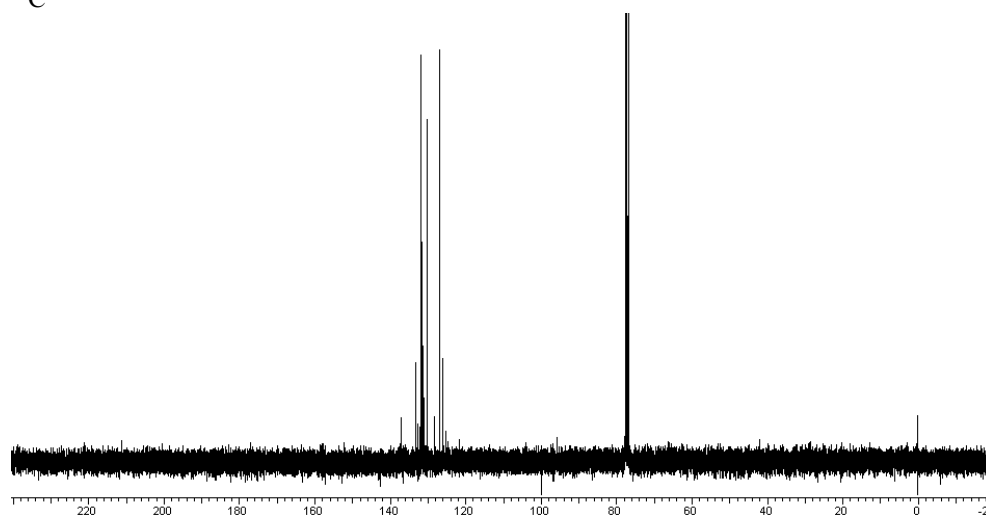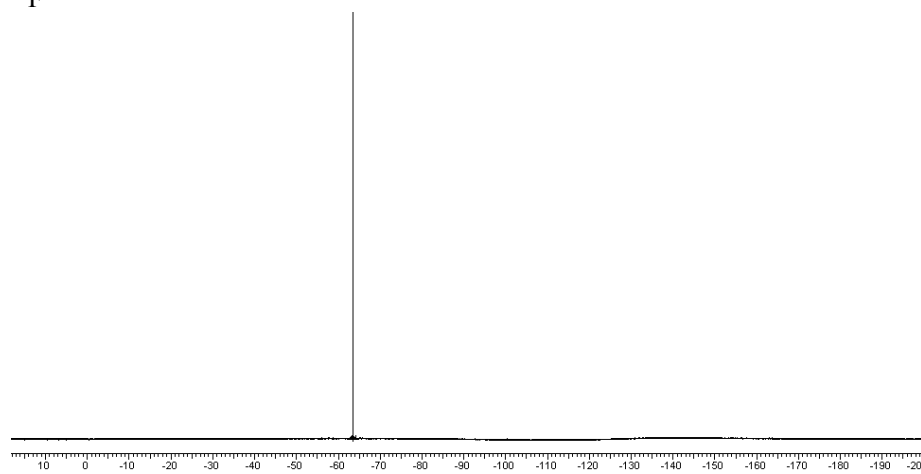
4,5-Dianisil-1,3-diphenyl-1H-imidazolium chloride (**3.3e**).
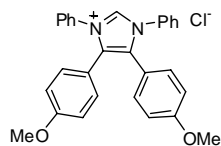
^{1}H NMR (CDCl$_3$): δ 10.58 (s, 1H, NCHN), 7.69 (m, 4H, aryl), 7.50 (m, 6H, aryl), 7.14 (m, 4H, aryl), 6.78 (m, 4H, aryl), 3.74 (s, 6H, CH_3). ^{13}C{^{1}H} NMR (CDCl$_3$): δ 161.0 (NCH), 137.0, 134.0, 132.7, 132.2, 130.5, 129.9, 126.8, 114.4 (aryl carbons), 117.2 (NC), 55.8 (CH_3). MS Cald'd: 433.1911, Found: 433.1944.

^{1}H

^{13}C
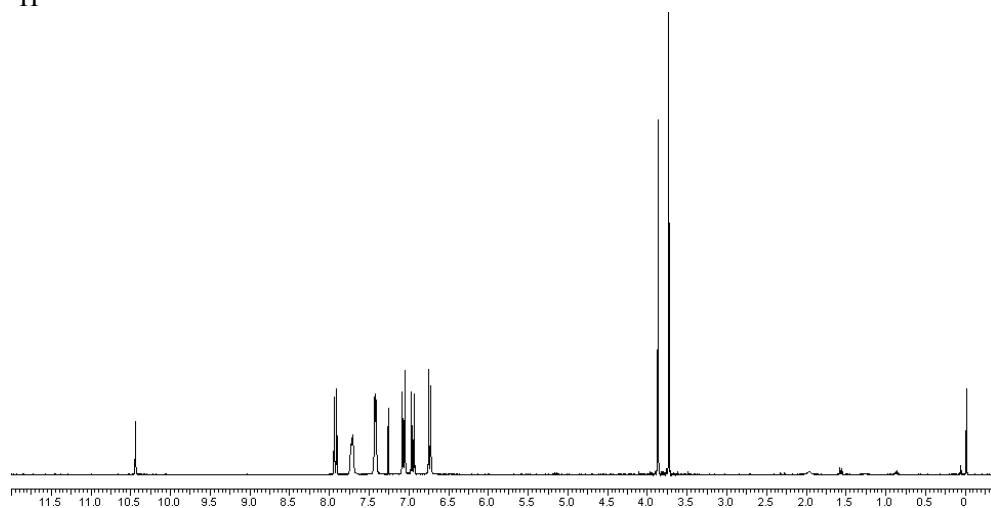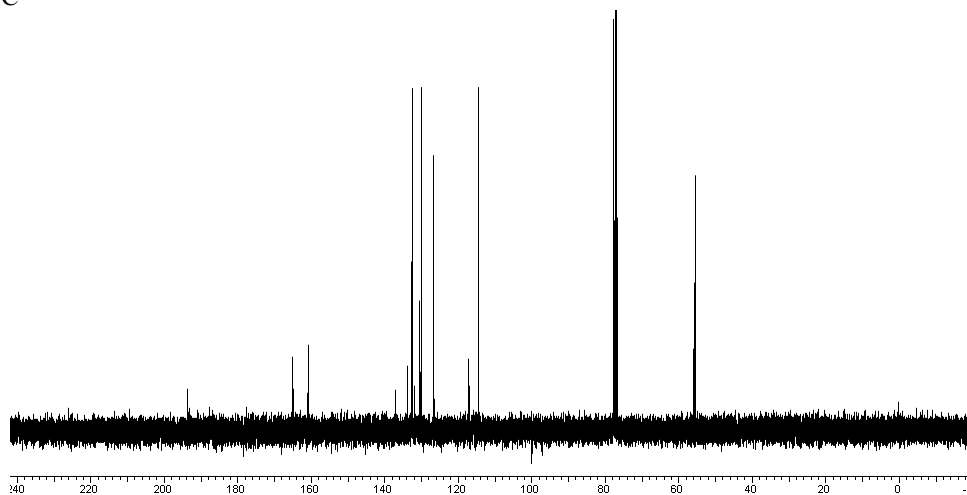
1,3-Di(4-fluorophenyl)-4,5-diphenyl-1H-imidazolium chloride (**3.3f**).
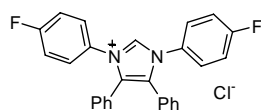
^{1}H NMR (CDCl$_3$): δ 10.88 (s, 1H, NC*H*N), 7.8 – 7.1 (m, 18H, aryl). ^{13}C{^{1}H} NMR (CDCl$_3$): δ 165.4 (NC*H*), 162.1 (N*C*), 138.2, 132.8, 131.5, 130.6, 129.3, 125.2, 117.3, 117.0 (aryl carbons). ^{19}F NMR (CDCl$_3$, δ): -109.3 (s). MS Calc'd: 409.1511, Found: 409.1539.

^{1}H
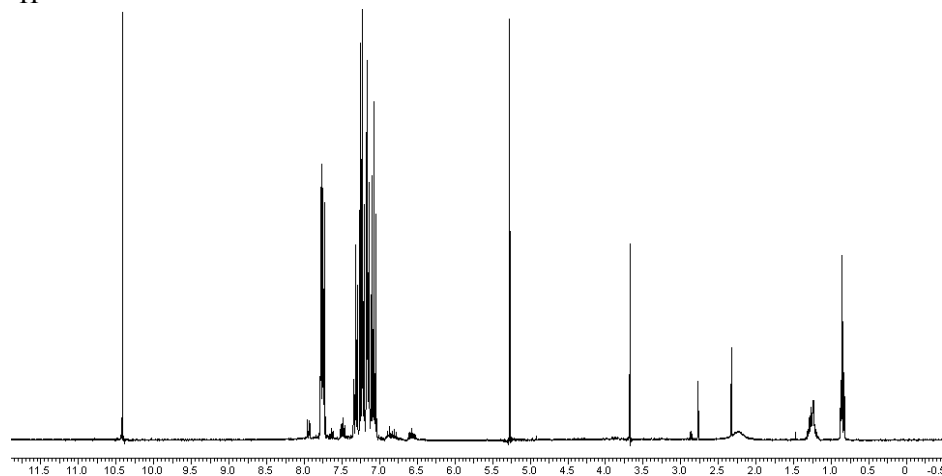
^{13}C
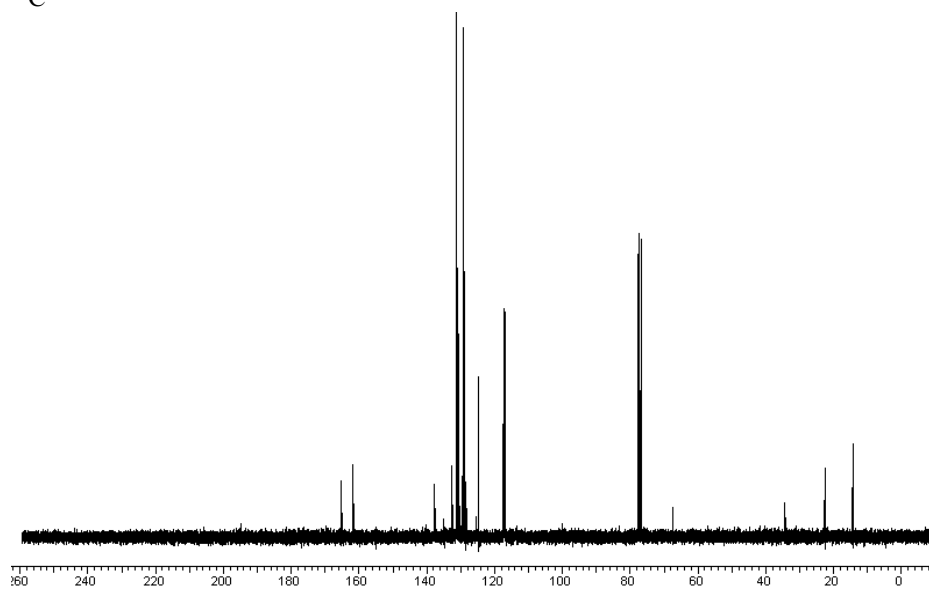
^{19}F
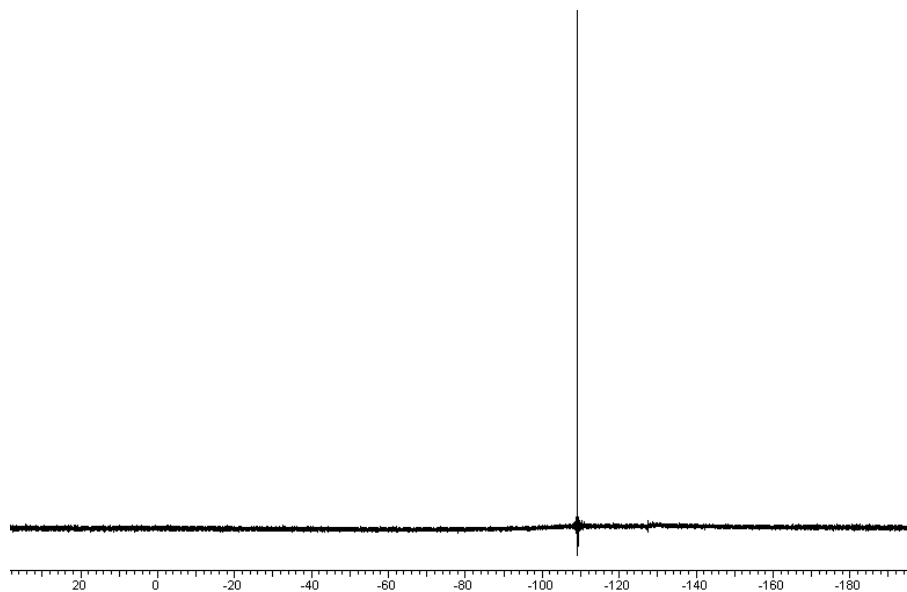
1,3,4,5-tetra(4-methylphenyl)-1H-imidazolium chloride (**3.3g**).
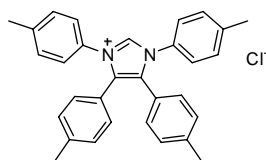
^{1}H NMR (CDCl$_3$): δ 10.62 (s,1H), 7.52 (d, 4H, *J* = 8.5 Hz), 7.21 (d, 4H, *J* = 8.2 Hz), 7.01 (dd, 8H, *J* = 5.1, 8.2 Hz), 2.34 (s, 6H), 2.28 (s, 6H). ^{13}C{^{1}H} NMR (75 MHz, CDCl$_3$): δ 140.7, 140.3, 132.0, 131.2, 130.9, 130.6, 129.9, 129.7, 126.3, 122.3, 21.6, 21.5. MS Calc'd: 429.2325, Found: 429.2312.

^{1}H

¹³C
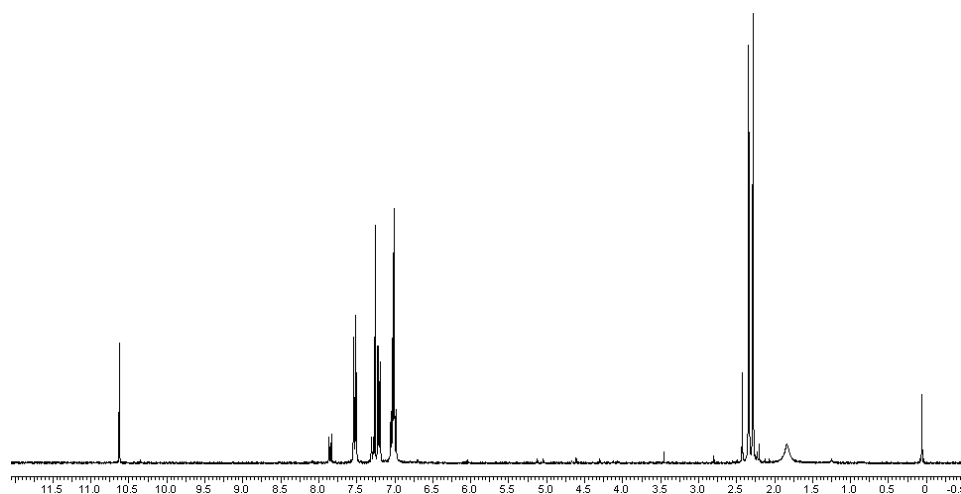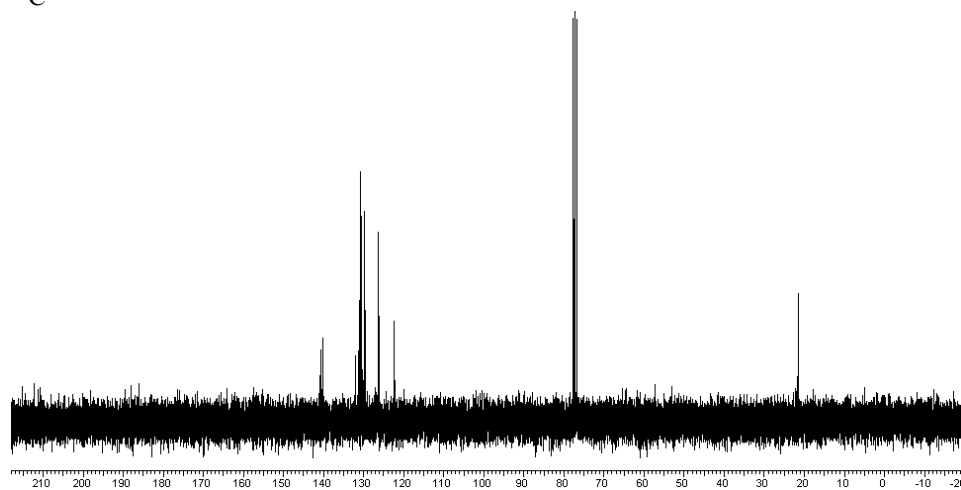
1,3-Dianisil-4,5-diphenyl-1H-imidazolium chloride (**3.3h**).
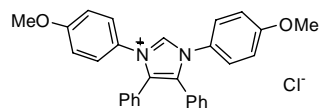
¹H NMR (CDCl₃): δ 10.44 (s, 1H), 7.61 (d, 4H, *J* = 9.1 Hz), 3.77 (s, 6H), 7.30-7.11 (m, 10H), 6.89 (d, 4H, *J* = 9.1 Hz). ¹³C{¹H} NMR (CDCl₃): δ 160.9, 154.2, 131.1, 130.2, 129.0, 128.0, 126.3, 125.2, 115.1, 104.8, 55.8. MS Calc'd: 433.1911, Found: 433.1936.

¹H
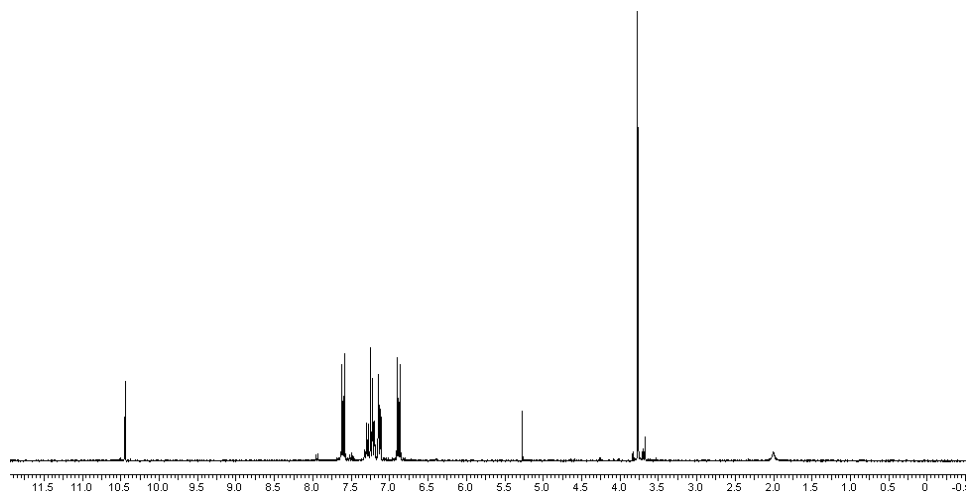
^{13}C
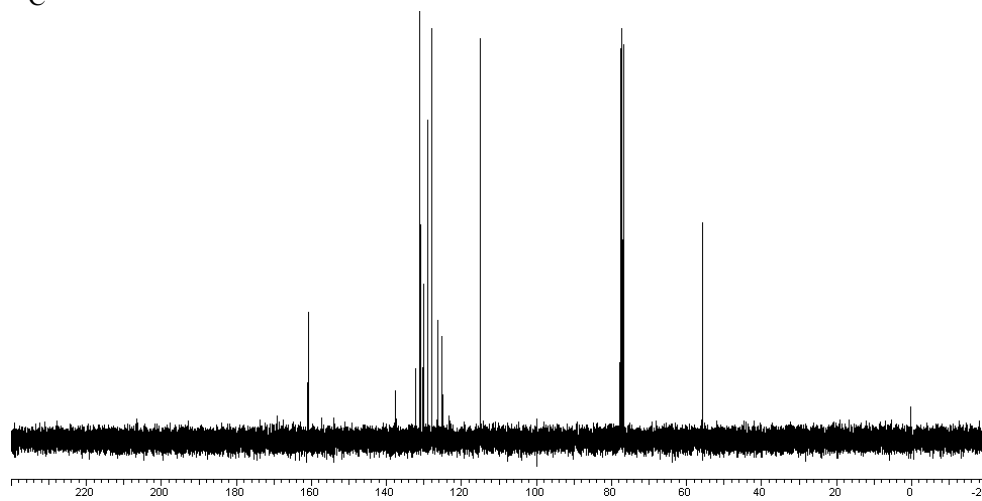
4,5-di(4-methylphenyl)-1,3-diphenyl imidazolium carbene.
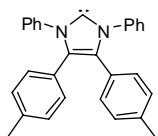
^{1}H NMR (C$_6$D$_6$): δ 7.6 – 6.6 (m, 18H, aryl), 1.88 (s, 6H, CH_3). ^{13}C{^{1}H} NMR (C$_6$D$_6$): δ 219.7 (NCN), 142.5, 137.8, 131.7, 131.2, 129.6, 129.0, 128.3, 127.3 (aryl carbons), 127.0 (NC), 21.4 (CH_3).

^{1}H
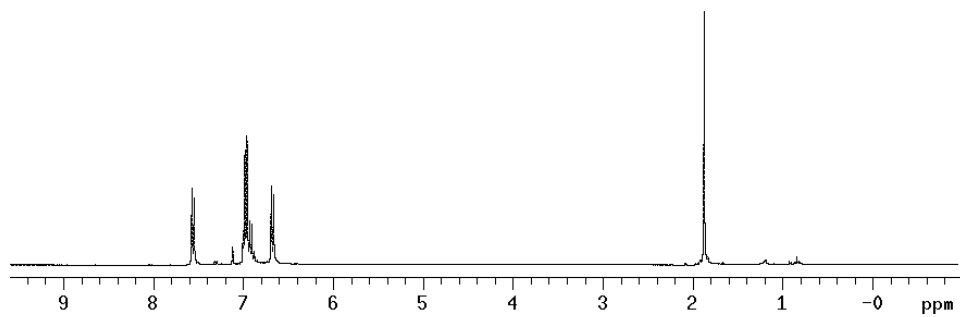
^{13}C
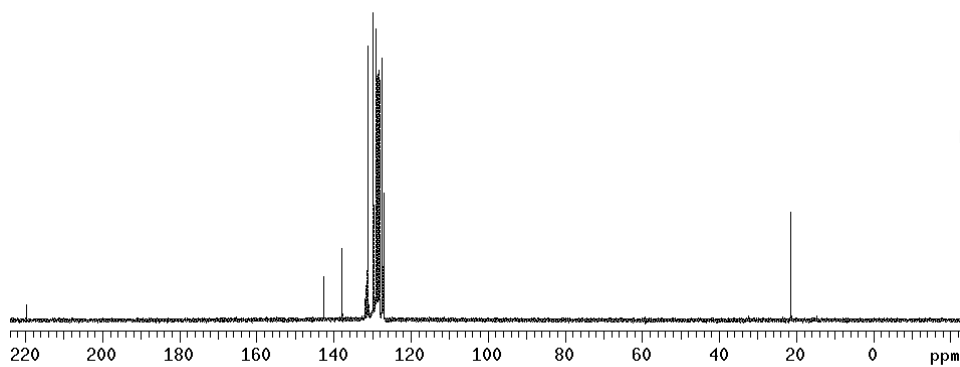
4,5-di(4-trifluorophenyl)-1,3-diphenyl imidazolium carbene.
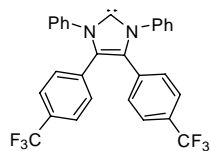
^{1}H NMR (C$_6$D$_6$): δ 7.4 – 6.7 (m, 18H, aryl). ^{13}C{^{1}H} NMR (C$_6$D$_6$): δ 220.6 (NCN), 141.0, 133.5, 130.9, 130.7, 129.8, 128.9, 127.3, 126.7 (phenyl carbons), 125.5 (q, J_{CF} = 4.0 Hz), 122.8 (NC).

^{1}H

¹³C
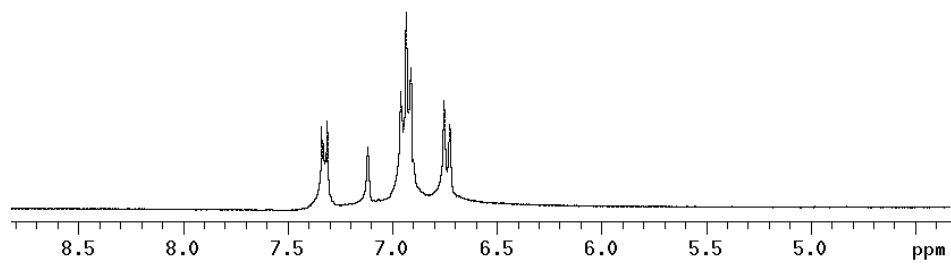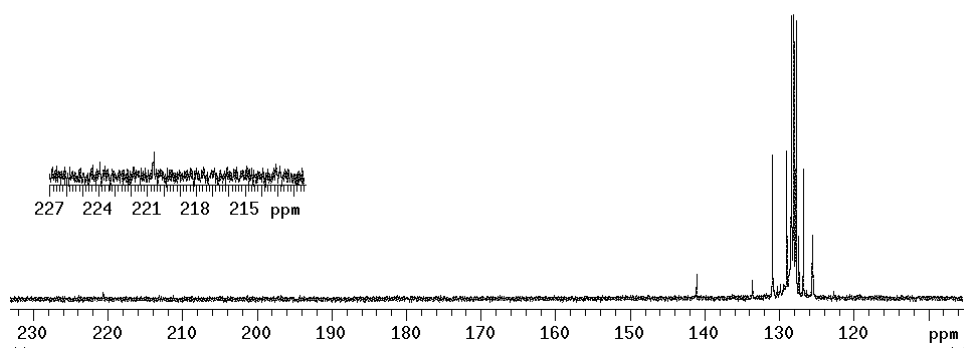
1,3,4,5-Tetraphenylimidazol-2-ylidene silver chloride (**3.4a**).
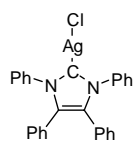
¹H NMR (CDCl₃): δ 7.11 - 7.43 (m, 16H, overlap, aryl), 6.93 - 7.00 (dd, 4H, *J* = 6.9 Hz, 1.0 Hz). ¹³C{¹H} NMR (CDCl₃): δ 138.8, 132.5, 130.7, 129.8, 129.4, 129.0, 128.7, 127.6, 127.2, the Ag*C* peak was not found.

¹H
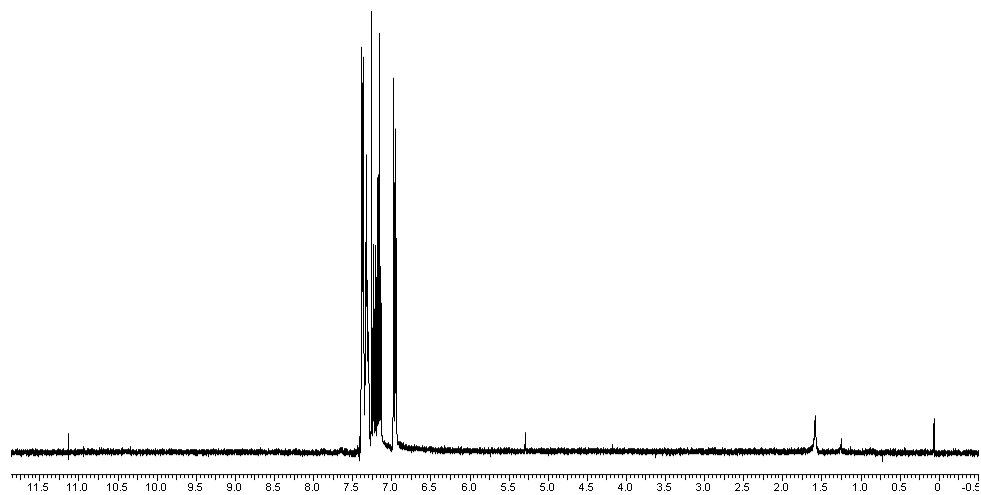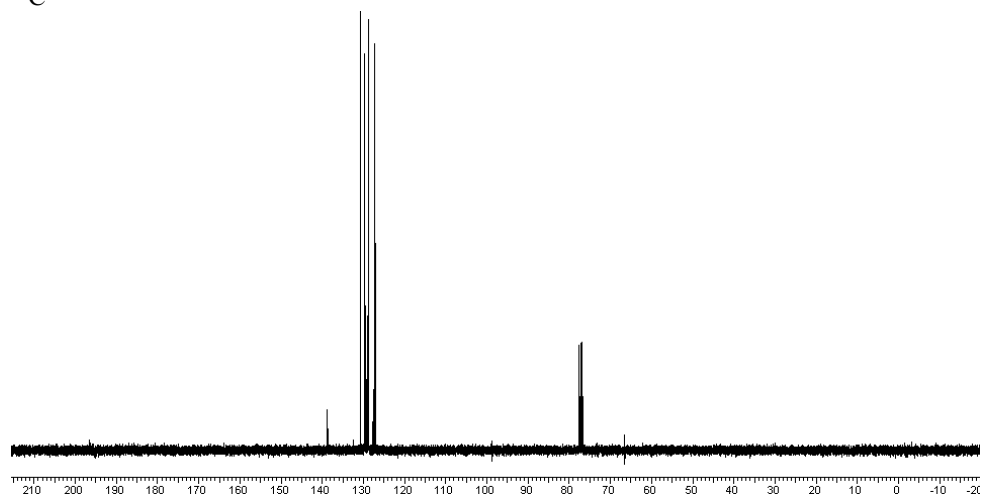
4,5-di(4-fluorophenyl)-1,3-diphenylimidazol-2-ylidene silver chloride (**3.4c**).
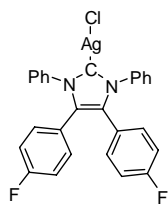
^{1}H NMR (CDCl$_3$): δ 7.44 – 7.36 (m, 6H), 7.33 – 7.27 (m, 4H), 6.98 - 6.84 (m, 8H). ^{13}C{^{1}H} NMR (CDCl$_3$): δ 138.5, 132.6, 129.9, 129.6, 127.2, 123.5, 123.5, 116.3, 116.0, the Ag*C* peak was not found. ^{19}F NMR (282 MHz, CDCl$_3$): δ -111.14 (s, 1 F).

^{1}H

^{13}C

^{19}F
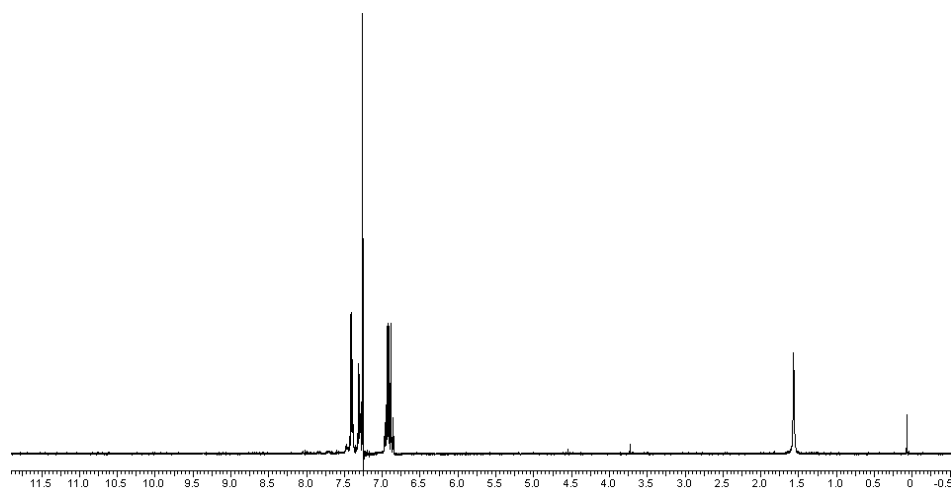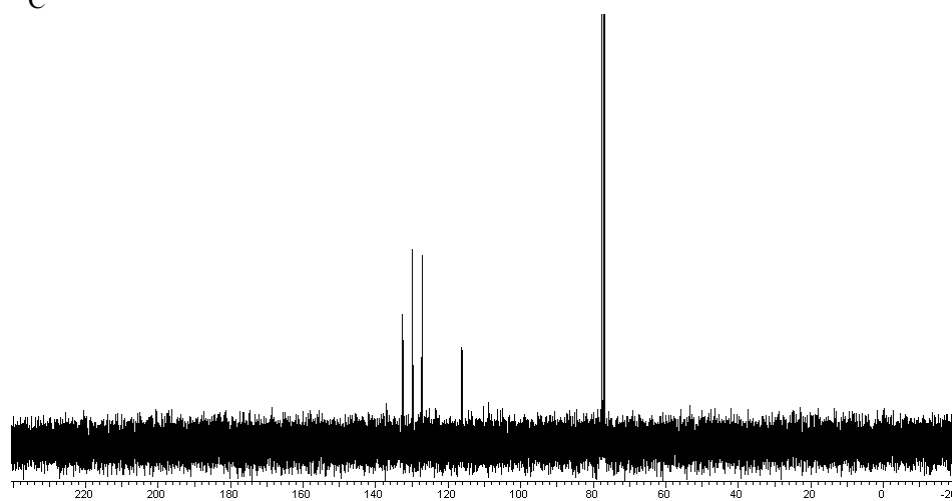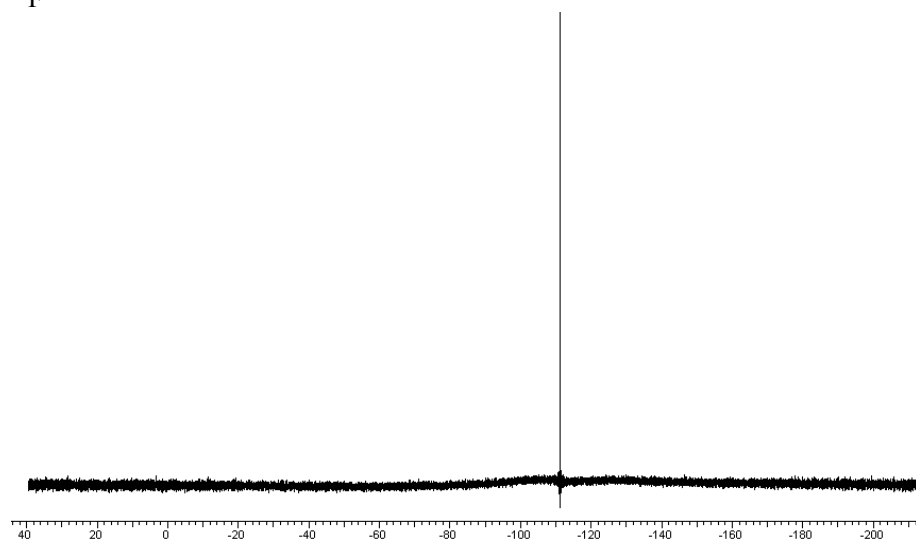
4,5-dianisil-1,3-diphenylimidazol-2-ylidene silver chloride (**3.4e**).
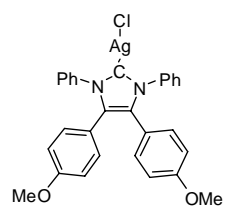
^{1}H NMR (CDCl$_3$): δ 7.37 (m, 6H, J = 5.7 Hz,), 7.33-7.26 (m, 4H) 6.87 (d, 4H, J = 0.8 Hz,), 6.68 (d, 4H, J = 9.1 Hz,), 3.72 (s, 6H). ^{13}C{^{1}H} NMR (CDCl$_3$): δ 159.9, 139.0, 132.0, 129.7, 129.2, 127.2, 119.9, 114.2, 100.1, 55.4, the Ag*C* peak was not found.

^{1}H

^{13}C
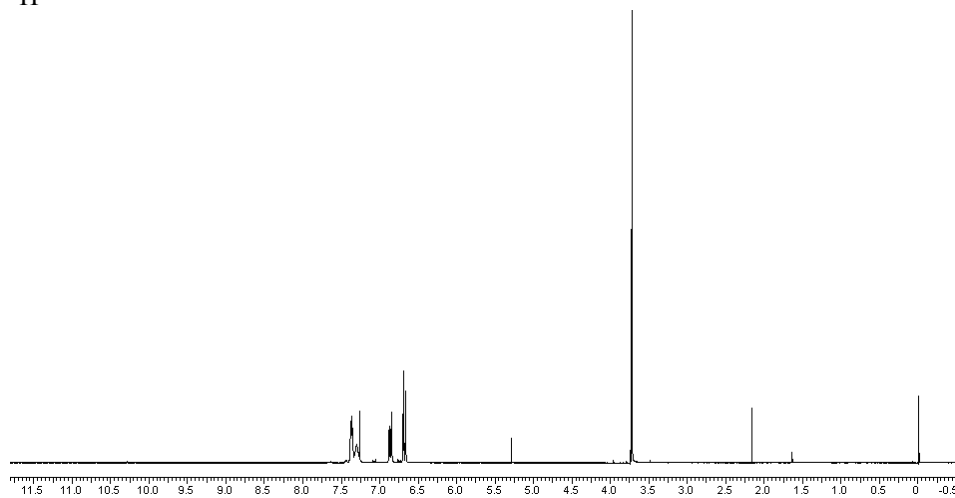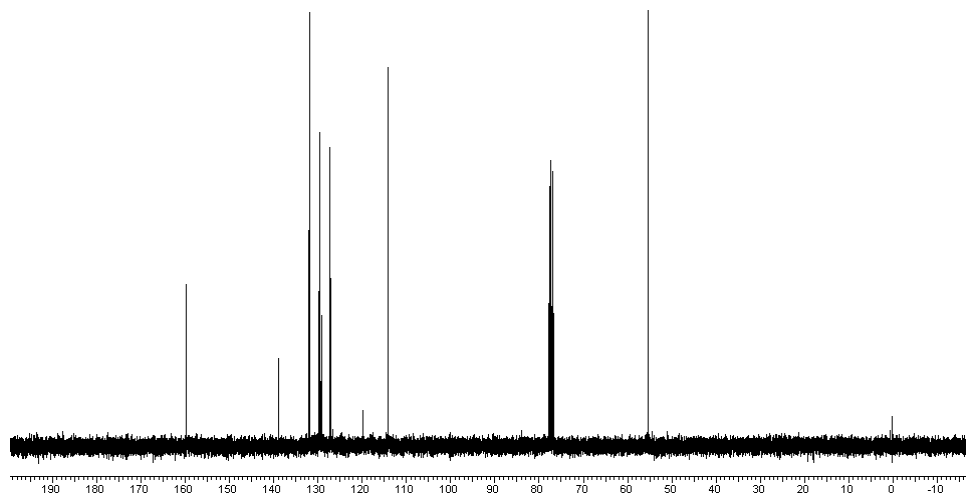
1,3-Di(4-fluorophenyl)-4,5-diphenylimidazol-2-ylidene silver chloride (**3.4f**).
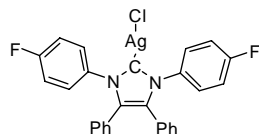
^{1}H NMR (CDCl$_3$): δ 7.41-7.36 (m, 6H), 7.33 - 7.26 (m, 4H), 6.97-6.85 (m, 8H). ^{13}C{^{1}H} NMR (CDCl$_3$): 161.3, 138.5, 132.5 (d, 2C, J = 8.0 Hz), 129.9, 129.6, 127.2, 123.5, 116.2, 116.0, the AgC peak was not found. ^{19}F (CDCl$_3$): -111.15. LRMS [C$_{27}$H$_{18}$N$_2$F$_2$AgCl+H$^+$] calculated: 550, Found 550.

^{1}H

^{13}C

¹⁹F

^{19}F
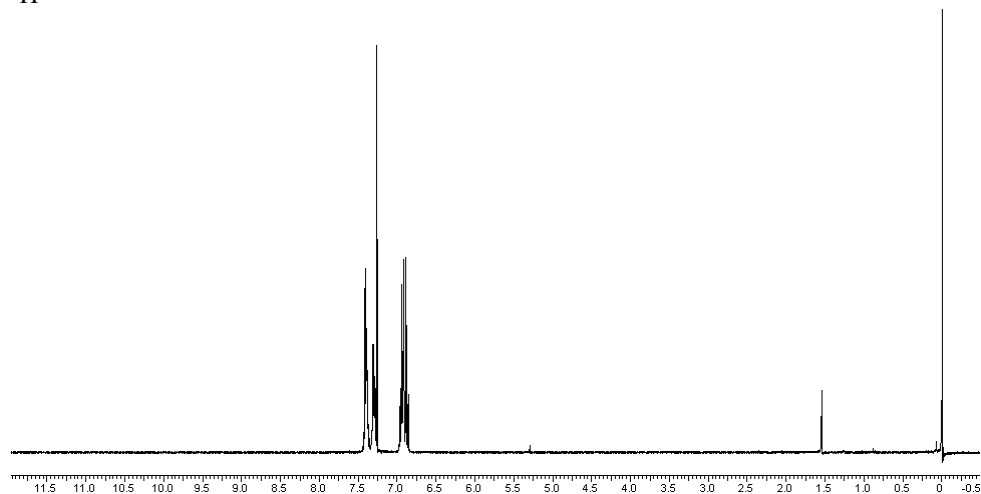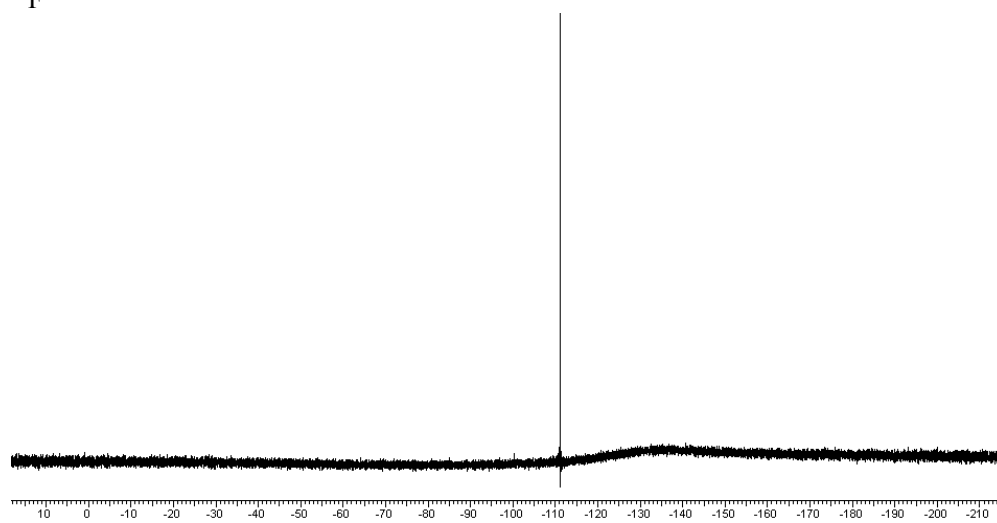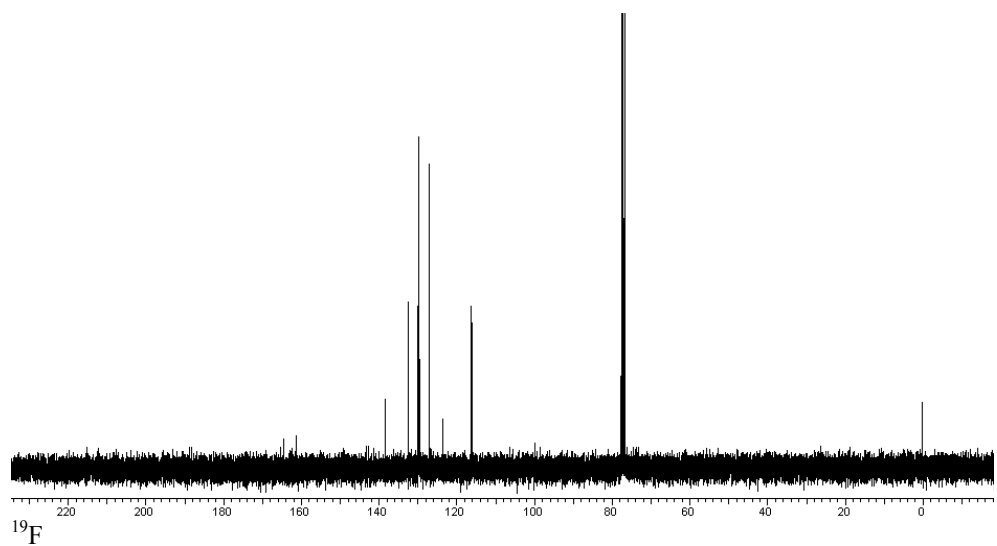
1,3-Dianisil-4,5-diphenylimidazol-2-ylidene silver chloride (**3.4h**).
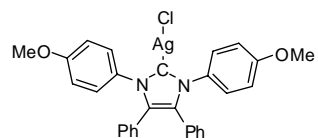
¹H NMR (CDCl$_3$): δ 7.14-7.22 (m, 10H), 6.96 (d, 4H, *J* = 7.9 Hz), 6.86 (d, 4H, *J* = 9.1 Hz), 3.61 (s, 6H).

^{13}C{^{1}H}NMR (CDCl$_3$): δ 160.0, 131.7, 130.7, 129.3, 128.7, 128.4, 128.3, 127.8, 114.9, 55.73, the Ag*C* peak was not found.

^{1}H
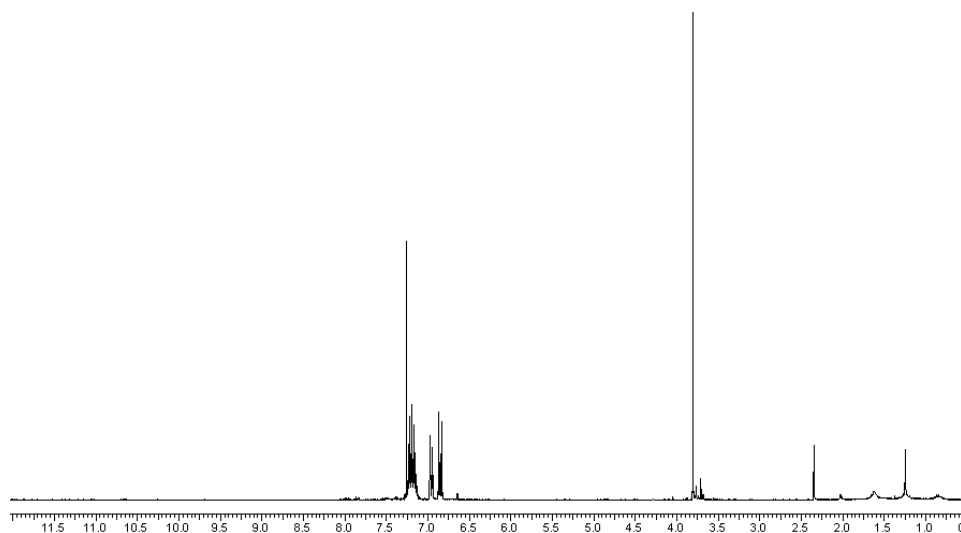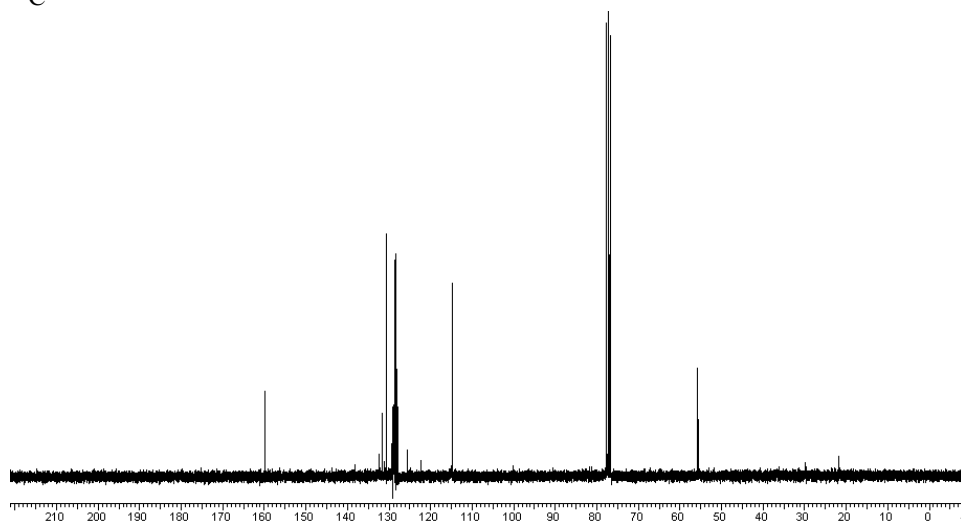
Synthesis of NHC-Ir(COD)Cl (3.5). Imidazolium chloride (1.0 eq., 0.5 mmol) was dissolved in THF. To this red solution, iridium cyclooctadiene chloride dimer (0.6 eq., 0.3 mmol, 202 mg) was added, followed by potassium *tert*-butoxide (1.2 eq., 0.6 mmol, 68 mg). The solution immediately turned a dark brown color, and was allowed to stir for 30 minutes, after which it was dissolved in 10 ml DCM, and washed twice with water (20 mL), dried over MgSO₄, filtered, and concentrated *in vacuo*, producing dark yellow-brown flakes. NMR analysis indicated that the complexes were pure at this stage.

1,3,4,5-Tetraphenylimidazolylidene Iridium Cyclooctadiene Chloride (3.5a).
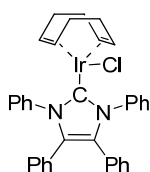
Yield 68%. ^{1}H: 7.68 (s, 4H), 7.31 (m, 6H), 7.10 (m, 10H), 4.31 (m, 2H), 2.62 (m, 2H), 1.68 (m, 2H), 1.40 – 1.20 (m, 6H). ^{13}C{^{1}H}: 181.9, 138.6, 132.2, 130.9, 129.0, 1285, 128.4, 128.3, 128.2, 83.2, 51.8, 33.2, 29.2. LRMS: calculated 708.1889, Found 708.19.

^{1}H

^{13}C
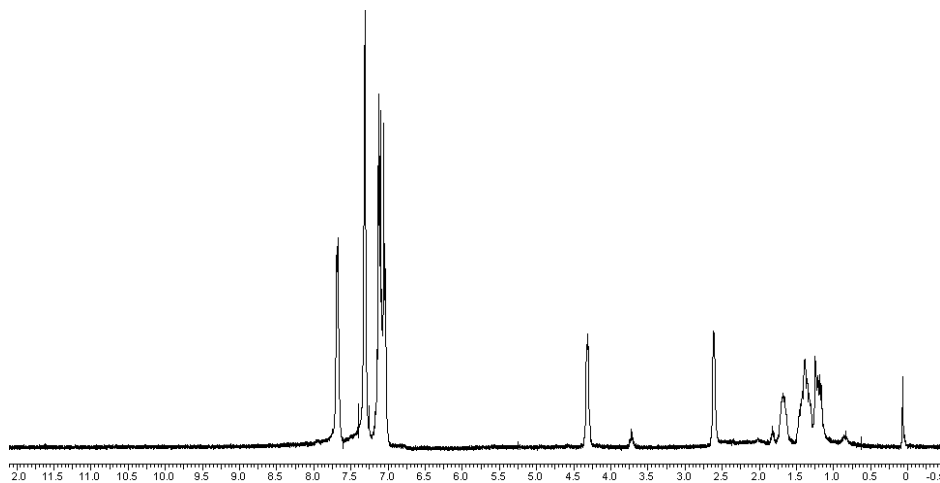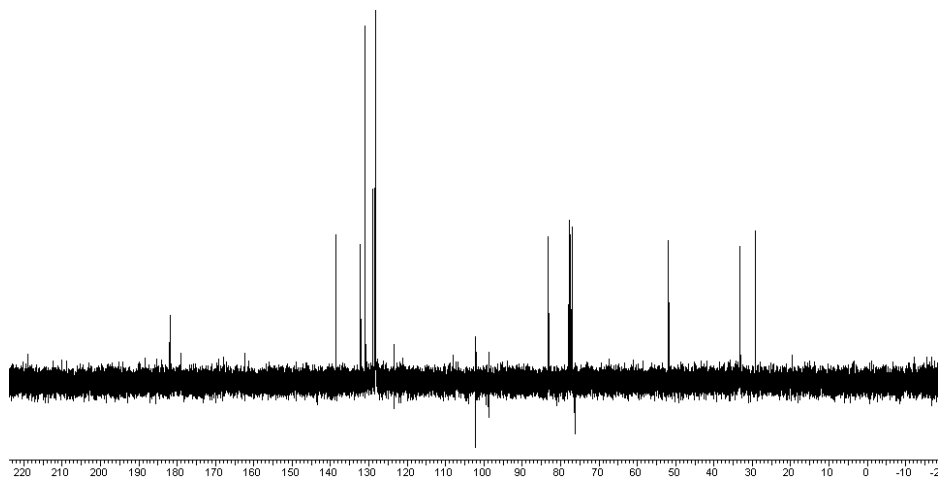
1,3-Di(4-fluorophenyl)-4,5-diphenylimidazolylidene Iridium Cyclooctadiene Chloride (3.5c).
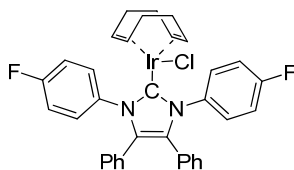
^{1}H 7.67 (m, 4H), 7.15 (m, 6H), 7.02 (m, 8H), 4.36 (m, 2H), 2.60 (m, 2H), 1.85 – 1.63 (m, 3H), 1.57 – 1.35 (m, 4H), 1.25 (m, 2H). ^{13}C{^{1}H} δ ppm: 182.1, 163.8, 160.5, 134.6, 132.3, 130.9, 128.5, 128.5, 127.9, 115.1 (d), 84.0, 52.0, 33.2, 29.2. ^{19}F: -113.4. Yield 93%. HRMS: calculated [M+H]$^+$ 745.1761, Found 745.1756.

^{1}H

^{13}C

^{19}F
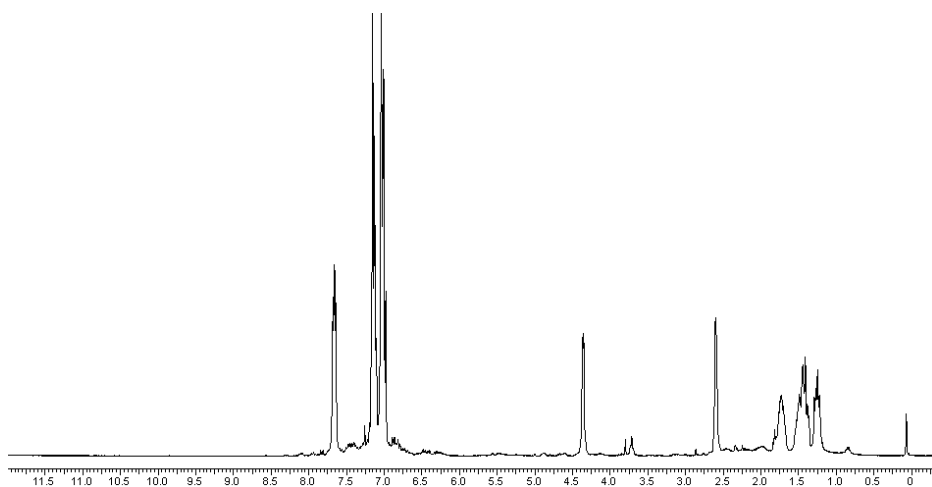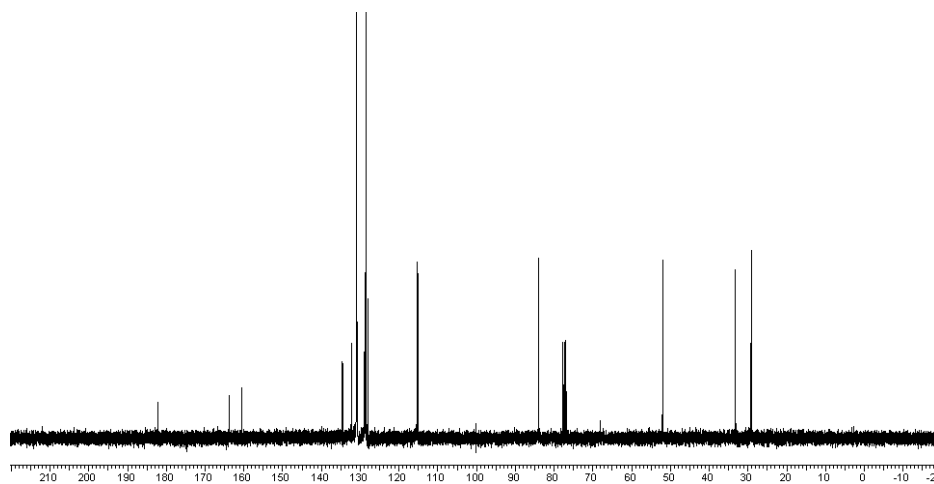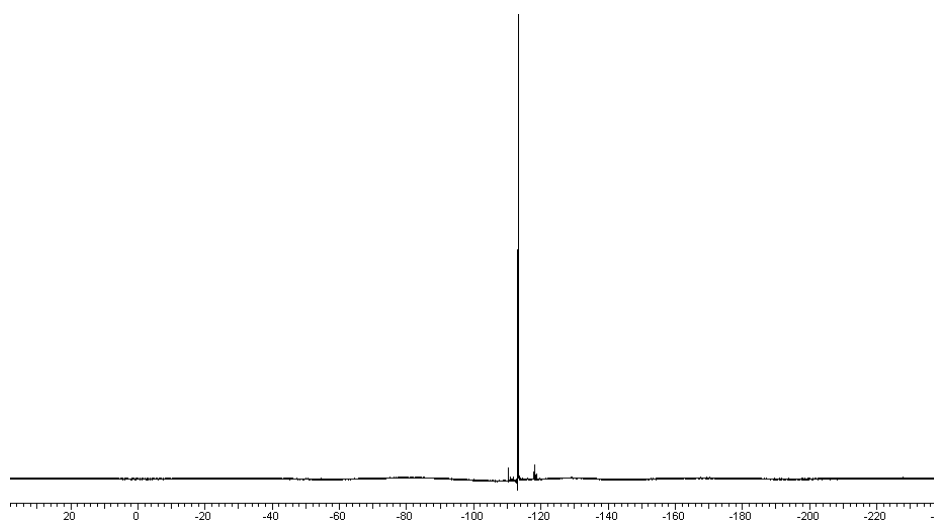
4,5-Dianysil-1,3-diphenylimidazolylidene Iridium cyclooctadiene chloride (3.5e).
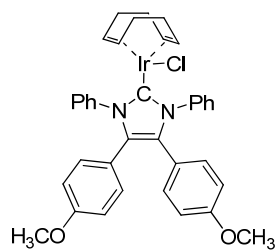
Yield 94%. ^{1}H: 7.68 (m, 4H), 7.32 (m, 6H), 6.97 (d, 4H, J = 8.8 Hz), 6.66 (d, 4H, J = 8.8 Hz), 4.31 (m, 2H), 3.64 (s, 6H), 2.55 (m, 2H), 1.65 (m, 2H), 1.38 (m, 4H), 1.17 (m, 2H). ^{13}C{^{1}H} NMR δ ppm 181.2, 159.5, 138.8, 132.2, 129.2, 131.7, 129.1, 128.2, 128.0, 120.7, 113.8, 82.9, 55.3, 51.7, 33.2. HRMS: calculated [M+H]$^+$ 769.2161, found 769.2154.

^{1}H

^{13}C
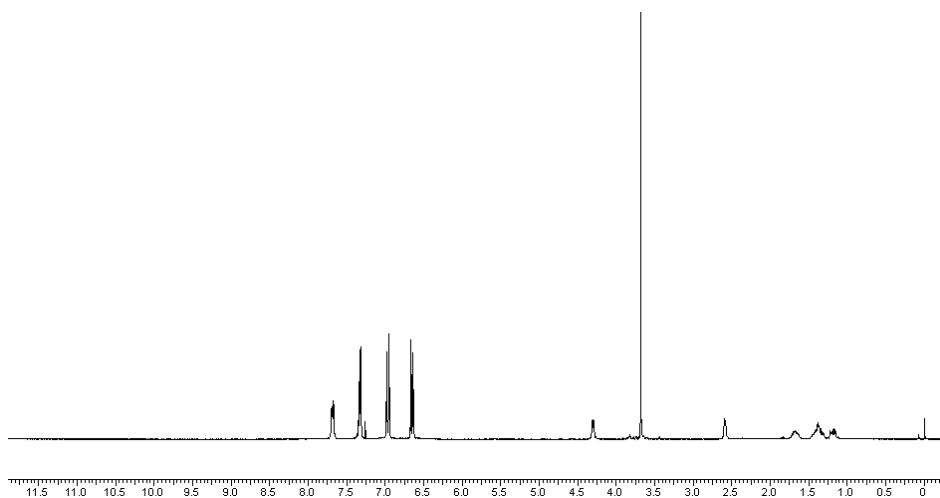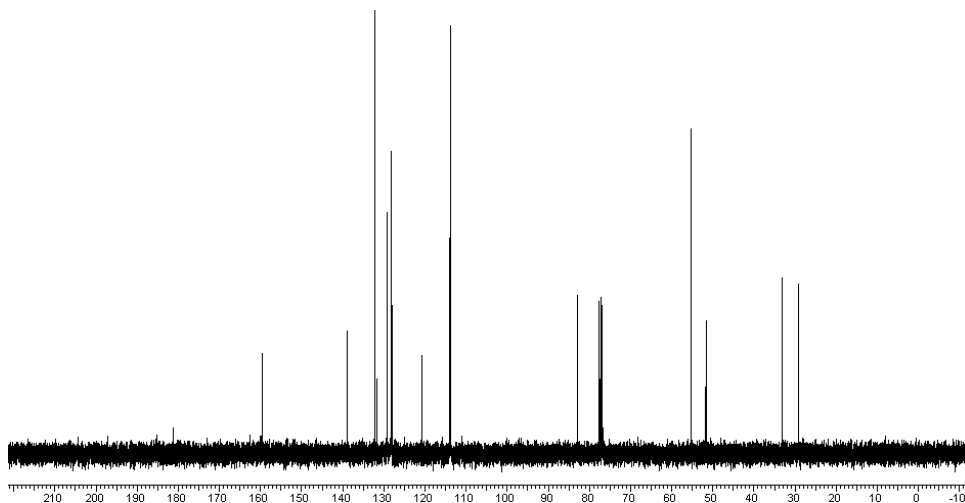
4,5-Di(4-fluorophenyl)-1,3-diphenylimidazolylidene Iridium Cyclooctadiene Chloride (3.5f).
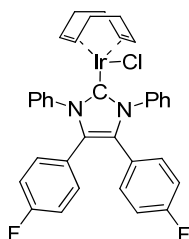
Yield 88%. ^{1}H: 7.64 (dd, 4H, J = 3.9, 4.7 Hz), 7.15 (m, 6H), 7.0 (m, 8H), 4.34 (m, 2H), 2.56 (m, 2H), 1.72 (m, 2H), 1.55 – 1.34 (m, 4H), 1.22 (m, 4H). ^{13}C{^{1}H}: 182.3, 164.3, 161.0, 138.3, 132.8 (d, J = 8.4 Hz), 131.3, 129.1, 128.4, 124.2, 115.9, 115.6, 51.9, 33.2, 29.2. ^{19}F: -113.3. HRMS: calculated [M+H]$^+$ 745. 1761, Found 745.1740.

^{1}H

^{13}C

^{19}F
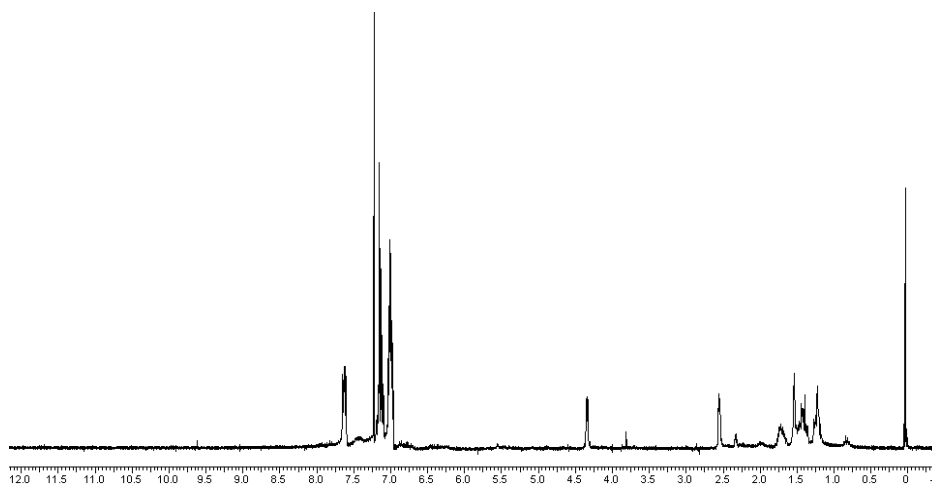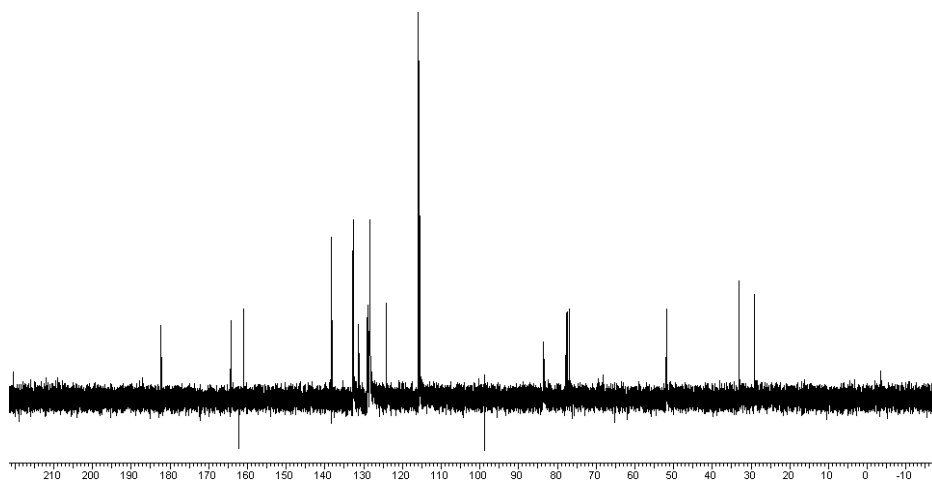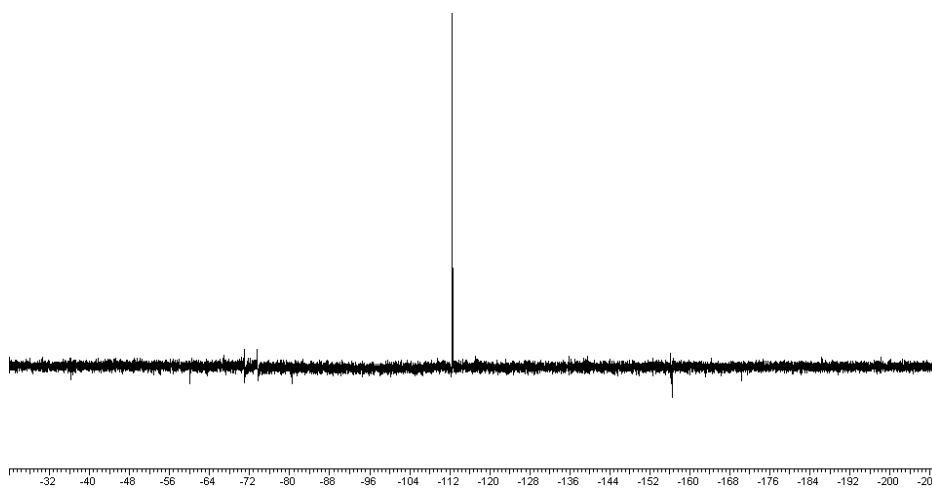
1,3-Dianysil-4,5-diphenylimidazolylidene Iridium cyclooctadiene chloride (3.5h).
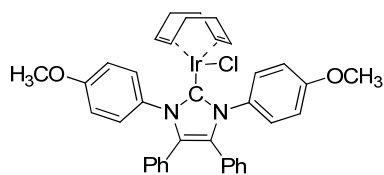
Quantitative yield. ^{1}H: 7.56 (d, 4H, J = 8.8 Hz), 7.09 (m, 10H), 5.82 (d, 4H, J = 9.1 Hz), 4.30 (m, 2H), 3.75 (s, 6H), 2.08 (m, 2H), 1.72 (m, 2H), 1.59 – 1.14 (m, 6H). ^{13}C{1H}: δ ppm 189.3, 159.18, 132.2, 131.6, 130.9, 130.1, 128.5, 128.4, 128.3, 119.7, 113.4, 82.9, 55.6, 51.7, 33.3. HRMS: calculated [M+H]$^+$ 769.2161, Found 769.2158.

^{1}H
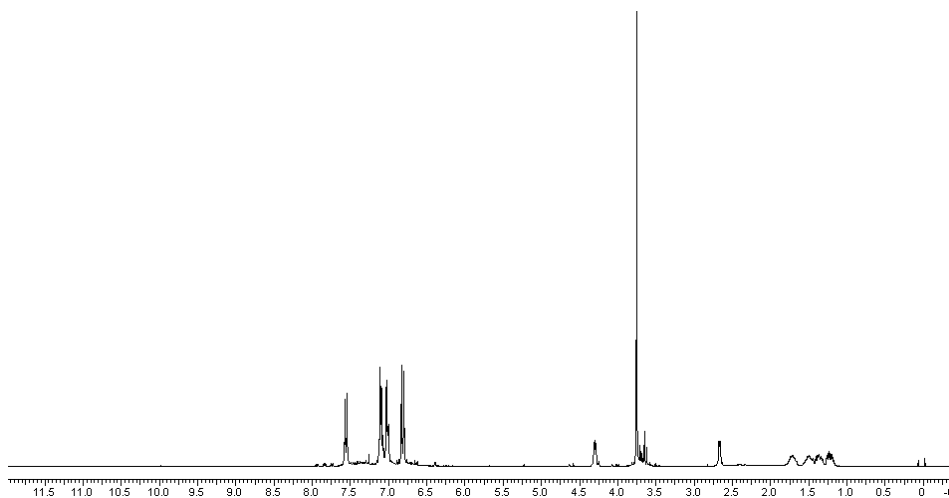
^{13}C
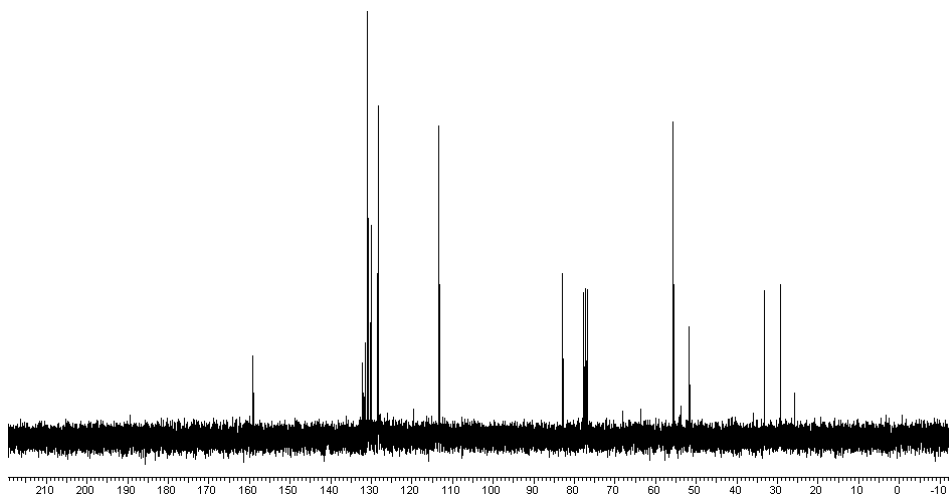
Synthesis of NHCIr(CO)₂Cl complexes 3.6. The NHCIr(COD)Cl complexes (0.02 mmol) were dissolved in 10 mL CH₂Cl₂, and a needle attached to a cylinder of CO gas was allowed to bubble through the solution slightly above atmospheric pressure for 3 seconds with vigorous stirring. A noticeable color change from dark yellow to lighter yellow was observed, after which the reactions were evacuated of solvent *in vacuo*. NMR analysis indicated that although the compounds were only aproximately 80% pure, no starting material remained, and the solutions would be pure enough for use in the IR studies, as no interference would occur in the CO stretching region.

(1,3,4,5-Tetraphenylimidazolylidene)dicarbonyliridium chloride (3.6a)

^{1}H NMR (CDCl$_3$) δ ppm 7.48 (m, 4 H), 7.39 (m, 6H) 7.25 - 7.11 (m, 6 H), 6.93 (d, J=7.1 Hz, 4 H). ^{13}C{1H}: δ ppm 180.8, 174.3, 168.1, 137.8, 132.7, 130.7, 129.3, 129.0, 128.9, 128.6, 127.5, the carbene carbon could not be resolved.

^{1}H

^{13}C
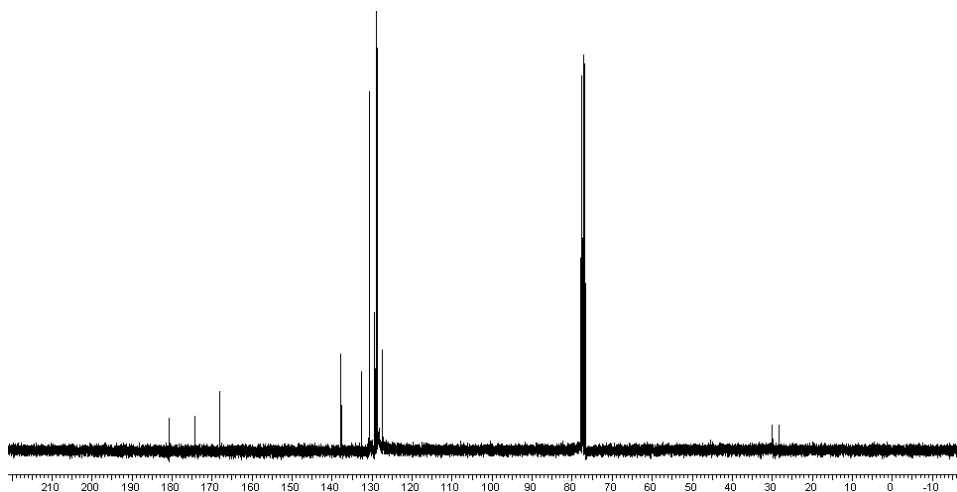
(1,3-Di(4-fluorophenyl)-4,5-diphenylimidazolylidene)iridiumdicarbonyl chloride (3.6c).
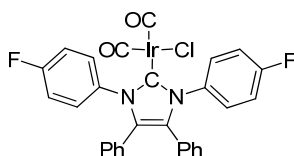
^{1}H NMR (CDCl$_3$) δ ppm: 7.46 (m, 4 H), 7.30-7.04 (m, 10 H), 6.97 (d, *J*=7.08 Hz, 4 H). ^{13}C{^{1}H} NMR (CDCl$_3$) δ ppm 180.6, 164.4, 133.7 (d, J=3.3 Hz, 2 C), 132.9, 130.8, 130.7, 129.2, 128.8, 127.1, 116.3, 116.0, the carbene peak could not be resolved. ^{19}F NMR (CDCl$_3$) δ ppm: -111.38 (s, 2 F).

^{1}H

^{13}C

^{19}F
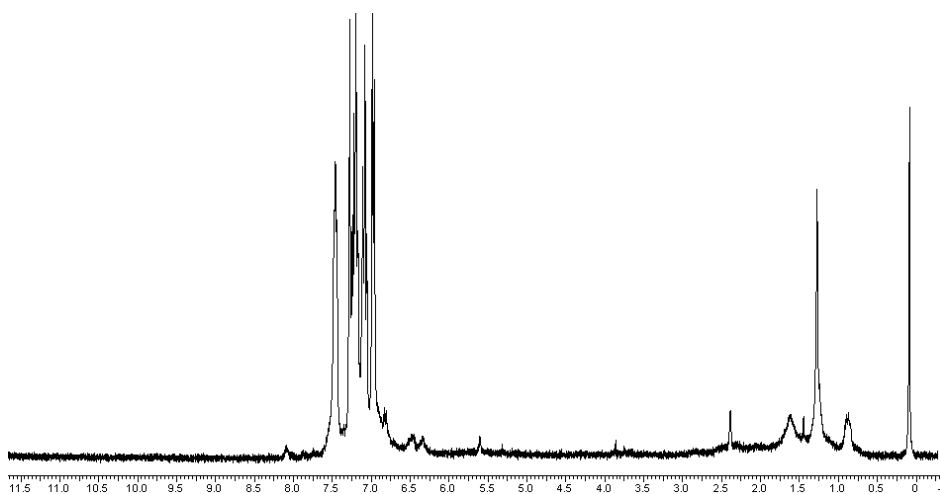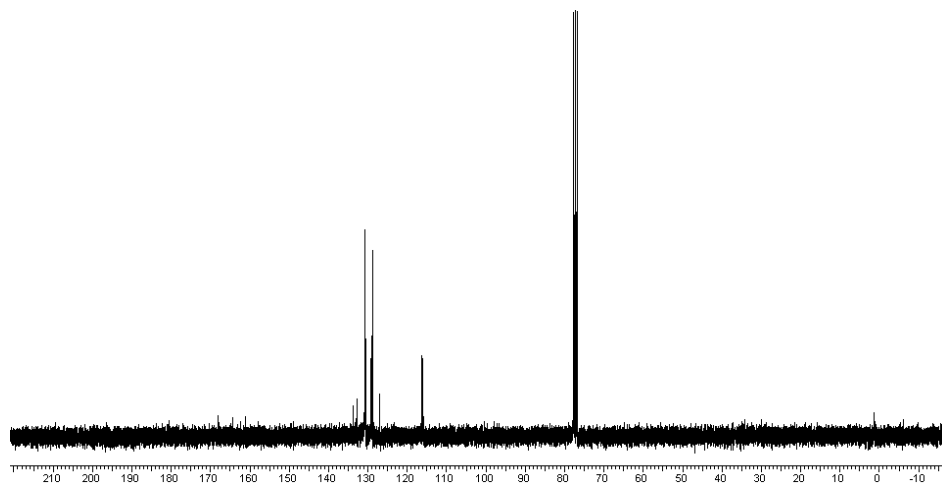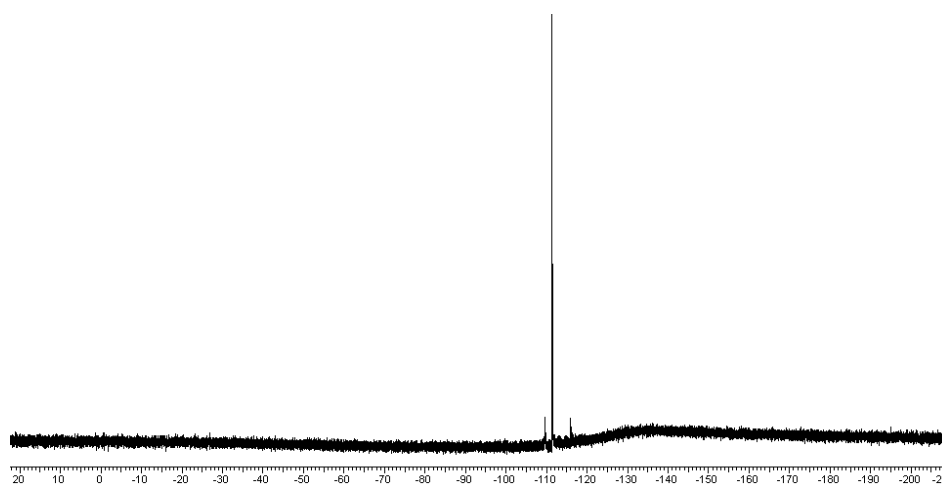
(4,5-Dianysil-1,3-diphenylimidazolylidene)dicarbonyliridium Chloride (3.6e).
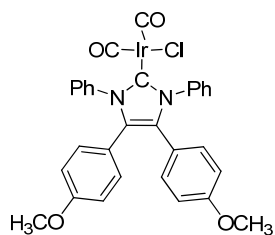
^{1}H NMR (CDCl$_3$) δ ppm 7.57 - 7.31 (m, 10 H), 6.87 (d, J=8.50 Hz, 4 H), 6.67 (d, J=8.65 Hz, 4 H), 3.72 (s, 6 H). ^{13}C{^{1}H} NMR (CDCl$_3$) δ ppm 181.0, 173.6, 168.2, 159.8, 138.0, 132.0, 129.0, 128.5, 119.8, 114.1, 55.36, the carbene carbon could not be resolved.

^{1}H

^{13}C
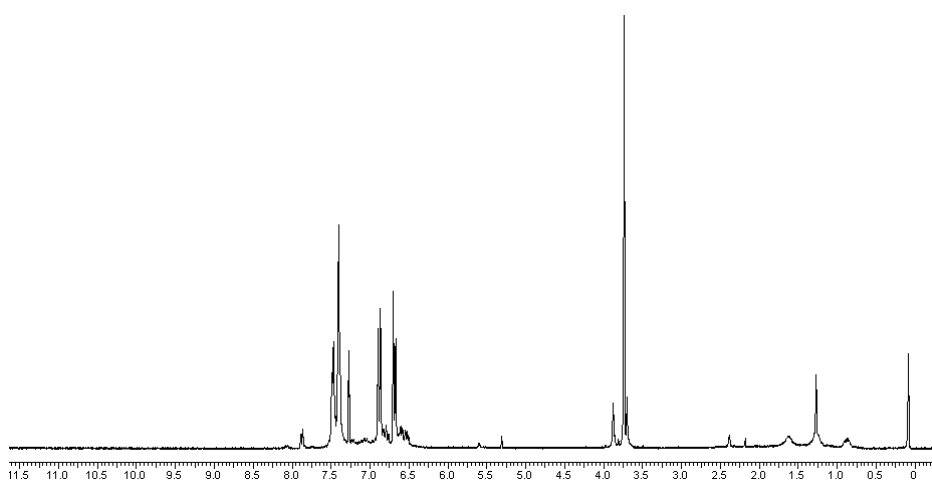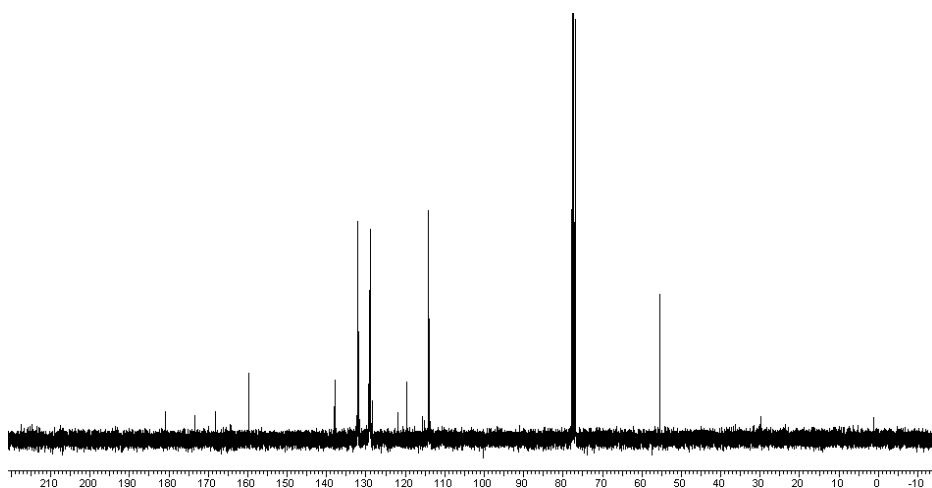
(4,5-Di(4-fluorophenyl)-1,3-diphenylimidazolylidene)dicarbonyliridium Chloride (3.6f).
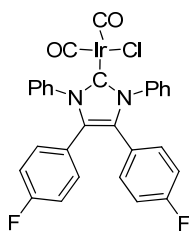
^{1}H NMR (CDCl$_3$) δ ppm 7.43 (m, 10 H), 6.92 (m, 8 H). ^{13}C{^{1}H} NMR (CDCl$_3$) δ ppm 180.7, 168.1, 164.6, 161.3, 137.5, 132.5 (d, *J*=8.42 Hz, 2 C), 129.5, 129.2, 128.9, 116.3, 116.0, the carbene peak did not resolve. ^{19}F NMR (CDCl$_3$) δ ppm -111.30 (s, 2 F).

^{1}H

^{13}C

^{19}F
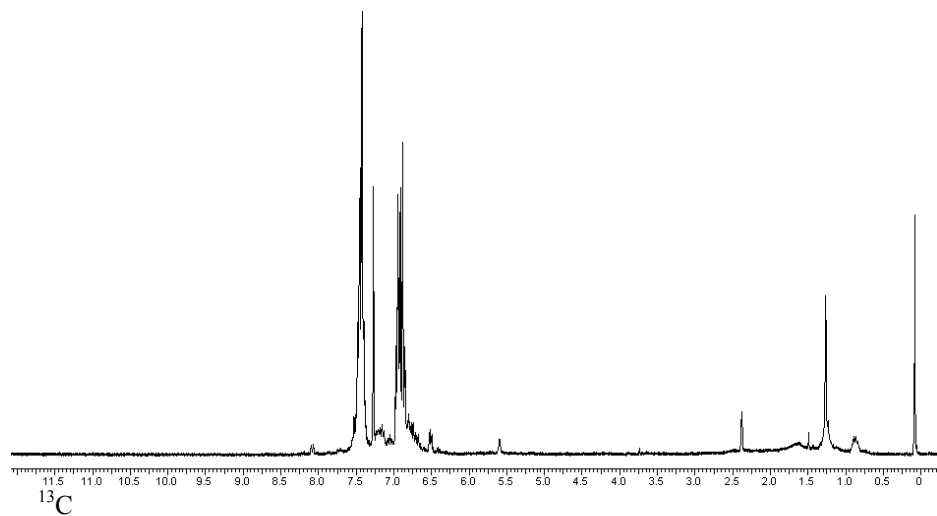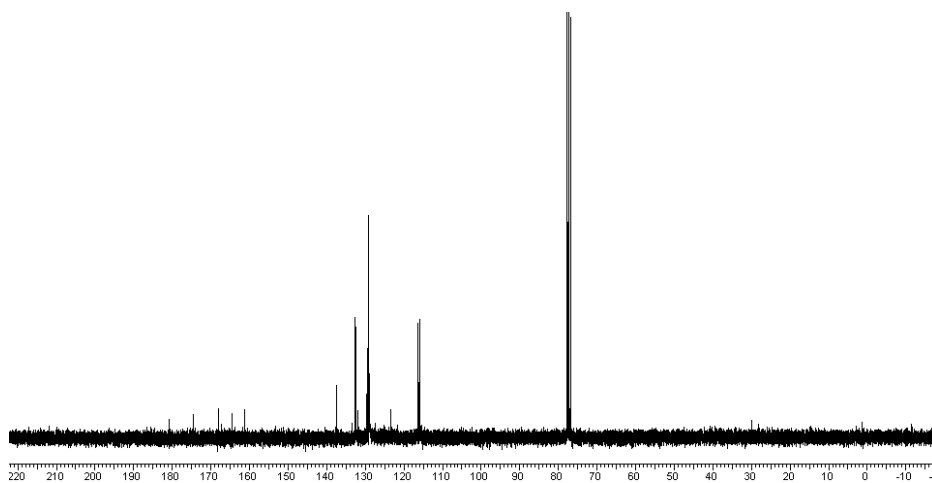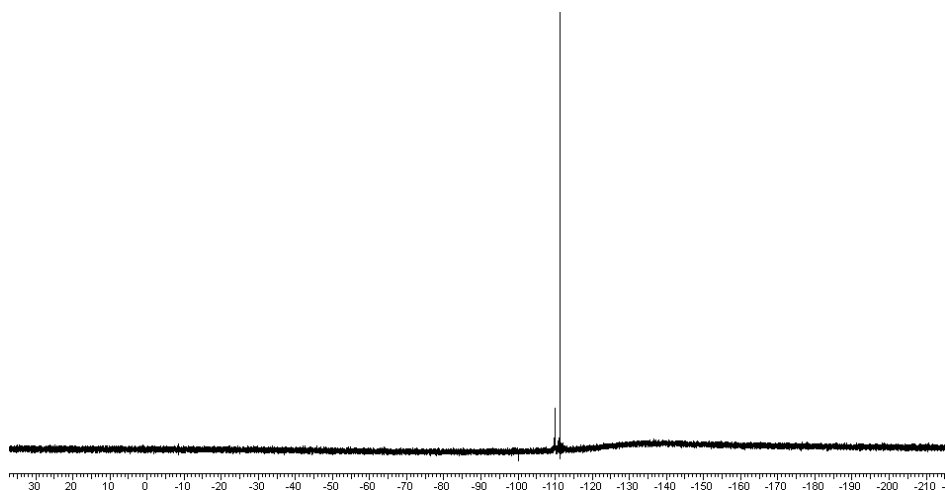
(1,3-Dianysil-4,5-diphenylimidazolylidene)dicarbonyliridium chloride (3.6h)
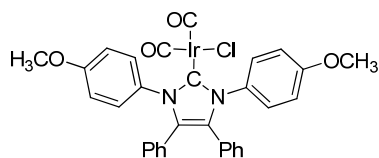
^{1}H NMR (CDCl$_3$) δ ppm 7.37 (d, *J* = 8.78 Hz, 4 H), 7.26 - 7.12 (m, 6 H), 6.99 (m, 4H) 6.88 (d, *J* = 8.78 Hz, 4 H), 3.38 (s, 6H). ^{13}C{^{1}H} NMR (CDCl$_3$) δ ppm 201.8, 181.1, 168.3, 159.9, 132.7, 130.7, 130.6, 128.8, 128.6, 127.7, 114.1, 55.6.

^{1}H
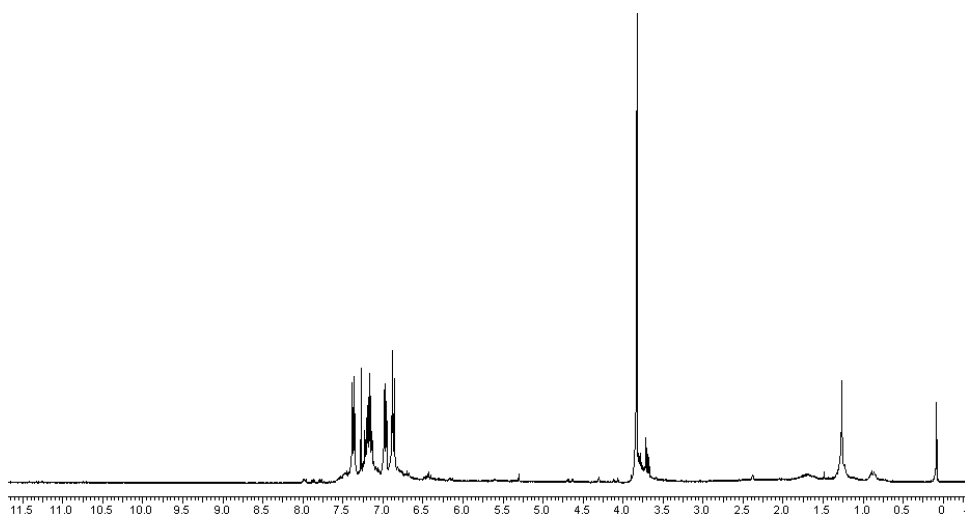
^{13}C
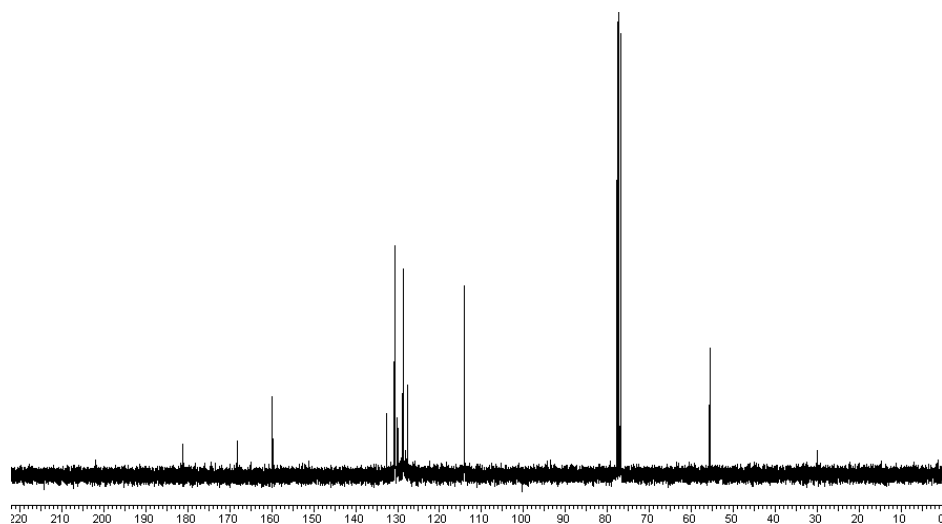
The full spectrum:
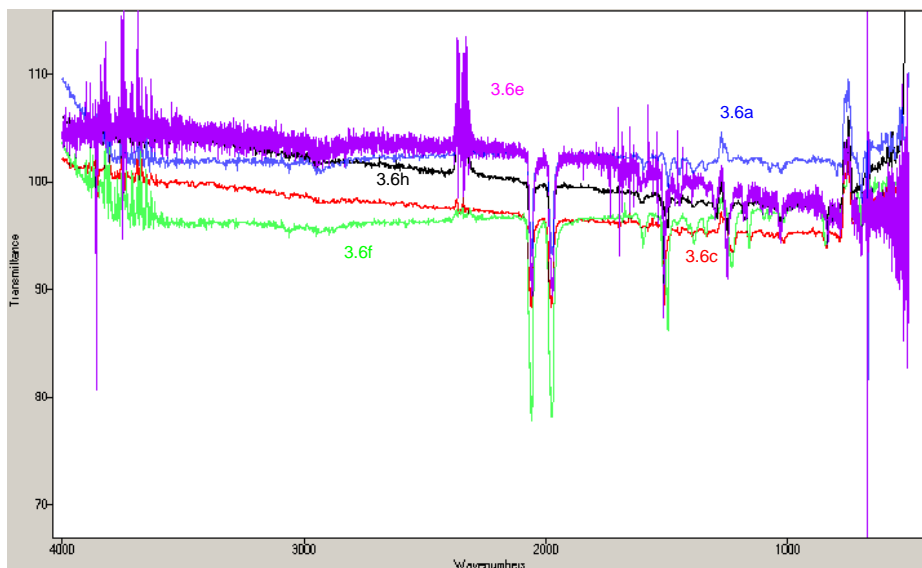
Enhanced view of the relevant peaks:
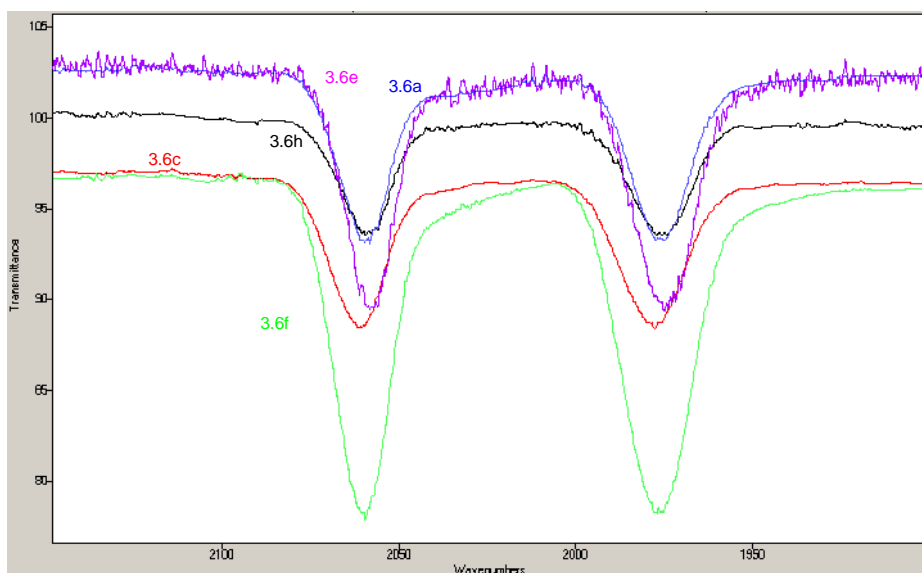
Figure B.1. IR Spectra of all compounds **3.6**.[a]

[a]Each measurement was taken five times from a dichloromethane solution of compounds **3.6a-f** from a thin film which was dried for aproximately 20 seconds with a heat on a NaCl plate prior to analysis. Three values for complex **3.6h** were taken, due to irremovable water content which greatly affected the IR CO shifts. The values were averaged as described in the text for the final IR CO stretch values. Shown below are one of the measurements without water present, overlayed.

LUMO   HOMO

X-ray

3.4a

optimized

X-ray

3.4e

optimized
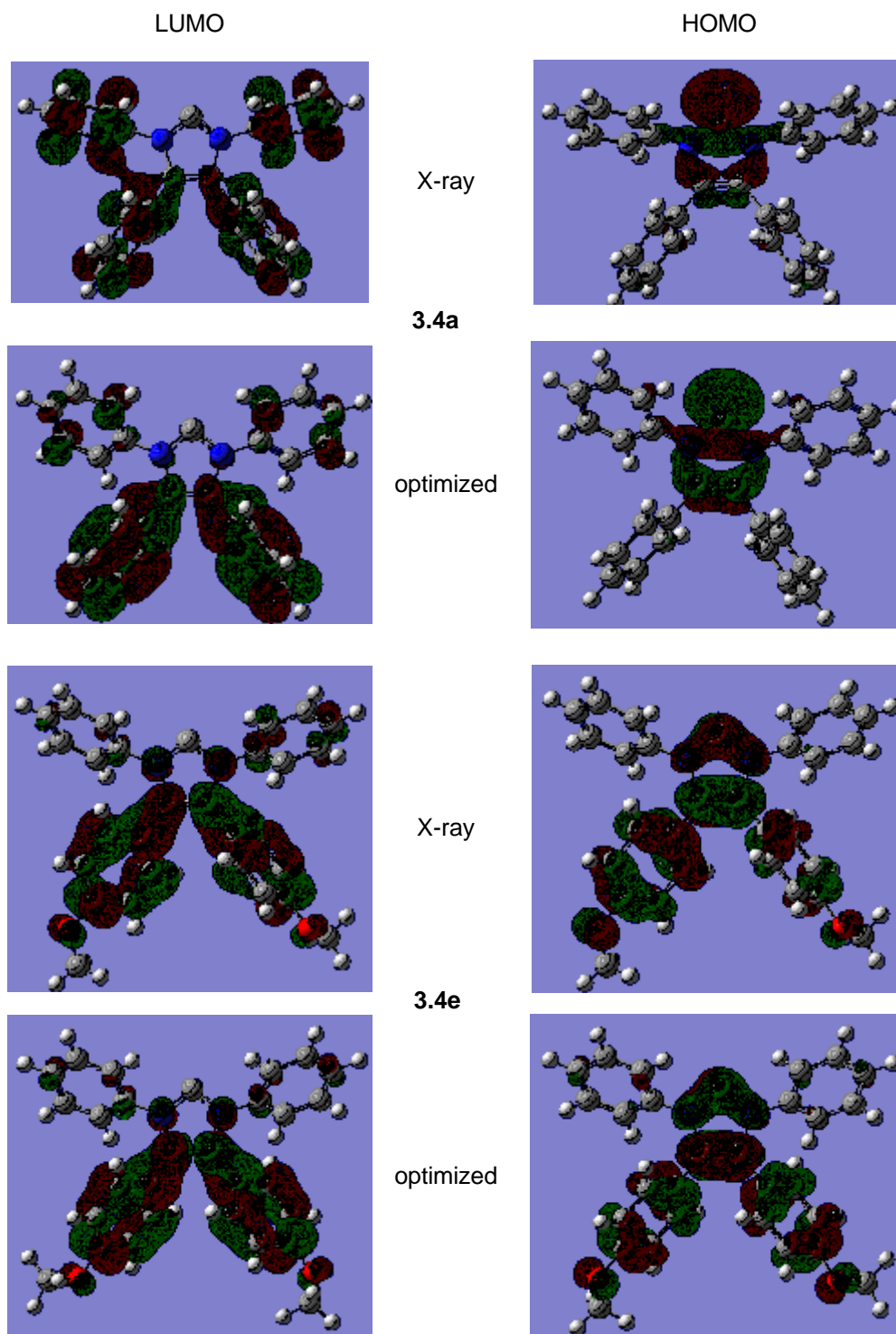
Figure B.2. Calculation results on free carbenes from imidazoliums 3.3. Gaussview was used for visualization after calculations (described in Chapter III). Continued on next page.

X-ray

3.4h

optimized

Figure B.2 Cont'd.

HOMO

LUMO

3.4e

3.4c
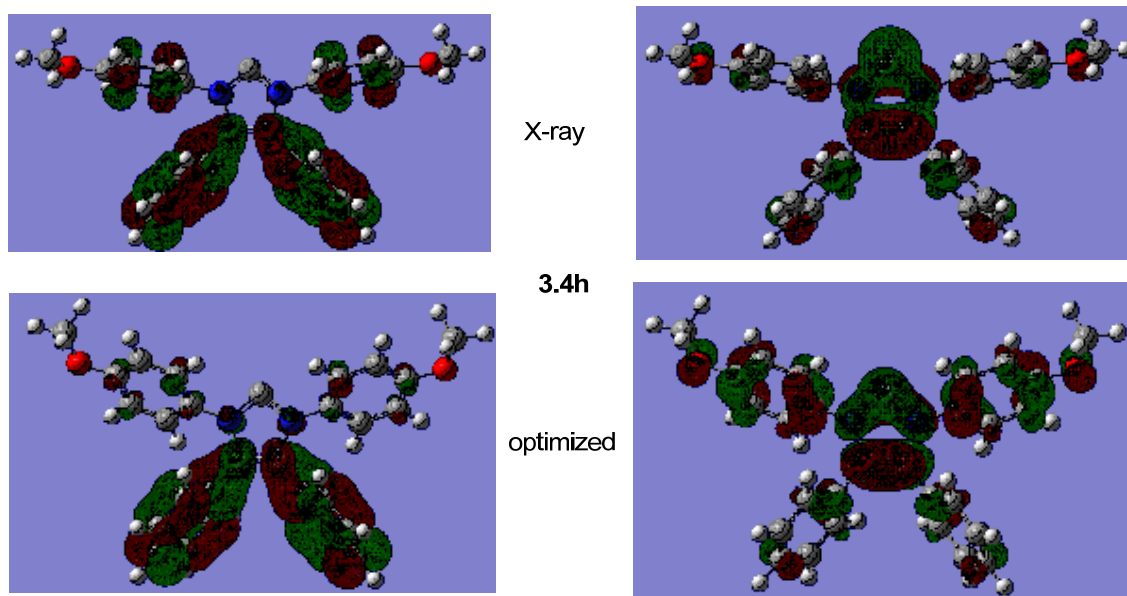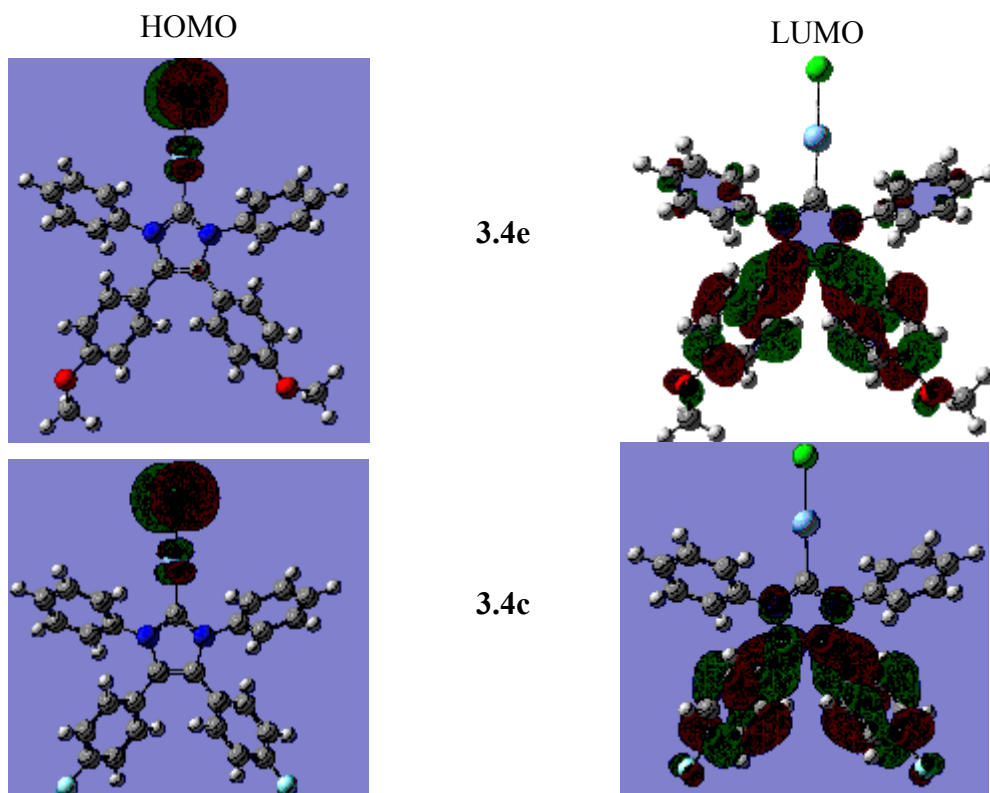
Figure B.3. Calculations on silver carbenes 3.4. Gaussview was used for visualization after calculations (described in Chapter III). Continued on next page.
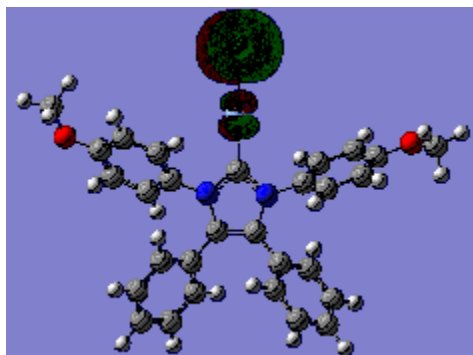
3.4h
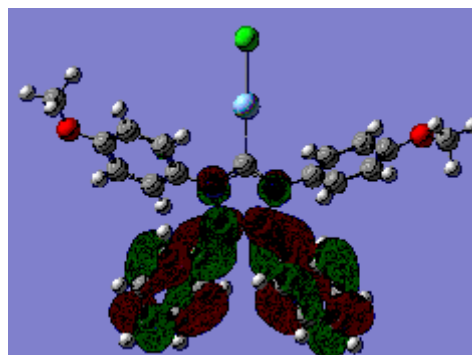
3.4f
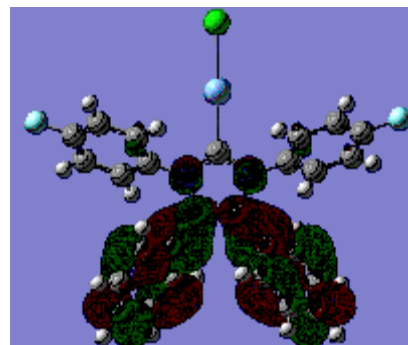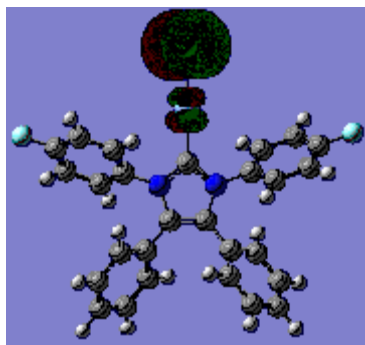
3.4a
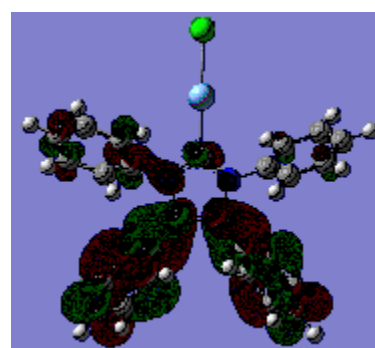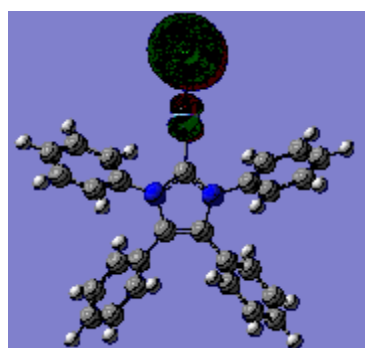
Figure B.3 Cont'd.

X-Ray Structure Data for 3.4a (ogle1)
$C_{27}H_{20}AgClN_2 \cdot CH_2Cl_2$
(solved by K. A. Abboud)
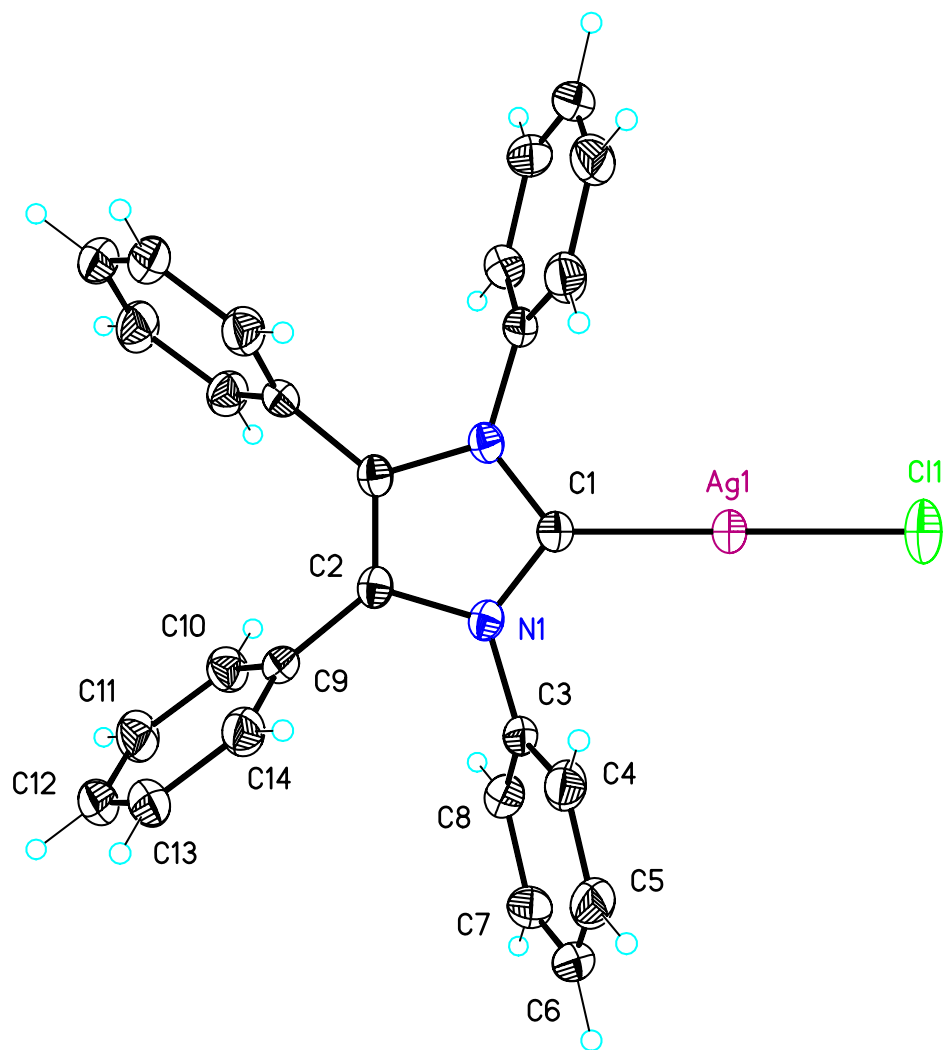
Labeled view with 50% probability ellipsoids

Table B .1. Crystal Data and Structure Refinement for ogle1 (**3.4a**).

Identification code	ogle1
Empirical formula	$C_{28}H_{22}AgCl_3N_2$ = $C_{27}H_{20}AgClN_2 \cdot CH_2Cl_2$
Formula weight	600.70
Temperature	173(2) K
Wavelength	0.71073 Å
Crystal system	Orthorhombic
Space group	Cmc2(1)
Unit cell dimensions	a = 16.9545(11) Å $\alpha = 90°$.
	b = 23.2586(15) Å $\beta = 90°$.
	c = 6.5773(4) Å $\gamma = 90°$.
Volume	2593.7(3) Å^3
Z	4
Density (calculated)	1.538 Mg/m^3
Absorption coefficient	1.106 mm^{-1}
F(000)	1208
Crystal size	0.09 x 0.09 x 0.05 mm^3
Theta range for data collection	1.49 to 27.49°.
Index ranges	$-12 \leq h \leq 22$, $-29 \leq k \leq 30$, $-8 \leq l \leq 8$
Reflections collected	8743
Independent reflections	3002 [R(int) = 0.0396]
Completeness to theta = 27.49°	100.0 %
Absorption correction	Integration
Max. and min. transmission	0.9424 and 0.8204
Refinement method	Full-matrix least-squares on F^2
Data / restraints / parameters	3002 / 1 / 166
Goodness-of-fit on F^2	1.035
Final R indices [I>2sigma(I)]	R1 = 0.0263, wR2 = 0.0623 [2874]
R indices (all data)	R1 = 0.0281, wR2 = 0.0630
Absolute structure parameter	-0.05(2)
Largest diff. peak and hole	0.483 and -0.434 e.Å^{-3}

$R1 = \Sigma(||F_o| - |F_c||) / \Sigma|F_o|$

$wR2 = [\Sigma[w(F_o^2 - F_c^2)^2] / \Sigma[w(F_o^2)^2]]^{1/2}$

$S = [\Sigma[w(F_o^2 - F_c^2)^2] / (n-p)]^{1/2}$

$w = 1/[\sigma^2(F_o^2)+(m*p)^2+n*p]$, p = $[max(F_o^2,0)+ 2* F_c^2]/3$, m & n are constants.

X-ray experimental: Data were collected at 173 K on a Siemens SMART PLATFORM equipped with A CCD area detector and a graphite monochromator utilizing MoKα radiation (λ = 0.71073 Å). Cell parameters were refined using up to 8192 reflections. A full sphere of data (1850 frames) was collected using the ω-scan method (0.3° frame width). The first 50 frames were re-measured at the end of data collection to monitor instrument and crystal stability (maximum correction on I was < 1 %). Absorption corrections by integration were applied based on measured indexed crystal faces.

The structure was solved by the Direct Methods in *SHELXTL6*, and refined using full-matrix least squares. The non-H atoms were treated anisotropically, whereas the hydrogen atoms were calculated in ideal positions and were riding on their respective carbon atoms. The asymmetric unit consists of a half complex and a half dichloromethane with each located on a mirror symmetry in the yz plane. A total of 166 parameters were refined in the final cycle of

refinement using 2874 reflections with $I > 2\sigma(I)$ to yield R_1 and wR_2 of 2.63% and 6.23%, respectively. Refinement was done using F^2.

SHELXTL6 (2000). Bruker-AXS, Madison, Wisconsin, USA.

Table B .2. Atomic Coordinates (x 10^4) and Equivalent Isotropic Displacement Parameters (Å^2x 10^3) for ogle1 (**3.4a**). U(eq) is defined as one third of the trace of the orthogonalized U^{ij} tensor.

	x	y	z	U(eq)
Ag1	-5000	10170(1)	-3569(1)	25(1)
Cl1	-5000	11176(1)	-3822(2)	35(1)
N1	-4372(1)	8922(1)	-3834(4)	21(1)
C1	-5000	9277(1)	-3739(9)	20(1)
C2	-4604(1)	8348(1)	-4081(3)	22(1)
C3	-3557(1)	9098(1)	-3732(6)	25(1)
C4	-3267(2)	9315(1)	-1921(5)	32(1)
C5	-2469(2)	9449(1)	-1804(5)	40(1)
C6	-1981(2)	9368(1)	-3422(8)	43(1)
C7	-2276(2)	9154(1)	-5223(5)	41(1)
C8	-3077(2)	9019(1)	-5387(5)	32(1)
C9	-4052(2)	7857(1)	-4176(4)	24(1)
C10	-3986(2)	7539(1)	-5964(4)	31(1)
C11	-3496(2)	7056(1)	-6009(5)	38(1)
C12	-3069(2)	6907(1)	-4304(5)	40(1)
C13	-3125(2)	7224(1)	-2541(5)	37(1)
C14	-3619(2)	7701(1)	-2473(4)	33(1)
Cl2	-5000	6390(1)	-9944(3)	108(1)
Cl3	-4823(3)	5711(1)	-13573(9)	139(2)
C15	-5000	6398(2)	-12590(10)	69(2)

Table B.3.   Bond Lengths [Å] and Angles [°] for ogle1 (**3.4a**).

Ag1-C1	2.079(3)
Ag1-Cl1	2.3446(8)
N1-C1	1.349(2)
N1-C2	1.402(3)
N1-C3	1.443(3)
C1-N1#1	1.349(2)
C2-C2#1	1.343(5)
C2-C9	1.477(3)
C3-C8	1.370(4)
C3-C4	1.384(4)
C4-C5	1.392(4)
C4-H4A	0.9500
C5-C6	1.361(5)
C5-H5A	0.9500
C6-C7	1.379(5)
C6-H6A	0.9500
C7-C8	1.399(4)
C7-H7A	0.9500
C8-H8A	0.9500

C9-C14	1.388(4)
C9-C10	1.394(3)
C10-C11	1.398(4)
C10-H10A	0.9500
C11-C12	1.379(4)
C11-H11A	0.9500
C12-C13	1.378(4)
C12-H12A	0.9500
C13-C14	1.390(4)
C13-H13A	0.9500
C14-H14A	0.9500
Cl2-C15	1.740(7)
Cl3-C15	1.748(6)
C15-Cl3#1	1.748(6)
C15-H15A	0.9600
C15-H15C	0.9600
C1-Ag1-Cl1	172.84(18)
C1-N1-C2	111.54(18)
C1-N1-C3	125.48(17)
C2-N1-C3	122.97(18)
N1-C1-N1#1	104.2(2)
N1-C1-Ag1	127.87(12)
N1#1-C1-Ag1	127.87(12)
C2#1-C2-N1	106.29(13)
C2#1-C2-C9	129.28(12)
N1-C2-C9	124.3(2)
C8-C3-C4	121.5(2)
C8-C3-N1	119.5(3)
C4-C3-N1	118.9(3)
C3-C4-C5	118.3(3)
C3-C4-H4A	120.8
C5-C4-H4A	120.8
C6-C5-C4	121.1(3)
C6-C5-H5A	119.4
C4-C5-H5A	119.4
C5-C6-C7	120.1(3)
C5-C6-H6A	119.9
C7-C6-H6A	119.9
C6-C7-C8	120.0(3)
C6-C7-H7A	120.0
C8-C7-H7A	120.0
C3-C8-C7	119.0(3)
C3-C8-H8A	120.5
C7-C8-H8A	120.5
C14-C9-C10	120.0(2)
C14-C9-C2	120.2(2)
C10-C9-C2	119.8(2)
C9-C10-C11	119.5(3)
C9-C10-H10A	120.3
C11-C10-H10A	120.3
C12-C11-C10	119.8(3)
C12-C11-H11A	120.1
C10-C11-H11A	120.1
C13-C12-C11	120.9(3)
C13-C12-H12A	119.5

C11-C12-H12A	119.5
C12-C13-C14	119.7(3)
C12-C13-H13A	120.1
C14-C13-H13A	120.1
C9-C14-C13	120.1(3)
C9-C14-H14A	120.0
C13-C14-H14A	120.0
Cl2-C15-Cl3	111.2(4)
Cl2-C15-Cl3#1	111.2(4)
Cl3-C15-Cl3#1	19.8(3)
Cl2-C15-H15A	108.6
Cl3-C15-H15A	109.2
Cl3#1-C15-H15A	125.1
Cl2-C15-H15C	109.4
Cl3-C15-H15C	92.2
Cl3#1-C15-H15C	109.9
H15A-C15-H15C	18.7

Symmetry transformations used to generate equivalent atoms:
#1 -x-1,y,z

Table B.4. Anisotropic Displacement Parameters $(\text{Å}^2 \text{x } 10^3)$ for ogle1 (**3.4a**). The anisotropic displacement factor exponent takes the form: $-2\pi^2[\, h^2 \, a^{*2}U^{11} + ... + 2 \, h \, k \, a^* \, b^* \, U^{12}\,]$

	U^{11}	U^{22}	U^{33}	U^{23}	U^{13}	U^{12}
Ag1	28(1)	18(1)	30(1)	-1(1)	0	0
Cl1	62(1)	21(1)	23(1)	-1(1)	0	0
N1	24(1)	19(1)	21(1)	-2(1)	1(1)	-2(1)
C1	24(1)	20(1)	15(2)	-2(2)	0	0
C2	26(1)	19(1)	20(1)	-1(1)	1(1)	-1(1)
C3	24(1)	17(1)	33(1)	2(1)	-4(1)	0(1)
C4	36(2)	24(1)	36(2)	-2(1)	-3(1)	-2(1)
C5	41(2)	28(1)	52(2)	-5(1)	-18(2)	-3(1)
C6	26(1)	26(1)	77(2)	6(2)	-13(2)	-3(1)
C7	24(1)	31(1)	67(2)	0(2)	11(1)	1(1)
C8	30(1)	25(1)	40(2)	-2(1)	1(1)	-3(1)
C9	21(1)	21(1)	31(1)	1(1)	2(1)	-2(1)
C10	32(1)	27(1)	32(1)	-2(1)	6(1)	3(1)
C11	41(2)	27(1)	45(2)	-8(1)	12(1)	4(1)
C12	31(2)	25(1)	63(2)	3(1)	8(1)	5(1)
C13	34(2)	26(1)	50(2)	4(1)	-9(1)	3(1)
C14	35(2)	26(1)	36(2)	-2(1)	-6(1)	-1(1)
Cl2	68(1)	175(2)	83(1)	36(1)	0	0
Cl3	103(5)	86(1)	227(3)	-38(3)	-17(4)	7(2)
C15	42(3)	75(4)	89(4)	8(3)	0	0

X-Ray Structure Data for 3.4c (ogle13)
$C_{27}H_{18}AgClF_2N_2$
(solved by K. A. Abboud)
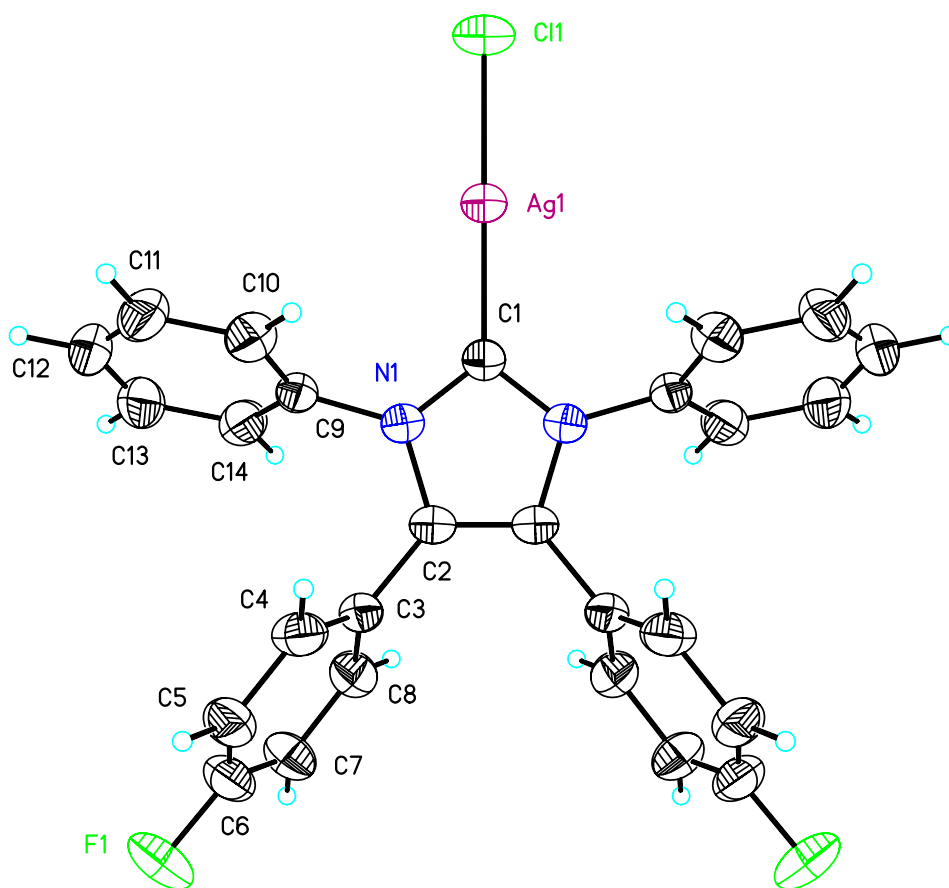
Labeled view with 50% probability ellipsoids

Table B.5. Crystal Data and Structure Refinement for ogle13 (**3.4c**).

Identification code	ogle13
Empirical formula	$C_{27}H_{18}AgClF_2N_2$
Formula weight	621.88
Temperature	173(2) K
Wavelength	0.71073 Å
Crystal system	Orthorhombic
Space group	Cmc2(1)
Unit cell dimensions	a = 17.5486(14) Å $\quad\alpha = 90°$.
	b = 23.6751(19) Å $\quad\beta = 90°$.
	c = 6.7198(5) Å $\quad\gamma = 90°$.
Volume	2791.8(4) Å^3
Z	4
Density (calculated)	1.480 Mg/m^3
Absorption coefficient	0.855 mm^{-1}
F(000)	1264
Crystal size	0.19 x 0.06 x 0.06 mm^3
Theta range for data collection	1.44 to 27.50°.
Index ranges	$-22 \leq h \leq 22, -23 \leq k \leq 30, -8 \leq l \leq 8$
Reflections collected	9030
Independent reflections	3147 [R(int) = 0.0391]
Completeness to theta = 27.50°	100.0 %
Absorption correction	Integration
Max. and min. transmission	0.9505 and 0.8545
Refinement method	Full-matrix least-squares on F^2
Data / restraints / parameters	3147 / 1 / 154
Goodness-of-fit on F^2	0.981
Final R indices [I>2sigma(I)]	R1 = 0.0265, wR2 = 0.0645 [2811]
R indices (all data)	R1 = 0.0309, wR2 = 0.0655
Absolute structure parameter	0.00(3)
Largest diff. peak and hole	0.327 and -0.333 e.Å^{-3}

$R1 = \Sigma(||F_o| - |F_c||) / \Sigma|F_o|$

$wR2 = [\Sigma[w(F_o^2 - F_c^2)^2] / \Sigma[w(F_o^2)^2]]^{1/2}$

$S = [\Sigma[w(F_o^2 - F_c^2)^2] / (n-p)]^{1/2}$

$w = 1/[\sigma^2(F_o^2)+(m*p)^2+n*p]$, p = $[max(F_o^2,0)+ 2* F_c^2]/3$, m & n are constants.

X-ray experimental: Data were collected at 173 K on a Siemens SMART PLATFORM equipped with A CCD area detector and a graphite monochromator utilizing MoKα radiation (λ = 0.71073 Å). Cell parameters were refined using up to 8192 reflections. A full sphere of data (1850 frames) was collected using the ω-scan method (0.3° frame width). The first 50 frames were re-measured at the end of data collection to monitor instrument and crystal stability (maximum correction on I was < 1 %). Absorption corrections by integration were applied based on measured indexed crystal faces.

The structure was solved by the Direct Methods in *SHELXTL6,* and refined using full-matrix least squares. The non-H atoms were treated anisotropically, whereas the hydrogen atoms were calculated in ideal positions and were riding on their respective carbon atoms. The complexes are located on 2-fold rotation axes; thus a half complex in the asymmetric unit. There is also a half pentane molecule on the asymmetric unit (located on mirror planes). The

latter was disordered and could not be modeled properly, thus program SQUEEZE, a part of the PLATON package of crystallographic software, was used to calculate the solvent disorder area and remove its contribution to the overall intensity data. A total of 154 parameters were refined in the final cycle of refinement using 2811 reflections with $I > 2\sigma(I)$ to yield R_1 and wR_2 of 2.65% and 6.45%, respectively. Refinement was done using F^2.

P. van der Sluis & A.L. Spek (1990). SQUEEZE, Acta Cryst. A46, 194-201.
SHELXTL6 (2000). Bruker-AXS, Madison, Wisconsin, USA.
Spek, A.L. (1990). PLATON, Acta Cryst. A46, C-34.

Table B.6. Atomic Coordinates (x 10^4) and Equivalent Isotropic Displacement Parameters (Å^2x 10^3) for ogle13 (**3.4c**). U(eq) is defined as one third of the trace of the orthogonalized U^{ij} tensor.

	x	y	z	U(eq)
Ag1	0	5202(1)	2500(1)	36(1)
N1	608(1)	3970(1)	2734(5)	30(1)
F1	2377(1)	1576(1)	3151(3)	74(1)
Cl1	0	6189(1)	2740(2)	46(1)
C1	0	4321(1)	2634(13)	30(1)
C2	382(1)	3411(1)	2928(3)	32(1)
C3	913(2)	2926(1)	2986(4)	35(1)
C4	1321(2)	2778(1)	1308(5)	44(1)
C5	1817(2)	2313(1)	1348(6)	49(1)
C6	1878(2)	2023(1)	3074(5)	51(1)
C7	1482(2)	2151(1)	4774(5)	48(1)
C8	1001(2)	2613(1)	4736(5)	41(1)
C9	1397(1)	4138(1)	2646(6)	35(1)
C10	1685(2)	4360(1)	913(5)	47(1)
C11	2460(2)	4474(2)	797(6)	58(1)
C12	2927(2)	4364(1)	2354(11)	61(1)
C13	2634(2)	4145(2)	4099(7)	61(1)
C14	1855(2)	4037(1)	4267(5)	45(1)

Table B.7. Bond Lengths [Å] and Angles [°] for ogle13 (**3.4c**).

Ag1-C1	2.087(3)
Ag1-Cl1	2.3440(9)
N1-C1	1.354(3)
N1-C2	1.386(3)
N1-C9	1.442(3)
F1-C6	1.374(3)
C1-N1#1	1.354(3)
C2-C2#1	1.341(5)
C2-C3	1.479(3)
C3-C4	1.380(4)
C3-C8	1.399(4)
C4-C5	1.404(4)
C4-H4A	0.9500
C5-C6	1.352(5)
C5-H5A	0.9500
C6-C7	1.371(4)
C7-C8	1.383(4)

C7-H7A	0.9500
C8-H8A	0.9500
C9-C14	1.374(5)
C9-C10	1.376(5)
C10-C11	1.388(5)
C10-H10A	0.9500
C11-C12	1.355(7)
C11-H11A	0.9500
C12-C13	1.382(7)
C12-H12A	0.9500
C13-C14	1.395(4)
C13-H13A	0.9500
C14-H14A	0.9500
C1-Ag1-Cl1	173.6(2)
C1-N1-C2	111.47(19)
C1-N1-C9	125.81(19)
C2-N1-C9	122.72(18)
N1-C1-N1#1	103.9(3)
N1-C1-Ag1	128.01(12)
N1#1-C1-Ag1	128.01(12)
C2#1-C2-N1	106.57(12)
C2#1-C2-C3	129.05(13)
N1-C2-C3	124.3(2)
C4-C3-C8	119.6(3)
C4-C3-C2	120.2(2)
C8-C3-C2	120.2(2)
C3-C4-C5	120.4(3)
C3-C4-H4A	119.8
C5-C4-H4A	119.8
C6-C5-C4	117.6(3)
C6-C5-H5A	121.2
C4-C5-H5A	121.2
C5-C6-C7	124.2(3)
C5-C6-F1	118.3(3)
C7-C6-F1	117.5(3)
C6-C7-C8	117.9(3)
C6-C7-H7A	121.0
C8-C7-H7A	121.0
C7-C8-C3	120.2(3)
C7-C8-H8A	119.9
C3-C8-H8A	119.9
C14-C9-C10	121.5(2)
C14-C9-N1	118.8(3)
C10-C9-N1	119.6(3)
C9-C10-C11	118.9(3)
C9-C10-H10A	120.6
C11-C10-H10A	120.6
C12-C11-C10	120.8(4)
C12-C11-H11A	119.6
C10-C11-H11A	119.6
C11-C12-C13	120.1(3)
C11-C12-H12A	119.9
C13-C12-H12A	119.9
C12-C13-C14	120.1(4)
C12-C13-H13A	119.9

C14-C13-H13A	119.9
C9-C14-C13	118.5(3)
C9-C14-H14A	120.7
C13-C14-H14A	120.7

Symmetry transformations used to generate equivalent atoms:
#1 -x,y,z

Table B.8. Anisotropic Displacement Parameters ($\text{Å}^2\text{x }10^3$) for ogle13 (**3.4c**). The anisotropic displacement factor exponent takes the form: $-2\pi^2[\, h^2 a^{*2}U^{11} + ... + 2\, h\, k\, a^*\, b^*\, U^{12}\,]$

	U^{11}	U^{22}	U^{33}	U^{23}	U^{13}	U^{12}
Ag1	39(1)	28(1)	41(1)	1(1)	0	0
N1	34(1)	27(1)	30(1)	1(1)	-1(1)	-1(1)
F1	76(1)	54(1)	92(2)	-3(1)	-1(1)	36(1)
Cl1	73(1)	31(1)	34(1)	2(1)	0	0
C1	34(1)	30(2)	26(2)	-3(2)	0	0
C2	39(1)	26(1)	30(2)	0(1)	0(1)	0(1)
C3	34(1)	27(1)	45(2)	-3(1)	-3(1)	-1(1)
C4	54(2)	32(1)	46(2)	2(1)	8(1)	-1(1)
C5	48(2)	39(2)	60(2)	-3(2)	14(2)	8(1)
C6	46(2)	37(2)	69(3)	-7(1)	-8(1)	13(1)
C7	51(2)	43(2)	49(2)	6(1)	-4(1)	14(1)
C8	43(2)	41(2)	41(2)	0(1)	-2(1)	4(1)
C9	32(1)	27(1)	45(2)	-4(2)	5(2)	0(1)
C10	46(2)	42(2)	53(2)	4(1)	5(2)	-2(1)
C11	50(2)	45(2)	78(3)	1(2)	23(2)	-7(2)
C12	36(1)	46(2)	101(3)	0(3)	15(3)	-4(1)
C13	37(2)	48(2)	96(3)	0(2)	-16(2)	-1(2)
C14	43(2)	41(2)	53(2)	5(1)	-4(1)	-5(1)

X-Ray Structure Data for 3.4e (ogle6)
$C_{29}H_{24}AgClN_2O_2$
(solved by K. A. Abboud)
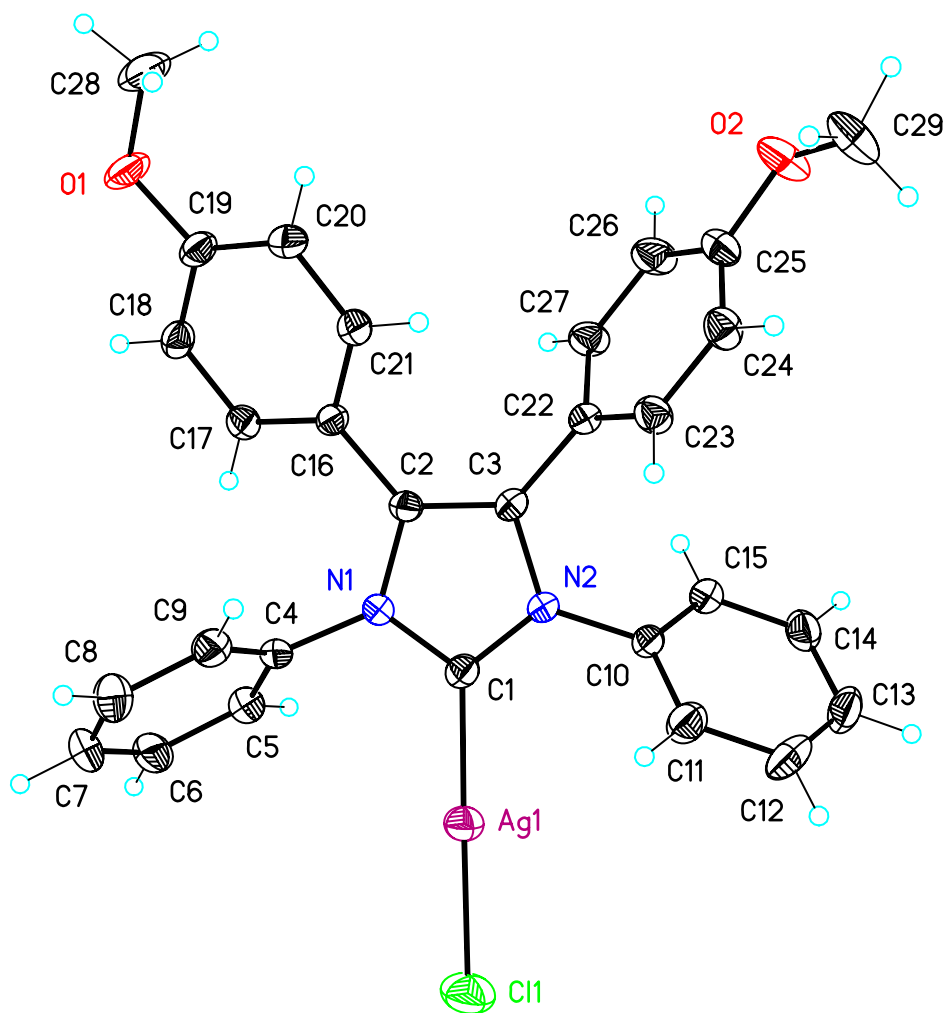
Labeled view with 50% probability ellipsoids

Table B.9. Crystal Data and Structure Refinement for ogle6 (**3.4e**).

Identification code	ogle6
Empirical formula	$C_{29}H_{24}AgClN_2O_2$
Formula weight	575.82
Temperature	173(2) K
Wavelength	0.71073 Å
Crystal system	Monoclinic
Space group	C2/c
Unit cell dimensions	a = 20.2507(13) Å $\quad$ $\alpha = 90°$.
	b = 14.730(1) Å $\quad$ $\beta = 111.846(1)°$.
	c = 17.8733(12) Å $\quad$ $\gamma = 90°$.
Volume	4948.6(6) Å^3
Z	8
Density (calculated)	1.546 Mg/m^3
Absorption coefficient	0.952 mm^{-1}
F(000)	2336
Crystal size	0.20 x 0.09 x 0.08 mm^3
Theta range for data collection	1.76 to 27.50°.
Index ranges	$-22 \leq h \leq 26, -16 \leq k \leq 19, -21 \leq l \leq 23$
Reflections collected	16517
Independent reflections	5661 [R(int) = 0.0277]
Completeness to theta = 27.50°	99.7 %
Absorption correction	Integration
Max. and min. transmission	0.9369 and 0.8159
Refinement method	Full-matrix least-squares on F^2
Data / restraints / parameters	5661 / 0 / 318
Goodness-of-fit on F^2	1.086
Final R indices [I>2sigma(I)]	R1 = 0.0384, wR2 = 0.1066 [4866]
R indices (all data)	R1 = 0.0481, wR2 = 0.1106
Largest diff. peak and hole	0.860 and -0.584 e.Å^{-3}

$R1 = \Sigma(||F_o| - |F_c||) / \Sigma|F_o|$

$wR2 = [\Sigma[w(F_o^2 - F_c^2)^2] / \Sigma[w(F_o^2)^2]]^{1/2}$

$S = [\Sigma[w(F_o^2 - F_c^2)^2] / (n-p)]^{1/2}$

$w = 1/[\sigma^2(F_o^2)+(m*p)^2+n*p]$, $p = [max(F_o^2,0)+ 2* F_c^2]/3$, m & n are constants.

X-ray experimental: Data were collected at 173 K on a Siemens SMART PLATFORM equipped with A CCD area detector and a graphite monochromator utilizing MoK$_\alpha$ radiation (λ = 0.71073 Å). Cell parameters were refined using up to 8192 reflections. A full sphere of data (1850 frames) was collected using the ω-scan method (0.3° frame width). The first 50 frames were re-measured at the end of data collection to monitor instrument and crystal stability (maximum correction on I was < 1 %). Absorption corrections by integration were applied based on measured indexed crystal faces.

The structure was solved by the Direct Methods in *SHELXTL6,* and refined using full-matrix least squares. The non-H atoms were treated anisotropically, whereas the hydrogen atoms were calculated in ideal positions and were riding on their respective carbon atoms. A total of 318 parameters were refined in the final cycle of refinement using 4866 reflections with I > 2σ(I) to yield R$_1$ and wR$_2$ of 3.84% and 10.66%, respectively. Refinement was done using F^2.

SHELXTL6 (2000). Bruker-AXS, Madison, Wisconsin, USA.

Table B.10. Atomic Coordinates (x 10^4) and Equivalent Isotropic Displacement Parameters ($Å^2$x 10^3) for ogle6 (**3.4e**). U(eq) is defined as one third of the trace of the orthogonalized U^{ij} tensor.

	x	y	z	U(eq)
Ag1	1622(1)	8043(1)	984(1)	28(1)
Cl1	2520(1)	8953(1)	932(1)	47(1)
O1	-521(1)	2328(2)	1284(2)	37(1)
O2	-2965(1)	6985(2)	1230(2)	37(1)
N1	833(1)	6334(2)	1172(2)	19(1)
N2	178(1)	7511(2)	1057(2)	19(1)
C1	829(2)	7251(2)	1090(2)	21(1)
C2	182(2)	6014(2)	1173(2)	19(1)
C3	-235(2)	6764(2)	1101(2)	20(1)
C4	1481(2)	5825(2)	1328(2)	20(1)
C5	1787(2)	5822(2)	754(2)	26(1)
C6	2438(2)	5384(2)	929(2)	34(1)
C7	2762(2)	4962(3)	1663(3)	39(1)
C8	2449(2)	4968(3)	2230(2)	38(1)
C9	1803(2)	5402(2)	2061(2)	27(1)
C10	-62(2)	8441(2)	931(2)	21(1)
C11	334(2)	9106(2)	1450(2)	30(1)
C12	109(2)	10006(2)	1306(2)	39(1)
C13	-498(2)	10226(2)	657(2)	37(1)
C14	-890(2)	9554(2)	153(2)	31(1)
C15	-674(2)	8655(2)	287(2)	25(1)
C16	10(2)	5049(2)	1217(2)	18(1)
C17	286(2)	4364(2)	878(2)	21(1)
C18	98(2)	3464(2)	912(2)	23(1)
C19	-375(2)	3234(2)	1274(2)	24(1)
C20	-662(2)	3906(2)	1605(2)	26(1)
C21	-469(2)	4799(2)	1575(2)	23(1)
C22	-955(2)	6862(2)	1114(2)	20(1)
C23	-1052(2)	7344(2)	1740(2)	24(1)
C24	-1715(2)	7406(2)	1795(2)	26(1)
C25	-2295(2)	6981(2)	1222(2)	25(1)
C26	-2208(2)	6519(2)	590(2)	31(1)
C27	-1546(2)	6460(2)	534(2)	26(1)
C28	-998(3)	2067(3)	1669(3)	50(1)
C29	-3064(2)	7380(3)	1909(2)	42(1)

Table B.11. Bond Lengths [Å] and Angles [°] for ogle6 (**3.4e**).

Ag1-C1	2.051(3)
Ag1-Cl1	2.2880(9)
O1-C19	1.369(4)

O1-C28	1.431(4)
O2-C25	1.363(4)
O2-C29	1.426(4)
N1-C1	1.358(4)
N1-C2	1.400(4)
N1-C4	1.445(4)
N2-C1	1.353(4)
N2-C3	1.402(4)
N2-C10	1.443(4)
C2-C3	1.368(4)
C2-C16	1.472(4)
C3-C22	1.473(4)
C4-C9	1.377(4)
C4-C5	1.382(4)
C5-C6	1.396(5)
C5-H5A	0.9500
C6-C7	1.378(5)
C6-H6A	0.9500
C7-C8	1.379(6)
C7-H7A	0.9500
C8-C9	1.385(5)
C8-H8A	0.9500
C9-H9A	0.9500
C10-C15	1.378(4)
C10-C11	1.382(4)
C11-C12	1.393(5)
C11-H11A	0.9500
C12-C13	1.378(6)
C12-H12A	0.9500
C13-C14	1.374(5)
C13-H13A	0.9500
C14-C15	1.387(5)
C14-H14A	0.9500
C15-H15A	0.9500
C16-C17	1.395(4)
C16-C21	1.396(4)
C17-C18	1.387(4)
C17-H17A	0.9500
C18-C19	1.383(4)
C18-H18A	0.9500
C19-C20	1.387(4)
C20-C21	1.378(4)
C20-H20A	0.9500
C21-H21A	0.9500
C22-C27	1.391(4)
C22-C23	1.399(4)
C23-C24	1.385(4)
C23-H23A	0.9500
C24-C25	1.387(4)
C24-H24A	0.9500
C25-C26	1.385(5)
C26-C27	1.385(4)
C26-H26A	0.9500
C27-H27A	0.9500
C28-H28A	0.9800
C28-H28B	0.9800

C28-H28C	0.9800
C29-H29A	0.9800
C29-H29B	0.9800
C29-H29C	0.9800
C1-Ag1-Cl1	177.00(9)
C19-O1-C28	117.0(3)
C25-O2-C29	117.8(3)
C1-N1-C2	111.5(2)
C1-N1-C4	120.4(2)
C2-N1-C4	127.8(2)
C1-N2-C3	111.5(2)
C1-N2-C10	122.8(2)
C3-N2-C10	125.5(2)
N2-C1-N1	104.7(2)
N2-C1-Ag1	128.2(2)
N1-C1-Ag1	127.0(2)
C3-C2-N1	106.1(2)
C3-C2-C16	129.4(3)
N1-C2-C16	124.5(3)
C2-C3-N2	106.2(2)
C2-C3-C22	131.1(3)
N2-C3-C22	122.6(3)
C9-C4-C5	121.4(3)
C9-C4-N1	119.6(3)
C5-C4-N1	118.9(3)
C4-C5-C6	118.9(3)
C4-C5-H5A	120.6
C6-C5-H5A	120.6
C7-C6-C5	119.7(3)
C7-C6-H6A	120.1
C5-C6-H6A	120.1
C6-C7-C8	120.8(3)
C6-C7-H7A	119.6
C8-C7-H7A	119.6
C7-C8-C9	119.8(3)
C7-C8-H8A	120.1
C9-C8-H8A	120.1
C4-C9-C8	119.4(3)
C4-C9-H9A	120.3
C8-C9-H9A	120.3
C15-C10-C11	121.0(3)
C15-C10-N2	119.6(3)
C11-C10-N2	119.4(3)
C10-C11-C12	118.9(3)
C10-C11-H11A	120.6
C12-C11-H11A	120.6
C13-C12-C11	120.4(3)
C13-C12-H12A	119.8
C11-C12-H12A	119.8
C14-C13-C12	120.0(3)
C14-C13-H13A	120.0
C12-C13-H13A	120.0
C13-C14-C15	120.4(3)
C13-C14-H14A	119.8
C15-C14-H14A	119.8

C10-C15-C14	119.3(3)
C10-C15-H15A	120.3
C14-C15-H15A	120.3
C17-C16-C21	117.8(3)
C17-C16-C2	122.3(3)
C21-C16-C2	119.8(3)
C18-C17-C16	120.7(3)
C18-C17-H17A	119.6
C16-C17-H17A	119.6
C19-C18-C17	120.2(3)
C19-C18-H18A	119.9
C17-C18-H18A	119.9
O1-C19-C18	115.8(3)
O1-C19-C20	124.4(3)
C18-C19-C20	119.9(3)
C21-C20-C19	119.7(3)
C21-C20-H20A	120.2
C19-C20-H20A	120.2
C20-C21-C16	121.6(3)
C20-C21-H21A	119.2
C16-C21-H21A	119.2
C27-C22-C23	118.3(3)
C27-C22-C3	121.9(3)
C23-C22-C3	119.8(3)
C24-C23-C22	121.3(3)
C24-C23-H23A	119.4
C22-C23-H23A	119.4
C23-C24-C25	119.6(3)
C23-C24-H24A	120.2
C25-C24-H24A	120.2
O2-C25-C26	116.1(3)
O2-C25-C24	124.3(3)
C26-C25-C24	119.6(3)
C25-C26-C27	120.7(3)
C25-C26-H26A	119.7
C27-C26-H26A	119.7
C26-C27-C22	120.5(3)
C26-C27-H27A	119.8
C22-C27-H27A	119.8
O1-C28-H28A	109.5
O1-C28-H28B	109.5
H28A-C28-H28B	109.5
O1-C28-H28C	109.5
H28A-C28-H28C	109.5
H28B-C28-H28C	109.5
O2-C29-H29A	109.5
O2-C29-H29B	109.5
H29A-C29-H29B	109.5
O2-C29-H29C	109.5
H29A-C29-H29C	109.5
H29B-C29-H29C	109.5

Table B.12.   Anisotropic Displacement Parameters (Å^2x 10^3) for ogle6 (**3.4e**). The anisotropic displacement
factor exponent takes the form: $-2\pi^2[\,h^2\,a^{*2}U^{11} + ... \; + 2\,h\,k\,a^*\,b^*\,U^{12}\,]$

	U^{11}	U^{22}	U^{33}	U^{23}	U^{13}	U^{12}
Ag1	24(1)	27(1)	33(1)	3(1)	11(1)	-2(1)
Cl1	35(1)	52(1)	58(1)	8(1)	22(1)	-8(1)
O1	48(2)	16(1)	58(2)	-3(1)	33(1)	-8(1)
O2	19(1)	60(2)	35(1)	-11(1)	12(1)	-4(1)
N1	16(1)	18(1)	23(1)	1(1)	7(1)	0(1)
N2	18(1)	15(1)	25(1)	-1(1)	8(1)	-2(1)
C1	22(2)	18(1)	21(1)	1(1)	7(1)	-1(1)
C2	17(1)	19(1)	21(1)	0(1)	8(1)	-2(1)
C3	21(1)	16(1)	22(1)	-2(1)	8(1)	-2(1)
C4	16(1)	17(1)	27(2)	-2(1)	7(1)	-2(1)
C5	24(2)	24(2)	29(2)	0(1)	11(1)	0(1)
C6	27(2)	32(2)	47(2)	-5(2)	19(2)	1(1)
C7	22(2)	32(2)	60(2)	4(2)	13(2)	8(1)
C8	32(2)	33(2)	41(2)	13(2)	4(2)	7(2)
C9	26(2)	25(2)	30(2)	5(1)	10(1)	-1(1)
C10	22(1)	17(1)	27(2)	0(1)	13(1)	-1(1)
C11	32(2)	23(2)	32(2)	-3(1)	9(1)	-2(1)
C12	52(2)	19(2)	46(2)	-7(2)	19(2)	-9(2)
C13	47(2)	18(2)	53(2)	4(2)	27(2)	6(2)
C14	27(2)	28(2)	40(2)	8(1)	15(2)	7(1)
C15	23(2)	20(2)	32(2)	2(1)	10(1)	1(1)
C16	18(1)	16(1)	20(1)	1(1)	5(1)	-1(1)
C17	21(1)	22(2)	23(1)	0(1)	10(1)	1(1)
C18	26(2)	18(2)	25(2)	-3(1)	9(1)	1(1)
C19	27(2)	17(2)	27(2)	-1(1)	8(1)	-4(1)
C20	26(2)	23(2)	34(2)	2(1)	16(1)	-3(1)
C21	23(2)	21(2)	28(2)	0(1)	13(1)	1(1)
C22	19(1)	16(1)	25(1)	1(1)	9(1)	-1(1)
C23	20(2)	27(2)	25(2)	-5(1)	7(1)	-1(1)
C24	24(2)	29(2)	24(2)	-5(1)	9(1)	2(1)
C25	18(1)	31(2)	27(2)	2(1)	8(1)	2(1)
C26	22(2)	36(2)	32(2)	-11(1)	8(1)	-8(1)
C27	24(2)	28(2)	29(2)	-10(1)	11(1)	-7(1)
C28	63(3)	23(2)	84(3)	1(2)	50(3)	-9(2)
C29	26(2)	64(3)	41(2)	-4(2)	19(2)	6(2)

X-Ray Structure Data for 3.4f (ogle12)
C$_{27}$H$_{18}$AgClF$_2$N$_2$ · ClH$_2$CCClH$_2$
(solved by K. A. Abboud)
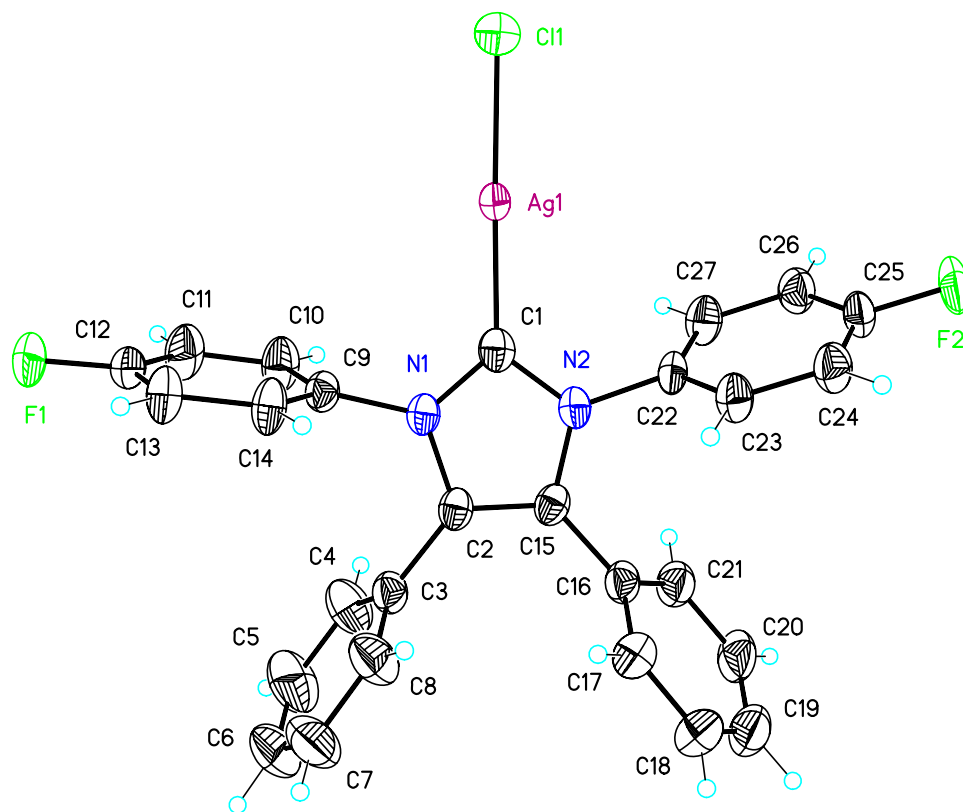
Labeled view with 50% probability ellipsoids

Table B.13. Crystal Data and Structure Refinement for ogle12 (**3.4f**).

Identification code	ogle12
Empirical formula	$C_{29}H_{22}AgCl_3F_2N_2$ = $C_{27}H_{18}AgClF_2N_2 \cdot ClH_2CCClH_2$
Formula weight	650.71
Temperature	173(2) K
Wavelength	0.71073 Å
Crystal system	Triclinic
Space group	P-1

Unit cell dimensions

$a = 6.659(2)$ Å	$\alpha = 73.452(4)°$.
$b = 13.924(4)$ Å	$\beta = 77.98°$.
$c = 15.986(4)$ Å	$\gamma = 76.16°$.

Volume	1363.9(7) Å^3
Z	2
Density (calculated)	1.584 Mg/m^3
Absorption coefficient	1.068 mm^{-1}
F(000)	652
Crystal size	0.24 x 0.13 x 0.04 mm^3
Theta range for data collection	1.34 to 27.50°.
Index ranges	$-8 \leq h \leq 8$, $-18 \leq k \leq 11$, $-20 \leq l \leq 19$
Reflections collected	9118
Independent reflections	6075 [R(int) = 0.0508]
Completeness to theta = 27.50°	97.1 %
Absorption correction	Integration
Max. and min. transmission	0.9585 and 0.7836
Refinement method	Full-matrix least-squares on F^2
Data / restraints / parameters	6075 / 0 / 333
Goodness-of-fit on F^2	1.212
Final R indices [I>2sigma(I)]	R1 = 0.0563, wR2 = 0.1801 [5447]
R indices (all data)	R1 = 0.0622, wR2 = 0.1835
Largest diff. peak and hole	1.785 and -1.122 e.Å^{-3}

$R1 = \sum(||F_o| - |F_c||) / \sum|F_o|$

$wR2 = [\sum[w(F_o^2 - F_c^2)^2] / \sum[w(F_o^2)^2]]^{1/2}$

$S = [\sum[w(F_o^2 - F_c^2)^2] / (n-p)]^{1/2}$

$w = 1/[\sigma^2(F_o^2)+(m*p)^2+n*p]$, $p = [max(F_o^2,0)+ 2* F_c^2]/3$, m & n are constants.

X-ray experimental: Data were collected at 173 K on a Siemens SMART PLATFORM equipped with A CCD area detector and a graphite monochromator utilizing MoK$_\alpha$ radiation ($\lambda = 0.71073$ Å). Cell parameters were refined using up to 8192 reflections. A full sphere of data (1850 frames) was collected using the ω-scan method (0.3° frame width). The first 50 frames were re-measured at the end of data collection to monitor instrument and crystal stability (maximum correction on I was < 1 %). Absorption corrections by integration were applied based on measured indexed crystal faces.

The structure was solved by the Direct Methods in *SHELXTL6,* and refined using full-matrix least squares. The non-H atoms were treated anisotropically, whereas the hydrogen atoms were calculated in ideal positions and were riding on their respective carbon atoms. There is a disordered dichloroethane molecule in the asymmetric unit and it has its CH2-CH2 unit disordered. The final refined model has two parts of the latter unit refined with dependent occupation factors. A total of 333 parameters were refined in the final cycle of refinement using 5447 reflections with I > 2σ(I) to yield R$_1$ and wR$_2$ of 5.63% and 18.01%, respectively. Refinement was done using F^2.

SHELXTL6 (2000). Bruker-AXS, Madison, Wisconsin, USA.

Table B.14. Atomic Coordinates (x 10^4) and Equivalent Isotropic Displacement Parameters (Å^2x 10^3) for ogle12 (**3.4f**). U(eq) is defined as one third of the trace of the orthogonalized U^{ij} tensor.

	x	y	z	U(eq)
Ag1	7579(1)	5106(1)	-229(1)	27(1)
Cl1	7304(2)	5385(1)	-1727(1)	35(1)
C1	7663(8)	4812(4)	1109(4)	29(1)
N2	8057(7)	3885(4)	1683(3)	28(1)
C9	6864(9)	6565(4)	1363(4)	30(1)
F1	5634(7)	9670(3)	864(3)	49(1)
N1	7270(7)	5462(4)	1646(3)	28(1)
C3	7040(10)	5484(5)	3256(4)	34(1)
C22	8670(9)	2929(4)	1421(4)	29(1)
C2	7424(8)	4945(4)	2531(4)	29(1)
C16	8256(10)	3049(5)	3312(4)	34(1)
C10	4873(10)	7085(5)	1236(5)	43(2)
C27	7278(10)	2596(5)	1095(5)	39(1)
F2	10392(8)	185(3)	787(3)	54(1)
C17	9926(12)	2887(5)	3763(5)	45(2)
C23	10662(9)	2363(5)	1522(4)	35(1)
C26	7862(11)	1662(5)	873(5)	40(1)
C8	8699(13)	5548(6)	3620(6)	52(2)
C5	4671(16)	6353(8)	4270(7)	70(3)
C11	4465(11)	8141(5)	1050(6)	47(2)
C25	9815(11)	1106(5)	995(5)	39(1)
C12	6063(11)	8632(5)	1008(4)	37(1)
C21	6891(12)	2366(5)	3579(5)	43(2)
C7	8328(16)	6019(7)	4327(6)	65(2)
C19	8822(15)	1405(6)	4775(5)	59(2)
C24	11249(10)	1431(5)	1311(5)	40(1)
C18	10172(15)	2074(6)	4507(5)	57(2)
C20	7174(14)	1548(5)	4311(5)	53(2)
C14	8451(10)	7060(5)	1297(5)	38(1)
C13	8059(10)	8133(5)	1120(5)	41(2)
C4	5024(13)	5880(6)	3587(6)	54(2)
C6	6337(17)	6403(7)	4652(6)	69(3)
C15	7923(9)	3939(4)	2553(4)	29(1)
Cl2	5913(5)	-314(3)	6701(2)	95(1)
Cl3	-216(6)	1524(3)	7017(2)	107(1)
C28	3870(50)	780(20)	6780(19)	122(10)
C29	1790(40)	521(18)	6817(17)	107(8)
C28'	2990(80)	290(40)	7120(30)	97(15)
C29'	2310(70)	1320(30)	6880(30)	90(15)

Table B.15. Bond Lengths [Å] and Angles [°] for ogle12 (**3.4f**).

Ag1-C1	2.070(6)
Ag1-Cl1	2.3537(17)

C1-N2	1.357(7)
C1-N1	1.365(8)
N2-C15	1.397(8)
N2-C22	1.450(7)
C9-C14	1.365(9)
C9-C10	1.376(8)
C9-N1	1.446(7)
F1-C12	1.365(7)
N1-C2	1.406(8)
C3-C4	1.380(10)
C3-C8	1.382(10)
C3-C2	1.500(8)
C22-C27	1.374(9)
C22-C23	1.387(8)
C2-C15	1.353(8)
C16-C17	1.389(10)
C16-C21	1.391(9)
C16-C15	1.477(8)
C10-C11	1.384(9)
C10-H24A	0.9500
C27-C26	1.390(9)
C27-H27A	0.9500
F2-C25	1.363(7)
C17-C18	1.395(10)
C17-H30A	0.9500
C23-C24	1.379(9)
C23-H32A	0.9500
C26-C25	1.366(10)
C26-H33A	0.9500
C8-C7	1.414(11)
C8-H43A	0.9500
C5-C4	1.381(12)
C5-C6	1.398(15)
C5-H44A	0.9500
C11-C12	1.378(10)
C11-H46A	0.9500
C25-C24	1.381(10)
C12-C13	1.367(10)
C21-C20	1.391(10)
C21-H55A	0.9500
C7-C6	1.358(14)
C7-H56A	0.9500
C19-C18	1.369(13)
C19-C20	1.394(13)
C19-H57A	0.9500
C24-H60A	0.9500
C18-H65A	0.9500
C20-H68A	0.9500
C14-C13	1.410(8)
C14-H71A	0.9500
C13-H73A	0.9500
C4-H74A	0.9500
C6-H75A	0.9500
Cl2-C28	1.80(3)
Cl2-C28'	1.98(5)
Cl3-C29'	1.62(4)

Cl3-C29	1.74(2)
C28-C29	1.50(4)
C28-H28A	0.9900
C28-H28B	0.9900
C29-H29A	0.9900
C29-H29B	0.9900
C28'-C29'	1.36(7)
C28'-H28C	0.9900
C28'-H28D	0.9900
C29'-H29C	0.9900
C29'-H29D	0.9900
C1-Ag1-Cl1	176.37(16)
N2-C1-N1	102.3(5)
N2-C1-Ag1	127.2(4)
N1-C1-Ag1	130.5(4)
C1-N2-C15	113.5(5)
C1-N2-C22	123.7(5)
C15-N2-C22	122.7(5)
C14-C9-C10	121.9(6)
C14-C9-N1	118.3(5)
C10-C9-N1	119.6(5)
C1-N1-C2	112.5(5)
C1-N1-C9	125.8(5)
C2-N1-C9	121.6(5)
C4-C3-C8	119.7(7)
C4-C3-C2	120.1(6)
C8-C3-C2	120.1(6)
C27-C22-C23	121.7(5)
C27-C22-N2	120.0(5)
C23-C22-N2	118.3(5)
C15-C2-N1	106.1(5)
C15-C2-C3	130.8(6)
N1-C2-C3	123.1(5)
C17-C16-C21	119.6(6)
C17-C16-C15	120.5(6)
C21-C16-C15	119.9(6)
C9-C10-C11	118.9(6)
C9-C10-H24A	120.6
C11-C10-H24A	120.6
C22-C27-C26	119.4(6)
C22-C27-H27A	120.3
C26-C27-H27A	120.3
C16-C17-C18	120.3(7)
C16-C17-H30A	119.9
C18-C17-H30A	119.9
C24-C23-C22	119.3(6)
C24-C23-H32A	120.3
C22-C23-H32A	120.3
C25-C26-C27	118.0(6)
C25-C26-H33A	121.0
C27-C26-H33A	121.0
C3-C8-C7	120.0(7)
C3-C8-H43A	120.0
C7-C8-H43A	120.0
C4-C5-C6	120.6(8)

C4-C5-H44A	119.7
C6-C5-H44A	119.7
C12-C11-C10	118.8(6)
C12-C11-H46A	120.6
C10-C11-H46A	120.6
F2-C25-C26	118.4(6)
F2-C25-C24	118.0(6)
C26-C25-C24	123.6(6)
F1-C12-C13	117.9(6)
F1-C12-C11	118.7(6)
C13-C12-C11	123.4(6)
C16-C21-C20	119.6(7)
C16-C21-H55A	120.2
C20-C21-H55A	120.2
C6-C7-C8	119.9(9)
C6-C7-H56A	120.1
C8-C7-H56A	120.1
C18-C19-C20	119.7(7)
C18-C19-H57A	120.1
C20-C19-H57A	120.1
C23-C24-C25	118.0(6)
C23-C24-H60A	121.0
C25-C24-H60A	121.0
C19-C18-C17	120.2(8)
C19-C18-H65A	119.9
C17-C18-H65A	119.9
C21-C20-C19	120.5(8)
C21-C20-H68A	119.7
C19-C20-H68A	119.7
C9-C14-C13	120.0(6)
C9-C14-H71A	120.0
C13-C14-H71A	120.0
C12-C13-C14	117.0(6)
C12-C13-H73A	121.5
C14-C13-H73A	121.5
C3-C4-C5	120.0(9)
C3-C4-H74A	120.0
C5-C4-H74A	120.0
C7-C6-C5	119.7(8)
C7-C6-H75A	120.1
C5-C6-H75A	120.1
C2-C15-N2	105.6(5)
C2-C15-C16	129.5(6)
N2-C15-C16	124.9(5)
C28-Cl2-C28'	29.5(14)
C29'-Cl3-C29	44.6(16)
C29-C28-Cl2	109.6(19)
C29-C28-H28A	109.7
Cl2-C28-H28A	109.7
C29-C28-H28B	109.7
Cl2-C28-H28B	109.7
H28A-C28-H28B	108.2
C28-C29-Cl3	110.2(18)
C28-C29-H29A	109.6
Cl3-C29-H29A	109.6
C28-C29-H29B	109.6

Cl3-C29-H29B	109.6
H29A-C29-H29B	108.1
C29'-C28'-Cl2	120(4)
C29'-C28'-H28C	107.3
Cl2-C28'-H28C	107.3
C29'-C28'-H28D	107.3
Cl2-C28'-H28D	107.3
H28C-C28'-H28D	106.9
C28'-C29'-Cl3	107(4)
C28'-C29'-H29C	110.3
Cl3-C29'-H29C	110.3
C28'-C29'-H29D	110.3
Cl3-C29'-H29D	110.3
H29C-C29'-H29D	108.6

Table B.16. Anisotropic Displacement Parameters ($Å^2$x 10^3) for ogle12 (**3.4f**). The anisotropic displacement factor exponent takes the form: $-2\pi^2[\,h^2\,a^{*2}U^{11} + ... + 2\,h\,k\,a^*\,b^*\,U^{12}\,]$

	U^{11}	U^{22}	U^{33}	U^{23}	U^{13}	U^{12}
Ag1	31(1)	20(1)	29(1)	-7(1)	-4(1)	-2(1)
Cl1	26(1)	44(1)	37(1)	-11(1)	-4(1)	-7(1)
C1	19(2)	28(3)	38(3)	-10(2)	0(2)	1(2)
N2	26(2)	22(2)	35(2)	-9(2)	-2(2)	-3(2)
C9	29(3)	23(3)	33(3)	-7(2)	-3(2)	0(2)
F1	62(3)	21(2)	60(3)	-9(2)	-13(2)	0(2)
N1	25(2)	22(2)	34(2)	-7(2)	-4(2)	-1(2)
C3	38(3)	26(3)	34(3)	-9(2)	0(2)	-2(2)
C22	29(3)	17(2)	36(3)	-6(2)	-2(2)	-1(2)
C2	24(2)	24(3)	35(3)	-7(2)	-2(2)	-1(2)
C16	37(3)	26(3)	33(3)	-9(2)	2(2)	-1(2)
C10	32(3)	31(3)	69(5)	-12(3)	-16(3)	-2(3)
C27	31(3)	30(3)	54(4)	-9(3)	-9(3)	0(2)
F2	69(3)	25(2)	70(3)	-25(2)	-14(2)	5(2)
C17	54(4)	36(3)	42(4)	-5(3)	-12(3)	-6(3)
C23	30(3)	29(3)	48(4)	-13(3)	-8(3)	-1(2)
C26	48(4)	29(3)	50(4)	-13(3)	-18(3)	-5(3)
C8	50(4)	55(5)	57(4)	-32(4)	-6(3)	-2(3)
C5	67(6)	68(6)	77(6)	-47(5)	16(5)	-3(5)
C11	37(3)	30(3)	71(5)	-11(3)	-21(3)	9(3)
C25	51(4)	22(3)	42(3)	-12(2)	-4(3)	-3(3)
C12	48(4)	24(3)	36(3)	-8(2)	-8(3)	0(3)
C21	51(4)	31(3)	40(3)	-6(3)	1(3)	-8(3)
C7	77(6)	66(6)	64(5)	-38(5)	-17(5)	-4(5)
C19	80(6)	36(4)	45(4)	-3(3)	-3(4)	3(4)
C24	34(3)	32(3)	50(4)	-14(3)	-8(3)	4(3)
C18	74(5)	45(4)	44(4)	-3(3)	-17(4)	0(4)
C20	75(5)	28(3)	46(4)	-2(3)	8(4)	-13(3)
C14	27(3)	22(3)	60(4)	-9(3)	-4(3)	1(2)
C13	37(3)	25(3)	61(4)	-9(3)	-4(3)	-8(2)
C4	46(4)	56(5)	64(5)	-36(4)	5(4)	-3(3)
C6	93(7)	62(5)	56(5)	-38(4)	0(5)	-4(5)
C15	24(3)	25(3)	33(3)	-4(2)	-1(2)	-2(2)
Cl2	97(2)	103(2)	80(2)	-2(2)	-24(2)	-23(2)
Cl3	117(3)	128(3)	71(2)	-30(2)	-25(2)	-1(2)

X-Ray Structure Data for 4h (ogle7)
$C_{29}H_{24}AgClN_2O_2 \cdot CH_2Cl_2$
(solved by K. A. Abboud)
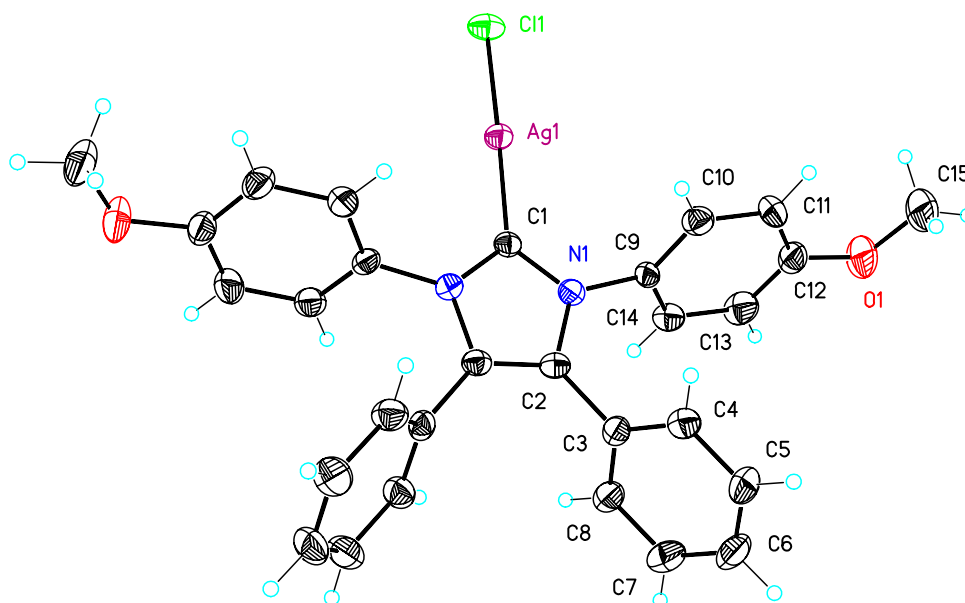
Labeled view with 50% probability ellipsoids

Table B.17. Crystal Data and Structure Refinement for ogle7 (**3.4h**).

Identification code	ogle7
Empirical formula	$C_{30}H_{26}AgCl_3N_2O_2$ = $C_{29}H_{24}AgClN_2O_2 \cdot CH_2Cl_2$
Formula weight	660.75
Temperature	173(2) K
Wavelength	0.71073 Å
Crystal system	Orthorhombic
Space group	Cmc2(1)
Unit cell dimensions	a = 18.7911(14) Å $\quad\quad$ $\alpha = 90°$.
	b = 23.0534(16) Å $\quad\quad$ $\beta = 90°$.
	c = 6.5177(5) Å $\quad\quad$ $\gamma = 90°$.
Volume	2823.5(4) Å^3
Z	4
Density (calculated)	1.554 Mg/m^3
Absorption coefficient	1.028 mm^{-1}
F(000)	1336
Crystal size	0.28 x 0.08 x 0.08 mm^3
Theta range for data collection	1.40 to 27.49°.
Index ranges	$-15 \leq h \leq 24$, $-21 \leq k \leq 29$, $-7 \leq l \leq 8$
Reflections collected	5420
Independent reflections	2963 [R(int) = 0.0330]
Completeness to theta = 27.49°	99.0 %
Absorption correction	Integration
Max. and min. transmission	0.9222 and 0.7616
Refinement method	Full-matrix least-squares on F^2
Data / restraints / parameters	2963 / 1 / 181
Goodness-of-fit on F^2	1.014
Final R indices [I>2sigma(I)]	R1 = 0.0308, wR2 = 0.0731 [2671]
R indices (all data)	R1 = 0.0358, wR2 = 0.0748
Absolute structure parameter	0.10(3)
Largest diff. peak and hole	0.405 and -0.380 e.Å^{-3}

$R1 = \Sigma(||F_o| - |F_c||) / \Sigma|F_o|$

$wR2 = [\Sigma[w(F_o^2 - F_c^2)^2] / \Sigma[w(F_o^2)^2]]^{1/2}$

$S = [\Sigma[w(F_o^2 - F_c^2)^2] / (n-p)]^{1/2}$

$w = 1/[\sigma^2(F_o^2)+(m*p)^2+n*p]$, $p = [max(F_o^2,0)+ 2* F_c^2]/3$, m & n are constants.

X-ray experimental: Data were collected at 173 K on a Siemens SMART PLATFORM equipped with A CCD area detector and a graphite monochromator utilizing MoKα radiation (λ = 0.71073 Å). Cell parameters were refined using up to 8192 reflections. A full sphere of data (1850 frames) was collected using the ω-scan method (0.3° frame width). The first 50 frames were re-measured at the end of data collection to monitor instrument and crystal stability (maximum correction on I was < 1 %). Absorption corrections by integration were applied based on measured indexed crystal faces.

The structure was solved by the Direct Methods in *SHELXTL6*, and refined using full-matrix least squares. The non-H atoms were treated anisotropically, whereas the hydrogen atoms were calculated in ideal positions and were riding on their respective carbon atoms. The asymmetric unit consists of a half complex and a half dichloromethane molecule. Each molecule is located on mirror plane symmetry. A total of 181 parameters were refined in the final

cycle of refinement using 2671 reflections with $I > 2\sigma(I)$ to yield R_1 and wR_2 of 3.08% and 7.31%, respectively. Refinement was done using F^2.

SHELXTL6 (2000). Bruker-AXS, Madison, Wisconsin, USA.

Table B.18. Atomic Coordinates (x 10^4) and Equivalent Isotropic Displacement Parameters ($\mathring{A}^2$x 10^3) for ogle7 (**3.4h**). U(eq) is defined as one third of the trace of the orthogonalized U^{ij} tensor.

	x	y	z	U(eq)
Ag1	0	5190(1)	-7452(1)	24(1)
Cl1	0	6205(1)	-7654(3)	31(1)
Cl2	5000	3289(1)	1534(3)	62(1)
Cl3	5000	4227(1)	-1406(3)	70(1)
O1	3478(1)	4350(1)	-7661(9)	49(1)
N1	566(1)	3929(1)	-7631(6)	21(1)
C1	0	4289(2)	-7543(16)	20(1)
C2	358(2)	3349(1)	-7785(6)	22(1)
C3	880(2)	2866(1)	-7927(5)	23(1)
C4	1296(2)	2724(2)	-6245(6)	31(1)
C5	1795(2)	2281(2)	-6387(7)	38(1)
C6	1876(2)	1986(2)	-8235(7)	40(1)
C7	1462(2)	2122(2)	-9897(7)	37(1)
C8	965(2)	2569(2)	-9769(6)	30(1)
C9	1306(1)	4102(1)	-7613(8)	22(1)
C10	1620(2)	4303(2)	-5864(6)	28(1)
C11	2348(2)	4408(2)	-5813(7)	32(1)
C12	2752(2)	4295(1)	-7537(11)	32(1)
C13	2430(2)	4105(2)	-9318(7)	37(1)
C14	1700(2)	4010(2)	-9380(6)	28(1)
C15	3847(2)	4493(2)	-5830(9)	57(1)
C16	5000	3486(3)	-1043(12)	63(2)

Table B.19. Bond Lengths [$\mathring{A}$] and Angles [°] for ogle7 (**3.4h**).

Ag1-C1	2.079(4)
Ag1-Cl1	2.3439(11)
Ag1-Ag1#1	3.3744(3)
Ag1-Ag1#2	3.3744(3)
Cl2-C16	1.740(8)
Cl3-C16	1.725(6)
O1-C12	1.372(3)
O1-C15	1.419(7)
N1-C1	1.350(3)
N1-C2	1.396(4)
N1-C9	1.445(3)
C1-N1#3	1.350(3)
C2-C2#3	1.346(6)
C2-C3	1.488(4)
C3-C4	1.386(5)
C3-C8	1.390(5)
C4-C5	1.390(5)

C4-H4A	0.9500
C5-C6	1.392(6)
C5-H5A	0.9500
C6-C7	1.370(6)
C6-H6A	0.9500
C7-C8	1.394(5)
C7-H7A	0.9500
C8-H8A	0.9500
C9-C10	1.365(6)
C9-C14	1.385(6)
C10-C11	1.391(5)
C10-H10A	0.9500
C11-C12	1.381(7)
C11-H11A	0.9500
C12-C13	1.380(7)
C13-C14	1.391(5)
C13-H13A	0.9500
C14-H14A	0.9500
C15-H15A	0.9800
C15-H15B	0.9800
C15-H15C	0.9800
C16-H16A	0.9900
C16-H16B	0.9900
C1-Ag1-Cl1	175.1(3)
C1-Ag1-Ag1#1	73.3(3)
Cl1-Ag1-Ag1#1	101.82(5)
C1-Ag1-Ag1#2	76.6(3)
Cl1-Ag1-Ag1#2	108.26(5)
Ag1#1-Ag1-Ag1#2	149.925(18)
C12-O1-C15	117.3(5)
C1-N1-C2	111.7(2)
C1-N1-C9	126.1(2)
C2-N1-C9	122.2(2)
N1#3-C1-N1	104.1(3)
N1#3-C1-Ag1	127.93(16)
N1-C1-Ag1	127.93(16)
C2#3-C2-N1	106.25(15)
C2#3-C2-C3	131.22(16)
N1-C2-C3	122.5(3)
C4-C3-C8	120.2(3)
C4-C3-C2	119.9(3)
C8-C3-C2	119.9(3)
C3-C4-C5	120.0(4)
C3-C4-H4A	120.0
C5-C4-H4A	120.0
C4-C5-C6	119.4(4)
C4-C5-H5A	120.3
C6-C5-H5A	120.3
C7-C6-C5	120.7(3)
C7-C6-H6A	119.6
C5-C6-H6A	119.6
C6-C7-C8	120.1(4)
C6-C7-H7A	119.9
C8-C7-H7A	119.9
C3-C8-C7	119.5(4)

C3-C8-H8A	120.2
C7-C8-H8A	120.2
C10-C9-C14	121.0(3)
C10-C9-N1	121.0(4)
C14-C9-N1	117.7(4)
C9-C10-C11	120.3(4)
C9-C10-H10A	119.8
C11-C10-H10A	119.8
C12-C11-C10	119.2(4)
C12-C11-H11A	120.4
C10-C11-H11A	120.4
O1-C12-C13	114.5(6)
O1-C12-C11	125.2(5)
C13-C12-C11	120.2(3)
C12-C13-C14	120.5(4)
C12-C13-H13A	119.8
C14-C13-H13A	119.8
C9-C14-C13	118.6(4)
C9-C14-H14A	120.7
C13-C14-H14A	120.7
O1-C15-H15A	109.5
O1-C15-H15B	109.5
H15A-C15-H15B	109.5
O1-C15-H15C	109.5
H15A-C15-H15C	109.5
H15B-C15-H15C	109.5
Cl3-C16-Cl2	113.0(4)
Cl3-C16-H16A	109.0
Cl2-C16-H16A	109.0
Cl3-C16-H16B	109.0
Cl2-C16-H16B	109.0
H16A-C16-H16B	107.8

Symmetry transformations used to generate equivalent atoms:
#1 -x,-y+1,z-1/2   #2 -x,-y+1,z+1/2   #3 -x,y,z

Table B.20. Anisotropic Displacement Parameters (Å^2x 10^3) for ogle7 (**3.4h**). The anisotropic displacement factor exponent takes the form: $-2\pi^2[\,h^2\,a^{*2}U^{11} + ... \; + 2\,h\,k\,a^*\,b^*\,U^{12}\,]$

	U^{11}	U^{22}	U^{33}	U^{23}	U^{13}	U^{12}
Ag1	24(1)	19(1)	30(1)	-1(1)	0	0
Cl1	47(1)	22(1)	25(1)	-1(1)	0	0
Cl2	76(1)	60(1)	51(1)	16(1)	0	0
Cl3	101(2)	40(1)	69(1)	13(1)	0	0
O1	21(1)	58(2)	69(2)	-2(2)	2(2)	-6(1)
N1	21(1)	20(1)	21(2)	-1(2)	-1(2)	-1(1)
C1	22(2)	20(2)	17(2)	-1(3)	0	0
C2	27(1)	18(1)	22(2)	0(1)	2(2)	-1(1)
C3	20(1)	20(1)	30(3)	4(1)	2(1)	-1(1)
C4	33(2)	25(2)	35(2)	-1(2)	-4(2)	1(2)
C5	33(2)	33(2)	48(3)	4(2)	-10(2)	9(2)

C6	31(2)	31(2)	57(3)	2(2)	5(2)	11(2)
C7	40(2)	30(2)	41(2)	-3(2)	9(2)	6(2)
C8	28(2)	27(2)	34(2)	1(2)	1(2)	4(2)
C9	20(1)	17(1)	28(2)	0(2)	-5(2)	-1(1)
C10	27(2)	25(2)	31(2)	-2(2)	4(2)	0(2)
C11	26(2)	31(2)	37(2)	-4(2)	-7(2)	-5(2)
C12	22(1)	25(1)	49(2)	2(2)	0(3)	-2(1)
C13	29(2)	36(2)	45(3)	-2(2)	14(2)	-2(2)
C14	31(2)	25(2)	29(2)	-2(2)	3(2)	-2(2)
C15	26(2)	55(3)	89(4)	-7(3)	-10(2)	-8(2)
C16	97(6)	35(3)	57(5)	6(3)	0	0

X-Ray Structure Data for 3.3d (sm121)
$C_{29}H_{19}ClF_6N_2 \cdot (CH_2Cl_2)_{0.375}$
(solved by J. A. Reibenspies)
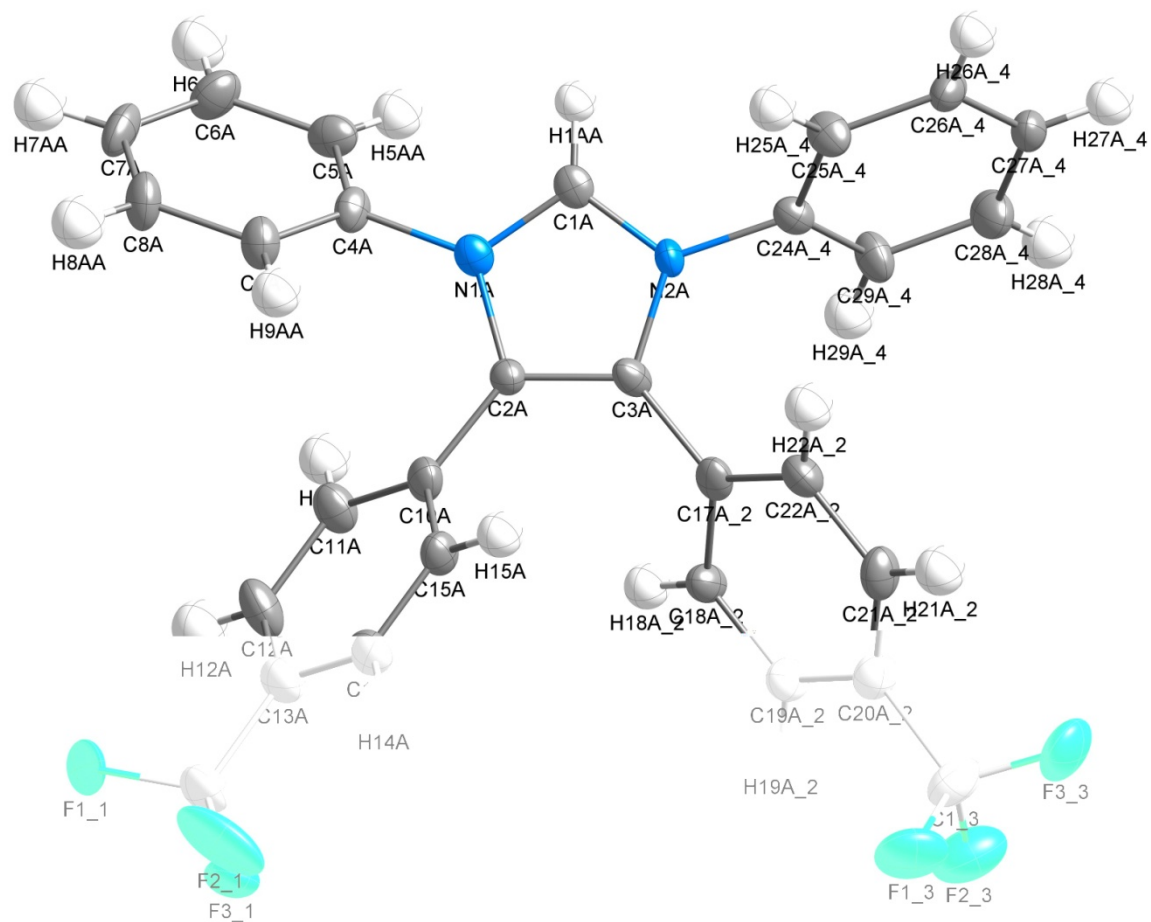
Labeled view with 50% probability ellipsoids
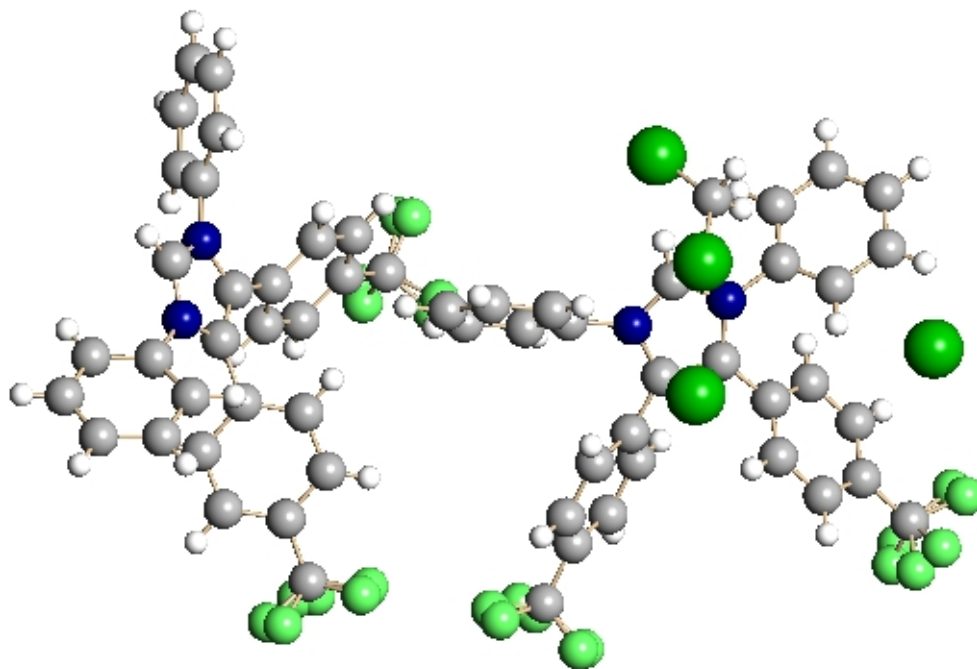
Note: 2 Chlorine anions and ¾ CH$_2$Cl$_2$ is located in the asymmetric volume of the unit cell. The anions and the CH$_2$Cl$_2$ are disordered over three possible CH$_2$Cl$_2$ positions.

Table B.21. Crystal Data and Structure Refinement for sm121 (**3.3d**).

Identification code	sm121
Empirical formula	$C_{29.375}H_{19.75}Cl_{1.75}F_6N_2$ = $C_{29}H_{19}ClF_6N_2 \cdot (CH_2Cl_2)_{0.375}$
Formula weight	567.90
Temperature	110(2) K
Wavelength	0.71073 Å
Crystal system	Triclinic
Space group	P-1
Unit cell dimensions	a = 10.757(3) Å α = 98.285(5)°.
	b = 15.673(5) Å β = 90.679(5)°.
	c = 15.764(5) Å γ = 95.983(5)°.
Volume	2614.6(13) Å^3
Z	4
Density (calculated)	1.443 Mg/m^3
Absorption coefficient	0.262 mm^{-1}
F(000)	1158
Crystal size	0.40 x 0.20 x 0.20 mm^3
Theta range for data collection	1.31 to 25.00°.
Index ranges	-12<=h<=12, -18<=k<=18, -18<=l<=18
Reflections collected	18703
Independent reflections	8310 [R(int) = 0.0394]
Completeness to theta = 25.00°	90.1 %
Absorption correction	Semi-empirical from equivalents
Max. and min. transmission	0.9494 and 0.9023
Refinement method	Full-matrix least-squares on F^2
Data / restraints / parameters	8310 / 366 / 833
Goodness-of-fit on F^2	1.003
Final R indices [I>2sigma(I)]	R1 = 0.0890, wR2 = 0.1784
R indices (all data)	R1 = 0.1056, wR2 = 0.1878
Largest diff. peak and hole	0.583 and -0.516 e.Å^{-3}

Table B.22. Atomic Coordinates (x 10^4) and Equivalent Isotropic Displacement Parameters (Å^{2}x 10^3) for sm121 (**3.3d**). U(eq) is defined as one third of the trace of the orthogonalized U^{ij} tensor.

	x	y	z	U(eq)
C(1ME)	1360(20)	420(90)	3670(40)	360(50)
C(2ME)	3740(50)	-1000(90)	705(9)	360(50)
C(3ME)	1030(40)	-720(50)	160(90)	360(50)
Cl(1)	1341(2)	105(2)	4661(1)	57(1)
Cl(2)	2652(2)	564(2)	3073(1)	47(1)
Cl(3)	3841(2)	-773(1)	1793(1)	40(1)
Cl(4)	2531(7)	-933(3)	19(3)	46(2)
Cl(5)	0	0	0	46(1)
N(1A)	1046(3)	-1844(2)	2575(2)	20(1)
N(2A)	2764(3)	-2033(2)	3206(2)	18(1)
C(1A)	1764(4)	-1602(3)	3281(3)	18(1)
C(2A)	1619(4)	-2458(3)	2015(3)	18(1)
C(3A)	2706(4)	-2576(3)	2425(3)	19(1)

C(4A)	-158(4)	-1541(3)	2446(3)	21(1)
C(5A)	-1008(5)	-1566(3)	3097(3)	27(1)
C(6A)	-2185(5)	-1304(4)	2969(3)	32(1)
C(7A)	-2487(4)	-1042(3)	2194(4)	30(1)
C(8A)	-1619(5)	-1007(3)	1564(3)	31(1)
C(9A)	-433(4)	-1263(3)	1682(3)	26(1)
C(10A)	1168(4)	-2847(3)	1154(3)	24(1)
C(11A)	-33(5)	-3278(3)	992(3)	28(1)
C(12A)	-407(5)	-3658(4)	167(3)	34(1)
C(13A)	416(5)	-3610(3)	-495(3)	30(1)
C(14A)	1612(5)	-3192(3)	-335(3)	28(1)
C(15A)	1983(4)	-2810(3)	476(3)	23(1)
C11	22(4)	-4033(3)	-1378(3)	39(1)
F11	-1073(7)	-3827(7)	-1647(6)	77(2)
F21	869(9)	-3836(6)	-1972(4)	67(2)
F31	-65(8)	-4895(2)	-1457(4)	34(2)
C12	22(4)	-4033(3)	-1378(3)	39(1)
F12	-1240(5)	-4165(11)	-1432(9)	42(3)
F22	335(15)	-3538(9)	-1992(7)	49(3)
F32	404(16)	-4806(6)	-1632(10)	43(3)
C17A2	3658(4)	-3140(3)	2140(3)	21(1)
C18A2	3319(4)	-4029(3)	1845(3)	23(1)
C19A2	4195(4)	-4567(3)	1566(3)	24(1)
C20A2	5453(4)	-4239(3)	1572(3)	27(1)
C21A2	5815(4)	-3362(3)	1866(3)	27(1)
C22A2	4923(4)	-2818(3)	2141(3)	25(1)
C13	6408(4)	-4809(3)	1238(2)	36(1)
F13	6661(15)	-4747(12)	416(4)	48(2)
F23	6075(14)	-5657(4)	1269(14)	52(2)
F33	7500(8)	-4603(11)	1666(9)	46(2)
C14	6408(4)	-4809(3)	1238(2)	36(1)
F14	7596(11)	-4504(16)	1460(20)	44(4)
F24	6200(20)	-5582(10)	1526(19)	38(3)
F34	6370(30)	-4990(20)	384(4)	46(3)
C24A4	3757(4)	-1941(3)	3851(3)	19(1)
C25A4	4444(4)	-1141(3)	4071(3)	23(1)
C26A4	5380(4)	-1050(3)	4707(3)	24(1)
C27A4	5624(4)	-1746(3)	5093(3)	24(1)
C28A4	4938(5)	-2545(3)	4850(3)	30(1)
C29A4	4001(5)	-2648(3)	4228(3)	27(1)
N1B4	-84(3)	-1713(2)	-2501(2)	20(1)
N2B4	-1809(3)	-1932(2)	-1839(2)	19(1)
C1B4	-687(4)	-1478(3)	-1789(3)	23(1)
C2B4	-851(4)	-2334(3)	-3042(3)	17(1)
C3B4	-1933(4)	-2470(3)	-2628(3)	20(1)
C4B4	1207(4)	-1396(3)	-2666(3)	22(1)
C5B4	1463(4)	-1102(3)	-3440(3)	22(1)
C6B4	2718(5)	-874(3)	-3605(3)	29(1)
C7B4	3666(5)	-925(3)	-3007(4)	32(1)
C8B4	3352(4)	-1187(3)	-2235(3)	27(1)
C9B4	2117(4)	-1445(3)	-2052(3)	26(1)
C10B4	-513(4)	-2747(3)	-3895(3)	19(1)
C11B4	577(4)	-3166(3)	-4003(3)	21(1)
C12B4	834(5)	-3589(3)	-4802(3)	26(1)
C13B4	7(4)	-3607(3)	-5493(3)	20(1)
C14B4	-1065(5)	-3197(3)	-5390(3)	25(1)

C15B4	-1311(4)	-2753(3)	-4584(3)	22(1)
C15	286(4)	-4089(3)	-6347(2)	27(1)
F15	65(13)	-4948(2)	-6362(7)	27(2)
F25	1484(6)	-3939(9)	-6576(9)	46(2)
F35	-425(15)	-3898(9)	-6982(5)	46(2)
C16	286(4)	-4089(3)	-6347(2)	27(1)
F16	-230(20)	-4913(6)	-6518(15)	26(3)
F26	1536(5)	-4125(17)	-6392(15)	30(3)
F36	-30(20)	-3699(14)	-7006(9)	33(3)
C17B6	-3072(4)	-3056(3)	-2897(3)	19(1)
C18B6	-2973(4)	-3926(3)	-3203(3)	19(1)
C19B6	-4030(4)	-4487(3)	-3464(3)	23(1)
C20B6	-5201(4)	-4180(3)	-3425(3)	26(1)
C21B6	-5307(4)	-3316(3)	-3129(3)	26(1)
C22B6	-4240(4)	-2757(3)	-2868(3)	24(1)
C17	-6337(4)	-4769(3)	-3753(3)	37(1)
F17	-6495(14)	-4856(12)	-4607(3)	43(2)
F27	-6337(13)	-5577(5)	-3550(13)	49(2)
F37	-7373(7)	-4471(9)	-3422(9)	37(2)
C18	-6337(4)	-4769(3)	-3753(3)	37(1)
F18	-6650(20)	-4648(16)	-4551(7)	35(3)
F28	-6130(20)	-5612(5)	-3810(20)	46(3)
F38	-7359(13)	-4690(20)	-3291(13)	50(4)
C24B8	-2718(4)	-1885(3)	-1168(3)	21(1)
C25B8	-3145(5)	-1108(4)	-880(3)	35(1)
C26B8	-4008(6)	-1080(4)	-213(4)	46(2)
C27B8	-4430(5)	-1829(4)	119(3)	37(1)
C28B8	-4026(6)	-2586(4)	-186(4)	45(2)
C29B8	-3153(6)	-2639(4)	-844(3)	40(1)

Table B.23.   Bond Lengths [Å] and Angles [°] for sm121 (**3.3d**).

C(1ME)-Cl(1)	1.700(11)
C(1ME)-Cl(2)	1.700(11)
C(1ME)-H(1MA)	0.9900
C(1ME)-H(1MB)	0.9900
C(2ME)-Cl(4)	1.699(11)
C(2ME)-Cl(3)	1.701(11)
C(2ME)-H(2MA)	0.9900
C(2ME)-H(2MB)	0.9900
C(3ME)-Cl(4)	1.697(11)
C(3ME)-Cl(5)	1.699(11)
C(3ME)-H(3MA)	0.9900
C(3ME)-H(3MB)	0.9900
Cl(5)-C(3ME)#1	1.699(11)
N(1A)-C(1A)	1.332(6)
N(1A)-C(2A)	1.407(6)
N(1A)-C(4A)	1.448(6)
N(2A)-C(1A)	1.327(6)
N(2A)-C(3A)	1.389(6)
N(2A)-C24A4	1.447(6)
C(1A)-H(1AA)	0.9500
C(2A)-C(3A)	1.371(6)

C(2A)-C(10A)	1.461(6)
C(3A)-C17A2	1.454(6)
C(4A)-C(9A)	1.378(7)
C(4A)-C(5A)	1.385(7)
C(5A)-C(6A)	1.392(7)
C(5A)-H(5AA)	0.9500
C(6A)-C(7A)	1.389(8)
C(6A)-H(6AA)	0.9500
C(7A)-C(8A)	1.375(7)
C(7A)-H(7AA)	0.9500
C(8A)-C(9A)	1.395(7)
C(8A)-H(8AA)	0.9500
C(9A)-H(9AA)	0.9500
C(10A)-C(15A)	1.393(7)
C(10A)-C(11A)	1.397(7)
C(11A)-C(12A)	1.387(7)
C(11A)-H(11A)	0.9500
C(12A)-C(13A)	1.382(8)
C(12A)-H(12A)	0.9500
C(13A)-C(14A)	1.385(7)
C(13A)-C11	1.489(6)
C(14A)-C(15A)	1.368(7)
C(14A)-H(14A)	0.9500
C(15A)-H(15A)	0.9500
C11-F31	1.332(5)
C11-F11	1.333(5)
C11-F21	1.358(5)
C17A2-C22A2	1.402(7)
C17A2-C18A2	1.412(7)
C18A2-C19A2	1.364(7)
C18A2-H18A2	0.9500
C19A2-C20A2	1.396(7)
C19A2-H19A2	0.9500
C20A2-C21A2	1.398(7)
C20A2-C13	1.483(6)
C21A2-C22A2	1.382(7)
C21A2-H21A2	0.9500
C22A2-H22A2	0.9500
C13-F33	1.334(5)
C13-F13	1.342(5)
C13-F23	1.348(5)
C24A4-C29A4	1.378(7)
C24A4-C25A4	1.383(6)
C25A4-C26A4	1.395(7)
C25A4-H25A4	0.9500
C26A4-C27A4	1.370(7)
C26A4-H26A4	0.9500
C27A4-C28A4	1.386(7)
C27A4-H27A4	0.9500
C28A4-C29A4	1.378(7)
C28A4-H28A4	0.9500
C29A4-H29A4	0.9500
N1B4-C1B4	1.327(6)
N1B4-C2B4	1.391(6)
N1B4-C4B4	1.464(6)
N2B4-C1B4	1.331(6)

N2B4-C3B4	1.395(6)
N2B4-C24B8	1.448(6)
C1B4-H1BA4	0.9500
C2B4-C3B4	1.354(6)
C2B4-C10B4	1.473(6)
C3B4-C17B6	1.472(6)
C4B4-C9B4	1.384(7)
C4B4-C5B4	1.386(7)
C5B4-C6B4	1.397(7)
C5B4-H5BA4	0.9500
C6B4-C7B4	1.397(8)
C6B4-H6BA4	0.9500
C7B4-C8B4	1.374(8)
C7B4-H7BA4	0.9500
C8B4-C9B4	1.393(7)
C8B4-H8BA4	0.9500
C9B4-H9BA4	0.9500
C10B4-C15B4	1.375(6)
C10B4-C11B4	1.403(6)
C11B4-C12B4	1.381(7)
C11B4-H11B4	0.9500
C12B4-C13B4	1.394(7)
C12B4-H12B4	0.9500
C13B4-C14B4	1.378(7)
C13B4-C15	1.495(6)
C14B4-C15B4	1.399(6)
C14B4-H14B4	0.9500
C15B4-H15B4	0.9500
C15-F35	1.339(5)
C15-F15	1.339(5)
C15-F25	1.349(5)
C17B6-C22B6	1.386(6)
C17B6-C18B6	1.395(6)
C18B6-C19B6	1.382(6)
C18B6-H18B6	0.9500
C19B6-C20B6	1.394(7)
C19B6-H19B6	0.9500
C20B6-C21B6	1.384(7)
C20B6-C17	1.492(6)
C21B6-C22B6	1.389(7)
C21B6-H21B6	0.9500
C22B6-H22B6	0.9500
C17-F37	1.336(5)
C17-F17	1.340(5)
C17-F27	1.350(5)
C24B8-C25B8	1.363(7)
C24B8-C29B8	1.393(7)
C25B8-C26B8	1.410(8)
C25B8-H25B8	0.9500
C26B8-C27B8	1.389(9)
C26B8-H26B8	0.9500
C27B8-C28B8	1.333(8)
C27B8-H27B8	0.9500
C28B8-C29B8	1.405(8)
C28B8-H28B8	0.9500
C29B8-H29B8	0.9500

Cl(1)-C(1ME)-Cl(2)	125.8(10)
Cl(1)-C(1ME)-H(1MA)	105.9
Cl(2)-C(1ME)-H(1MA)	105.9
Cl(1)-C(1ME)-H(1MB)	105.9
Cl(2)-C(1ME)-H(1MB)	105.9
H(1MA)-C(1ME)-H(1MB)	106.2
Cl(4)-C(2ME)-Cl(3)	130.1(12)
Cl(4)-C(2ME)-H(2MA)	104.8
Cl(3)-C(2ME)-H(2MA)	104.8
Cl(4)-C(2ME)-H(2MB)	104.8
Cl(3)-C(2ME)-H(2MB)	104.8
H(2MA)-C(2ME)-H(2MB)	105.8
Cl(4)-C(3ME)-Cl(5)	143.4(17)
Cl(4)-C(3ME)-H(3MA)	101.1
Cl(5)-C(3ME)-H(3MA)	101.1
Cl(4)-C(3ME)-H(3MB)	101.1
Cl(5)-C(3ME)-H(3MB)	101.1
H(3MA)-C(3ME)-H(3MB)	104.5
C(3ME)-Cl(4)-C(2ME)	134(5)
C(3ME)#1-Cl(5)-C(3ME)	179.999(1)
C(1A)-N(1A)-C(2A)	109.2(4)
C(1A)-N(1A)-C(4A)	124.0(4)
C(2A)-N(1A)-C(4A)	126.7(4)
C(1A)-N(2A)-C(3A)	109.8(4)
C(1A)-N(2A)-C24A4	124.3(4)
C(3A)-N(2A)-C24A4	125.9(4)
N(2A)-C(1A)-N(1A)	108.4(4)
N(2A)-C(1A)-H(1AA)	125.8
N(1A)-C(1A)-H(1AA)	125.8
C(3A)-C(2A)-N(1A)	105.9(4)
C(3A)-C(2A)-C(10A)	127.7(4)
N(1A)-C(2A)-C(10A)	126.3(4)
C(2A)-C(3A)-N(2A)	106.6(4)
C(2A)-C(3A)-C17A2	129.3(4)
N(2A)-C(3A)-C17A2	124.0(4)
C(9A)-C(4A)-C(5A)	122.4(4)
C(9A)-C(4A)-N(1A)	119.6(4)
C(5A)-C(4A)-N(1A)	118.0(4)
C(4A)-C(5A)-C(6A)	118.6(5)
C(4A)-C(5A)-H(5AA)	120.7
C(6A)-C(5A)-H(5AA)	120.7
C(7A)-C(6A)-C(5A)	119.8(5)
C(7A)-C(6A)-H(6AA)	120.1
C(5A)-C(6A)-H(6AA)	120.1
C(8A)-C(7A)-C(6A)	120.6(4)
C(8A)-C(7A)-H(7AA)	119.7
C(6A)-C(7A)-H(7AA)	119.7
C(7A)-C(8A)-C(9A)	120.4(5)
C(7A)-C(8A)-H(8AA)	119.8
C(9A)-C(8A)-H(8AA)	119.8
C(4A)-C(9A)-C(8A)	118.2(5)
C(4A)-C(9A)-H(9AA)	120.9
C(8A)-C(9A)-H(9AA)	120.9
C(15A)-C(10A)-C(11A)	119.1(4)
C(15A)-C(10A)-C(2A)	118.6(4)

C(11A)-C(10A)-C(2A)	122.3(4)
C(12A)-C(11A)-C(10A)	120.2(5)
C(12A)-C(11A)-H(11A)	119.9
C(10A)-C(11A)-H(11A)	119.9
C(13A)-C(12A)-C(11A)	119.6(5)
C(13A)-C(12A)-H(12A)	120.2
C(11A)-C(12A)-H(12A)	120.2
C(12A)-C(13A)-C(14A)	120.3(5)
C(12A)-C(13A)-C11	119.6(5)
C(14A)-C(13A)-C11	120.1(5)
C(15A)-C(14A)-C(13A)	120.4(5)
C(15A)-C(14A)-H(14A)	119.8
C(13A)-C(14A)-H(14A)	119.8
C(14A)-C(15A)-C(10A)	120.4(4)
C(14A)-C(15A)-H(15A)	119.8
C(10A)-C(15A)-H(15A)	119.8
F31-C11-F11	106.9(5)
F31-C11-F21	103.8(4)
F11-C11-F21	106.6(5)
F31-C11-C(13A)	112.4(4)
F11-C11-C(13A)	114.1(5)
F21-C11-C(13A)	112.4(5)
C22A2-C17A2-C18A2	118.4(4)
C22A2-C17A2-C(3A)	121.2(4)
C18A2-C17A2-C(3A)	120.3(4)
C19A2-C18A2-C17A2	121.2(4)
C19A2-C18A2-H18A2	119.4
C17A2-C18A2-H18A2	119.4
C18A2-C19A2-C20A2	119.9(5)
C18A2-C19A2-H19A2	120.1
C20A2-C19A2-H19A2	120.1
C19A2-C20A2-C21A2	120.1(4)
C19A2-C20A2-C13	120.4(4)
C21A2-C20A2-C13	119.5(4)
C22A2-C21A2-C20A2	119.9(4)
C22A2-C21A2-H21A2	120.0
C20A2-C21A2-H21A2	120.0
C21A2-C22A2-C17A2	120.5(5)
C21A2-C22A2-H22A2	119.7
C17A2-C22A2-H22A2	119.7
F33-C13-F13	105.5(5)
F33-C13-F23	106.6(5)
F13-C13-F23	106.2(5)
F33-C13-C20A2	112.2(6)
F13-C13-C20A2	112.0(6)
F23-C13-C20A2	113.7(7)
C29A4-C24A4-C25A4	121.5(4)
C29A4-C24A4-N(2A)	119.6(4)
C25A4-C24A4-N(2A)	118.9(4)
C24A4-C25A4-C26A4	118.7(4)
C24A4-C25A4-H25A4	120.7
C26A4-C25A4-H25A4	120.7
C27A4-C26A4-C25A4	120.3(4)
C27A4-C26A4-H26A4	119.8
C25A4-C26A4-H26A4	119.8
C26A4-C27A4-C28A4	119.9(4)

C26A4-C27A4-H27A4	120.1
C28A4-C27A4-H27A4	120.1
C29A4-C28A4-C27A4	120.8(5)
C29A4-C28A4-H28A4	119.6
C27A4-C28A4-H28A4	119.6
C28A4-C29A4-C24A4	118.8(5)
C28A4-C29A4-H29A4	120.6
C24A4-C29A4-H29A4	120.6
C1B4-N1B4-C2B4	109.2(4)
C1B4-N1B4-C4B4	125.1(4)
C2B4-N1B4-C4B4	125.7(4)
C1B4-N2B4-C3B4	108.4(4)
C1B4-N2B4-C24B8	125.0(4)
C3B4-N2B4-C24B8	126.6(4)
N1B4-C1B4-N2B4	108.7(4)
N1B4-C1B4-H1BA4	125.6
N2B4-C1B4-H1BA4	125.6
C3B4-C2B4-N1B4	106.5(4)
C3B4-C2B4-C10B4	128.3(4)
N1B4-C2B4-C10B4	125.2(4)
C2B4-C3B4-N2B4	107.2(4)
C2B4-C3B4-C17B6	130.1(4)
N2B4-C3B4-C17B6	122.8(4)
C9B4-C4B4-C5B4	123.5(4)
C9B4-C4B4-N1B4	117.8(4)
C5B4-C4B4-N1B4	118.7(4)
C4B4-C5B4-C6B4	117.0(5)
C4B4-C5B4-H5BA4	121.5
C6B4-C5B4-H5BA4	121.5
C7B4-C6B4-C5B4	121.3(5)
C7B4-C6B4-H6BA4	119.4
C5B4-C6B4-H6BA4	119.4
C8B4-C7B4-C6B4	119.2(5)
C8B4-C7B4-H7BA4	120.4
C6B4-C7B4-H7BA4	120.4
C7B4-C8B4-C9B4	121.6(5)
C7B4-C8B4-H8BA4	119.2
C9B4-C8B4-H8BA4	119.2
C4B4-C9B4-C8B4	117.4(5)
C4B4-C9B4-H9BA4	121.3
C8B4-C9B4-H9BA4	121.3
C15B4-C10B4-C11B4	119.9(4)
C15B4-C10B4-C2B4	119.1(4)
C11B4-C10B4-C2B4	120.9(4)
C12B4-C11B4-C10B4	119.6(4)
C12B4-C11B4-H11B4	120.2
C10B4-C11B4-H11B4	120.2
C11B4-C12B4-C13B4	120.1(4)
C11B4-C12B4-H12B4	119.9
C13B4-C12B4-H12B4	119.9
C14B4-C13B4-C12B4	120.5(4)
C14B4-C13B4-C15	120.3(4)
C12B4-C13B4-C15	119.2(4)
C13B4-C14B4-C15B4	119.4(4)
C13B4-C14B4-H14B4	120.3
C15B4-C14B4-H14B4	120.3

C10B4-C15B4-C14B4	120.5(4)
C10B4-C15B4-H15B4	119.7
C14B4-C15B4-H15B4	119.7
F35-C15-F15	106.0(4)
F35-C15-F25	106.5(5)
F15-C15-F25	105.9(5)
F35-C15-C13B4	112.4(5)
F15-C15-C13B4	111.5(5)
F25-C15-C13B4	114.0(5)
C22B6-C17B6-C18B6	119.3(4)
C22B6-C17B6-C3B4	121.2(4)
C18B6-C17B6-C3B4	119.4(4)
C19B6-C18B6-C17B6	120.4(4)
C19B6-C18B6-H18B6	119.8
C17B6-C18B6-H18B6	119.8
C18B6-C19B6-C20B6	119.8(4)
C18B6-C19B6-H19B6	120.1
C20B6-C19B6-H19B6	120.1
C21B6-C20B6-C19B6	120.2(4)
C21B6-C20B6-C17	119.6(4)
C19B6-C20B6-C17	120.0(4)
C20B6-C21B6-C22B6	119.7(4)
C20B6-C21B6-H21B6	120.2
C22B6-C21B6-H21B6	120.2
C17B6-C22B6-C21B6	120.6(4)
C17B6-C22B6-H22B6	119.7
C21B6-C22B6-H22B6	119.7
F37-C17-F17	106.2(5)
F37-C17-F27	105.9(5)
F17-C17-F27	106.7(5)
F37-C17-C20B6	111.1(6)
F17-C17-C20B6	113.2(7)
F27-C17-C20B6	113.2(6)
C25B8-C24B8-C29B8	121.6(5)
C25B8-C24B8-N2B4	119.3(4)
C29B8-C24B8-N2B4	119.0(4)
C24B8-C25B8-C26B8	117.9(5)
C24B8-C25B8-H25B8	121.1
C26B8-C25B8-H25B8	121.1
C27B8-C26B8-C25B8	120.5(5)
C27B8-C26B8-H26B8	119.7
C25B8-C26B8-H26B8	119.7
C28B8-C27B8-C26B8	120.6(5)
C28B8-C27B8-H27B8	119.7
C26B8-C27B8-H27B8	119.7
C27B8-C28B8-C29B8	120.5(6)
C27B8-C28B8-H28B8	119.7
C29B8-C28B8-H28B8	119.7
C24B8-C29B8-C28B8	118.7(5)
C24B8-C29B8-H29B8	120.6
C28B8-C29B8-H29B8	120.6

Symmetry transformations used to generate equivalent atoms:
#1 -x,-y,-z

Table B.24. Anisotropic Displacement Parameters ($\text{Å}^2\text{x }10^3$) for sm121 (**3.3d**). The anisotropic displacement factor exponent takes the form: $-2\pi^2[\,h^2\,a^{*2}U^{11} + ... \ + 2\,h\,k\,a^*\,b^*\,U^{12}\,]$

	U^{11}	U^{22}	U^{33}	U^{23}	U^{13}	U^{12}
Cl(1)	47(1)	71(2)	42(1)	-18(1)	14(1)	-11(1)
Cl(2)	47(1)	62(1)	34(1)	1(1)	-2(1)	14(1)
Cl(3)	51(1)	36(1)	36(1)	10(1)	5(1)	8(1)
Cl(4)	88(5)	23(3)	29(3)	2(2)	5(3)	17(3)
Cl(5)	62(1)	50(1)	17(1)	-1(1)	-1(1)	-28(1)
N(1A)	20(2)	25(2)	16(2)	5(2)	2(2)	1(2)
N(2A)	14(2)	22(2)	16(2)	1(2)	-4(1)	2(2)
C(1A)	19(2)	19(2)	17(2)	8(2)	2(2)	-3(2)
C(2A)	18(2)	17(2)	17(2)	3(2)	-1(2)	2(2)
C(3A)	15(2)	26(2)	16(2)	-1(2)	1(2)	-2(2)
C(4A)	13(2)	20(2)	28(3)	7(2)	-1(2)	-1(2)
C(5A)	36(3)	25(3)	20(2)	6(2)	4(2)	6(2)
C(6A)	26(3)	38(3)	35(3)	7(2)	10(2)	10(2)
C(7A)	15(2)	26(3)	51(3)	6(2)	-3(2)	6(2)
C(8A)	26(3)	37(3)	34(3)	15(2)	-5(2)	9(2)
C(9A)	24(2)	29(3)	28(3)	12(2)	-1(2)	5(2)
C(10A)	24(2)	29(3)	19(2)	5(2)	-3(2)	8(2)
C(11A)	26(3)	36(3)	21(2)	6(2)	-1(2)	-1(2)
C(12A)	34(3)	40(3)	26(3)	9(2)	-10(2)	-8(2)
C(13A)	42(3)	28(3)	21(3)	5(2)	-7(2)	7(2)
C(14A)	28(3)	37(3)	19(2)	5(2)	2(2)	10(2)
C(15A)	15(2)	31(3)	22(2)	3(2)	1(2)	3(2)
C11	53(3)	41(2)	21(2)	1(2)	-10(2)	12(2)
F11	110(4)	94(5)	33(4)	-16(4)	-43(3)	75(4)
F21	107(5)	72(5)	15(3)	7(3)	-3(3)	-28(4)
F31	43(4)	34(2)	23(3)	-5(2)	1(2)	8(2)
C12	53(3)	41(2)	21(2)	1(2)	-10(2)	12(2)
F12	50(4)	52(7)	26(6)	5(5)	-17(4)	18(4)
F22	67(7)	55(6)	24(5)	14(4)	-27(5)	1(5)
F32	56(7)	49(5)	23(6)	-4(4)	-4(6)	20(5)
C17A2	20(2)	32(3)	13(2)	5(2)	1(2)	4(2)
C18A2	16(2)	26(3)	24(2)	-3(2)	1(2)	1(2)
C19A2	22(2)	25(3)	25(2)	3(2)	1(2)	1(2)
C20A2	23(2)	36(3)	24(3)	8(2)	6(2)	6(2)
C21A2	16(2)	38(3)	28(3)	10(2)	1(2)	2(2)
C22A2	26(2)	26(3)	21(2)	0(2)	-5(2)	1(2)
C13	30(2)	40(2)	40(2)	7(2)	13(2)	14(2)
F13	49(5)	54(5)	41(3)	-2(3)	25(3)	8(4)
F23	49(4)	40(3)	70(6)	6(3)	24(5)	12(3)
F33	25(3)	59(5)	58(4)	9(4)	9(3)	19(3)
C14	30(2)	40(2)	40(2)	7(2)	13(2)	14(2)
F14	31(5)	50(7)	53(7)	8(6)	12(5)	8(4)
F24	39(6)	35(5)	42(7)	2(4)	17(6)	17(4)
F34	48(7)	56(8)	36(4)	3(4)	15(4)	23(6)
C24A4	17(2)	22(2)	17(2)	1(2)	3(2)	0(2)
C25A4	28(3)	19(2)	23(2)	8(2)	-2(2)	-3(2)
C26A4	17(2)	23(2)	31(3)	-1(2)	-3(2)	6(2)
C27A4	18(2)	31(3)	22(2)	0(2)	-3(2)	6(2)
C28A4	37(3)	26(3)	30(3)	7(2)	-7(2)	5(2)

C29A4	30(3)	28(3)	23(2)	8(2)	-8(2)	0(2)
N1B4	19(2)	21(2)	16(2)	-3(2)	3(2)	-2(2)
N2B4	21(2)	18(2)	16(2)	-2(2)	2(2)	2(2)
C1B4	22(2)	26(3)	18(2)	-6(2)	1(2)	7(2)
C2B4	14(2)	20(2)	17(2)	2(2)	-2(2)	5(2)
C3B4	21(2)	22(2)	19(2)	-1(2)	3(2)	8(2)
C4B4	23(2)	21(2)	18(2)	-6(2)	1(2)	-2(2)
C5B4	27(2)	17(2)	21(2)	1(2)	1(2)	-2(2)
C6B4	33(3)	23(3)	30(3)	2(2)	5(2)	-4(2)
C7B4	18(2)	33(3)	43(3)	-4(2)	4(2)	2(2)
C8B4	19(2)	21(2)	39(3)	-1(2)	-7(2)	1(2)
C9B4	24(2)	33(3)	19(2)	2(2)	1(2)	4(2)
C10B4	19(2)	15(2)	22(2)	0(2)	2(2)	0(2)
C11B4	18(2)	26(2)	22(2)	6(2)	1(2)	4(2)
C12B4	26(2)	27(3)	25(3)	2(2)	10(2)	11(2)
C13B4	27(2)	17(2)	16(2)	4(2)	4(2)	-1(2)
C14B4	29(3)	29(3)	16(2)	-1(2)	-4(2)	-1(2)
C15B4	15(2)	31(3)	20(2)	-2(2)	-2(2)	9(2)
C15	36(2)	28(2)	17(2)	0(2)	5(2)	0(2)
F15	33(4)	22(2)	22(4)	-8(2)	-1(3)	-2(2)
F25	48(3)	59(5)	21(4)	-9(3)	23(2)	-26(3)
F35	78(5)	45(4)	16(3)	1(2)	-3(3)	20(4)
C16	36(2)	28(2)	17(2)	0(2)	5(2)	0(2)
F16	33(7)	31(4)	14(7)	3(4)	-2(5)	-3(4)
F26	33(4)	37(7)	15(7)	-5(5)	14(4)	-6(4)
F36	55(8)	33(6)	10(5)	4(4)	12(5)	3(6)
C17B6	17(2)	27(2)	14(2)	4(2)	3(2)	7(2)
C18B6	17(2)	18(2)	22(2)	1(2)	-1(2)	5(2)
C19B6	28(3)	17(2)	24(2)	2(2)	-1(2)	2(2)
C20B6	21(2)	33(3)	24(2)	9(2)	-2(2)	-5(2)
C21B6	19(2)	35(3)	25(3)	8(2)	-1(2)	3(2)
C22B6	27(2)	19(2)	25(2)	-1(2)	2(2)	6(2)
C17	29(2)	38(2)	44(2)	10(2)	-6(2)	-3(2)
F17	41(5)	44(5)	37(3)	-11(3)	-11(3)	-5(4)
F27	43(5)	36(3)	66(6)	14(3)	-8(4)	-8(3)
F37	22(3)	39(4)	50(4)	14(3)	2(2)	-10(2)
C18	29(2)	38(2)	44(2)	10(2)	-6(2)	-3(2)
F18	28(6)	31(7)	44(4)	-3(4)	-14(4)	12(5)
F28	30(6)	37(4)	72(8)	22(5)	-18(6)	-12(4)
F38	30(5)	55(8)	63(6)	14(6)	5(4)	-20(5)
C24B8	17(2)	30(3)	17(2)	1(2)	2(2)	13(2)
C25B8	40(3)	39(3)	31(3)	8(2)	8(2)	19(3)
C26B8	47(4)	55(4)	41(3)	3(3)	10(3)	36(3)
C27B8	22(3)	60(4)	29(3)	8(3)	8(2)	5(2)
C28B8	55(4)	43(4)	36(3)	9(3)	16(3)	-4(3)
C29B8	57(4)	32(3)	30(3)	0(2)	15(3)	6(3)

Table B.25. Hydrogen Coordinates (x 10^4) and Isotropic Displacement Parameters ($\mathring{A}^2$x 10^3)
for sm121 (**3.3d**).

	x	y	z	U(eq)
H(1MA)	985	970	3733	436
H(1MB)	769	-15	3308	436
H(2MA)	4450	-635	505	436
H(2MB)	3940	-1604	571	436
H(3MA)	942	-741	780	436
H(3MB)	570	-1269	-124	436
H(1AA)	1589	-1191	3756	22
H(5AA)	-793	-1757	3619	32
H(6AA)	-2779	-1304	3410	39
H(7AA)	-3302	-886	2099	36
H(8AA)	-1829	-808	1045	37
H(9AA)	169	-1245	1247	31
H(11A)	-596	-3311	1449	34
H(12A)	-1225	-3950	57	41
H(14A)	2178	-3170	-792	33
H(15A)	2801	-2517	579	27
H18A2	2465	-4257	1842	27
H19A2	3950	-5163	1369	29
H21A2	6672	-3141	1876	32
H22A2	5170	-2220	2332	30
H25A4	4281	-663	3794	28
H26A4	5850	-503	4874	28
H27A4	6262	-1682	5526	29
H28A4	5115	-3027	5116	36
H29A4	3533	-3196	4063	32
H1BA4	-371	-1056	-1322	27
H5BA4	814	-1058	-3840	26
H6BA4	2930	-682	-4134	35
H7BA4	4517	-779	-3131	39
H8BA4	3992	-1193	-1816	33
H9BA4	1909	-1646	-1526	31
H11B4	1136	-3158	-3530	26
H12B4	1576	-3868	-4880	31
H14B4	-1631	-3215	-5861	30
H15B4	-2035	-2453	-4513	27
H18B6	-2174	-4135	-3233	23
H19B6	-3958	-5080	-3670	28
H21B6	-6105	-3107	-3105	31
H22B6	-4313	-2163	-2668	29
H25B8	-2869	-602	-1121	42
H26B8	-4304	-545	11	55
H27B8	-5012	-1802	568	44
H28B8	-4330	-3094	42	54
H29B8	-2866	-3178	-1063	48

VITA

JAMES WILLIAM OGLE

c/o Department of Chemistry

Texas A&M University

MS 3255

College Station, TX 77843-3255

EDUCATIONAL BACKGROUND

2008   Texas A&M University, Ph.D, Chemistry

2002   Texas A&M University, Kingsville, M.S., Chemistry

2000   Texas A&M University, Kingsville, B.S., Chemistry

PUBLICATIONS

1. Cui, X.; Ogle, J. W.; Burgess, K. *Chem.Commun.*, **2005**, 672-674.
2. Grill, J. M.; Ogle, J. W.; Miller, S. A. *J. Org. Chem.*, **2006**, 71, 9291-9296.
3. Zhou, J.; Ogle, J. W.; Fan, Y.; Banphavichit, V.; Zhu, Y.; Burgess, K. *Chemistry--A European Journal*, **2007**, 13, 7162-7170.
4. Ogle, J. W.; Zhang, J.; Reibenspies, J. H.; Abboud, K. A.; Miller, S. A. *Org. Lett.* ASAP, August 6, **2008**.

PRESENTATIONS

1. Givins, B.; Camarillo, E.; Mann, S.; Cruz, S.; Sendejo, Z.; Montemayor, M.; Gonzalez, J.; Jimenez, Y.; Bynum, Q.; Cruz, R.; Ogle, J.; Argullin, H.; Asgar, T.; Thomas, R. *Abstracts of Papers*, 225th ACS National Meeting, New Orleans, LA, United States, March 23-27, **2003**.
2. Ogle, J. W. IUCCP, College Station, TX, United States, October 10, **2005**.